

Development of Novel Ligands Influencing Neurotransmission in the Central Nervous System

Dissertation
zur Erlangung des Doktorgrades
der Naturwissenschaften

vorgelegt beim Fachbereich Biochemie, Chemie und Pharmazie
der Johann Wolfgang Goethe-Universität
in Frankfurt am Main

von
Britta Caroline Sasse
aus Bad Nauheim

Frankfurt am Main (2007)
(D 30)

vom Fachbereich Biochemie, Chemie und Pharmazie der Johann Wolfgang
Goethe-Universität als Dissertation angenommen.

Dekan: Prof. Dr. H. Schwalbe

1. Gutachter: Prof. Dr. H. Stark

2. Gutachter: Prof. Dr. G. Schneider

Datum der Disputation: 16.04.2007

Danksagung

Für die vorbildliche und engagierte wissenschaftliche Betreuung möchte ich meinem Doktorvater Professor Dr. Holger Stark danken. Durch seine innovativen Ideen und vielseitigen Interessen hat Professor Stark es mir ermöglicht, nicht nur einen tieferen Einblick in mein Forschungsgebiet zu erhalten, sondern darüber hinaus, Kenntnisse und Weitsicht in multidisziplinäre wissenschaftliche Forschungsgebiete zu bekommen.

Mein Dank gilt Professor Dr. Gisbert Schneider, Herrn Alexander Böcker und Herrn Dr. Evgeny Byvatov, Institut für Organische Chemie und Chemische Biologie, Johann Wolfgang-Goethe Universität, Frankfurt am Main, für die effektive Kooperation und enge wissenschaftliche Zusammenarbeit im Rahmen der Virtuellen Screening Methoden am Dopamin-D₃-Rezeptor. Vor allem der Enthusiasmus von Professor Dr. Gisbert Schneider und seine Freude am wissenschaftlichen Arbeiten haben mich sehr geprägt.

Dr. Pierre Sokoloff und seinen Mitarbeitern der Unité de Neurobiologie et Pharmacologie Moléculaire de l'INSERM in Paris, Frankreich, danke ich für die Einführung in Radioliganden-Bindungsstudien am Dopamin-D₂- und -D₃-Rezeptor und die Bereitstellung der humanen Dopamin-D₂- und -D₃-Rezeptorzelllinien. Bei Professor Dr. Rob Leurs und Professor Dr. Hendrik Timmerman, Free University of Amsterdam, The Netherlands, bedanke ich mich für das Überlassen der humanen Histamin-H₁-Rezeptorzelllinie. Professor Dr. John Shine, The Garvan Institute of Medical Research, Sydney, Australia, danke ich für die Bereitstellung der humanen Dopamin-D₂-Rezeptorzelllinie.

Ich möchte mich bei meinen Kollegen am Institut für Pharmazeutische Chemie für die Kollegialität und gute Zusammenarbeit bedanken. Vor allem bei Herrn Dr. Jukka Leppänen, Herrn Dr. Ulrich Mach und Herrn Oliver Saur möchte ich mich für die Synthese der in dieser Arbeit untersuchten Testliganden bedanken, sowie Herrn Tim Kottke für die fruchtbaren pharmakologischen Diskussionen. Frau Carina Richter danke ich für ihr Engagement im Labor. Vor allem ihre Freude in der Zellkultur hat das Zellwachstum positiv beeinflusst. Mein besonderer Dank gilt Frau Dr. Sieglinde Überall für die wertvolle und freudige Zusammenarbeit im Praktikum „Pharmazeutische Chemie II - Arzneibuchuntersuchung“, die diese Zeit für mich zu einer schönen Erinnerung werden lassen. Meinem Kollegen Dr. Matthias Linder, Institut für Pharmakologie, Johann Wolfgang-Goethe Universität, Frankfurt am Main, danke ich für die zahlreichen wissenschaftlichen Anregungen, Ratschläge und aufmunternde Unterstützung.

Besonderen Dank gilt meiner Familie und meinen Freunden für ihre andauernde Motivation und sowie moralischen Beistand.

1 INTRODUCTION	1
1.1 G Protein-Coupled Receptors	2
1.2 Dopamine	4
1.2.1 Dopamine Receptors	8
1.2.2 Signal Transduction of Dopamine D ₂ and D ₃ Receptors	12
1.2.3 Distribution and Function of Dopamine D ₂ and D ₃ Receptors	14
1.2.4 Therapeutic Relevance of Selective Dopamine D ₃ Receptor Ligands	15
1.2.5 Ligand Binding Mode at Dopamine D ₂ and D ₃ Receptors	22
1.2.6 Ligands for Dopamine D ₂ and D ₃ Receptors	23
1.3 Histamine	27
1.3.1 Histamine H ₁ Receptors	29
1.3.2 Signal Transduction of Histamine H ₁ Receptors	29
1.3.3 Distribution and Function of Histamine H ₁ Receptors	30
1.3.4 Therapeutic Relevance of Histamine H ₁ Receptor Ligands	31
1.3.5 Ligand Binding Mode at Histamine H ₁ Receptors	31
1.3.6 Ligands for Histamine H ₁ Receptors	32
1.4 The Drug Discovery Process	33
1.5 Radioligand Binding Studies	34
2 AIM OF THESIS	36
3 MATERIALS AND METHODS	38
3.1 Materials	39
3.1.1 Reference Substances and Test Compounds	39
3.1.2 Cells, Cell Culture and Protein Assay	40
3.1.3 Chemicals	40
3.1.4 Buffers and Solutions	41
3.1.5 Radiochemicals and Material for Radioligand Binding Assays	42
3.1.6 Technical Equipment	42
3.2 Methods	43
3.2.1 Cell culture	43
3.2.2 Preparation of Membrane Homogenates	45
3.2.3 Radioligand Binding Studies on Human Dopamine D _{2S} and D ₃ Receptors	46
3.2.4 Radioligand Binding Studies on Human Histamine H ₁ Receptors	47
3.2.5 GTP Shift Competition Binding Experiments	48
3.2.6 Data Analysis and Statistics	49
3.2.7 Virtual Screening Methods	53
4 RESULTS AND DISCUSSION	54
4.1 Assay Validation	55
4.1.1 Saturation Binding Experiments	55
4.1.2 Competition Binding Experiments	59

4.1.3 GTP Shift Assay for Discriminating Agonists	63
4.2 Pharmacological Results and Structure-Affinity Relationships	76
4.2.1 Analogues of BP 897 and ST 198	76
4.2.2 Benzhydrylpiperazine Derivatives	83
4.2.3 Pramipexole and Etrabamine Derivatives	94
4.3 Virtual Screening Leading to New Scaffolds	108
4.3.1 Support Vector Machine Based Virtual Screening	108
4.3.2 Lead Identification Strategies for Dopamine D ₃ Receptor Ligands	113
5 SUMMARY	119
6 ZUSAMMENFASSUNG	122
7 AUSFÜHRLICHE ZUSAMMENFASSUNG	125
8 ABBREVIATIONS	131
9 REFERENCES	135
10 PHARMACOLOGICAL EXPERIMENTAL PROCEDURES	150
10.1 Radioligand Binding Assays	151
10.1.1 Dopamine D _{2S} and D ₃ Receptor Binding Assays	151
10.1.2 Preliminary Dopamine D _{2S} and D ₃ Receptor Binding Screening	152
10.1.3 Histamine H ₁ Receptor Binding Assay	153
10.1.4 GTP Shift Assay	154
11 APPENDIX	155
12 CURRICULUM VITAE	169
13 PUBLICATIONS	171

1 Introduction

1.1 G Protein-Coupled Receptors

G protein-coupled receptors (GPCRs) comprise the largest family of cell surface receptors and share the characteristics of seven transmembrane helices (TM1-7) linked by three extracellular loops and three intracellular loops.¹ An additional short helix (H8), directly linked to TM7, is located parallel to the cytoplasmic surface of the membrane.² It is worth mentioning, that the bovine rhodopsin GPCR has been the only crystallized structure solved.² The human genome project has revealed more than 800 GPCR genes, and only approximately 30 genes are targets of drugs presently on the market, while 50% of all launched drugs exert their actions on them.^{3,4} Conclusively, GPCRs represent one of the most important families as pharmaceutical targets in the drug discovery process.^{3,5}

GPCRs communicate extracellular signals into the cell to give an intracellular response. The nature of the signals is highly diverse and includes extracellular signal molecules, such as biogenic amines, peptide and protein hormones, nucleosides and nucleotides, sensory signals such as light signals and even more (glutamate, ions, eicosanoids).⁴ The binding of these signal ligands to the extracellular site or transmembrane region induces a conformational change of the receptor which triggers the heterotrimeric guanine nucleotide binding proteins, consequently promoting the intracellular response.¹ Generally, activation of the receptor induces the exchange of guanosine-5'-triphosphate (GTP) for guanosine-5'-diphosphate (GDP) bound to the $G\alpha$ unit, following the dissociation of the heterotrimeric G protein into $GTP\alpha$ and $\beta\gamma$.¹ Both subunits regulate the activity of the effector systems, mainly adenylyl cyclase, phospholipase or ion channels.^{1,6,7} The production of second messengers strongly depends on the distinct G protein. The G protein becomes inactivated by hydrolysis of the $G\alpha$ bound GTP to GDP.^{1,8}

GPCRs are classified into different families according to their structural and genetic characteristics: family A (rhodopsin-like), family B (glucagon-receptor-like), and family C (metabotropic glutamate receptors).⁴ The rhodopsin-like family is by far the largest subgroup and is characterized by various highly conserved amino acids and a disulphide bridge that connects the first and second extracellular loops.⁴ As an example of a rhodopsin-like GPCR a homology model of the human dopamine D₃ receptor is shown in Figure 1.1.

Among the family A, the subfamily of biogenic amine binding GPCRs is of particular interest due to its interaction with predominant neurotransmitters such as acetylcholine, serotonin, histamine, and the catecholamines dopamine, epinephrine, and norepinephrine.

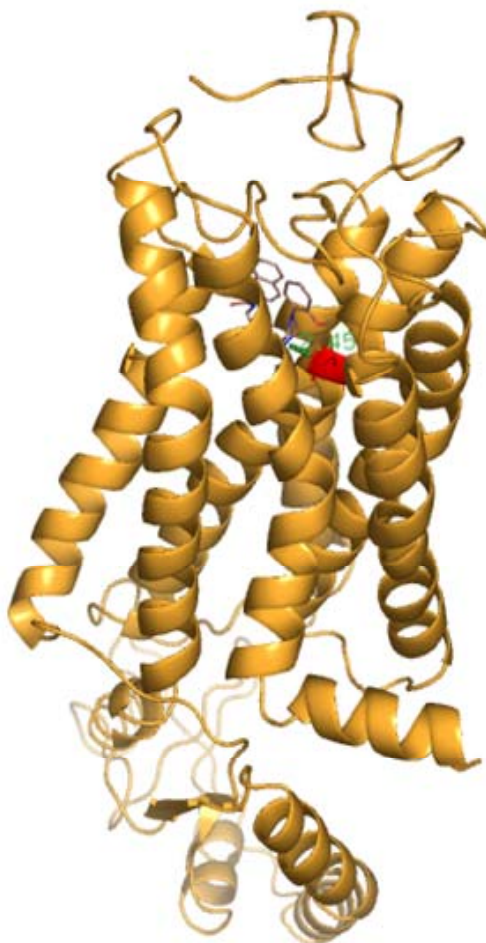


Figure 1.1 Homology model of the human dopamine D₃ receptor with ligand BP 897 interacting with Asp 110 (distance of basic nitrogen to carboxylic acid of Asp 110: 2.45 Å). The homology model was obtained by Byvatov et al., 2005.⁹ The dopamine binding pocket was defined by Asp 110. BP 897 was docked into the binding pocket using GOLD (version 2.2) with default parameter settings. Results were visualized using PyMOL (version 0.99).

A phylogenetic dendrogram of biogenic amine receptors is shown in Figure 1.2 (human sequences of the aminergic GPCRs were extracted from GPCRDB;^{10,11} multiple sequence alignment and dendrogram display were performed with ClustalW^{12,13}). The class of biogenic amine receptors has displayed a tremendous drug target for the treatment of several diseases, such as schizophrenia, Parkinson's disease, depression, and allergies.^{4,14} Recently, increasing evidence has been suggested that the rhodopsin-like GPCRs, but also other members of the GPCR family form dimers or high-order oligomers.¹⁵ Studies on the formation of oligomers have been based on results received by a variety of biophysical techniques.¹⁶ Arrangements of homo-oligomers with identical GPCRs or hetero-oligomers by forming complexes with different GPCRs have been identified.¹⁷ There is still a requirement of investigations in the influence on ligand binding and the functional relevance of oligomerized GPCRs.

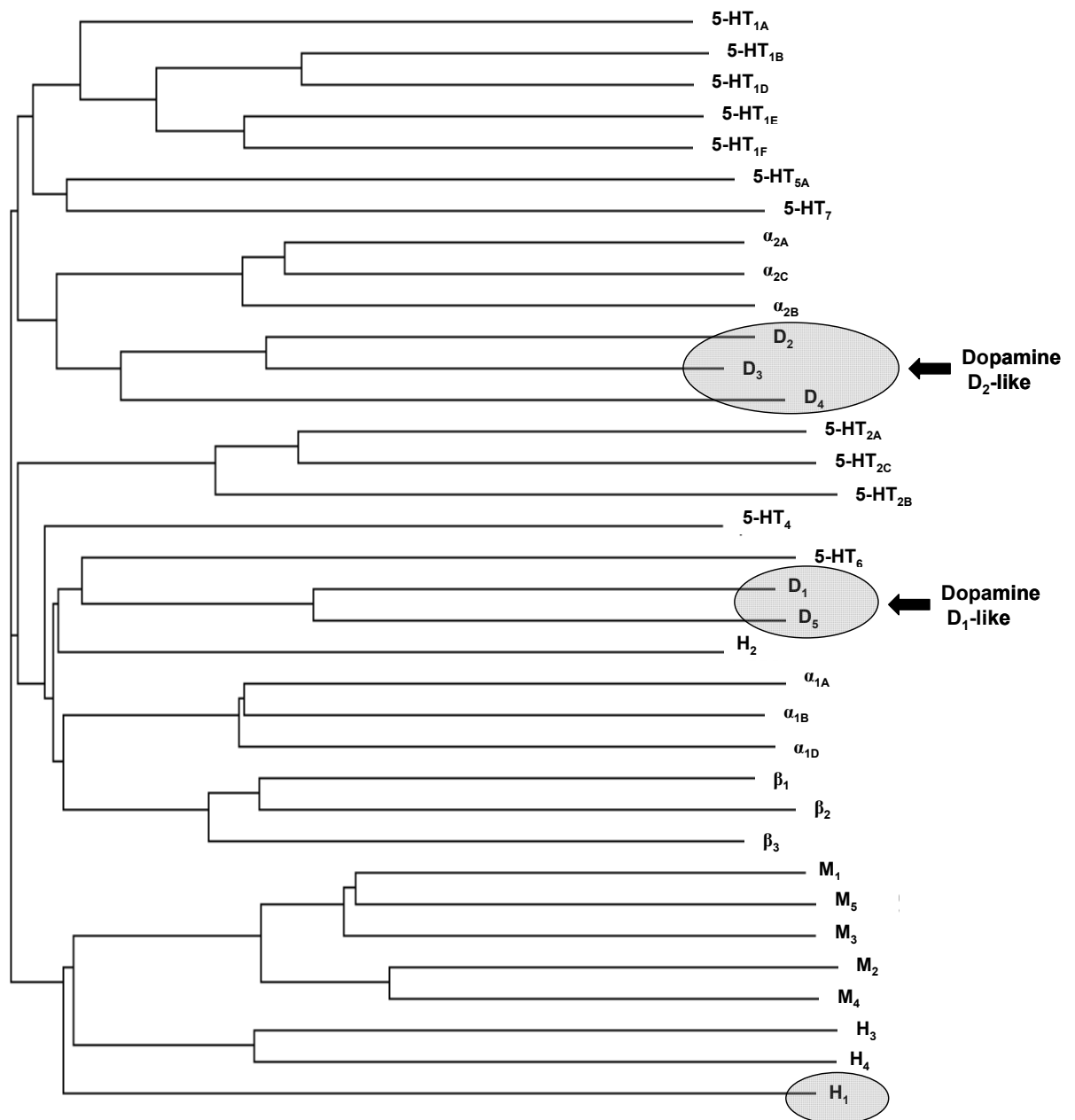


Figure 1.2 Phylogenetic dendrogram of biogenic amine receptors. Dopamine D₁- and D₂-like receptors as well as the histamine H₁ receptor are indicated by gray shaded circles.

1.2 Dopamine

The biogenic monoamine dopamine (DA) (2-(3,4-dihydroxyphenyl)ethanamine) is one of the most important neurotransmitter in the central nervous system (CNS) and firstly identified by Arvid Carlsson in 1958, who was awarded for the Nobel Prize for his pioneering work on dopamine systems in 2000.¹⁸ Dopamine belongs to the group of catecholamine neurotransmitters, structurally characterized by a catechol nucleus (a benzene ring with two adjacent hydroxyl groups), and is also the biogenic precursor of

norepinephrine and epinephrine. Dopamine agitates through interaction with G protein-coupled membrane bound receptors, and functions as a major regulator for processes of emotion, motivated behavior, cognition, voluntary movements, positive reinforcement, and hormone production in the mammalian brain.^{19,20} Imbalance in dopaminergic neurotransmission is associated with pathological disorders linked to neurological movement dysfunctions like Parkinson's disease (PD), Huntington's disease, attention deficit hyperactivity disorder (ADHD), Tourette syndrome, but also neuropsychiatric disorders, like schizophrenia, and drug addiction.²¹⁻²³ In the periphery dopamine modulates cardiovascular and renal functions; hormone secretion, vascular tone and gastrointestinal motility.²⁴

Dopamine is mainly biosynthesized in the central nervous system by mesencephalic neurons of the substantia nigra and ventral tegmental area, and by hypothalamic neurons. Therefore, the aromatic amino acid L-tyrosine is hydroxylated by the enzyme tyrosine 3-hydroxylase (TH) in a rate-limiting step to form levodopa, L-3,4-dihydroxyphenylalanine (L-DOPA). Subsequently, L-3,4-dihydroxyphenylalanine is decarboxylated by the cytoplasmic enzyme aromatic L-amino acid decarboxylase (AADC, L-DOPA decarboxylase) to give dopamine (Figures 1.3 and 1.4).²⁵ TH is activated by the calcium/calmodulin-dependent protein kinase and this enzyme is consequently activated by calcium-bound calmodulin.²⁵

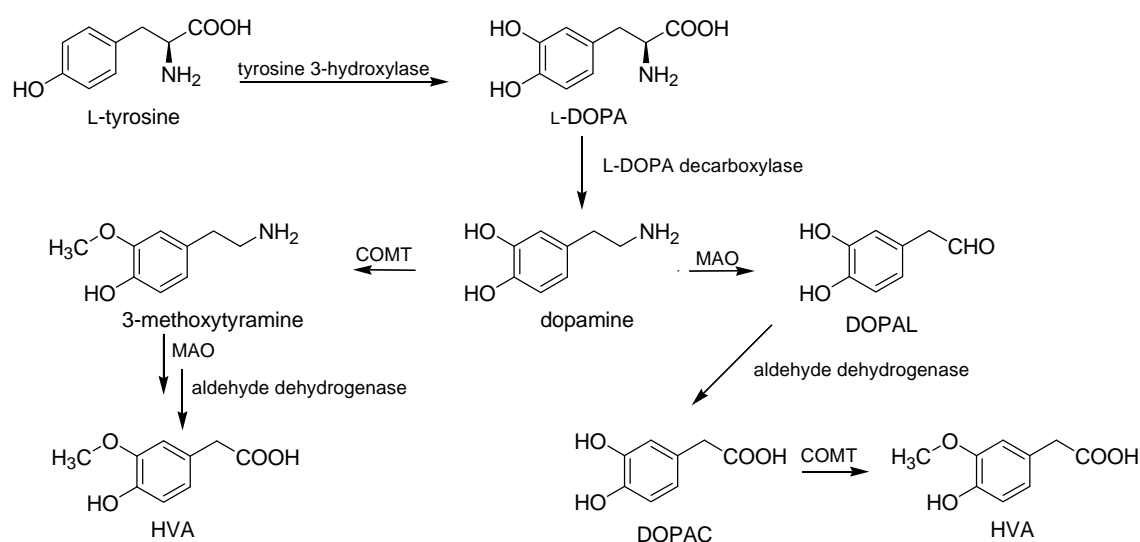


Figure 1.3 Biosynthesis and metabolism of dopamine.

The synthesized dopamine is stored in vesicles and is released into the synaptic cleft by depolarization of the presynaptic neuron due to Ca^{2+} influx. In the synaptic cleft it

stimulates postsynaptic D₁-like and D₂-like receptors and/or negatively modulates the release of dopamine and dopamine synthesis by stimulating presynaptic dopamine D₂ or D₃ autoreceptors via inhibition of tyrosine hydroxylase (negative feedback mechanism). The reuptake of synaptic dopamine into presynaptic neurons is regulated by dopamine transporter (DAT). Hence, dopamine is metabolized by monoamine oxidase (MAO-A, mainly MAO-B) to form 3,4-dihydroxyphenylacetaldehyde (DOPAL), following oxidation to give 3,4-dihydroxyphenylacetat (DOPAC). DA and DOPAC are also metabolized by catechol-*O*-methyltransferase (COMT) to form homovanilic acid (HVA). Synaptic dopamine is metabolized by COMT via 3-methoxytyramin to give HVA (Figures 1.3 and 1.4).²⁶

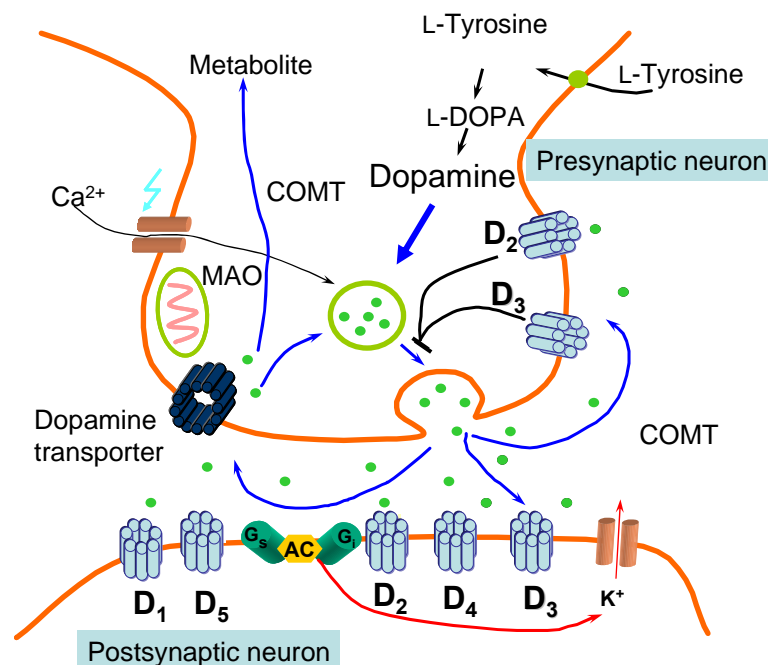


Figure 1.4 Schematic synaptically dopaminergic transmission.

Recently, the neuroprotective and neurotoxic effects of dopamine, which may form autotoxic metabolites, on distinct areas of neurons have been the focus of research.²⁷ Additionally, there is some evidence, that levodopa itself is a neurotransmitter candidate, but further investigation is required.^{28,29}

In the central nervous system the dopaminergic neuron system primarily originates from three major groups of neurons located in the midbrain (mesencephalon) and from neurons presented in the hypothalamus (nuclei arcuate and periventricular) (Figure 1.5).

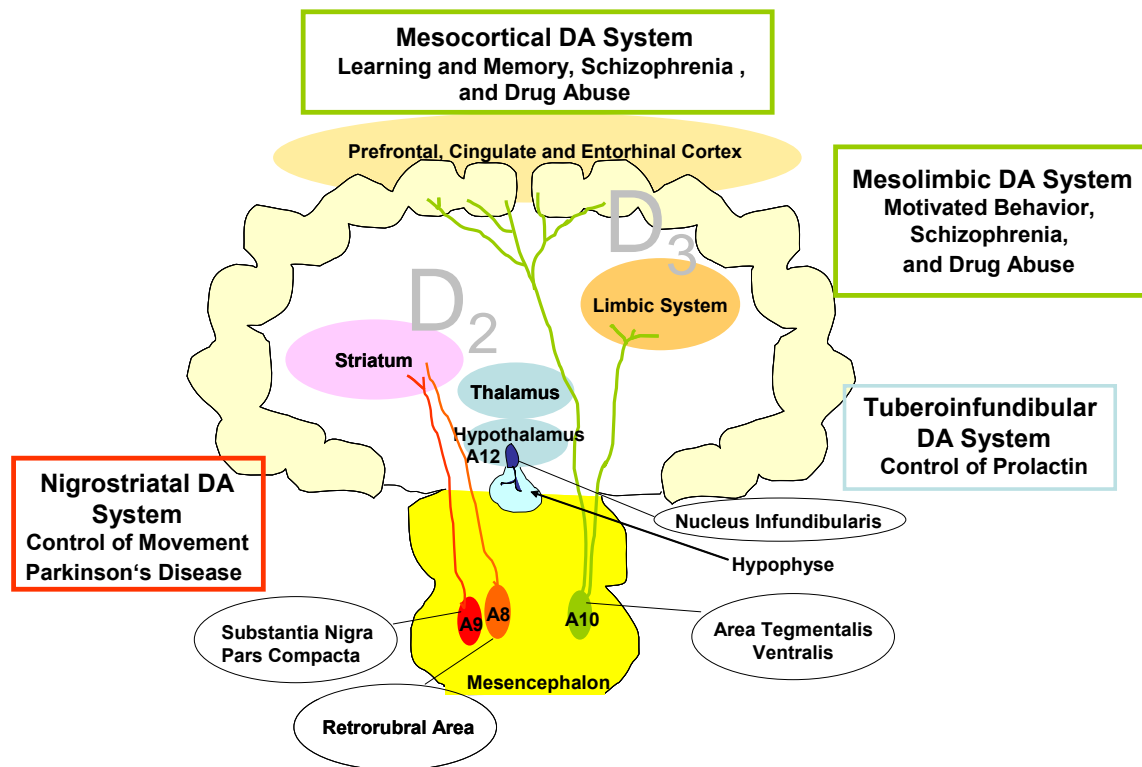


Figure 1.5 Schematic dopaminergic pathway.

The midbrain dopaminergic neurons are nominated as the A8 group in the retrorubral area (RRA), A9 group designates the substantia nigra pars compacta (SNc), and A10 group corresponds to the ventral tegmental area (VTA). The nigrostriatal dopaminergic system arises from dopaminergic cell groups in RRA (A8) and SNc (A9), and projects their axons to the dorsal striatum (nucleus caudatus, putamen).³⁰ This pathway is primarily associated with the control of movement and involved in Parkinson's disease. The dopaminergic neurons located in the ventral tegmental area (A10) project to limbic area (ventral striatum (nucleus accumbens), corpus amygdaloideum, and hippocampus). This innervation is referred as mesolimbic pathway, while projection to cortical areas (medial, prefrontal, cingulate and entorhinal cortex) represents the mesocortical pathway. The former pathway is implicated in motivated behavior, while the later is linked to aspects of learning and memory. Both dopaminergic pathways are associated with reward and schizophrenia. The arcuate and periventricular nuclei (nucleus infundibularis, A12) of the hypothalamus project to the eminentia mediana and to the intermediate lobe of the pituitary via the tuberoinfundibular pathway. This dopaminergic system plays an important role in the inhibitory control of prolactin. A short overview of dopaminergic pathways is given in Table 1.1.

Table 1.1 Overview of dopaminergic pathways.

Dopaminergic Pathway	Dopaminergic Neurons	Projection to	Disease
nigrostriatal	substantia nigra	caudate/putamen (dorsal striatum)	•Parkinson's disease •drug abuse
mesolimbic	ventral tegmental area	limbic areas (nucleus accumbens, ventral striatum, amygdale)	•schizophrenia (positive symptoms) •drug abuse
mesocortical	ventral tegmental area	cortex (medial, prefrontal, cingulate, entorhinal cortex)	•schizophrenia (negative & cognitive symptoms) •drug abuse
tuberoinfundibular	hypothalamus	pituitary, median eminence	•hyperprolactinaemia

1.2.1 Dopamine Receptors

Dopamine receptors belong to the rhodopsin-like G protein-coupled receptor family A. In 1972, the first evidence for the existence of dopamine receptors in brain was confirmed by demonstrating the modulation of adenylyl cyclase (AC) activity by dopamine.³¹ Soon after and on the basis of pharmacological and biochemical investigations, the assumption of diverse dopamine receptors was proposed. At that time, two receptor populations or subtypes were suggested to nominate dopamine D₁ the receptor population that was capable to stimulate adenylyl cyclase, and dopamine D₂ the receptor population, that was independent of AC or not coupled to this effector.³² This dual classification system was established by further pharmacological, physiological, biochemical and anatomic investigations and remained for more than a decade. In the following years novel gene cloning techniques were introduced, and as a result, three new dopamine receptor subtypes have been identified, namely dopamine D₃, D₄ and D₅.^{33,34,35} Although some differences among subtypes within a family have been recognized, dopamine receptors are classified into two subtype receptor families according to homology in their transmembrane sequences and signaling pathways. Dopamine D₁-like receptors comprise dopamine D₁ and D₅ receptors; and dopamine D₂-like receptors consist of dopamine D₂, D₃ and D₄ receptors (see Figure 1.2).²⁴ The dopamine D₁-like receptors are coupled to G_{αs}/G_{α_{olf}} and activate adenylyl cyclase type, consequently increasing the production of the second messenger cyclic adenosine-3',5'-monophosphate (cAMP), activate the cAMP-dependent protein kinase A (PKA) and protein phosphatase-1-inhibitor DARPP-32 (dopamine and cyclic AMP-regulated phosphoprotein, 32kDa).^{24,36} Both mechanisms are involved in the following regulation of enzymes, ion channels, receptors and transcription factors. By

coupling to $G\alpha_q$ a phospholipase C-dependent (PLC), but cAMP-independent mechanism modulates the intracellular Ca^{2+} concentration and protein kinase C (PKC). Dopamine D_2 -like receptors signal via pertussis-toxin sensitive $G\alpha_i/G\alpha_o$ protein.^{36,37} The $G\alpha_{i/o}$ subunit induces inhibition of adenylyl cyclase type 5, as a result downregulating the concentration of cAMP and activation of PKA, while the $G\beta\gamma$ subunit is involved in activating adenylyl cyclase type 2 (AC2) and the modulation of ion channels, phospholipases, protein kinases, and receptor tyrosine kinases.^{24,36} Besides interaction between dopamine receptors and G proteins, dopamine receptors couple to a complex signaling cascade including calcium channels, potassium channels, phospholipase C, arachidonic acid release (AA), Na^+/H^+ exchangers, $Na^+-H^+-ATPase$, and mediate with further signal-modulating proteins.^{24,36,38}

Structure of Dopamine Receptors

Dopamine receptors as GPCRs contain the putative characteristic of seven transmembrane domains (see Figure 1.1). The *N*-terminus of the receptor protein is located on the extracellular side of the membrane and contains *N*-linked glycosylation sites. The protein forms seven helical regions (I-VII) that span the membrane and ends with the short helix (H8) and the *C*-terminal tail on the cytoplasmic side of the membrane. Three extracellular loops (E-1, E-2, and E-3) connect the helices on the extracellular surface, and three intracellular loops (C-1, C-2, and C-3) bond the helices on the intracellular side. Phosphorylation sites are located on the third intracellular loop and on the *C*-terminus.³⁹ Dopamine D_2 -like receptors display a shorter *C*-terminal tail and an increased third intracellular loop compared to D_1 -like receptors. This increase in length is found in receptors coupling with G_i proteins and inhibiting AC, while D_1 -like receptors, coupling to G_s proteins and activating AC, present a short third intracellular loop.²⁴ Within the same dopamine subtype family, receptors share considerable homology of amino acid sequences. The dopamine D_2 and D_3 receptors demonstrate 75% similarity in the TM domains, while its signal-transduction pathway, pharmacological profile and brain distribution is dissimilar.³³ The dopamine D_2 and D_4 receptors share 53% identity in the TM domains.³⁴ For the D_1 -like family, there is 80% identity in the TM domain between dopamine D_1 and D_5 receptors. The genomic structure of dopamine receptors is based on two gene families that principally diverge in the absence and the presence of introns in the coding regions.⁴⁰ Dopamine D_1 and D_5 receptor genes do not possess introns in their coding region, while dopamine D_2 -like receptor genes contain introns.

Receptor-receptor interactions and dimerization/oligomerization have been recognized for all five dopamine receptor subtypes in *in vitro* heterologous expression systems.⁴¹ It has been demonstrated that dopamine D₁ and D₂ receptors each generate homo-oligomers and/or together form robust hetero-oligomers.^{42,43} Within a homo-oligomer or hetero-oligomer complex the ligand binding properties and signaling pathways have changed, but a functional synergism between dopamine D₁ and D₂ receptors has been proposed. A co-activation of co-expressed dopamine D₁ and D₂ receptors results in an increase in Ca²⁺ signaling mediated by phospholipase C and is unlike to the signaling cascade of dopamine D₁ and D₂ receptor homo-oligomers.⁴³ Besides the oligomerization of dopamine D₁ and D₂ receptors, further hetero-dimerization has been reported of dopamine D₂ and D₃ receptors,^{44,45} but also adenosine A₁/dopamine D₁ receptors, adenosine A_{2A}/dopamine D₂ receptors, adenosine A_{2A}/dopamine D₃ receptors, and somatostatin SSTR₅/dopamine D₂ receptors.^{17,46,47}

Dopamine Receptor Subtypes

The rat dopamine D₂ receptor was cloned and isolated for the first time in 1988.⁴⁸ Due to the sixth exon within the coding region of dopamine D₂ receptors, two alternative spliced isoforms, a short variant named D_{2short} (D_{2S}, D₂₍₄₁₄₎ or D_{2B}) and a long isoform known as D_{2long} (D_{2L}, D₂₍₄₄₃₎ or D_{2A}) was revealed, which differ by 29 amino acids in the third cytoplasmic loop.^{48,49} As known so far the isoforms demonstrate minor differences in regional brain distribution, response of signaling pathways⁵⁰ and sequestration rate, but display the same pharmacological profile concerning binding affinities.⁵¹ The distribution of dopamine D₂ receptor mRNA has been localized by *in situ* hybridization with high density in the caudate putamen, substantia nigra, olfactory tubercle and low density in nucleus accumbens.

The dopamine D₃ receptor was identified by screening rat brain cDNA library using the D₂ receptor sequence by Sokoloff et al.³³ Alternative splice variants have been identified,⁵² but only mouse spliced isoforms display a pharmacological profile. The dopamine D₃ receptor is predominantly localized in the ventral striatum, specifically in the islands of Calleja and shell of nucleus accumbens, but exists in lower levels in substantia nigra pars compacta and caudate putamen.^{53,54} Figure 1.6 shows dopamine D₃ receptor mRNA expression in human horizontal cryosection from the right hemisphere of the brain at the level of the anterior commissure using *in situ* hybridization.⁵⁴ Highest densities of dopamine D₃

receptor mRNA were found in the islands of Calleja (left panel) and within the nucleus accumbens (right panel).

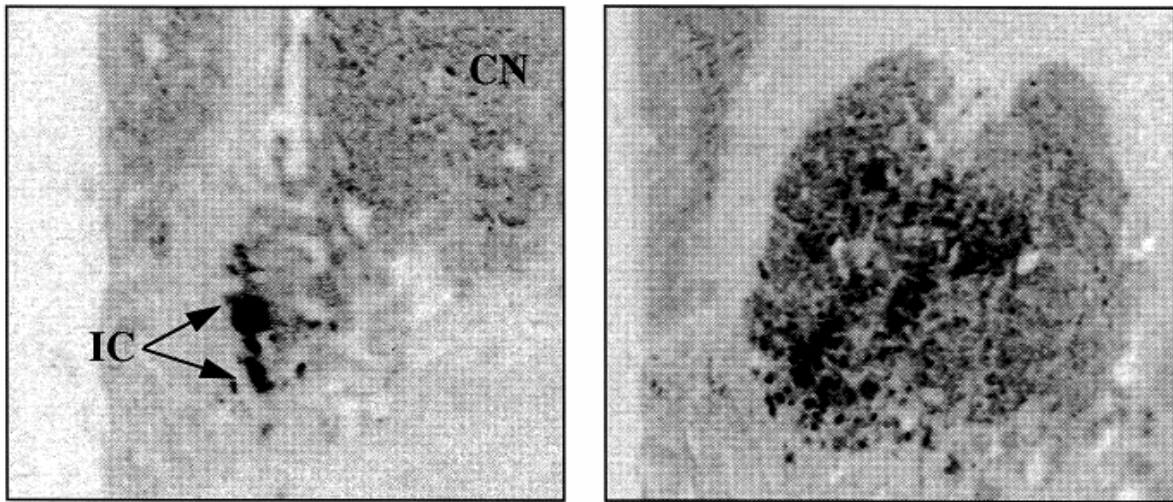


Figure 1.6 Dopamine D₃ receptor mRNA expression in the human brain using in situ hybridization. Left panel: islands of Calleja, IC; caudate nucleus, CN; right panel: nucleus accumbens (adapted from Suzuki et al., 1998).⁵⁴

In 1991, the dopamine D₄ receptor was first cloned by van Tol et al. by screening a library from the human neuroblastoma cell line SK-N-MC.³⁴ Investigation in the gene revealed the presence of polymorphic variations within the coding sequence. The major form in human with 60% is the D_{4.4} variation; the D_{4.7} is present in 14%, while D_{4.2} exists in 10% of the population.⁵⁵ The dopamine D₄ mRNA is localized in frontal cortex, amygdale, olfactory bulb, hippocampus, hypothalamus and mesencephalon.

The dopamine D₁ receptor was cloned by using screening of libraries and polymerase chain reaction based on the sequence of the dopamine D₂ receptor in 1990.⁵⁶ High levels of dopamine D₁ receptor mRNA have been discovered in the striatum, nucleus accumbens, and olfactory tubercle. In 1991, the dopamine D₅ receptor was isolated using the sequence of the D₁ receptor.³⁵ Pseudogenes of the dopamine D₅ receptor have been identified on chromosome 1 and 2, being 98% alike, and 95% identical to the human D₅ receptor. Dopamine D₅ mRNA is of abundant density in the thalamus, hippocampus, and mammillary nucleus. A summary of dopamine receptor subtypes is given in Table 1.2.

The endogen neurotransmitter dopamine discriminates between the five dopamine receptor subtypes. Dopamine has a higher affinity for the dopamine D₃ receptor than for the dopamine D₂ receptor that is explained by the sequence differences in the third intracellular loop.³³ The affinity binding for dopamine D₅ is 10 times higher than for the D₁ receptor (Table 1.2).⁵⁷

Table 1.2 Summary of properties of the dopamine receptor subtypes.

	D₁-like Receptor Family		D₂-like Receptor Family		
	D₁	D₅	D₂(short)/(long)	D₃	D₄
Alternative name	D1, D _{1A}	D5, D _{1B}	D2	D3	D4
Amino acids	446 (h, r)	477 (h) 475 (r)	414/443 (h) 415/445 (r)	400 (h) 446 (r)	387 (h, r)
Major transduction	G α_s , G α_{olf} , G α_q	G α_s , G α_{olf}	G α_{i2} , G α_{i3} , G α_o , G $\beta\gamma$	G α_o , G $\beta\gamma$	G α_{i2} , G α_{i3} , G α_o , G $\beta\gamma$
Response	AC5 \uparrow	AC5 \uparrow	AC5 \downarrow , AC2 \uparrow	AC5 \downarrow , (AC2 \uparrow)	AC5 \downarrow , AC2 \uparrow
Effector/ second messenger	cAMP \uparrow , PKA \uparrow , DARPP-32 \uparrow , PLC \uparrow , Ca ²⁺ \uparrow , PKC \uparrow	cAMP \uparrow , PKA \uparrow , DARPP-32 \uparrow , PLC \uparrow , Ca ²⁺ \uparrow , PKC \uparrow	cAMP \downarrow , PKA \downarrow , AA \uparrow ,	cAMP \downarrow , PKA \downarrow ,	cAMP \downarrow , PKA \downarrow , AA \uparrow ,
Dopamine low affinity state (K _i) [nM]	2,000 ⁵⁸	228 ⁵⁸	1,705 ³³	27 ³³	148 ⁵⁷
Major receptor distribution	caudate/ putamen, nucleus accumbens, olfactory tubercle, (hypo) thalamus, frontal cortex	hippocampus, thalamus, lateral mammillary nucleus, striatum, cerebral cortex	caudate/ putamen, olfactory tubercle, nucleus accumbens, cerebral cortex	Islands of Calleja, olfactory tubercle, nucleus accumbens, cerebral cortex	frontal cortex, midbrain, amygdalae, hippo- campus, hypo- thalamus, medulla, retina

The human and rat forms of the receptors are indicated by (h) and (r), respectively. \uparrow , stimulation; \downarrow , inhibition.

1.2.2 Signal Transduction of Dopamine D₂ and D₃ Receptors

The G protein-coupled dopamine D₂ and D₃ receptors belong to the dopamine D₂-like family. The dopamine D₂ receptors are coupled to a pertussis-toxin sensitive G α_i /G α_o , and being activated, they release G $\alpha_{i/o}$ and $\beta\gamma$ subunits. The G $\alpha_{i/o}$ subunit inhibits adenylyl cyclase 5, consequently reduces the concentration of cAMP and thereby the activation of protein kinase A. The G $\beta\gamma$ subunit activates adenylyl cyclase type 2 and regulates intracellular signaling by direct interaction with numerous types of ion channels and additionally, assists Ca²⁺ release from intracellular Ca²⁺ stores. Furthermore, it is able to activate MAP (mitogen-activated protein) kinase system via different pathways, involving phosphoinositide 3-kinase, Ras, and transactivation of a growth factor receptor.³⁶ Recently, additional and new insights into the signaling pathways of dopamine D₂ receptors and its regulation by intracellular binding partners have been discovered. Park et al. have

introduced prostate apoptosis response 4 (Par-4), a proapoptotic protein, which interacts through its leucine zipper motif at the calmodulin binding domain in the third cytoplasmic loop of the dopamine D₂ receptor.⁵⁹ This association induces the coupling of the dopamine D₂ receptor to G α_i and consequently the inhibition of cAMP activity. Increasing concentrations of intracellular Ca²⁺ activate calmodulin, which competes with Par-4 at the calmodulin binding domain. Displacement of Par-4 by calmodulin results in an uncoupling of the receptor from the G α_i and gives a negative feedback on D₂-mediated cAMP reduction. It has been observed, that mutant mouse with a deletion in the leucine zipper domain of Par-4 (Par-4 Δ LZ) display a depression-like syndrome, but further investigations have to be done to clearly interpret these results. A new role of β -arrestin in the signaling pathway of dopamine D₂ receptors, in addition to its role in receptor internalization, has been proclaimed recently.⁶⁰ Activation of the dopamine receptor induces the arrangement of a signaling complex containing the intracellular proteins β -arrestin 2, serine threonine kinase Akt, and protein phosphatase PP2A, that mediates the effects independently of G $\alpha_{i/o}$ -coupled mechanisms. Dopamine D₂ receptors regulate Akt by dopamine: prolonged dopamine stimulation inactivates Akt via dephosphorylation and activates its substrate glycogen synthase kinase 3 (GSK3), while a loss of stimulation activates Akt through phosphorylation and inhibits GSK3. The signaling pathways of dopamine D₂ receptors have been illustrated in Figure 1.7.

Although the dopamine D₃ receptor has been extensively characterized, the main second messenger signaling pathways still remain to be elusive. So far, the signaling pathways highly depend on the expression system of recombinant D₃ receptors. Stimulation as well as inhibition of adenylyl cyclase has been demonstrated, highly depending on host cells. Nevertheless, it has been reported, that inhibition of AC seems less efficiently than for D₂ receptors.²⁴ Inhibition of forskolin-stimulated adenylyl cyclase was found in CHO cells.⁶¹ The dopamine D₃ receptor modulates activity of potassium and calcium channels, protein kinase cascades and transcription factor c-fos expression in several expression systems. Additionally, an increased extracellular acidification and mitogenesis has been reported.⁶² Signaling mechanisms in brain remain to be determined. An additional function is the modulation of intracellular Ca²⁺ concentrations, inducing changes in the activity of Ca²⁺-regulated signaling proteins like protein phosphatase calcineurin (PP2B).⁶³

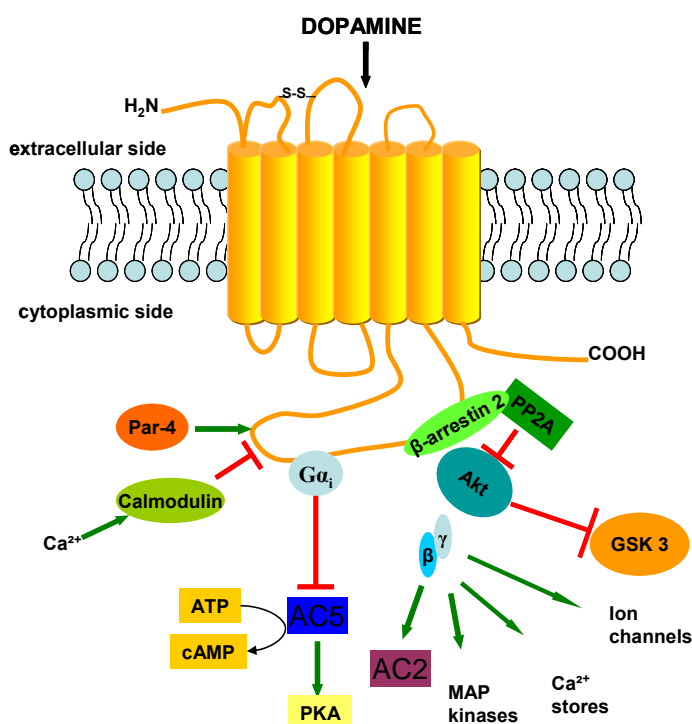


Figure 1.7 Signaling pathways of dopamine D₂ receptors (adapted from Kottke & Stark, 2005).⁶⁴

1.2.3 Distribution and Function of Dopamine D₂ and D₃ Receptors

Since the identification of the dopamine D₃ receptor in 1990 by Sokoloff et al.,³³ considerable effort has been undertaken in this prospective target for antipsychotic and antiparkinsonian drugs due to its restricted distribution in limbic regions of the brain.^{22,65} The dopamine D₃ receptor also plays a major role in drug addiction and strong evidence has been accumulated that it is implicated in the motivation to self-administer drugs and in influencing environmental stimuli on drug-seeking behavior.^{21,66} Dopamine D₃ receptors are present in a 10 - 100-fold lower density in brain regions as compared to that of dopamine D₂ receptors.⁶⁷ In rat brain, dopamine D₃ mRNA and receptors are expressed in a restricted distribution pattern with highest abundance in granule cells of islands of Calleja and moderate levels in medium-sized spiny neurons of the rostral and ventromedial shell of nucleus accumbens.⁶⁵ The neurons co-express the dopamine D₁ receptor, substance P, dynorphin and/or neurotensin and induce in an interactive influence on diverse effector systems.^{68,69} These limbic regions of the striatum are implicated in the dopaminergic mesolimbic pathway and control emotion, motivation, reward and behavior, and are consequently involved in schizophrenia and drug addiction.⁶⁵ Dopamine D₃ receptors are also localized in the cerebral cortex, ventral tegmental area, amygdalae, ventral pallidum and mediodorsal thalamus in rodents. In human brain, the distribution is alike with highest

levels in islands of Calleja and nucleus accumbens, but an extended distribution in the caudate putamen and the cerebral cortex.^{65,70} The existence of the dopamine D₃ autoreceptor and consequently its influence on dopamine release and synthesis is still questioned, but recent studies using a selective dopamine D₃ antibody have supported its presynaptic localization on dopaminergic neurons of the ventral tegmental area and substantia nigra.^{69,71-73} It has been reported that dopamine D₃ receptor mRNA and D₂ receptor mRNA are co-expressed in dopaminergic neurons and projection areas, assuming a functional interaction between both subreceptors.^{22,45}

The dopamine D₂ receptor is predominantly expressed in brain regions, such as the caudate nucleus, putamen and olfactory tubercle, lower levels are found in the nucleus accumbens, where the receptor is expressed by GABAergic neurons co-expressing enkephalins.^{24,70} In these areas, the receptor is mainly expressed postsynaptically (D_{2L}).⁷⁰ Additionally, it is distributed in the substantia nigra pars compacta and in the ventral tegmental area and is mostly presynaptic generated (D_{2S}), capable of regulating dopamine synthesis and release.⁷⁰ Dopamine D₂ receptors are involved in functions related to the nigrostriatal dopaminergic system. Its cell degeneration results in an imbalance of the two output pathways, namely the direct projection neurons, regulate via dopamine D₁ receptors, and indirect projection neurons, controlled by dopamine D₂ receptors, both generated in the striatum. Consequently, disproportion causes movement disorders associated with Parkinson's disease.^{24,70}

1.2.4 Therapeutic Relevance of Selective Dopamine D₃ Receptor Ligands

Alterations in the dopaminergic pathways are involved in a variety of neurological and psychiatric disorders, like Parkinson's disease, schizophrenia and drug abuse. Degeneration of dopaminergic neurons in the substantia nigra causes striatal dopamine depletion in Parkinson's disease. Imbalance of the mesolimbic dopaminergic pathway is involved in schizophrenia and addictive types of behavior. Further diseases associated with dysfunction of the dopaminergic system are restless legs syndrome, depression, Huntington's disease, epilepsy, attention deficit hyperactivity disorder, and ischaemia. The extended improvement in immunocytochemical methods, like polyclonal antibodies, *in situ* hybridization, recombinant receptors and knock-out animals, and the availability of highly affine and selective receptors allow the scientist to enlighten the role of each dopamine receptor subtype and its function in various pathological processes.

Parkinson's Disease

Parkinson's disease (PD), firstly described by James Parkinson in 1817,⁷⁴ is a progressive neurodegenerative movement disorder, characterized by rigidity, tremor, bradykinesia or akinesia, additionally allied with concomitant syndromes, such as anxiety and depression, and affects about 1% of the general population. The loss of dopaminergic cells in the substantia nigra pars compacta results in a deficiency of dopamine in the striatum, causing the major motor symptoms of the disease. Further progression of cell death involves areas of the origin of the mesolimbic dopamine system and is associated with deficits in cognitive functions and goal-directed behavior. The neuropathology of PD is well characterized, but etiology still remains unknown. Environmental and endogenous neurotoxicants, such as neurotoxicity of levodopa⁷⁵ or dopamine-induced autotoxicity,²⁷ finally leading to oxidative stress, as well as mitochondrial dysfunction, infection⁷⁶, or genes, such as α -synuclein and parkin, are considered to be implicated.

The symptomatic treatment of Parkinson's disease involves the stimulation of remaining dopamine receptors in order to balance dopamine transmission. Levodopa and dopamine agonists are highly effective for the treatment of the motor symptoms.⁷⁷ Since dopamine does not cross the blood-brain barrier, the precursor levodopa in combination with the peripheral decarboxylase inhibitors carbidopa (Nacom[®]) or benserazide (Madopar[®]) is administered. Levodopa penetrates into the central nervous system and is subsequently converted to dopamine by enzymatic decarboxylation. Levodopa treatment results in instant motor benefits, but long-term levodopa therapy consequences a significant loss of efficacy, motor fluctuations (on-off, wearing off, freezing) and dyskinesia (hyperkinetic movements) after 3 – 5 years.⁷⁸ In recent times, administration of dopamine receptor agonists, used in early monotherapy or adjunctive therapy with levodopa, has become common.⁷⁹ Dopamine agonists can be categorized in ergot and non-ergot derivatives. Ergot dopamine agonists comprise bromocriptine (Pravidel[®]), α -dihydroergocriptine (Almirid[®]), cabergoline (Cabaseril[®]), lisuride (Dopergin[®]), and pergolide (Parkotil[®]), and non-ergot dopamine agonists include ropinirole (Requip[®]), pramipexole (Sifrol[®]), rotigotine (Neupro[®]), and apomorphine (Apomorphine-Woelm[®]) (cf. 1.2.6). All dopamine receptor agonists have proved to be effective in clinical practice but display considerable differences in their binding profiles at dopaminergic receptor subtypes and other neurotransmitter receptors as well as in their pharmacokinetic properties.⁸⁰ Cardiac side effects, in particular fibrotic valvular heart disease, have been associated with ergot derivatives but further studies are still under investigation; consequently they are used

more cautiously.⁸¹ The recently launched drug rotigotine is the first transdermally delivered dopamine receptor agonist for the treatment of early PD and allows a continuous administration and dopaminergic stimulation.⁸² Ropinirole and pramipexole have demonstrated clinical benefits over levodopa, reduce motor deficits, minimize the risk of dyskinesia and additionally, they possess neuroprotective effects. Although stimulation of the dopamine D₂ receptor has been mainly considered for antiparkinsonian effects, the majority of the dopamine agonists used in the treatment of PD have high or higher affinity at the dopamine D₃ receptor than at the dopamine D₂ receptor. Consequently, it is assumed that the D₃ receptor, which is located in high abundance located in the limbic striatum, plays an important role in PD and might contribute to movement dysregulation.^{78,83}

Studies with a primate model of PD have revealed that levodopa-induced dyskinesia (LID) was associated with over expression of dopamine D₃ receptors. Administration of dopamine D₃ receptor partial agonists has relieved LID, without influencing the therapeutic success of levodopa, while dopamine D₃ receptor antagonists increased PD-like symptoms.⁵¹ It has been suggested that an additional diagnosis of dementia or non-responder to parkinsonian medication was correlated with a lower number of dopamine D₃ receptor.²² The D₃ receptor-preferring non-ergot dopamine agonist pramipexole has shown effectively to reduce the risk of motor complications.⁸⁴ Furthermore, pramipexole has been shown to be neuroprotective against 1-methyl-4-phenyl-1,2,3,6-tetrahydropyridine (MPTP) toxicity in non-human primates.⁸⁵ The MPTP administration produces parkinsonian-like symptoms and can also used as a model to study neuroprotection. MPTP is metabolized by monoamine oxidase B to the active metabolite *N*-methyl-4-phenylpyridinium (MPP⁺) and causes loss of dopaminergic neurons of the substantia nigra. Some evidence has been accumulated that the neuroprotective effect of pramipexole is due to its biological effect on dopaminergic neuron-associated genes, including dopamine transporter, vesicular monoamine transporter 2, and transcription factor Nurr1, but further studies need to confirm the assumption.⁸⁶ A positive influence on depression symptoms relieved by pramipexole has also be reported.⁸⁷ It has been shown that activation of dopamine D₁ receptors results in a relief of Parkinson symptoms and additionally, stimulation of dopamine D₁ and D₂ produces synergistic effects, but clear evidence is still lacking. Functional interaction of the dopamine D₁/D₃ receptors has been assumed due to its co-expression and similarities in reply to rodent Parkinson model.⁶⁸

Restless Legs Syndrome

The restless legs syndrome (RLS), firstly described by Karl-Axel Ekbom in 1945,⁸⁸ is a neurological sensorimotor disorder characterized by abnormal leg sensations (paresthesias) that occur mainly at rest and during the evening and night, leading to severe insomnia and daytime tiredness.⁸⁹ The paresthesias induce an irresistible urge to move the limbs following a temporal relieve of the symptoms. In the majority of RLS patients periodic limb movements (PLMs), a disorder with repetitive movements of the lower limbs during sleep, have been observed. RLS affects 3% to 15% of the general population, women twice as often as men, but many patients go undiagnosed because the syndrome has only recently recognized, its pathophysiology is rarely understood and standardizes diagnostic criteria were first developed in 1995 and recently updated guidelines on management of RLS were published.⁹⁰ The pathophysiology of primary (idiopathic) RLS includes changes in central dopaminergic transmitter systems, which may result in alteration of the spinal cord function, and abnormal brain iron metabolism. The hypothesis of the hypofunction in brain dopamine signaling is supported by the first-line treatment of RLS with dopamine D₂-like receptor agonist, predominantly the non-ergot derived, D₃ receptor-preferring compounds such as pramipexole (Sifrol[®]),⁹¹ ropinirole (Requip[®]),⁹² rotigotine (Neupro[®]),⁹³ which alleviate sensory and motor symptoms in 70 - 100% of patients (cf. 1.2.6).⁸⁹ A decreased dopamine D₂ receptor binding and hypofunction of the dopaminergic nigrostriatal system has been obtained in PET and SPECT investigations in RLS patients.⁸⁹ Studies on experimental lesions of hypothalamic A11 nucleus and in D₃ receptor knockout mice by Clemens et al. led to the hypothesis of a dysfunction of a supraspinal located dopaminergic region in the dorsal-posterior hypothalamus and subsequent alterations in spinal network, finally contributing to RLS.⁹⁴ Future experimental investigations need to confirm the hypothesis, but these results and the effective treatment of RLS with dopamine D₃ receptor-preferring agonists reflect the potential relevance of dopamine D₃ receptors in mechanisms of primary RLS pathophysiology.

Schizophrenia

Schizophrenia is a devastating mental disorder and affects about 1% of the world's population. The incidence is similar throughout diverse economical limits or cultures. The clinical symptoms of schizophrenia comprise several clinical features and are generally occurring at ages of 15 – 45. The psychiatric disorder is characterized by the appearance of positive symptoms, such as hallucinations, delusions, disorganization of thought, bizarre

behavior, and negative symptoms, including diminished affect, loss of motivation and the inability to experience pleasure. In some cases, cognitive impairments are also noticed, for example deficits in verbal fluency and memory recall. The etiology still remains elusive, although several environmental risk factors have been recognized, including maternal malnutrition, prenatal and perinatal birth complications. But also viral infections and genetic factors might be implicated.^{95,96} For over forty years the neurochemical pathophysiology has based on the “hyperdopaminergic hypothesis” of schizophrenia, which is revisited and not singly valid anymore.^{97,98} This theory is explained by the observation that direct or indirect dopamine agonists induce paranoia, while antagonists at the dopamine D₂ receptor relief psychosis.⁹⁹ An augment of dopamine release increases the positive psychotic symptoms, but do not influence the negative symptoms. Brain imaging studies have demonstrated that the imbalance of the dopaminergic system results from a hyperstimulation of striatal dopamine D₂ receptors, which is related to positive symptoms, and hypostimulation of cortical dopamine D₁ receptors, causing negative symptoms.¹⁰⁰ It is assumed that the origin of the synaptic dysconnectivity is a consequence of changes in *N*-methyl-D-aspartate (NMDA) and glutamatergic action, finally leading to NMDA hypoactivity in the prefrontal cortex.¹⁰¹ The “glutamate hypofunction hypothesis” of schizophrenia is based on studies of the noncompetitive NMDA receptor antagonist phencyclidine which has shown to induce positive, negative and cognitive symptoms of schizophrenia in healthy patients and exacerbate these symptoms in schizophrenics.¹⁰² Conclusively, drugs with enhanced activity at prefrontal dopamine D₁ transmission and NMDA transmission are assumed to contribute to schizophrenia.¹⁰³ The limbic areas of the striatum play a key role in schizophrenia. This region is associated by high abundance of the dopamine D₃ receptor. Post-mortem studies demonstrated an enhanced expression of dopamine D₃ receptors in the ventral striatum of untreated schizophrenia patients, but a reduction in antipsychotic-treated patients.¹⁰⁴ It has been supposed that antipsychotic drugs normalize the dopamine D₃ expression and stable the ventral striatal activity. Consequently, dopamine D₃ receptor antagonists are assumed to have antipsychotic effects.¹⁰⁵ It has also been shown that dopamine D₃ receptor antagonists improve cognitive functions in models of rodents due to enhancing frontocortical cholinergic transmission.¹⁰⁶ In summary, selective antagonism of dopamine D₃ receptors, which are mostly located in the limbic regions, may reduce negative and cognitive symptoms of schizophrenia and prevent undesirable extrapyramidal side-effects (EPS).

Antipsychotic drugs of the first generation (cf. 1.2.6) demonstrate some preference for dopamine D₂ receptors, but although exhibit affinity for dopamine D₃ receptors. Their interaction with dopamine D₂ receptors in limbic brain regions releases positive symptoms, while antagonism in the dorsal striatum causes EPS.⁷⁸ Second generation, so-called atypical antipsychotics (cf. 1.2.6), have a low incidence of EPS, display moderate dopamine D₂ and D₃ receptor antagonism and have additional effects on other neurotransmitter systems including histamine H₁ receptors, serotonin 5-HT_{1a}, 5-HT_{2a}, 5-HT_{2c} receptors, adrenergic α_1/α_2 receptors and muscarinic acetylcholine M₁ receptors (multireceptor targeting), which has been assumed to advance the therapeutic profile.¹⁰⁷ Atypical antipsychotics have demonstrated to improve in particular negative symptoms, cognitive impairment and have shown a lower prevalence of tardive dyskinesia.¹⁰⁸ Additionally, this class of drugs has also provided neuroprotective effects in animal model.¹⁰⁹ Since the atypical antipsychotic clozapine (Clozaril[®]) has demonstrated a higher affinity for the dopamine D₄ receptor than for the dopamine D₂ receptor and additionally interacts with various neurotransmitter receptors, this former observation suggested that the dopamine D₄ antagonism might contribute to its unique clinical profile (cf. 1.2.6).³⁴ Supported by additional post-mortem neuropathological and pharmacological studies selective and high affine dopamine D₄ receptor antagonists were developed for the treatment of schizophrenia.¹¹⁰ However, clinical trials of dopamine D₄-selective ligands, among them sonepiprazole, have demonstrated to be ineffective against psychotic symptoms.¹¹¹ Likely, the promiscuous binding behavior of atypical antipsychotic contributes to the clinical efficacy.

Depression

Major depression is a severe disorder with a prevalence of 10-15% and genetic, developmental, and environmental factors are involved in its etiology. The cardinal symptoms include depressed mood (sadness) and the inability to experience pleasure (melancholy or anhedonia), but depression is also characterized by various other features such as insomnia, hypersomnia, pain or lethargy. Depression often co-occurs with comorbid disorders, for example Parkinson's disease.¹¹² For decades, the neuropathology of depression is based on the serotonergic and noradrenergic hypothesis, but latest investigations implicate an important role of the dopaminergic system and a deficit in dopaminergic transmission might contribute to depression.¹¹² Recently, dopamine D₃ receptor agonists have demonstrated antidepressant effects and mood enhancement in

depressive patients but also in depressed Parkinson's patients. Ropinirole has been used effectively in combination with antidepressants in treatment-resistant depression.¹¹³ Antidepressant properties of rotigotine (Neupro[®]) have been reported in experimental rat models of depression at low doses (cf. 1.2.6).¹¹⁴ Pramipexole (Sifrol[®]) has been effective in the treatment of depression in Parkinson's disease and bipolar depression (cf. 1.2.6).^{115,116} These results reveal the beneficial effect of agonists at dopamine D₃ receptors for the treatment of depression, but additional studies are of absolute necessity.

Drug Addiction

Drug abuse and addiction are long-lasting conditions and are associated with drug-induced neuroadaptations in the brain. Drugs of abuse, such as opiates, nicotine, cannabis, cocaine, produce reward and are involved in reinforcement and drug dependence. This chronic relapsing disease is not only of scientific interest, but also socially important due to its enormous and rising economic cost.¹¹⁷ The mesocorticolimbic system, projecting from the ventral tegmental area to the nucleus accumbens and frontal cortex, is implicated in reward and reinforcement effects of abused drugs (alcohol, heroin, cocaine, tetrahydrocannabinol and nicotine) and it is well evidenced that drugs of abuse increase dopamine levels in the shell of nucleus accumbens.^{21,118} Cocaine and amphetamine inhibit the uptake of dopamine by the dopamine transporter (DAT), leading to an increased synaptically dopamine concentration, a mechanism which is responsible for their rewarding and reinforcing properties.^{117,119} Post-mortem studies of human brains from cocaine addicts have demonstrated that dopamine D₃ mRNA and binding are increased in the nucleus accumbens, but there is no alteration in dopamine D₁ and D₂ receptor expression.¹²⁰ The dopamine D₃ receptor is highly expressed and co-localized with dopamine D₁ receptors, dynorphin and substance P in brain regions involved in drug dependence. Current investigations using highly selective dopamine D₃ receptor ligands, either partial agonists or antagonists, and dopamine D₃-deficient mice have revealed that dopamine D₃ receptors participate in the motivation to self-administer drugs and in the control of environmental stimuli on drug-seeking behavior. Consequently, the therapeutic concept in the treatment of drug addiction and prevention of relapse includes the inhibition of dopamine D₃ receptors using partial agonists or antagonists. The expression of dopamine D₃ receptors is regulated by brain-derived neurotrophic factor (BDNF).¹⁰⁴ Administration of drugs of abuse results in a transient increase in BDNF expression, inducing an increase in D₃ receptors.¹⁰⁴ So both dopamine D₃ receptors and BDNF are involved in drug conditioning.

1.2.5 Ligand Binding Mode at Dopamine D₂ and D₃ Receptors

The three dimensional (3D) crystal structure of the G protein-coupled receptor bovine rhodopsin has been identified in 2000.² Since that time the high-resolution structure has been used as a template to generate homology models in order to design novel ligands for GPCRs, including the human dopamine D₃ receptor.^{9,121} The computer-assisted method to receive a 3D model of dopamine D₃ elucidates the function of highly conserved GPCR residues, ligand binding mode and enables structure-based drug design. However, it is worth mentioning that the rhodopsin template corresponds to the inactive conformation of the receptor with an inverse agonist as an endogenous ligand, consequently models have to be interpreted with caution.

The predicted binding site of dopamine D₂ receptors for dopamine and other agonists involves TM domains 3, 4, 5, and 6. Aspartate residue Asp-114 in TM3 forms a tight salt bridge with the basic amino group of the ligand. The Asp is highly conserved among human biogenic amine receptors.¹²² Two serine residues Ser-193 and Ser-197 in TM5 contribute to hydrogen bond via binding hydroxyl groups of the catechol moiety and are essential for activation of the receptor.¹²³ Agonists interact with both conserved serine residues. Ser-194 serves as an option to Ser-193 for hydrogen-bonding. Agonists hold tight binding of TM3 and TM6. Additional residues such as His-394 (TM6), Trp-386 (TM6) and Phe-390 (TM6) form hydrophobic interactions with aromatic moieties. Antagonist binding mode mainly includes TM helices 2, 3, 4, 6, and 7. Prominently, Asp-114 (TM3) binds via salt bridge to the cationic moiety, Ser-193 (TM5) or Ser-197 (TM5) gives one hydrogen bond, and Trp-386 (TM6) is important for a hydrophobic pocket. His-393 (TM6) stabilizes the inactive form of the receptor. Especially TM3 and TM6 involve tight antagonist binding.

The predicted binding mode for dopamine D₃ focuses on Ser-192 (TM5) as a hydrogen-bond donor and Asp-110 (TM3) that forms an interaction with a positively charged group of the ligand.¹²⁴ Phenylalanine Phe-345 and Phe-346 have demonstrated to be implicated in aromatic and hydrophobic interactions, respectively.¹²¹ For the dopamine D₃ receptor, more evidence to confirm the prediction, for example site-directed mutagenesis, is requested.

Basically, agonists for dopamine D₂ and D₃ receptors comprise the structural feature of a basic amine group in a defined distance to an aromatic moiety with the characteristic of a hydrogen-bond acceptor. Intensive investigation has been done on the pharmacophore

model of dopamine D₂ and D₃ receptors for antagonists or partial agonists.^{9,125,126} Fundamental structural features for ligands with antagonist properties require an aryl moiety, a hydrogen acceptor pharmacophore at the position of the oxygen amide, a hydrophobic or aromatic pharmacophore in the spacer region and a cationic and an aromatic pharmacophore in the basic amine aryl residue. The aryl residue can be represented by extended bi- and tricyclic aryl rings, additionally substituted with heteroatoms, or by a conjugated olefinic phenyl ring system.¹²⁷ A general structural scheme exemplified by the structure of BP 897 is shown in Figure 1.8. Dopamine D₃ receptor ligands prefer an extended and more linear conformation, while dopamine D₂ receptor ligands adopt a more bent conformation. Consequently the distance between hydrogen acceptor and positively charged nitrogen for dopamine D₃ spans about 6.5 Å and for dopamine D₂ stretches 5.5 Å.¹²⁶

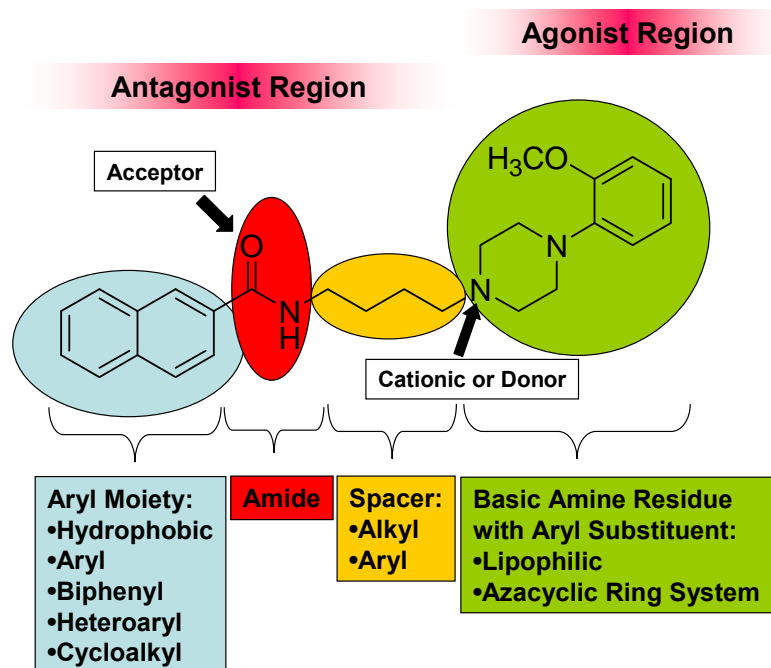


Figure 1.8 General structural scheme of dopamine D₂ and D₃ receptor ligands with antagonist or partial agonist properties.

1.2.6 Ligands for Dopamine D₂ and D₃ Receptors

Classical pharmacological receptor studies, the introduction of molecular cloning techniques and development of radioligand competition binding studies using recombinant dopamine receptor subtypes allow determining affinity binding of novel ligands.

Dopamine D₂-like Receptor Ligands

The development of dopamine D₂-like receptor agonists was based on the rigidification of the neurotransmitter dopamine and itemization of the dopamine agonist apomorphine (Apomorphin-Woelm[®]). This effort resulted in the 2-aminotetralin derivative 7-hydroxy-*N,N*-dipropyl-2-aminotetralin (7-OH-DPAT) and its related modification PD128907 (Chart 1.1).^{67,128} Both compounds have demonstrated high affinity and moderate dopamine D₃ receptor-preference. Due to metabolic instability the ligands are only used as pharmacological tools. The antiparkinsonian drug ropinirole (Requip[®]), which is also used for the treatment of restless legs syndrome, has demonstrated low affinity for dopamine D₁-like and D₄ receptors, but has bound with slightly higher affinity for dopamine D₂ than for D₃ receptors.¹²⁹ The pyrimidine derivative piribedil (Trivastal[®], France) is a dopamine D₂/D₃ agonist with additional α_2 -noradrenergic properties. It is used for the treatment of Parkinson's disease and it has additional pro-cognitive effects.¹³⁰ Compounds are shown in Chart 1.1.

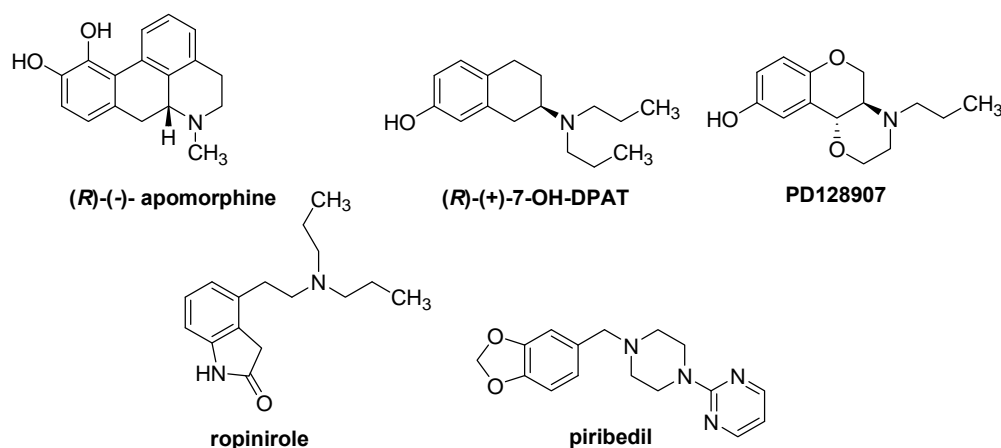


Chart 1.1 Dopamine D₂-like receptor agonists.

The butyrophenone derivative and antagonist haloperidol (Haldol[®]) demonstrates 10 to 20-fold higher affinity for dopamine D₂ versus D₃ receptors.¹³¹ Since 1958, haloperidol has been an important representative of “classical” antipsychotic drugs and its pharmacological effects, but also extrapyramidal side effects are mediated by interacting with other central nervous system neurotransmitter receptors. Its neuroleptic activity depends on the tertiary amino group linked to the butyrophenone structure. Variation in the piperazine ring to give a spiro analogue of haloperidol resulted in spiperone (spiroperidol), just as haloperidol slightly preferring dopamine D₂ over D₃ receptors.¹³² The 2-methoxybenzamide derivatives sulpiride (Dolmatil[®]) and raclopride comprise an aminomethylpyrrolidine residue and are

antipsychotics with high affinities for both dopamine D₂ and D₃ receptors.¹³² The dibenzazepine derivative and atypical antipsychotic clozapine (Clozaril[®]) has a unique pharmacological behavior due to its low affinities for dopamine D₁, D₂, and D₃, but moderate affinity for dopamine D₄ receptors. It is assumed that its therapeutic effect results from interaction with several of neurotransmitter receptors, such as histaminergic, serotonergic, muscarinic receptor. Typical (haloperidol, spiperone, raclopride) and atypical antipsychotics (sulpiride, clozapine) are shown in Chart 1.2.

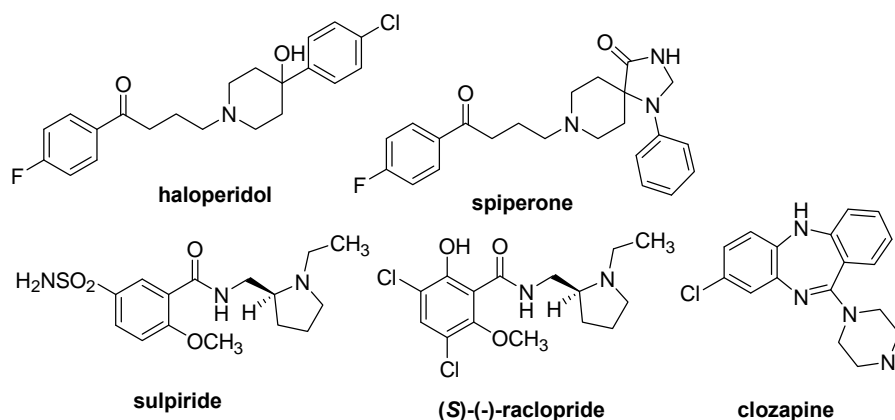


Chart 1.2 Dopamine D₂-like receptor antagonists.

Selective Dopamine D₃ Receptor Ligands

Pramipexole (Sifrol[®], Mirapex[®]) is an analogue of (*R*)-(+)-7-OH-DPAT revealed by bioisosteric replacement of the phenol residue with a metabolically more stable 2-aminothiazole moiety.^{133,134} Pramipexole is a full dopamine receptor agonist and binds at presynaptic and postsynaptic dopamine D₂-like receptors with highest affinity for dopamine D₃ receptors and has shown only low affinities at adrenoceptors and serotonin receptors.¹³⁵ It has been effective in the treatment of Parkinson's disease. Recently, it has been introduced for the treatment of restless legs syndrome (Chart 1.3).⁹¹ The aminotetralin derivative rotigotine (Neupro[®]) is a dopamine receptor agonist used in a transdermal delivery system and for the treatment of Parkinson's disease (Chart 1.3).^{82,136} Rotigotine demonstrated agonist activity with 20-fold preference for the dopamine D₃ over the D₂ and about 100-fold over the D₁ receptor. FAUC 88 has been introduced as a novel class of nonaromatic dopamine D₃ receptor agonist (Chart 1.3).¹³⁷ The conjugated enyne residue represents a bioisosteric replacement of the catechol structure.

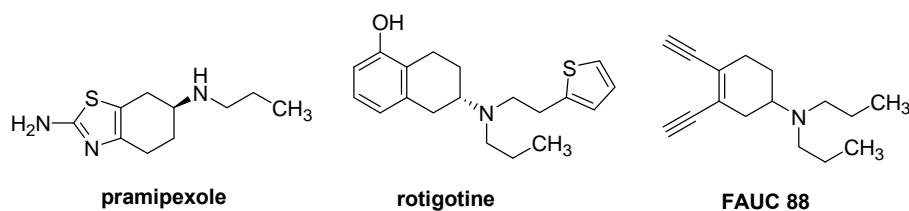


Chart 1.3 Dopamine D₃ receptor agonists.

A set of dopamine D₃ receptor selective antagonists and partial agonists is shown in Chart 1.4. Among the first dopamine D₃ receptor antagonists with significant selectivity for D₃ versus D₂ was U99194A.¹³⁸ Development of analogues of the dopamine D₂-like receptor antagonist sulpiride (see Chart 1.2) resulted in the benzamide derivative nafadotride. Its levoisomer has subnanomolar affinity and a 20-fold preference for dopamine D₃ receptors.¹³⁸ The 1,2,3,4-tetrahydroisoquinoline antagonist SB 277011 has nanomolar affinity and 100-fold selectivity for dopamine D₃.¹³⁹ It has been used as a pharmacological agent in animal models of drug abuse and reduces cocaine-, nicotine-, ethanol-, and heroin-seeking behaviors.^{21,127} BP 897 was identified as a selective dopamine D₃ receptor partial agonist with high affinity binding at human dopamine D₃ receptors and a 70-fold selectivity over human D₂, which behaves as an antagonist at this subtype.^{66,140}

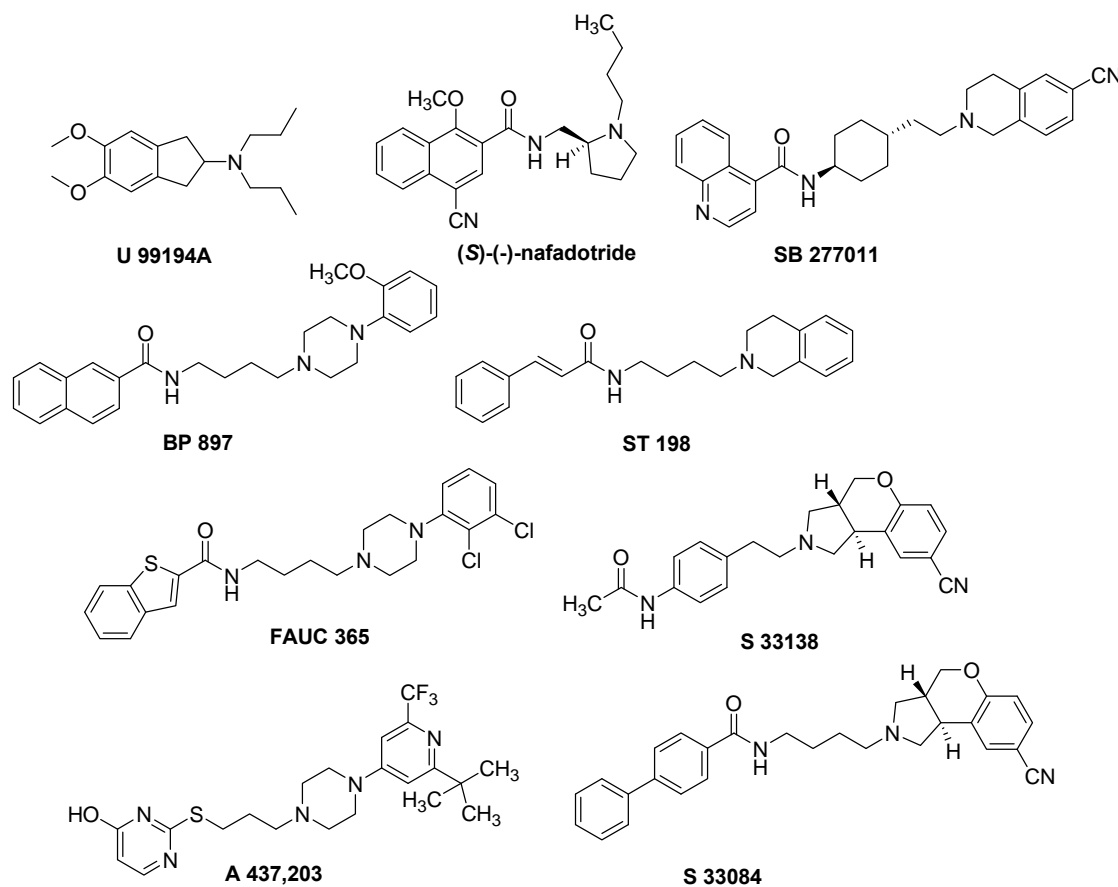


Chart 1.4 Dopamine D₃ receptor antagonists and partial agonists.

Further evaluation of *in vitro* models showed, that BP 897 has demonstrated antagonist dopamine D₃ receptor profile in addition to its partial agonist properties.^{141,142} BP 897 has attenuated the behavioral and reinforcing effects of cocaine, showing a promising property for the treatment of drug abuse. Considering further interactions of BP 897 with multiple classes of monoaminergic receptors, the only pivotal role of dopamine D₃ receptors in the mechanism of reduced cocaine-seeking behavior is not confirmed yet.^{21,143} To date BP 897 is ongoing phase II of clinical studies as a therapeutic target for the treatment of cocaine abuse and related central nervous disorders.¹⁴⁴ Another related development in this lead structure is FAUC 365, an antagonist bearing a heteroatome substituted bicyclic ring system and a (2,3-dichlorophenyl)piperazine substructure. The compound demonstrated high affinity for hD₃, while the affinity for hD₂ was depending on different assay conditions, but provided an impressive high selectivity for hD₃ over hD₂¹²⁵ although this could not be confirmed by other groups.¹⁴⁵ Further development is represented by the 1,2,3,4-tetrahydroisoquinoline compound ST 198. It has been reported that the antagonist normalizes dopamine D₃ receptor function and subsequently attenuates levodopa-induced dyskinesia.⁸³ The benzopyranopyrrole derivative S 33084 behaves also as an antagonist and has displayed high dopamine D₃ binding affinity and >100-fold selectivity ratio for dopamine D₃ receptors.¹⁴⁶ S 33138 and A 437,203 are promising agents and are in Phase II trials for the treatment of schizophrenia. Both compounds behave as selective dopamine D₃ over D₂ receptor antagonists. The pyrimidylpiperazine derivative A 437,203 has an influence on brain dopamine activity and has demonstrated antipsychotic properties in the absence of EPS. *In vitro* data have confirmed the former as a highly potent D₃ receptor ligand acting as antagonist.^{147,148}

1.3 Histamine

The monoamine histamine (2-(1*H*-imidazol-4-yl)ethanamine), a neurotransmitter and neuromodulator in the mammalian brain, acts via biogenic amine binding GPCRs and as seen for dopamine receptors, histamine receptors also comprise the highly conserved aspartate acid in TM3. The central histaminergic system is involved in the regulation of various neurotransmitters, particularly in the activity of dopamine (see 1.2) transmission, and therefore has a high influence on neurotransmission in the central nervous system.¹⁴⁹ Histaminergic cell bodies in brain are sited in the tuberomammillary nucleus of the posterior hypothalamus. Their neurons project to all brain areas with a strong innervation of the limbic system. Consequently, the brain histamine system is involved in various CNS functions, such as sleep/wakefulness, feeding behavior, circadian rhythm, cardiovascular

control, catecholamine release and the neuroendocrine regulation.¹⁴⁹ Neuronal histamine additionally regulates the release of acetylcholine in brain and is therefore implicated in cognitive functions, learning and memory processes.¹⁵⁰ The role of the central histaminergic system on schizophrenia is highly discussed.¹⁵¹

Histamine is synthesized from the amino acid L-histidine by the enzyme L-histidine decarboxylase with pyridoxal phosphate as a cofactor (Figure 1.9). Histamine is rapidly metabolized in brain by the intracellular enzyme *N*-methyltransferase to give *N*-methylhistamine and subsequently oxidized by monoamine oxidase and aldehyde oxidase to result in *N*-methylimidazole acetic acid. In the periphery, histamine is mainly oxidized by diamine oxidase (histaminase) to form imidazole acetic acid.

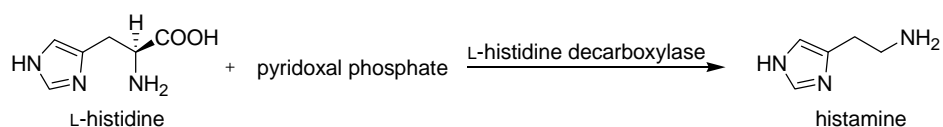


Figure 1.9 Biosynthesis of histamine.

Furthermore, histamine is located in the periphery; high density is concentrated in tissue mast cells and enterochromaffin-like cells in the gastrointestinal tract. Lower amount of histamine is found in basophil leukocytes and platelets. Histamine has shown to play a pivotal role in a variety of physiological processes including allergic responses and regulation of gastric-acid release and accordingly it is implicated in pathophysiological conditions counting allergic reactions, immunological disorders, and gastric-acid-related diseases.

Histamine Receptors

Histamine mediates its function through histamine receptors, which belong to the family of the aminergic G protein-coupled receptors. Until present, the existence of four histamine receptor subtypes, histamine H₁, H₂, H₃, and H₄ receptors, has been identified and they translate extracellular signals via the G proteins, G_q, G_s, G_{i/o}, and G_{i/o}, respectively.¹⁵² Although all four histamine receptor subtypes have been recognized in the periphery, only histamine H₁, H₂ and H₃ have been identified in the mammalian central nervous system. Stimulation of histamine H₁ receptors is involved in inflammatory effects, associated with smooth muscle contraction and edema linked to allergic responses.¹⁴⁹ The cloning of histamine H₁ receptor was reported in 1991.¹³⁸ Stimulating effects on gastric-acid secretion via histamine H₂ receptors has been known for a long time and provided an important

target for acid-related diseases such as peptic ulcer and gastro-esophageal reflux disease. The cloning of the cDNA for canine histamine H₂ receptors was reported in 1991.^{153,154} The histamine H₃ receptor was identified by Arrang in 1983¹⁵⁵, cloned by Lovenberg in 1999¹⁵⁶ and it is a presynaptic autoreceptor, inhibiting the synthesis and release of the endogenous ligand in histaminergic neurons in the CNS. It further functions as a heteroreceptor and regulates the release of other neurotransmitters such as dopamine, serotonin, glutamate, GABA, acetylcholine, noradrenaline in the CNS and periphery.¹⁴⁹ The use of its antagonists in the treatment of obesity, neurological disorders such as Alzheimer's disease, epilepsy, schizophrenia, sleep disturbance, and attention deficit hyperactivity disorder, is currently under investigation. Research in histamine H₃ receptor variants resulted in the finding of histamine H₄ receptors and its subsequent cloning in 2000.¹⁵⁷ Histamine H₄ receptors are mainly expressed in cells of the immune system and mast cells; they are also located on lymphocyte T cells, dendritic cells and basophils, which implicate its influence on immune response and inflammatory disease. Histamine H₃ receptors are closely related to histamine H₄ receptors (37 - 43% overall H₄ homology to H₃), but displayed differences to cloned histamine H₁ and H₂ receptors (19 - 22 and 18 - 20% homology, respectively).¹⁵⁸ The four histamine receptor subtypes have demonstrated agonist-independent activity, referred as constitutive activity *in vitro* at physiological concentrations; consequently antagonists have to be reclassified as inverse agonists.¹⁵⁸

1.3.1 Histamine H₁ Receptors

The G protein-coupled human histamine H₁ receptor consists of 487 amino acids and shows the putative seven transmembrane domains. The proposed structure possesses a large third intracellular loop and a short intracellular C terminal tail. The bovine adrenal medulla histamine H₁ receptor was cloned by expression cloning in the *Xenopus* oocyte system in 1991,¹⁵⁴ followed by the cloning of histamine H₁ receptor from various species including rat, guinea pig, mouse, and human (chromosome 3).¹⁵⁹⁻¹⁶²

1.3.2 Signal Transduction of Histamine H₁ Receptors

The histamine H₁ receptor stimulation activates phospholipase C (PLC) via a pertussis toxin-insensitive G protein, related to the G_{q/11} family of G proteins, consequently forming inositol-1,4,5-triphosphate (IP₃) and 1,2-diacylglycerol (DAG), resulting in an increase in intracellular calcium concentration.¹⁶³ Additionally, its stimulation results in the activation

of a variety of signaling pathways, mostly to be secondary to changes in intracellular calcium concentration or activation of protein kinase C (PKC), such as stimulation of nitric oxide synthetase (NOS) activity, phospholipase A₂ (PLA₂) activity and therefore release of arachidonic acid from cell membrane, changes in cAMP accumulation, and promotion of transcription of genes controlled by nuclear factor kappa B (NF- κ B) (Figure 1.10).^{149,164} For the histamine H₁ receptor, constitutively activity has been described, but however its (patho)physiological relevance is unknown.

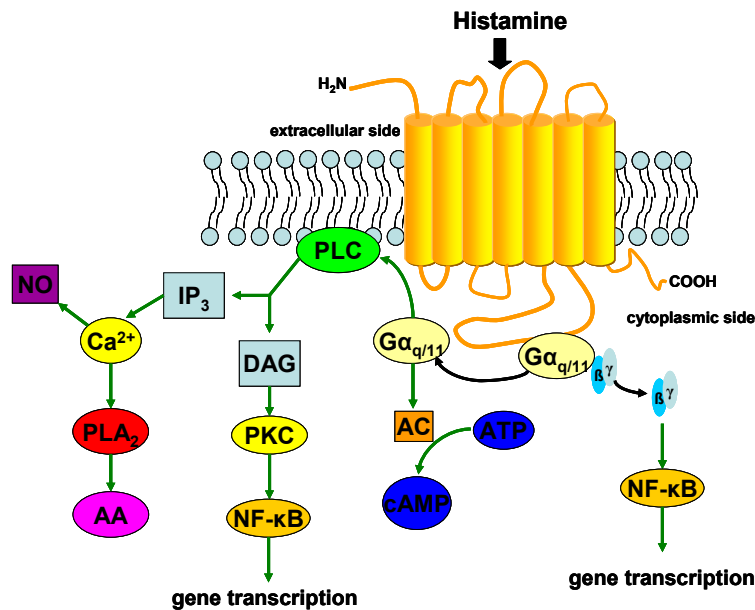


Figure 1.10 Signaling pathways of histamine H₁ receptors.

1.3.3 Distribution and Function of Histamine H₁ Receptors

Histamine H₁ receptors are distributed in the mammalian brain and in the periphery. In the human brain high concentrations are located in nucleus accumbens, thalamus, neocortex, hippocampus, and posterior hypothalamus; however basal ganglia demonstrate low abundance. Stimulation of histamine H₁ receptors consequences inhibition of firing and hyperpolarization in hippocampal neurons, but it causes excitation in brainstem, thalamic and cortical neurons. Histamine strongly influences sleep and wakefulness via the histamine H₁ receptor in brain, therefore the receptor plays an important role in sedative effects. Histamine H₁ receptor activation stimulates tyrosine hydroxylase in mammalian brain. In the periphery, histamine H₁ receptors are localized on smooth muscles in the respiratory tract and gastrointestinal tract, cardiovascular system, and genitourinary system. Additionally they are abundant on endothelial cells and lymphocytes. Activation of histamine H₁ receptors results in contraction of smooth muscle, vascular permeability due

to endothelial cell contraction, release of nitric oxide, negative inotropic effects on myocardium, and facilitates the release of adrenaline and noradrenaline in the adrenal medulla.¹⁴⁹ A number of the effects are described as the “triple response”: red spot, itch and swelling; which are symptoms of allergic reactions and inflammatory disorders and represent the key role of histamine H₁ receptors.

1.3.4 Therapeutic Relevance of Histamine H₁ Receptor Ligands

Histamine H₁ receptor antagonists or so-called ‘antihistamines’ have been used for many decades and are still the most important drugs in the treatment of various allergic disorders, such as hay fever, allergic rhinitis, and urticaria. First generation histamine H₁ receptor antagonists (cf. 1.3.6) interfere with cholinergic, dopaminergic and serotonergic receptors and cause adverse central nervous system effects such as sedation, decreased cognitive functions and sleepiness. For that reason, these drugs have been administered for sleep disorders, emesis, and allergic disorders in pediatrics or with topical application. Other side effects were obtained such as anxiety, appetite stimulation and tachycardia; peripheral cholinergic antagonism resulted in dry mouth and urinary retention. The next generation antihistamines have improved side-effect profiles, causing less sedation, but a few demonstrate severe cardiovascular effects (cf. 1.3.6). Chlorpromazine, a phenothiazine derivative, was initially developed from H₁ receptor antagonists for its antiallergic properties by Delay and Deniker in 1952. Finally, chlorpromazine entered the market as the first neuroleptic drug causing sedative effects due to its antagonist binding profile for central histamine H₁ receptors. In most cases classical and atypical antipsychotics are antagonists at histamine H₁ receptors, and besides the sedative effect, an anxiolytic effect has been reported.⁶⁶ Currently the histamine H₁ receptor is under investigation due to its effect to induce weight gain in antipsychotic treated patients.^{107,165} The therapeutic use of histamine H₁ receptor agonists is still unclear. Betahistine, a histamine H₁ receptor agonist, has been used in the treatment of vertebrobasilar insufficiency,¹⁶⁶ Ménière’s disease and as a prophylaxis of migraine,¹⁶⁷ but the therapeutic effect has not been obviously linked to its histamine H₁ agonism.

1.3.5 Ligand Binding Mode at Histamine H₁ Receptors

Site-directed mutagenesis has confirmed that the conserved aspartic acid (107) in TM3 of the human histamine H₁ receptor is crucial for the binding of histamine and histamine H₁

receptor antagonists. Aspartate in TM3 is highly conserved among aminergic rhodopsin-like G protein-coupled receptors and provides the negative counter-ion for the protonated amine group of the ligand.¹⁶⁸ For histamine binding, the asparagine (207) in TM5 interacts via hydrogen bond with the nitrogen of the imidazole ring and lysine (200) in TM5 links with the nitrogen of the aliphatic primary amine.¹⁶⁹

1.3.6 Ligands for Histamine H₁ Receptors

Due to the uncertain therapeutic relevance of agonists, the centre of attention is put on ligands with antagonist properties. The first histamine H₁ receptor antagonists were synthesized two decades after the discovery of histamine. One of the first introduced compounds with selectivity and high affinity for histamine H₁ receptors was mepyramine (pyrilamine), an ethylenediamine derivative, which is still used as a radioligand for pharmacological testing. Other histamine H₁ receptor antagonists followed such as diphenhydramine (Benadryl[®], Vomex A[®]), chlorpheniramine (Polaronil[®]) and bamipine (Soventol[®]) in order to release allergic symptoms (Chart 1.5). These compounds are very lipophilic and able to penetrate into the CNS and elicit sedative side effects by antagonism of histamine H₁ receptors. Therefore, they are mainly used for the treatment of travel sickness (antiemetics), sleeping disorders or with topical application for allergic reactions.¹⁶³ The tetracyclic compound mianserin (Mianeurin[®]), a rigidized derivative of mepyramine, was developed as a compound with not only high antihistamine activity, but also high antiserotonin potency to improve antiallergic activity and reduce the central nervous system depressant effect (Chart 1.5).¹⁷⁰

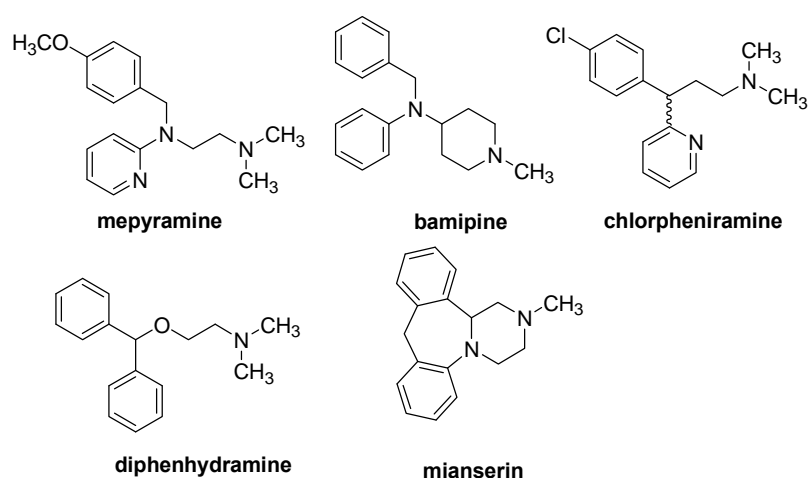


Chart 1.5 First generation of histamine H₁ receptor antagonists.

In the last decades, new histamine H₁ receptor antagonists with reduced lipophilic structures have been synthesized such as cetirizine (Zyrtec[®]) and fexofenadine (Telfast[®]), comprising diphenylmethyl substituents with high affinity for histamine H₁ receptors, and loratadine (Lisino[®]) and ketotifen (Zaditen[®]), bearing a tricyclic ring system (Chart 1.6).

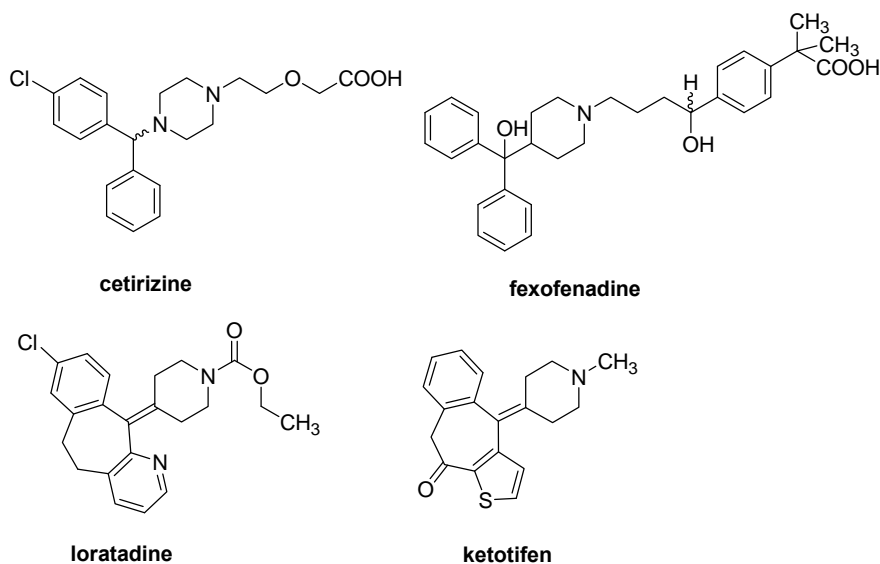


Chart 1.6 “Non sedative” second generation of histamine H₁ receptor antagonists.

These compounds poorly cross the blood-brain barrier and are commonly referred as non sedating “second generation” histamine H₁ receptor antagonists because they are almost free from sedative side effects at the recommended clinical dose. Moreover, the second generation class has an improved side effect profile regarding unwanted ventricular arrhythmias.¹⁴⁹ It is noteworthy, that due to the constitutive activity *in vitro* of histamine H₁ receptors (see 1.3), most histamine H₁ receptor antagonists has been reclassified as histamine H₁ receptor (partial) inverse agonists.

1.4 The Drug Discovery Process

The development of potential drug candidates in drug discovery has mainly concentrated on testing synthesized compounds in order to evaluate the ligand affinity and selectivity for the selected target. Based on the *in vitro* screening results, ligands have been identified as lead compounds and further optimized by iterative chemical modifications to obtain structure-activity relationships. Conventional drug discovery and development of novel ligands has resulted in a long-term, costly and highly risky procedure and the past average of 90% attrition rate did not provide long-term success.¹⁷¹ In order to optimize the development of novel ligands and to contribute to a more efficient drug discovery process,

new lead identification strategies have been implemented in the early drug development stages.¹⁷²

The drug discovery process for the selected target can be divided into three phases: the lead identification phase, the lead optimization phase and the clinical development. In the lead identification phase large compound collections received from combinatorial chemistry, parallel synthesis and generated compound libraries are tested at the target of interest with (ultra)high-throughput screening (HTS), a miniaturized and automated *in vitro* assay, to obtain novel hits and lead candidates. As a complement to HTS, structure-based and ligand-based virtual screening (VS) have been introduced to identify novel structural hit classes. The former method relies on the target structure, while the latter approach includes topological search from well-known ligands of the target.¹⁷³ Ligand-based VS methods can be divided into data mining techniques (e. g. clustering¹⁷⁴ and recursive partitioning¹⁷⁵), similarity searching, pharmacophore modeling¹⁷⁶ and more complex techniques employing models received by support vector machines (SVM)¹⁷⁷ or neural networks (NN)¹⁷⁸. These chemoinformatic techniques allow handling and analyzing the resulting large amount of data and support the medicinal chemist to gain deeper insight into the relationship between pharmacological data and structural features of compounds.

1.5 Radioligand Binding Studies

Development of novel ligands in drug discovery requires a robust assay system for compound screening, and the selection and development of an assay is of immense importance. Radioligand binding studies allow to accurately determining the affinity of ligands at the receptor of interest, its selectivity and to identify novel chemical scaffolds. The technique is basically a very straightforward method, applicable in a very wide range of preparations and has strongly improved receptor research for many decades. Furthermore, it comprises the ability to identify, characterize and elucidate receptors in their natural environment and also those transfected into cell lines. It enables to merely detect ligands that demonstrate affinity and receive large amounts of data, using smallest amounts of tissue and ligand, in a robust and fast high-throughput screening; therefore it has become an essential tool within the drug discovery process. The power of binding studies to provide valid quantitative estimates and high quality of binding data depends crucially on the assay system under investigation and experimental assay conditions need to be chosen carefully. Buffer composition, incubation temperature, pH value, ionic strength, and radioligand depletion are important parameters within the assay and significantly influence binding data. Particular attention has to be paid to the kinetic; the

appropriate incubation time has to allow ligands, especially with high affinities, to reach the equilibrium state. It is of importance to notice that a radioligand binding assay estimates the affinity of a ligand specific binding site, while a functional assay determines the intrinsic efficacy of the ligand. Agonist competition curves display mostly a shallow and biphasic shape due to the existence of multiple agonist affinity states. Nevertheless, it is possible for G protein-coupled receptors to assess whether the ligand is an agonist or antagonist by conducting a guanosine-5'-triphosphate (GTP) shift experiment. High-affinity binding of agonists depends on the association of a receptor/G protein complex. In the presence of either salt and/or guanine nucleotides the complex dissociates and results in a significant reduction in agonist binding affinity, while antagonist binding is not decreased. Although radioligand binding assays are an extremely powerful tool to investigate in ligand-receptor interactions, some limitations have to be considered. The per-assay costs are highly expensive and include a high affine and selective radioligand, cell culture, solutions, reagents, disposable items, multiwell assay plates and precise instrumentations. Determined K_i affinity values of screening compounds might be different using dissimilar binding assay conditions, including varying radioligands, incubation buffers, and incubation times.

Radioligand binding is also used to estimate ligand-receptor interactions *in vivo* in both animals and humans, applying positron emission tomography (PET) or single photon emission computed tomography (SPECT), in order to monitor receptor dynamics in many diseases, particularly in the central nervous system.

2 Aim of Thesis

The aim of the thesis is the development of novel ligands influencing neurotransmission in the central nervous system. Due to its important role in various neurological and neuropsychiatric disorders such as Parkinson's disease, schizophrenia and drug addiction, the focus is concentrated on the dopamine D₃ receptor. The strategy is the development of radioligand binding assays to investigate in structure-affinity relationships (SAR) of novel structural classes of ligands.

Radioligand binding assays for human dopamine D₃ receptors and, for reasons of structural homology and selectivity, human dopamine D_{2S} receptors, stably expressed in Chinese hamster ovary cells (CHO), are implemented. To gain insight into the cross affinity receptor profile of related biogenic amine receptors, a radioligand binding assay for human histamine H₁ receptors stably expressed in CHO cells is validated. For functional classification of agonists in radioligand binding assays and consequently discrimination of agonists from antagonists, a GTP shift assay is performed.

To develop novel ligands for dopamine D₃ receptors, derivatives of the leads BP 897 and ST 198 are tested for binding affinities. Variations of discrete elements of the lead structures and therefore alterations of functionalities in the ligand are studied to enlighten structural requirements for high affinity binding and selectivity at dopamine D₃ receptors.

Ligands with antagonistic properties at dopamine D₂-like receptors and at histamine H₁ receptors comprise close structural similarity. A hybrid structure approach of histamine H₁ receptor antagonists and dopamine D₂/D₃ receptor structural features is investigated. The aim is to elucidate the SAR of the histamine H₁/dopamine D₂-like receptor profile and to identify highly affine dopamine D₃ receptor selective ligands.

Structural variations of the dopamine D₃ receptor agonist pramipexole and the structurally related dopamine agonist etrabamine are investigated. The strategy is to introduce the selective dopamine D₃ receptor binding profile, the advanced pharmacokinetic and neuroprotective properties of pramipexole into novel ligands. The influence on affinity binding of an additional dopamine D₃ receptor pharmacophore element combined with the dopamine agonists is assessed. The aim of this approach is to develop ligands with high affinity and improved selectivity for dopamine D₃ receptors.

Investigation in the identification of novel lead structures with altered chemical scaffold for dopamine D₃ receptors is performed. Radioligand binding assays are applied on molecules resulting from chemoinformatic virtual screening techniques. By combining radioligand binding studies with computational methods the aim is to achieve a deeper insight into the SAR of ligands and the ligand binding mode at the dopamine D₃ receptor.

3 Materials and Methods

3.1 Materials

3.1.1 Reference Substances and Test Compounds

Bamipine (Dr. Rentschler, Laupheim, Germany)

BP 897 (Dr. P. Sokoloff, Paris, France, synthesized in our laboratories by Prof. Dr. H. Stark, Frankfurt, Germany)

Cetirizine dihydrochloride (European Pharmacopoeia, Strasbourg, France)

(*R/S*)-Chlorpheniramine maleate (Sigma-Aldrich Chemie GmbH, Steinheim, Germany)

Ciprofloxacin hydrochloride (Bayer, Leverkusen, Germany)

Diphenhydramine hydrochloride (Sigma-Aldrich Chemie GmbH, Steinheim, Germany)

Fexofenadine hydrochloride (Prof. Dr. S. Elz, Regensburg, Germany)

Haloperidol (Sigma-Aldrich Chemie GmbH, Steinheim, Germany)

Ketotifenhydrogenfumarate (Stada, Bad Vilbel, Germany)

Loratadine (Prof. Dr. G. Lambrecht, Frankfurt, Germany)

Mianserin hydrochloride (Sanofi-Aventis, Frankfurt, Germany)

(*S*)-(-)-Nafadotride (Dr. P. Sokoloff, Paris, France)

Pramipexole dihydrochloride (Böhringer Ingelheim, Ingelheim, Germany)

Pyrilamine maleate (Sigma-Aldrich Chemie GmbH, Steinheim, Germany)

(*S*)-(-)-Raclopride L(+)-tartaric salt (Sigma-Aldrich Chemie GmbH, Steinheim, Germany)

Spiperone (Sigma-Aldrich Chemie GmbH, Steinheim, Germany)

ST 198 (synthesized in our laboratories by Prof. H. Stark, Frankfurt, Germany)

Terfenadine (Sigma-Aldrich Chemie GmbH, Steinheim, Germany)

U 99194A (Tocris Bioscience, Bristol, UK)

Analogues of benzhydrylpiperazine, Pramipexole and BP897 were synthesized in our laboratories by Prof. Dr. H. Stark and co-workers, Institute of Pharmaceutical Chemistry, Frankfurt am Main, Germany.

Virtually screened synthetic compounds were ordered from SPECS, 2628 XH Delft, The Netherlands, and Interbioscreen (IBS), 121019 Moscow, Russia.

3.1.2 Cells, Cell Culture and Protein Assay

Cells

CHO-K1 cells stably expressing human D_{2S} receptors (Dr. J. Shine, Sydney, Australia).

CHO-K1 cells stably expressing human D₃ receptors (Dr. P. Sokoloff, Paris, France).

CHO-K1 cells stably expressing human H₁ receptors (Prof. R. Leurs, Amsterdam, The Netherlands).

Cell Culture and Protein Assay

Bovine serum albumin (Sigma-Aldrich Chemie GmbH, Steinheim, Germany)

Cell culture dishes (TPP AG, Trasadingen, Switzerland, Greiner bio-one GmbH, Frickenhausen, Germany)

Coomassie® Brilliant Blue G250 (Merck KGaA, Darmstadt, Germany)

Dulbecco's Modified Eagle's Medium (PAA Laboratories GmbH, Cölbe, Germany)

Dulbecco's Modified Eagle's Medium/F12 (1:1) (Invitrogen GmbH, Karlsruhe, Germany)

Fetal bovine serum, dialyzed (PAA Laboratories GmbH, Cölbe, Germany)

Fetal bovine serum, inactivated (PAA Laboratories GmbH, Cölbe, Germany)

G418 sulphate (PAA Laboratories GmbH, Cölbe, Germany)

L-Glutamine (PAA Laboratories GmbH, Cölbe, Germany)

Non-essential amino acids (PAA Laboratories GmbH, Cölbe, Germany)

Penicillin G/streptomycin mixture (PAA Laboratories GmbH, Cölbe, Germany)

Trypsin/EDTA (PAA Laboratories GmbH, Cölbe, Germany)

3.1.3 Chemicals

All chemicals are of highest analytical grade purity commercially available.

Dimethylsulfoxide (DMSO) (Sigma-Aldrich Chemie GmbH, Steinheim, Germany)

Disodium hydrogen phosphate dihydrate (Merck KGaA, Darmstadt, Germany)

Ethanol (Merck KGaA, Darmstadt, Germany)

5'-Guanylylimidodiphosphate trisodium (Sigma-Aldrich Chemie GmbH, Steinheim, Germany)

N-(2-Hydroxyethylpiperazine)-*N'*-2-ethanesulfonic acid sodium salt (HEPES) (Carl Roth GmbH, Karlsruhe, Germany)

Magnesium chloride hexahydrate (Merck KGaA, Darmstadt, Germany)

Phosphoric acid (87%)(Merck KGaA, Darmstadt, Germany)

Sodium chloride (Carl Roth GmbH, Karlsruhe, Germany)

1 M Sodium hydroxide (Merck KGaA, Darmstadt, Germany)

Tris(hydroxymethyl)aminomethane (Tris) (Carl Roth GmbH, Karlsruhe, Germany)

3.1.4 Buffers and Solutions

Buffers and solutions were made of analytical grade purity chemicals and Milli-Q water. PBS was autoclaved.

HEPES Buffer

HEPES	20 mM
MgCl ₂	10 mM
NaCl	100 mM
NaOH	ad pH 7.4

Membrane Buffer

Tris	10 mM
MgCl ₂	5 mM
HCl	ad pH 7.4

Binding Buffer

Tris	50 mM
KCl	5 mM
CaCl ₂	1 mM
MgCl ₂	1 mM
NaCl	120 mM
HCl	ad pH 7.4

Wash Buffer

Tris	50 mM
NaCl	120 mM
HCl	ad pH 7.4

Phosphate-Buffered Saline (PBS)

NaCl	140 mM
KCl	3 mM
Na ₂ HPO ₄	8 mM
KH ₂ PO ₄	1.5 mM
H ₃ PO ₄ (8.5%)	ad pH 7.4

GTP-Binding Buffer (GTP Shift)

NaCl	120 mM
	(4-fold concentrated)
Tris	50 mM
KCl	5 mM
CaCl ₂	1 mM
MgCl ₂	2 mM
HCl	ad pH 7.4

Control Buffer (GTP Shift)

Tris	50 mM
KCl	5 mM
CaCl ₂	1 mM
MgCl ₂	2 mM
HCl	ad pH 7.4

Bradford Reagent (Aqueous Solution)

Coomassie® Brilliant Blue G250	0.01% (w/v)
Ethanol	4.7% (v/v)
H ₃ PO ₄	8.5% (v/v)

3.1.5 Radiochemicals and Material for Radioligand Binding Assays

Betaplate scint (Perkin Elmer Life and Analytical Sciences, Rodgau-Jügesheim, Germany)

Glass fibre filter; filtermat B (Perkin Elmer Life and Analytical Sciences, Rodgau-Jügesheim, Germany)

Polyethylenimine 50% (w/v) aqueous solution (PEI) (Sigma-Aldrich Chemie GmbH, Steinheim, Germany)

[Pyridinyl-5-³H]Pyrilamine (SA 28.0 Ci/mmol) = [³H]Mepyramine (Amersham Biosciences Europe GmbH, Freiburg, Germany)

Sample bag (Perkin Elmer Life and Analytical Sciences, Rodgau-Jügesheim, Germany)

[³H]Spiperone (SA 106.0 Ci/mmol) (Amersham Biosciences Europe GmbH, Freiburg, Germany)

3.1.6 Technical Equipment

Analytical scales sartorius basic (Sartorius AG, Göttingen, Germany)

Autoclave (Getinge AB, Getinge, Sweden)

Centrifuge ZK 380 (Hermle Labortechnik GmbH, Wehingen, Germany)

Dispensette III Variable (Brand GmbH & Co KG, Wertheim, Germany)

Freezer -20 °C (Liebherr Logistik GmbH, Kirchdorf, Germany)

Freezer -70 °C (G. Kisker GbR, Steinfurt, Germany)

Glass-glass hand held homogenizer (hand potter) (Carl Roth GmbH, Karlsruhe, Germany)

Heater (Ehret GmbH & Co KG, Emmendingen, Germany)

Heraeus Suprafuge 22 (Heraeus Holding GmbH, Hanau, Germany)

Hitachi U 2000 Spectrophotometer (Hitachi Europe GmbH, Düsseldorf, Germany)

Ika-Ultra-Turrax T 25 basic (Janke & Kunkel GmbH & Co KG, Staufen, Germany)

Incubator Heraeus Instruments (Heraeus Holding GmbH, Hanau, Germany)

Inotech Cell Harvester (Inotech AG, Dottikon, Switzerland)

Laboratory-dishwasher G 7783 CD Mielabor (Miele & Cie GmbH & Co, Gütersloh, Germany)

Laminar Air Flow Clean Air (Clean Air Deutschland GmbH, Haan/Rheinland, Germany)

Liquid nitrogen container GT 35 (Air Liquide, Bussysaint George, France)

Liquid nitrogen container GT 40 (Air Liquide, Bussysaint George, France)

Magnetic hotplate IKAMAG RCT (Janke & Kunkel GmbH & Co KG, Staufen, Germany)

Mettler MT 5-scales (Mettler Toledo, Gießen, Germany)

MicroBeta Trilux (Perkin Elmer Life Sciences GmbH, Rodgau, Germany)

MicroBeta Workstation ((Perkin Elmer Life Sciences GmbH, Rodgau, Germany)

Mikroskope Telaval 31 (Karl Zeiss AG, Oberkochen, Germany)

Multipipette plus (Eppendorf, Hamburg, Germany)

pH-Meter CG 820 (Schott Geräte GmbH, Mainz, Germany)

Pipetboy acu (IBS Integra Biosciences AG, Fernwald, Germany)

Pipette Reference (Eppendorf, Hamburg, Germany)

Refrigerator (Bosch GmbH, Gerlingen, Germany)

Shaker GFL 1083 (GFL mbH, Burgwedel, Germany)

Sonication Bandelin Sonopul HD 200 (Bandelin electronic GmbH & Co KG, Berlin)

Varioclave Steam Sterilizator (H + P Labortechnik GmbH, Oberschleißheim, Germany)

Vortexer Genie 2 (Scientific Industries, Bohemia, USA)

Vortexer VF 2 (Janke & Kunkel GmbH & Co KG, Staufen, Germany)

Wallac 1295-012 Heat Sealer (Perkin Elmer Life Sciences GmbH, Rodgau, Germany)

3.2 Methods

3.2.1 Cell culture

CHO-Cells Expressing Human Dopamine D_{2S} and D₃ Receptors

CHO-K1 cells, expressing the recombinant human dopamine D_{2(short)} receptor gene, were grown in Dulbecco's Modified Eagle's Medium/F12 (1:1) supplemented with 10% inactivated fetal bovine serum, 100 I.U./mL penicillin G, 100 µg/mL streptomycin and 2 mM glutamine in an atmosphere of 5% CO₂ at 37 °C.¹⁷⁹ Human D₃ receptors stably expressed in CHO cells were cultured in Dulbecco's Modified Eagle's Medium supplemented with 10% dialyzed fetal bovine serum, 2 mM glutamine and were grown in an atmosphere of 5% CO₂ at 37 °C in monolayer culture.³³ For cell culture 1 mL stocks

were quickly thawed in hands or in a 37 °C water bath, suspended in 10 mL cold medium and centrifuged at 800 rpm for 5 min at 4 °C. The cells were suspended in 10 mL growth medium in a 75 cm² cell culture flask. Cell passage was done at cell confluence three times a week, pointing out that CHO-D₃ cells need more time for growing compared to CHO-D_{2s} expressing cells. The whole medium was removed; cells were carefully washed with 5 mL 37 °C warmed phosphate-buffered saline (PBS), loosened with 1 mL trypsin/EDTA and resuspended in fresh 37 °C warmed medium. Depending on cell density the splitting ratio was 1:4 to 1:5. Stock aliquots were obtained by washing the cells with 5 mL PBS, removing cells from cell culture flask with 1 mL trypsin/EDTA, inactivating trypsin with 4 mL medium and additionally the cells were collected by centrifugation (800 rpm, 4 °C, 15 min). The cells were resuspended in growth medium supplemented with 10% dimethylsulfoxide (DMSO) and slowly frozen to -70 °C before stored in liquid nitrogen. Two 1mL aliquots were obtained by one 75 cm² cell culture flask.

CHO-Cells Expressing Human Histamine H₁ Receptors

CHO-K1 cells, stably expressing the recombinant human histamine H₁ receptor gene, were grown in Dulbecco's Modified Eagle's Medium supplemented with 10% fetal bovine serum, 2 mM glutamine, 100 I.U./mL penicillin G, 100 µg/mL streptomycin and 0.1 mM non-essential amino acids in an atmosphere of 5% CO₂ at 37 °C in monolayer culture. 1 mL of stock was thawed in hands, suspended in 10 mL cold medium and centrifuged at 800 rpm for 5 min at 4 °C. The cells were suspended in 10 mL cold medium and added into 20 mL of warmed growth medium in a 150 cm² cell culture flask. Cells were passaged three times a week and therefore the medium was removed, cells were washed with 15 mL 37 °C PBS, 3 mL trypsin/EDTA were added to remove cells and they were resuspended in fresh medium. Due to fast growing splitting ratios of cells were 1:4 to 1:8. For preparing stock aliquots, cells were rinsed with PBS, trypsinized and centrifuged at 800 rpm for 15 min at 4 °C. Consequently, the cells were resuspended in growth medium supplied with 10% DMSO and stored at -70 °C before putting the aliquots in liquid nitrogen. Three stock aliquots were obtained from one 150 cm² cell culture flask.

3.2.2 Preparation of Membrane Homogenates

Membrane Preparations of CHO-Cells Expressing Human Dopamine D_{2S} and D₃ Receptors

Preparation of membrane homogenates were carried out 2-3 passages after thawing, and human dopamine D_{2S} and D₃ receptor expressing cell lines were grown to confluence (80 – 100%). The medium was disposed and the cells were washed with 10 mL ice-cold PBS buffer. The cells were scraped from the flasks into 15 mL ice-cold medium and centrifuged at 3,000 rpm for 10 min at 4 °C. After centrifugation the medium was removed and the cell membranes resuspended in 10 mL ice-cold membrane buffer, disrupted with an Ultra-Turax (setting 1.5, twice for 10 seconds-exposure), filled up with membrane buffer to 25 ml volume, and finally membranes were pelleted at 20,000 rpm for 30 min at 4 °C. The pellets were rehomogenized in ice-cold membrane buffer (hD₃: 250 µL/75 cm² flask, hD_{2S}: 125 µL/75 cm² flask) by ultrasonic waves (duty cycle constant, 8 - 10 seconds) and membrane aliquots were stored at -70 °C. During the time of storage no change of binding parameters could be detected. Determination of membrane protein was carried out by the method of Bradford.¹⁸⁰

Membrane Preparations of CHO-Cells Expressing Human Histamine H₁ Receptors

After thawing CHO-K1 cells expressing histamine H₁ receptors, four passages were carried out before membrane homogenates were prepared. At confluence of 80 – 100%, the cells were rinsed with 10 mL ice-cold PBS buffer, scraped into ice-cold HEPES binding buffer and homogenized three times with ultrasonic waves for 15 seconds (duty cycle constant, 8 - 10 seconds). Membranes were pelleted at 20,000 rpm for 30 min at 4 °C and resuspended in HEPES buffer (hH₁: 200 µL/75 cm² flask) using a hand potter. Aliquots were stored in liquid nitrogen. No change in binding parameters appeared during storage. The method of Bradford was used for protein determination.¹⁸⁰

Protein Assay

The protein concentration of the membrane preparation was determined with Coomassie Blue G 25 reagent and bovine serum albumin (0.5 mg/mL) diluted in membrane buffer as the standard, according to the method of Bradford¹⁸⁰. The absorptions of the standard preparation and membrane preparation were determined at 595 nm in a spectrophotometer, using a blank as zero. The standard curve and unknown protein concentration were analyzed by linear-regression curve-fitting procedures using GraphPad PrismTM software (cf. 3.2.6).

3.2.3 Radioligand Binding Studies on Human Dopamine D_{2S} and D₃ Receptors

Radioligand binding assays at dopamine D_{2S} and D₃ receptors stably expressed in CHO-K1 cells were employed according to Sokoloff et al. with few modifications.⁶¹ Assay conditions were established to yield the highest signal-to-noise ratio. Assays were carried out in triplicates and at least 3 independent experiments using 96-well plates. Test compounds were diluted in DMSO to make a 1 or 10 mM stock solution, depending on its solubility and were further diluted to the required volume with incubation buffer. BP 897 was diluted in DMSO to receive a 1 mM stock solution and further dissolved in incubation buffer. The radioligand dilution of [³H]spiperone was prepared with incubation buffer. Incubations were run at 25 °C for 2 h and terminated by rapid filtration through GF/B glass fibre filters, presoaked for 30 min and at 4 °C in 0.3% polyethylenimine solution, using a cell harvester. Unbound radioligand was removed with four washes of 300 µL ice-cold wash buffer. Filters were dried at 55 °C for 50 – 60 min in the oven and afterwards soaked in 9 mL scintillant. Bound radioactivity was counted (5 min/well) in a β-counter at 45% counter efficiency.

Saturation Binding Experiments

Saturation binding experiments were performed to determine the total number of receptors (B_{max}) of the membrane preparation and the equilibrium binding dissociation constant (K_d) of the radioligand. A constant amount of cell membrane preparation with the subtype receptor of interest was incubated with increasing concentrations of radioligand in the absence and presence of unlabeled ligand used to define non-specific binding. Assays were

carried out by diluting [³H]spiperone to 10 concentrations in the range of 0.01 – 10 nM (final concentration). Cell membrane preparations with human dopamine D_{2s} or D₃ receptors were thawed and rehomogenized in incubation buffer using ultrasonic waves (duty cycle constant, 10 sec) at 4 °C. The amount of protein was 10 µg/200 µL for dopamine D₂ receptors and 2 µg/200 µL for D₃ receptors. 50 µL of incubation buffer to determine total binding or 50 µL 10 µM BP 897 for monitoring non-specific binding, 50 µL diluted [³H]spiperone and 100 µL cell membrane suspension were incubated. Data were analyzed by the software GraphPad PrismTM (cf. 3.2.6).

Competition Binding Experiments

To obtain the inhibition constant K_i of unlabeled test compounds, competition binding experiments were investigated. A constant concentration of labeled ligand and seven varying concentrations of the unlabeled test compound were incubated with cell membrane preparation containing the receptor of interest. Therefore test compound and [³H]spiperone were diluted and cell membrane preparations with human dopamine D_{2s} or D₃ receptors were thawed, rehomogenized in incubation buffer using ultrasonic waves (duty cycle constant, 10 sec) at 4 °C. Final membrane protein concentrations of dopamine D_{2s} receptors was 10 µg/200 µL and for D₃ receptors 2 µg/200 µL. 50 µL of test compound dilution or 50 µL of incubation buffer to determine total binding or 50 µL of 10 µM BP 897 to measure non-specific binding were incubated with 50 µL 0.2 nM [³H]spiperone (final concentration) and 100 µL cell membrane suspension. Data were analyzed by the software GraphPad PrismTM (cf. 3.2.6).

3.2.4 Radioligand Binding Studies on Human Histamine H₁ Receptors

The assay procedure for radioligand binding studies on histamine H₁ receptors stably expressed in CHO-K1 cells was carried out according to Smit et al. with some alteration, considering the best signal-to-noise ratio.¹⁸¹ The experimental ingredients were added in triplicates into 96-well plates and binding data were received by at least 3 independent experiments. DMSO was used to prepare a 1 or 10 mM stock of test compound, which was further diluted in HEPES buffer. (*R/S*)-Chlorpheniramine maleate and the radioligand [³H]mepyramine were diluted in HEPES buffer. Incubations were run at 25 °C for 2 h and terminated by rapid filtration through GF/B glass fibre filters, presoaked for 30 min at 4 °C in 0.3% polyethylenimine solution, using a cell harvester. Unbound radioligand was

removed with four washes of 300 μL ice-cold HEPES buffer. Before the filters were soaked in 9 mL scintillant, they were dried at 55 $^{\circ}\text{C}$ for 50 – 60 min in the oven. Bound radioactivity was counted for 5 min per well in a β -counter at 45% counter efficiency.

Saturation Binding Experiments

General procedures and considerations have been described above.

A serial dilution of 10 concentrations in the range 0.05 – 50 nM (final concentration) of [^3H]mepyramine were prepared and cell membrane preparations with human histamine H_1 receptors were thawed and rehomogenized in HEPES buffer using ultrasonic waves (duty cycle constant, 10 sec) at 4 $^{\circ}\text{C}$. The amount of protein was 30 $\mu\text{g}/200 \mu\text{L}$ for histamine H_1 receptors. 50 μL HEPES buffer to monitor total binding or 50 μL of 10 μM (*R/S*)-Chlorpheniramine maleate for non-specific binding, 50 μL diluted radioligand [^3H]mepyramine and 100 μL cell membrane suspension were mixed. Data were analyzed by the software GraphPad PrismTM (cf. 3.2.6).

Competition Binding Experiments

General procedures and considerations have been described above. Cell membrane preparations with human histamine H_1 receptors were thawed and rehomogenized in HEPES buffer using ultrasonic waves (duty cycle constant, 10 sec) at 4 $^{\circ}\text{C}$ (protein concentration: 30 $\mu\text{g}/200 \mu\text{L}$). 50 μl of 1.0 nM [^3H]mepyramine (final concentration), 50 μL of test compound dilution or 50 μL of HEPES buffer to determine total binding or 50 μL of 10 μM (*R/S*)-Chlorpheniramine maleate to define non-specific binding and 100 μL cell membrane suspension were incubated to equilibrium. Data were analyzed by the software GraphPad PrismTM (cf. 3.2.6).

3.2.5 GTP Shift Competition Binding Experiments

GTP shift competition binding experiments are carried out under similar assay conditions to competition binding experiments for dopamine $\text{D}_{2\text{S}}$ and D_3 receptors with few modifications (cf. 3.2.3). Assays were carried out in triplicates and at least 3 independent experiments using 96-well plates. Frozen cell membrane preparations with human dopamine $\text{D}_{2\text{S}}$ or D_3 receptors were thawed, rehomogenized in control buffer (GTP-shift) using ultrasonic waves (duty cycle constant, 10 sec) at 4 $^{\circ}\text{C}$. Final membrane protein concentrations of dopamine $\text{D}_{2\text{S}}$ receptors was 10 $\mu\text{g}/200 \mu\text{L}$ and for D_3 receptors 2 $\mu\text{g}/200$

μL . Test compound and [^3H]spiperone were diluted in control buffer (GTP-shift) (final concentration 0.2 nM). Either 50 μL of test compound dilution or 50 μL of control buffer (GTP-shift) to determine total binding or 50 μL of 10 μM BP897 in control buffer (GTP-shift) to measure non-specific binding were applied. In the next step, 50 μL GTP-binding buffer, 50 μL control buffer (GTP-shift) or 50 μL 100 μM Gpp(NH)p in GTP-binding buffer were added to the microtiter plate, respectively. Finally, 50 μL 0.2 nM [^3H]spiperone (final concentration) and 50 μL cell membrane suspension were applied. Samples were incubated at 25 °C for 2 h and terminated by rapid filtration through GF/B glass fibre filters, presoaked for 30 min and at 4 °C in 0.3% polyethylenimine solution, using a cell harvester. Unbound radioligand was removed with four washes of 300 μL ice-cold wash buffer. Filters were dried at 55 °C for 50 – 60 min in the oven and afterwards soaked in 9 mL scintillant. Bound radioactivity was counted (5 min/well) in a β -counter at 45% counter efficiency. Data were analyzed by the software GraphPad PrismTM (cf. 3.2.6).

3.2.6 Data Analysis and Statistics

Data were analyzed by the software GraphPad PrismTM (GraphPad Software Inc., 2000, version 3.02, San Diego, CA, USA). Binding experiments were calculated using non-linear least squares fit. Specific binding was analyzed by subtracting the non-specific binding from the measured total binding for each data point.

Saturation Binding Experiments

One-site binding model

Data from saturation studies were fitted to the equation 3.1 to determine the equilibrium dissociation constant (K_d) of the radioligand and the total amount of binding sites (B_{max}) [cpm]. K_d is a constant that is equal to the concentration of radioligand at which half of the total number of receptors are occupied,

$$y = \frac{B_{\text{max}} \cdot x}{(K_d + x)} \quad (3.1)$$

y is the amount of specific binding [cpm] and x is the concentration of radioligand [nM].

To calculate the concentration values [nM] from determined cpm data, equation 3.2 was used:

$$\text{concentration [nM]} = \frac{\text{cpm} \cdot e}{2200 \cdot V \cdot SA}, \quad (3.2)$$

e is the counting efficacy factor (2.222), V is the assay volume, SA is the specific activity of the radioligand [Ci/mmol].

For displaying data, saturation experiments were transformed to create a Scatchard plot. Bound/free ligand was plotted versus specific binding [cpm] before linear regression was conducted.

Two-site binding model

Data from saturation binding experiments were fitted to the equation 3.3 using a two-site binding model.

$$y = \frac{B_{\max 1} \cdot x}{(K_{d1} + x)} + \frac{B_{\max 2} \cdot x}{(K_{d2} + x)} \quad (3.3)$$

Fitting data calculated by equations 3.1 and 3.3 were compared with an F -test.

Competition Binding Experiments

One-site binding model

Data from competition binding experiments were fitted to the equation 3.4 to calculate Hill coefficient (n_H).

$$y = \frac{B_0}{1 + 10^{(\log IC_{50} - x) \cdot n_H}} \quad (3.4)$$

Data were fitted to equation 3.5 to calculate the IC_{50} value of the competing compound.

$$y = \frac{B_0}{1 + 10^{x - \log IC_{50}}} \quad (3.5)$$

y is the specific binding of radioligand, x is the logarithm of the competitor concentration. B_0 is the amount of specific radioligand binding in a single experiment in the absence of competitor (or its concentration is infinitesimal).

To obtain the inhibition constant (K_i) of the competing ligand from the determined IC_{50} value, which is the concentration of unlabeled competitor displacing 50% of the specifically bound radioligand, the Cheng-Prusoff equation¹⁸² 3.6 was applied. K_i value is equal to its equilibrium dissociation binding constant and defines its affinity.

$$K_i = \frac{IC_{50}}{\left(1 + \frac{L}{K_d}\right)} \quad (3.6)$$

where L is the radioligand concentration, K_d is the equilibrium dissociation constant of the radioligand.

Two-site binding model

If the obtained Hill coefficient was significantly different from unity the competition curves were reanalyzed and fitted to a two-site binding model of high- and low-affinity binding. The equation 3.7 describes the competition of a competing ligand for two binding sites with different affinities while the radioligand has identical affinity for both sites.

$$y = \frac{B_0 \cdot fraction1}{1 + 10^{(x - \log IC_{50_1})}} + \frac{B_0 \cdot (1 - fraction1)}{1 + 10^{(x - \log IC_{50_2})}} \quad (3.7)$$

fraction 1 is the fraction of the receptors that have an affinity described by $\log IC_{50_1}$, while the remaining receptors have an affinity described by $\log IC_{50_2}$. If $\log IC_{50_1}$ is smaller than $\log IC_{50_2}$, then fraction₁ is the fraction of high affinity sites.

For comparing non-linear regression fits for one- and two-site binding models, data were calculated by equations 3.5 and 3.7 and compared with an *F*-test (equation 3.8).

$$F = \frac{(SS_1 - SS_2)/(df_1 - df_2)}{SS_2/df_2} \quad (3.8)$$

where SS is the residual sum of the squares, df are the degrees of freedom ($_1 =$ one-site model, $_2 =$ two-site model). The two-site model is assumed to be a better fit than the one-site model if the F value has a $P < 0.05$.

GTP Shift

The comparison of the non-linear regression fits was performed according to Graeser and Neubig.¹⁸³ One- and two-site binding models of control data (c) and Gpp(NH)p treated data (e) were calculated by equations 3.5 and 3.7 and each set of data was compared by applying F -test statistics (equation 3.8).

$$F = \frac{(SS_1 - SS_2)/(df_1 - df_2)}{SS_2/df_2} \quad (3.8)$$

SS is the residual sum of the squares, df is the degrees of freedom ($_1 =$ one-site model, $_2 =$ two-site model). The two-site model is assumed to give a better fit than the one-site model if the F value has a $P < 0.05$. In competition binding that was fitted best by a two-site binding model, inhibition constants for the higher (K_H) and lower (K_L) affinity site and the % higher affinity sites (R_H) were obtained.

A third data set was created by combining control data (c) and Gpp(NH)p treated data (e) and were analyzed by the one-site binding model (3.5) to generate SS_{ce} and df_{ce} . Statistical significance of differences between c and e was determined by calculating the F -test ($P < 0.05$) from equation (3.9).

$$F = \frac{[SS_{ce} - (SS_c + SS_e)]/[df_{ce} - (df_c + df_e)]}{[(SS_c + SS_e)/(df_c + df_e)]} \quad (3.9)$$

SS_c and SS_e represent the residual sum of the squares of c and e, respectively, df_c and df_e are the degrees of freedom of c and e, respectively.

Statistics

Unless it is stated otherwise, data are presented as means with standard deviation (\pm SD) of at least three independent experiments carried out in triplicates. Statistical significance was assessed using Student's t -test with $P < 0.05$.

3.2.7 Virtual Screening Methods

Virtual Screening methods were performed by the working group of Professor Gisbert Schneider, Johann Wolfgang Goethe-University, Department of Biochemistry, Chemistry and Pharmaceutical Sciences, Frankfurt/Main.

Software program packages

MOE (Version 2005, Molecular Operating Environment, Chemical Computing Group Ltd., Montreal, Canada),

CORINA (Molecular Networks GmbH, Erlangen, Germany),

GOLD (Version 2.2, The Cambridge Crystallographic Data Centre, Cambridge, UK),

SIMCA-P+ 10.5 (Umetrics, Umea, Sweden),

LIBSVM (Version 2.5, <http://www.csie.ntu.edu.tw/~cjlin/libsvm>),¹⁸⁴

PyMOL (Version 0.99, DeLano Scientific LLC., Palo Alto, USA).

4 Results and Discussion

4.1 Assay Validation

The principle method for the determination of ligand binding affinity is the competition radioligand binding assay. To obtain accurate estimates of the equilibrium dissociation constant K_d of the radioligand in saturation binding experiments and of the inhibition constant K_i for the test ligand in competition binding experiments, a subsequent validation of the assay system was of absolute necessity. For setting up a new binding assay general considerations were investigated and best assay conditions were established by carrying out a series of preliminary experiments to provide the best signal-to-noise ratio.¹⁸⁵ To validate the binding assay, ligand binding has to confirm the law of mass action.¹⁸⁶ Due to a finite number of receptors in the tissue, specific binding has to be saturable with increasing radioligand concentrations. Non-specific binding continues to increase as a function of radioligand, however displays minimal non-specific binding (< 20% of the total binding), consequently increasing the precision of the assay by an escalating signal-to-noise ratio. Radioligand binding has to be reversible, consistent with its physiological mechanism. It is recommended that the used radioligand concentration should be in the range of the radioligand K_d , but in order to avoid depletion, less than 10% of the added radioligand is allowed to bound to the receptors.^{185,186} Parameters within the assay such as buffer composition, incubation temperature, pH value, tissue preparation and ionic strength were carefully chosen (cf. 3.2). Initial binding experiments regarding the incubation time, tissue preparation, amount of protein and cell-harvesting with varying rinses were investigated on a trial-and error basis to increase the precision of the assay. Incubation time is important to allow competitor and radioligand to attain equilibrium. At equilibrium the rate of association and dissociation of the ligand-receptor complex are equal, leading to a constant concentration of the ligand-receptor complex. Kinetic binding experiments have not been performed due to previous characterizations of the receptor subtypes and radioligands by other groups in related studies.^{33,181,187} Suitable incubation times (cf. 3.2) have been adapted according to literature protocols.^{125,181,186,188}

4.1.1 Saturation Binding Experiments

In order to determine the equilibrium binding dissociation constant K_d of the radioligand and the total number of specific binding sites B_{max} of the membrane preparation with the receptor of interest, saturation binding experiments were performed. A constant amount of cell membrane preparation, containing either dopamine hD_{2S}, hD₃ (cf. 3.2.3) or histamine

hH₁ receptors (cf. 3.2.4), was incubated with increasing concentrations of radioligand until virtually all of the receptors were occupied. At each radioligand concentration the total binding and non-specific binding were defined in the absence and presence of an unlabeled ligand, respectively. The specific binding is the total binding minus the non-specific binding. Figures 4.1 - 4.3 show total, specific and non-specific binding determined in saturation binding experiments.

Dopamine hD_{2S} and hD₃ Receptors

Representative saturation binding isotherms and Scatchard plots of [³H]spiperone at dopamine hD_{2S} and hD₃ receptors stably expressed in CHO-cells were analyzed (cf. 3.2.6) and are shown in Figures 4.1 and 4.2. In the experiments BP 897 was used in a concentration of 10 μM for dopamine hD_{2S} receptors (Figure 4.1), while either 10 μM BP 897 (Figure 4.2A) or 10 μM haloperidol (Figure 4.2B) was investigated for hD₃ receptors to achieve non-specific binding.

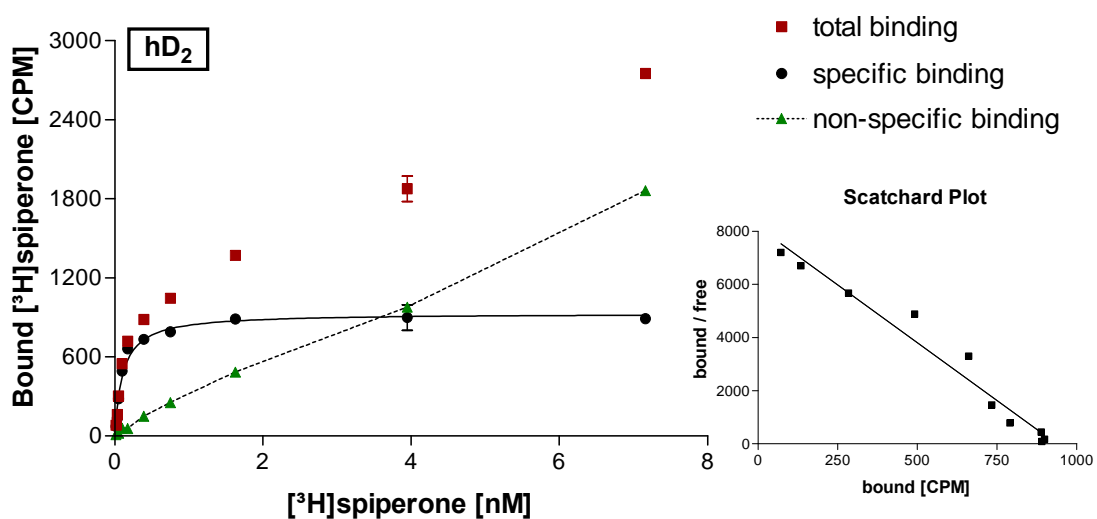
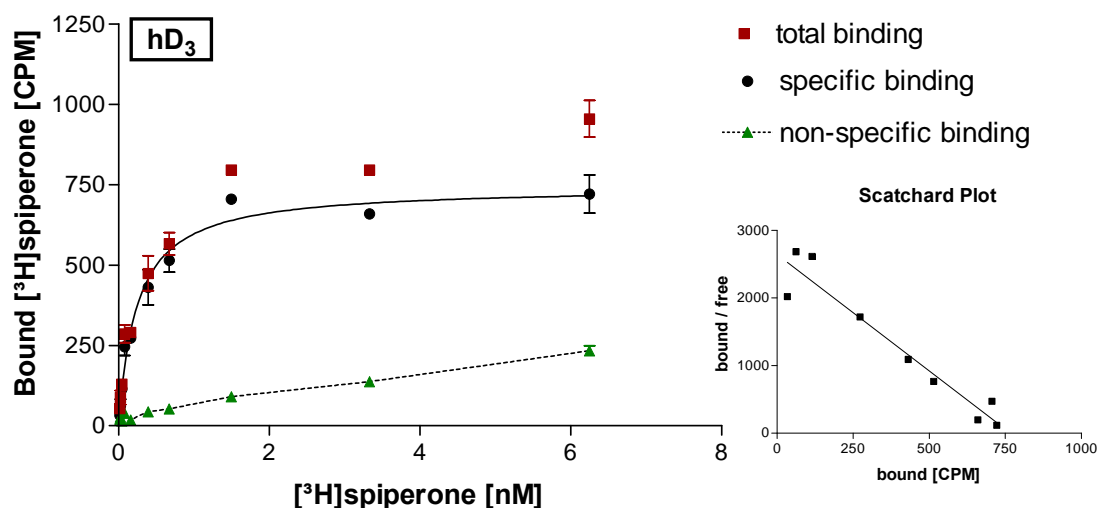


Figure 4.1 Saturation binding isotherms and Scatchard plot of [³H]spiperone at dopamine hD_{2S} receptors. Non-specific binding was determined with 10 μM BP 897.

In all saturation binding experiments specific binding of [³H]spiperone calculated for dopamine hD_{2S} and hD₃ was saturable as the concentration of the radioligand increased and consistent with a one-site binding model. Non-specific binding was not saturated with radioligand and therefore it was linear within increasing concentrations of radioligand. Non-specific binding was negligible (< 20% of the total binding) and confirmed the precision of the assay. Scatchard analysis of the specific [³H]spiperone binding at both receptor subtypes resulted in linear plots consistent with a single class of binding sites

without any co-operativity. Equilibrium dissociation constants K_d and the total number of specific binding sites B_{max} values of [3H]spiperone binding to CHO-cell membranes stably expressing dopamine hD_{2S} or hD₃ obtained are presented in Table 4.1.

A



B

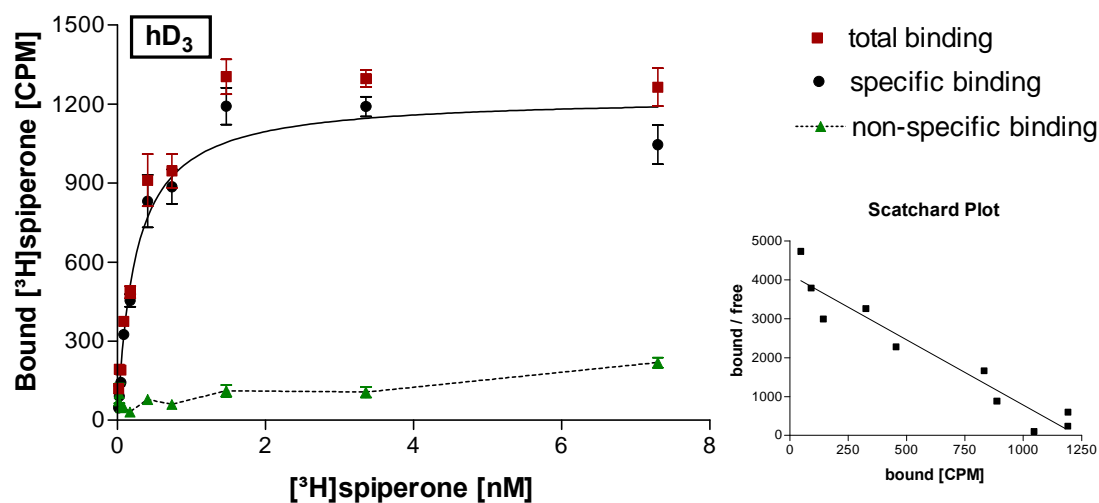


Figure 4.2 Saturation binding isotherms and Scatchard plot of [3H]spiperone at dopamine hD₃ receptors. **A** Non-specific binding was determined with 10 μ M BP 897. **B** Non-specific binding was determined with 10 μ M haloperidol.

Table 4.1 Equilibrium dissociation constants and total number of specific binding sites derived from [3H]spiperone saturation binding experiments.

Receptor	Non-specific binding	K_d [nM]	B_{max} [fmol/ μ g]
hD _{2S}	10 μ M BP897	0.11 ± 0.01	0.41 ± 0.02
hD ₃	10 μ M BP897	0.22 ± 0.02	4.53 ± 0.22
hD ₃	10 μ M haloperidol	0.22 ± 0.02	3.77 ± 0.19

The estimated K_d values are in good agreement with results previously described for dopamine hD_{2S} ($K_d = 0.10$ nM)¹⁸⁹ or hD_3 receptors ($K_d = 0.26$ nM)¹⁸⁹ expressed in CHO-cells. In transfected cell lines, including CHO-cells, K_d values for [³H]spiperone are reported as 0.04 to 0.15 nM at dopamine D_{2S} receptors,^{10,190,187,191} and 0.2 to 0.5 nM at dopamine D_3 receptors.¹⁸⁹ Highest concentrations of binding sites were determined for membranes containing the dopamine hD_3 receptor subtype, while lower concentrations were revealed for dopamine hD_{2S} receptors.¹⁹² The density of sites and specific binding varies within CHO-cell lines.¹⁸⁶ Although there was no difference between the K_d values of dopamine hD_3 determined with 10 μ M BP 897 and 10 μ M haloperidol, the B_{max} was significantly lower ($P < 0.05$, unpaired t -test) using 10 μ M haloperidol. A possible explanation might be that haloperidol is an inverse agonist^{193,194} on dopamine D_2 -like receptors while BP 897 behaves as a partial dopamine D_3 receptor agonist and stabilizes different conformational states of the receptor. Due to the close structural similarity of the butyrophenone derivatives haloperidol and [³H]spiperone, BP 897 was chosen to determine non-specific binding for further assay development in order to avoid isotope dilution.¹⁸⁶ The non-specific binding of a radioligand is assessed in the presence of a high concentration of an unlabeled ligand, which is recommended to be chemically different from the radioligand, polar and affine, and adequate to prevent radioligand binding to its target site. The data received from saturation binding experiments confirmed a well established assay system for further determination of binding affinity constants of novel compounds in competition binding assays.

Histamine H_1 Receptors

Saturation binding isotherms and Scatchard plots of [³H]mepyramine at histamine H_1 receptors stably expressed in CHO-cells were analyzed (3.2.6) and are demonstrated in Figure 4.3. 10 μ M chlorpheniramine was investigated for hH_1 receptors to achieve non-specific binding. The binding of [³H]mepyramine at the human H_1 receptor expressed in CHO-cells was specific and saturable at higher concentration of radioligand. Non-specific binding increased with rising concentrations of radioligand and were less than 20% of total binding in the concentration range of interest. Scatchard transformation of the [³H]mepyramine saturation isotherm resulted in a linear plot and displayed that the binding was to single class of binding sites without any co-operativity. The estimated K_d value (cf. 3.2.6) is in good agreement with the K_d data of 1.2 nM previously described by Anthes et al. for histamine hH_1 receptors in CHO-cells (Table 4.2).^{181,195}

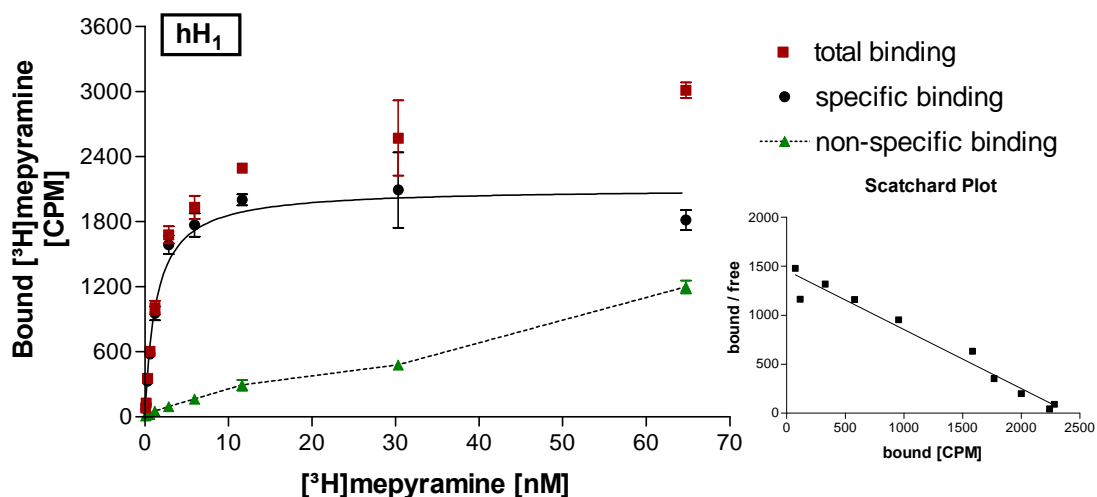


Figure 4.3 Saturation binding isotherms and Scatchard plot of [³H]mepyramine to histamine hH₁ receptors.

Table 4.2 Equilibrium dissociation constant and total number of specific binding sites derived from [³H]mepyramine saturation binding experiments.

Receptor	Non-specific binding	K_d [nM]	B_{max} [fmol/ μ g]
hH ₁	10 μ M chlorpheniramine	1.28 ± 0.06	1.87 ± 0.36

4.1.2 Competition Binding Experiments

In order to validate competition binding assays a variety of well characterized reference drugs with antagonist properties at dopamine hD_{2S}, hD₃ (cf. 3.2.3) or histamine hH₁ receptors (cf. 3.2.4) were tested. Increasing concentrations of unlabeled ligand competed for the receptor with a constant concentration of radioligand. The concentration of competitor which inhibits 50% of specific binding, the IC_{50} , and the slope of the inhibition curve, the Hill slope n_H , have been estimated to determine the dissociation constant of the competitor, K_i (cf. 3.2.6). It is of importance that the non-specific binding is less than 20% of the total binding at the radioligand concentration equivalent to its K_d . The selection of reference compounds considered an affinity range of at least three orders of magnitude to give variations in selectivity profile. The obtained inhibition constants (K_i) of unlabeled test compounds were compared to literature data.

Dopamine hD_{2S} and hD₃ Receptors

For validation of the competition radioligand binding assay with [³H]spiperone at dopamine hD_{2S} and hD₃ receptors, reference compounds with antagonist properties at dopamine D₂-like receptors were assessed. Representative competition binding curves are shown in Figures 4.4 and 4.5 for dopamine hD_{2S} and hD₃ receptors, respectively. Data are presented as a percentage of maximal specific binding. The determined inhibition constants K_i (cf. 3.2.6) of reference substances investigated for assay validation at dopamine hD_{2S} and hD₃ receptors are presented in Table 4.3.

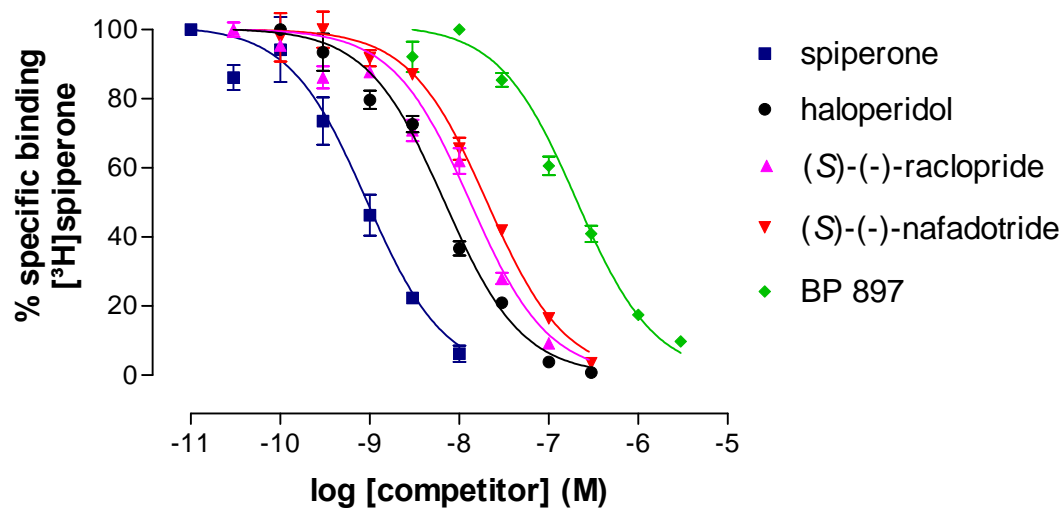


Figure 4.4 Competition curves of reference drugs at [³H]spiperone binding sites for hD_{2S} receptors.

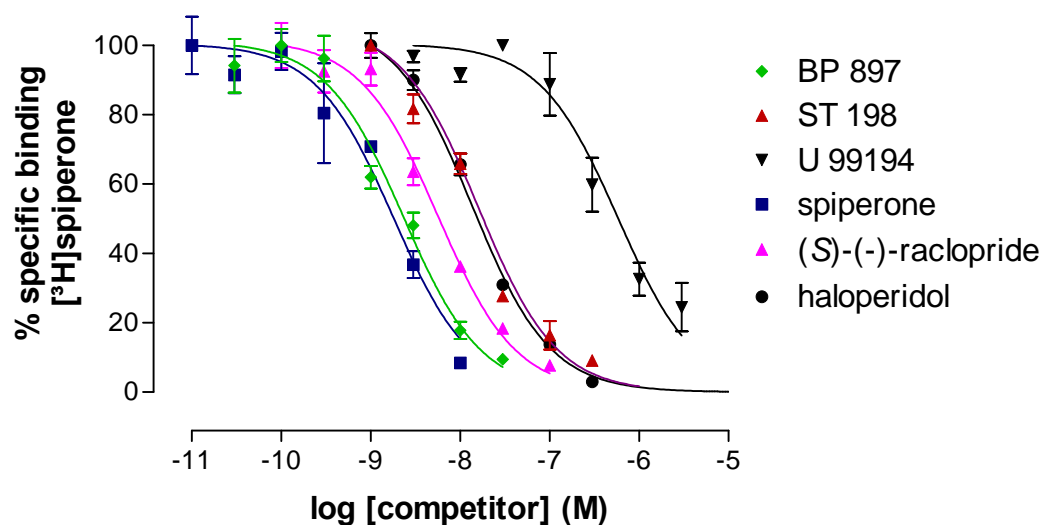


Figure 4.5 Competition curves of reference drugs at [³H]spiperone binding sites for hD₃ receptors.

Competition between the radioligand [^3H]spiperone and inhibitor was consistent with the law of mass action and has demonstrated constantly a one-site binding model for dopamine $\text{hD}_{2\text{S}}$ and hD_3 receptors (cf. 3.2.6). The Hill coefficients were mostly not significantly different from unity, otherwise it has been mentioned. The non-specific binding was less than 20% of the total binding and in addition, less than 10% of the added radioligand was depleted by the receptor. The determined K_i values of tested reference drugs were consistent with results performed by other groups (reference data: BP 897: K_i (D_2) = 61 nM, K_i (D_3) = 0.92 nM;^{140,61} haloperidol: K_i (D_2) = 2.4 nM, K_i (D_3) = 4.8 nM;¹⁰ (*S*)-(-)-nafadotride: K_i (D_2) = 3 nM;¹³⁸ (*S*)-(-)-raclopride: K_i (D_2) = 2.9 nM, K_i (D_3) = 3.5 nM;¹⁹⁶ spiperone: K_i (D_2) = 0.25 nM, K_i (D_3) = 0.61 nM;¹⁰ ST 198: K_i (D_2) = 780 nM, K_i (D_3) = 12 nM;⁸³ U 99194A: K_i (D_2) = 2280 nM, K_i (D_3) = 223 nM¹⁰⁴).

Spiperone/[^3H]spiperone competition binding experiments using dopamine $\text{hD}_{2\text{S}}$ and hD_3 receptors yielded spiperone dissociation constants (K_i) higher than K_d values of [^3H]spiperone assessed in saturation binding experiments. These results are in agreement with literature data, indicating that the K_i value of a compound deviates with the affinity of its radiolabeled complement.¹⁸⁸ In summary, the binding assays provided a good signal-to-noise ratio and determined data were reproducible and reliable.

Table 4.3 Inhibition constants K_i and Hill coefficients (in parentheses) of determined dopamine reference compounds.

Compound	K_i [nM] $\text{hD}_{2\text{S}}$	K_i [nM] hD_3
BP 897	52 ± 11.7 (1.12 ± 0.30)	0.91 ± 0.23 (0.98 ± 0.28)
Haloperidol	2.26 ± 0.30 (0.95 ± 0.05)	4.65 ± 0.22 (1.04 ± 0.15)
(<i>S</i>)-(-)-Nafadotride	6.46 ± 0.21 (1.03 ± 0.05)	n.d. ^a
(<i>S</i>)-(-)-Raclopride	4.51 ± 0.11 (1.07 ± 0.12)	2.50 ± 0.87 (0.85 ± 0.14)
Spiperone	0.27 ± 0.01 (0.99 ± 0.15)	0.68 ± 0.07 (1.02 ± 0.22)
ST 198	1272 ± 99 (0.95 ± 0.11)	8.72 ± 0.21 (0.76 ± 0.11)
U 99194A	3852 ± 672 (0.84 ± 0.16)	314 ± 92 (0.82 ± 0.06)

^an.d., not determined.

Histamine H_1 Receptors

For the evaluation of the radioligand competition binding assay at histamine H_1 receptors (cf. 3.2.4), a variety of reference histamine H_1 receptor antagonists, first and second

generation of antihistamines, has been tested for competition binding with [^3H]mepyramine. A selection of representative competition binding curves for histamine H_1 receptors is shown in Figure 4.6.

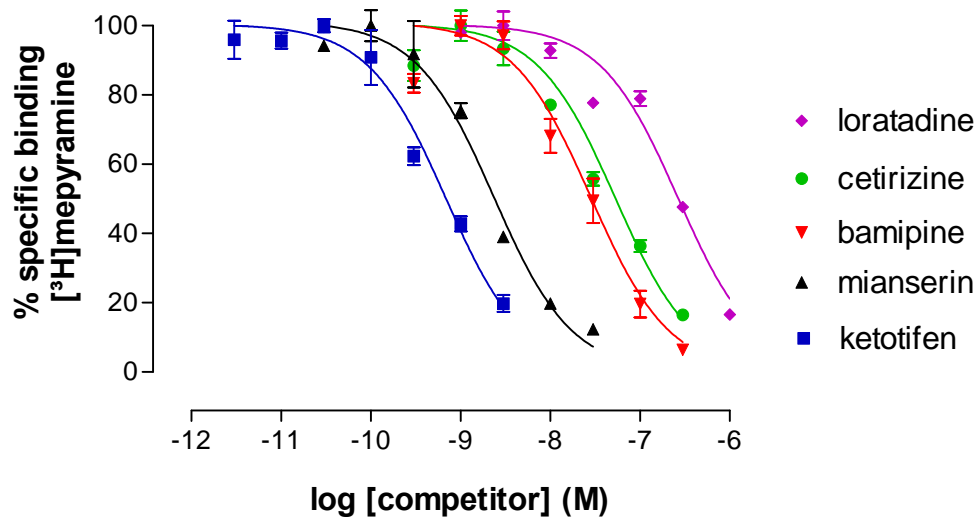


Figure 4.6 Competition curves of reference drugs at [^3H]mepyramine binding for hH_1 receptors.

Data are presented as a percentage of maximal specific binding. The determined inhibition constants (K_i) of reference drugs were analyzed (cf. 3.2.6) and are summarized in Table 4.4.

Table 4.4 Inhibition constants K_i and Hill coefficients (in parentheses) of determined histamine reference compounds.

Compound	K_i [nM] hH_1
Bamipine	12 ± 0.9 (1.16 ± 0.51)
Cetirizine	28 ± 7.0 (0.79 ± 0.18)
Chlorpheniramine	17 ± 2.56 (1.00 ± 0.19)
Diphenhydramine	35 ± 1.6 (0.86 ± 0.07)
Fexofenadine	34 ± 2.0 (0.86 ± 0.12)
Ketotifen	0.34 ± 0.07 (1.05 ± 0.13)
Loratadine	130 ± 54 (1.00 ± 0.06)
Mepyramine	1.75 ± 0.12 (0.79 ± 0.02)
Mianserin	0.84 ± 0.26 (1.18 ± 0.12)

The compounds behaved as competitive inhibitors of [³H]mepyramine binding and competition binding curves were consistent with the law of mass action and indicated a one-site binding model due to the Hill coefficients, not significantly different from unity (cf. 3.2.6). The non-specific binding was less than 20% of the total binding. Less than 10% of the added radioligand was depleted by the receptor. The determined K_i values of tested reference drugs were consistent with results performed by other groups (reference data: bamipine: no reference K_i data are available at cloned histamine hH₁ receptors; cetirizine: K_i (H₁) = 30 nM; chlorpheniramine: K_i (H₁) = 14 nM; diphenhydramine: K_i (H₁) = 45 nM; fexofenadine: K_i (H₁) = 52 nM; ketotifen: K_i (H₁) = 0.14 nM; mepyramine: K_i (H₁) = 1.7 nM; mianserin: K_i (H₁) = 0.85 nM; loratadine: K_i (H₁) = 138 nM).^{149,195,197} As already observed for [³H]spiperone and spiperone in competition binding experiments at dopamine hD_{2S} and hD₃ receptors, the K_i value for mepyramine is higher than the K_d data of [³H]mepyramine. Conclusively, the assessed data were reproducible, reliable and in good agreement with literature data, providing precise assay conditions.^{149,181,195}

4.1.3 GTP Shift Assay for Discriminating Agonists

Agonist binding is in general more complex than antagonist binding to G protein-coupled receptors. This different binding behavior allows distinguishing agonists from antagonists in simple radioligand competition binding studies. The use of disrupted cell membrane preparations in low ionic strength media containing magnesium and lack of sodium forms a high-affinity agonist/receptor/G protein ternary complex.¹⁹⁸ Under these assay conditions, binding curves of agonists demonstrate a shallow shape, appear multiphasic and are analyzed according to a multiple, independent-site model. At least two apparent affinity states are determined; described K_H (high affinity) and K_L (low affinity). This agonist-induced isomerisation is also recognized for dopamine receptors. The high affinity ternary complex is effectively modulated by guanine nucleotides such as guanosine-5'-triphosphate (GTP) (Chart 4.1). In the presence of GTP the high-affinity binding state of the receptor is eliminated, and results in a rightward shift of the competition curve, the so-called "GTP shift", and a monophasic binding curve, mostly with steepening of the shallow Hill slope to unity. It represents the lower affinity of the bimolecular agonist-receptor complex (K_{iGTP}), but it is noteworthy that the K_L is not equivalent to K_{iGTP} (Figure 4.7).¹⁸⁵

In this study the effect of the nonhydrolysable GTP analogue 5'-guanylyl-imidodiphosphate [Gpp(NH)p] (Chart 4.1) on ligand binding to dopamine D_{2S} and D₃ receptors has been investigated.

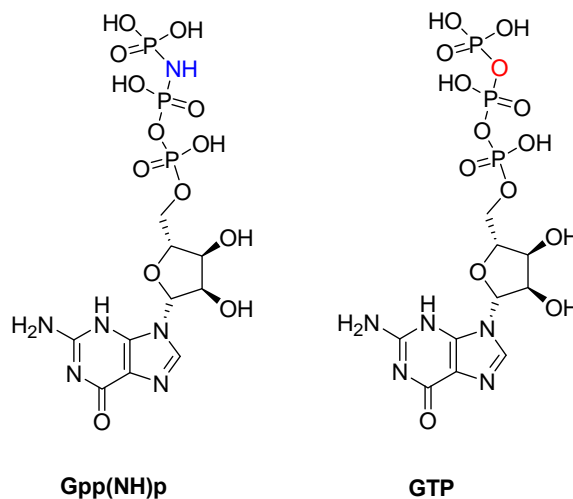


Chart 4.1 Structures of Gpp(NH)p and GTP.

It was of great interest to examine whether there are high and low affinity states for both receptor subtypes in the presence of an agonist, antagonist and partial agonist, and whether there is an alteration in affinity binding of ligands induced by added Gpp(NH)p resulting in a GTP shift at dopamine D_{2S} and D₃ receptors. For a more detailed discussion of the GTP shift see Figure 4.16.

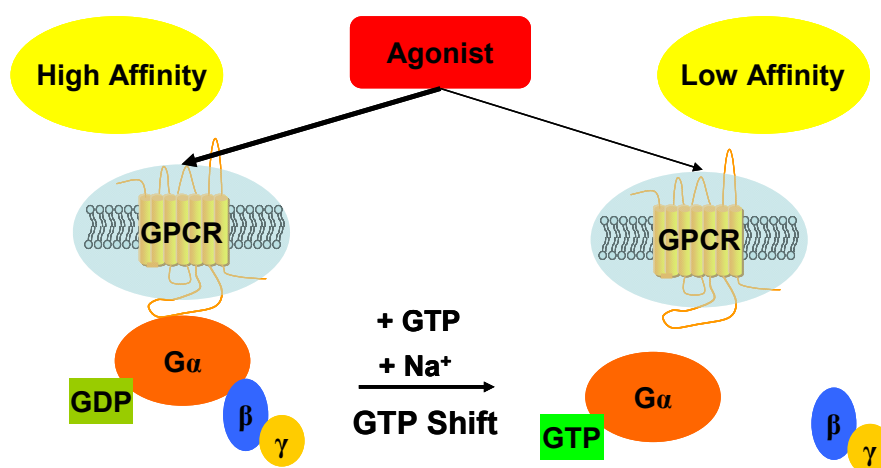
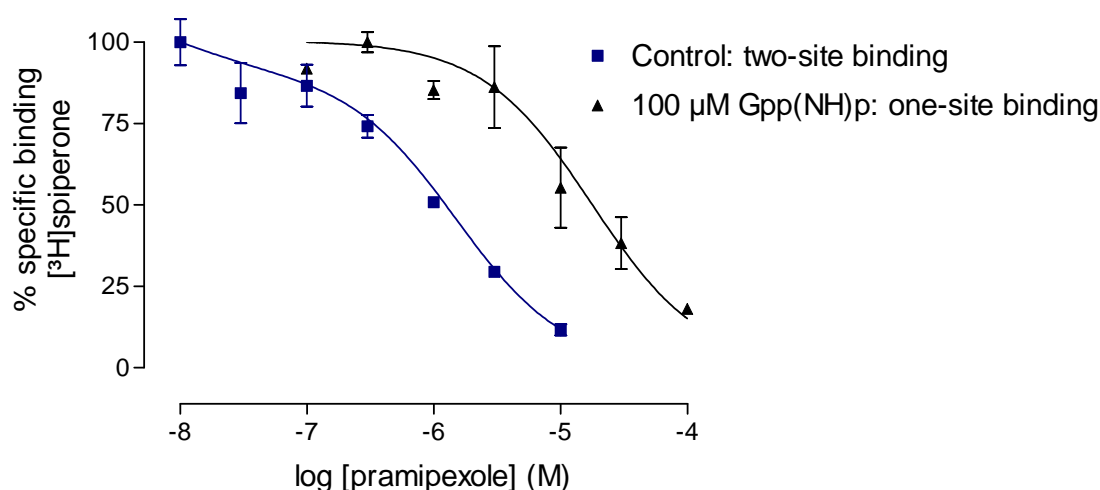


Figure 4.7 Scheme of the GTP shift.

Radioligand competition binding studies were performed using [³H]spiperone and selected ligands were assessed under different assay conditions as described by Mierau et al.¹³⁵ According to literature, the binding of [³H]spiperone has not been effected by the addition of Gpp(NH)p or sodium ions.¹⁹⁹

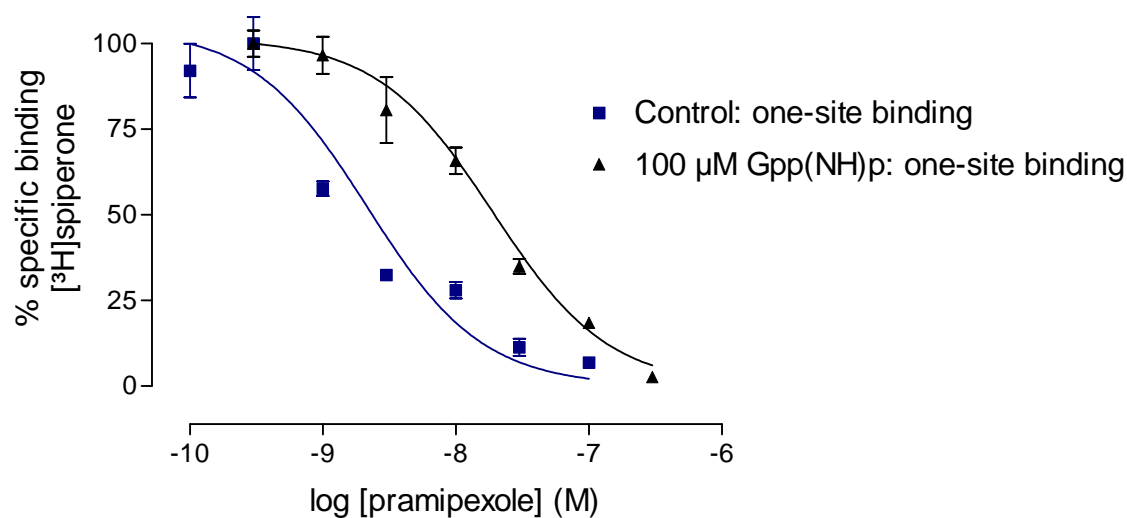
100 μM Gpp(NH)p and 120 mM NaCl were applied to observe the effect on affinity binding in order to produce a GTP shift (cf. 3.2.5). These concentrations have been used on regular basis by other groups in related studies, and produced maximal response and ensured complete conversion of higher affinity sites to lower affinity sites.¹⁹⁹ For dopamine D_{2S} and D₃ receptor agonist binding pramipexole (cf. 1.2.6) and its seleno analogue compound **54** (2-amino-6-(ethylamino)-4,5,6,7-tetrahydrobenzo[1.3]selenazole) (cf. 4.2.3) were selected. The methoxyphenylpiperazine derivative BP 897 was chosen as a partial agonist at dopamine D₃ and antagonist at dopamine D₂ and 1,2,3,4-tetrahydroisoquinoline compound ST 198 represented the antagonist at dopamine D₂ and D₃ receptors (cf. 1.2.6).

In the absence of Gpp(NH)p, competition binding experiments for pramipexole and compound **54** at dopamine D_{2S} receptors were best described by a two-site binding model (*F*-test, *P* < 0.001) (cf. 3.2.6) and the affinities of higher and lower affinity sites (*K_H* and *K_L*) and their proportion (*R_H*) were derived (Figures 4.8 and 4.10). In the presence of 100 μM Gpp(NH)p competition curves were best described by a one-site binding model (*F*-test, *P* < 0.05) and *K_i* Gpp(NH)p was assessed (cf. 3.2.6) as illustrated in Figures 4.8 and 4.10.



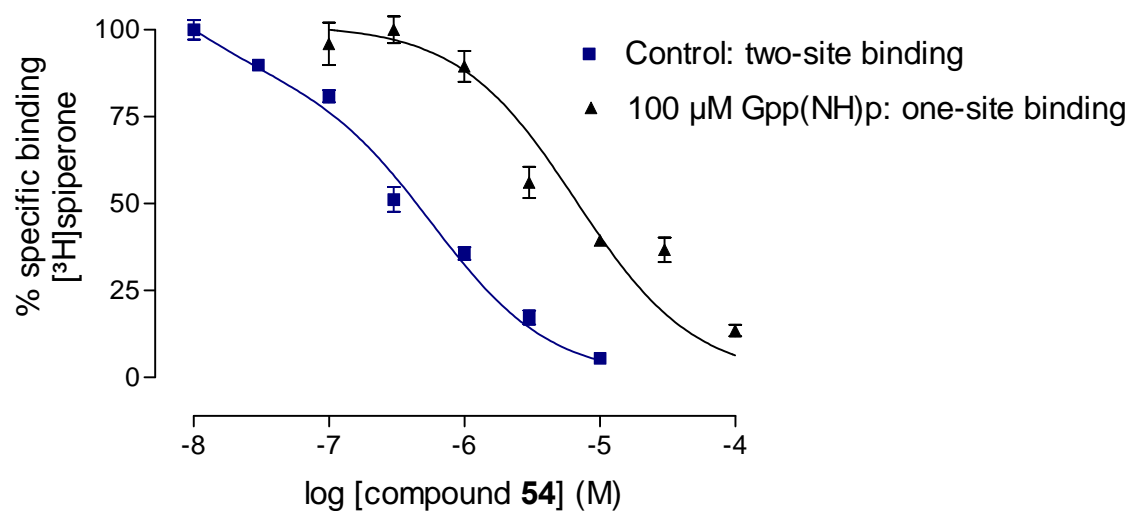
	<i>K_H</i> [nM]	% <i>R_H</i>	<i>K_L</i> [nM]	n	<i>K_i</i> Gpp(NH)p [nM]	n
hD_{2S}	3.07 ± 0.83	23 ± 7	348 ± 143	3	4989 ± 865 (0.80 ± 0.12)	4

Figure 4.8 Pramipexole binding at dopamine D_{2S} receptors (Hill coefficients in parentheses).



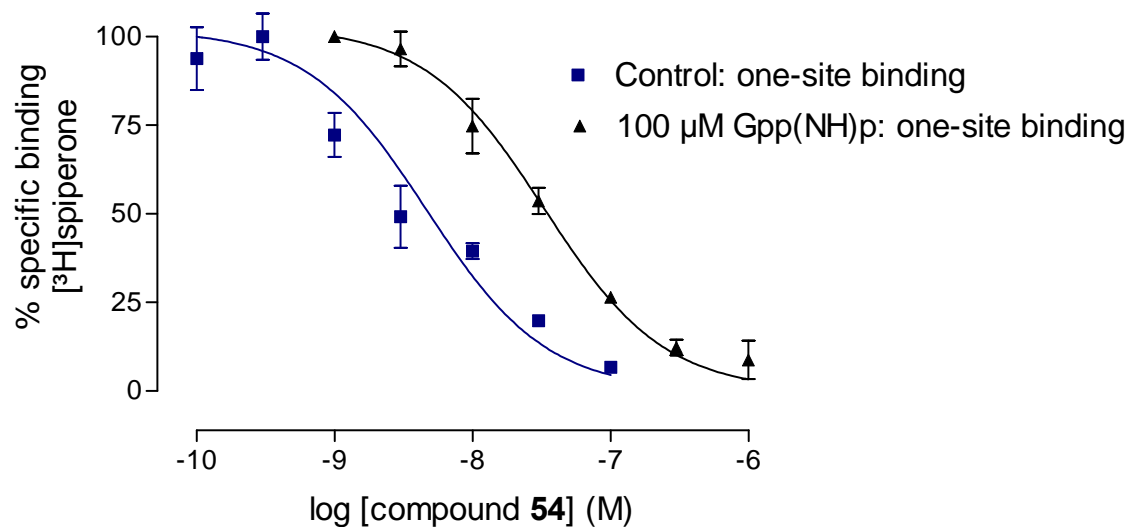
	K_{control} [nM]	n	K_i Gpp(NH)p [nM]	n
hD₃	1.19 ± 0.06 (0.72 ± 0.21)	3	12 ± 3.0 (0.94 ± 0.20)	4

Figure 4.9 Pramipexole binding at dopamine D₃ receptors (Hill coefficients in parentheses).



	K_H [nM]	% R_H	K_L [nM]	n	K_i Gpp(NH)p [nM]	n
hD_{2S}	2.54 ± 1.24	33 ± 5	185 ± 33	3	2449 ± 250 (0.69 ± 0.09)	4

Figure 4.10 Compound 54 binding at dopamine D_{2S} receptors (Hill coefficients in parentheses).



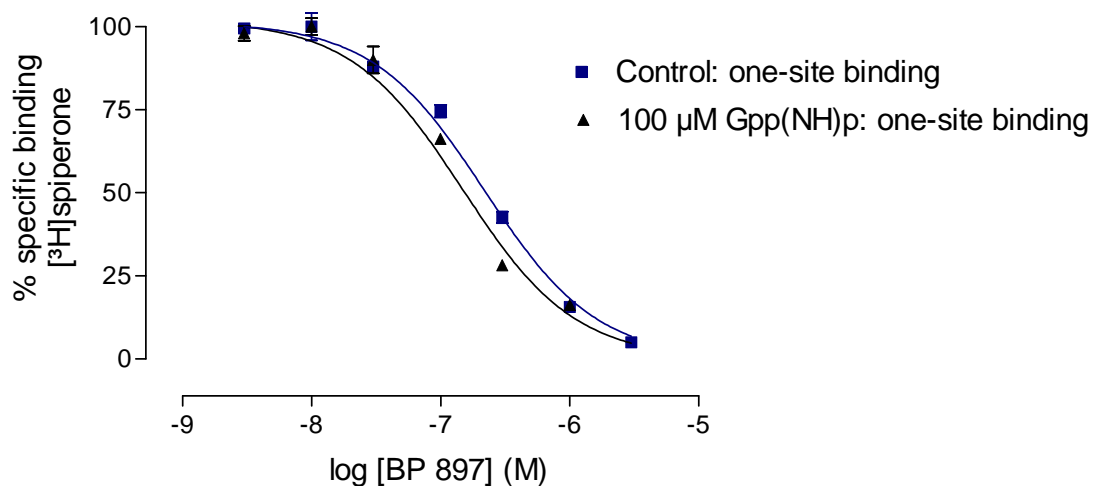
	K_i control [nM]	n	K_i Gpp(NH)p [nM]	n
hD₃	3.18 ± 0.72 (0.78 ± 0.17)	3	19 ± 3.6 (0.89 ± 0.22)	3

Figure 4.11 Compound **54** binding at dopamine D₃ receptors (Hill coefficients in parentheses).

The affinity of the lower affinity site (K_L) assessed in the absence of Gpp(NH)p compared to the single site observed in the presence of Gpp(NH)p (K_i Gpp(NH)p) were not similar for pramipexole and also for compound **54**. This observation has already been reported for pramipexole.¹³⁵ The percentage of the high-affinity binding site (R_H) for pramipexole and compound **54** was $23 \pm 7\%$, and $33 \pm 5\%$, respectively. In the case of binding at dopamine D₃ receptors, the competition curves in the absence and presence of Gpp(NH)p were best described by a one-site binding model for both ligands (F -test, $P < 0.05$) as demonstrated in Figures 4.9 and 4.11. There was a significant decrease in affinity binding and consequently an observed GTP shift for pramipexole and compound **54** in the presence of the guanine nucleotide analogue (F -test, $P < 0.05$). The studies have shown that pramipexole has a preference for binding to human D₃ receptors over the D_{2S} receptor.¹³⁵ By comparing data received from the high affinity state (K_H) at dopamine D_{2S} with the K_i control value in the absence of Gpp(NH)p at dopamine D₃ for compound **54**, similar dissociation constants were assessed displaying neither preference for one of the receptor subtypes.

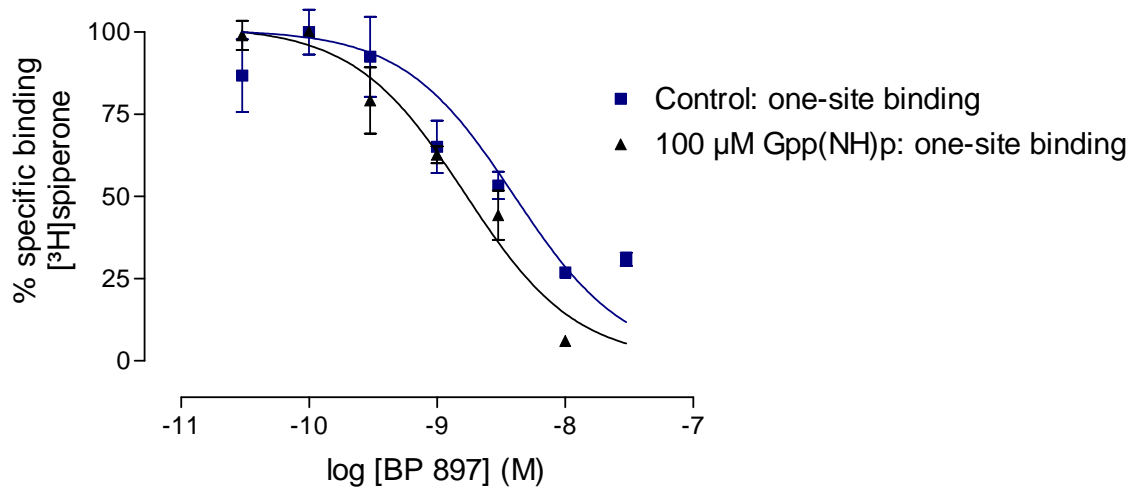
Competition binding curves for the partial agonist BP 897 at dopamine D₃ and antagonist at D_{2S} receptors were best described by a one-site binding model (cf. 3.2.6) in the absence and presence of Gpp(NH)p (F -test, $P < 0.05$) and were characterized by Hill slopes not significantly different from unity (Figures 4.12 and 4.13). Binding data at dopamine D_{2S}

receptors demonstrated no significant difference between the absence and presence of Gpp(NH)p, but an increase in affinity binding of BP 897 in the presence of guanine nucleotide at dopamine D₃ receptors (*F*-test, *P* < 0.05).



	K_i control [nM]	n	K_i Gpp(NH)p [nM]	n
hD_{2S}	79 ± 0.5	3	53 ± 2.2	3
	(1.18 ± 0.27)		(1.30 ± 0.20)	

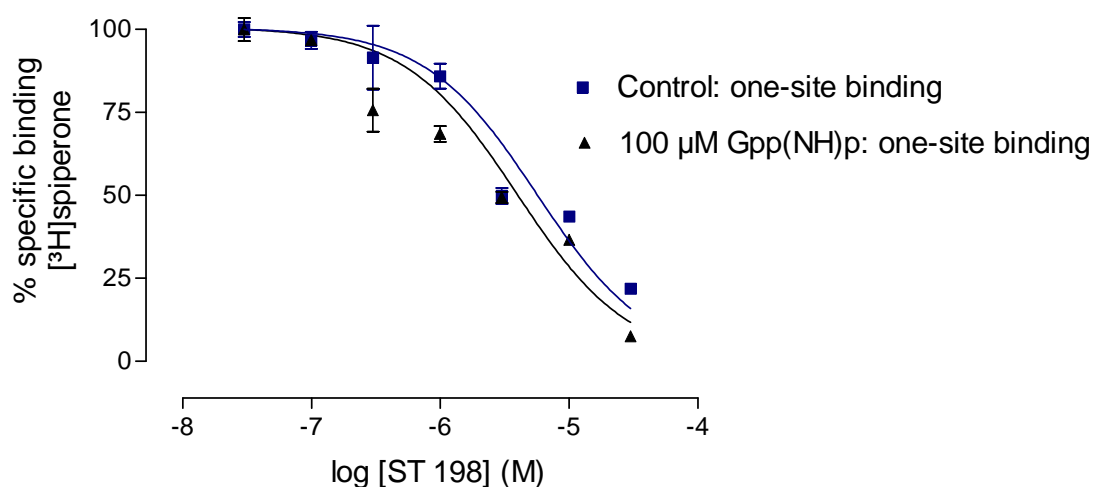
Figure 4.12 BP 897 binding at dopamine D_{2S} receptors (Hill coefficients in parentheses).



	K_i control [nM]	n	K_i Gpp(NH)p [nM]	n
hD₃	1.74 ± 0.16	3	0.76 ± 0.12	3
	(0.80 ± 0.21)		(1.10 ± 0.03)	

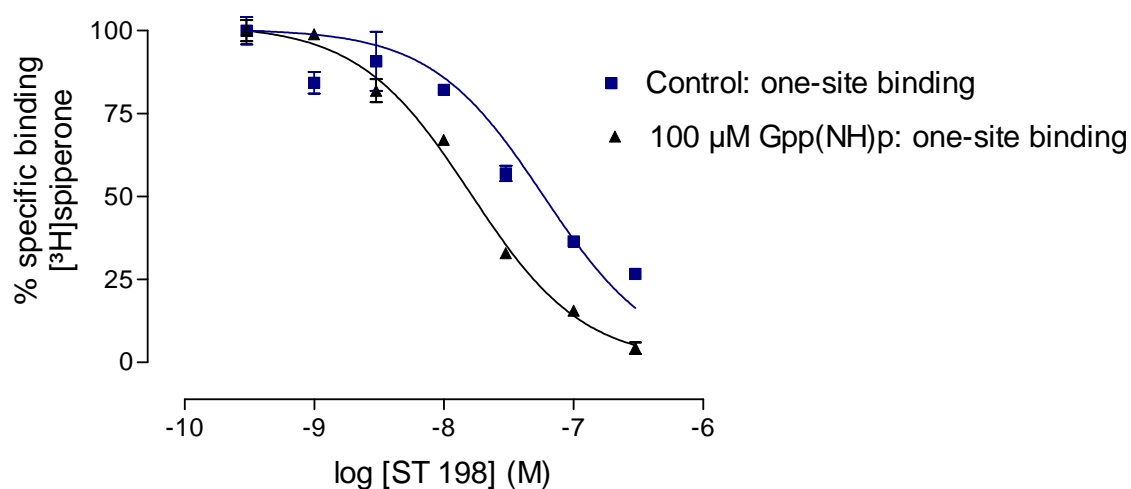
Figure 4.13 BP 897 binding at dopamine D₃ receptors (Hill coefficients in parentheses).

For the antagonist ST 198 tested in each dopamine receptor subtype cell line in the absence and presence of Gpp(NH)p the competition curves were considered by Hill slopes not significantly different from unity and were best fitted by a one-site binding model (cf. 3.2.6) (F -test, $P < 0.05$) as shown in Figures 4.14 and 4.15. There was no difference between competition binding curves in the absence and presence of Gpp(NH)p at dopamine D_{2S} receptors. However an apparent effect of guanine nucleotide was observed for dopamine D_3 receptors and it faintly shifted the competition binding curve to the left sight and resulted in an improved affinity profile (F -test, $P < 0.05$).



	K_i control [nM]	n	K_i Gpp(NH)p [nM]	n
hD_{2S}	1830 ± 142 (0.84 ± 0.10)	4	1071 ± 143 (0.86 ± 0.18)	4

Figure 4.14 ST 198 binding at dopamine D_{2S} receptors (Hill coefficients in parentheses).



	K_i control [nM]	n	K_i Gpp(NH)p [nM]	n
hD₃	55 ± 8.4 (0.86 ± 0.06)	3	7.67 ± 1.20 (0.93 ± 0.16)	4

Figure 4.15 ST 198 binding at dopamine D_3 receptors (Hill coefficients in parentheses).

The model of the ternary complex and its extension allow to illustrate a GTP shift.¹⁹⁸ In the ternary complex model (Figure 4.16A) the receptor (R) can bind simultaneously an agonist (A) and a G protein (G) to form a ternary complex (ARG).

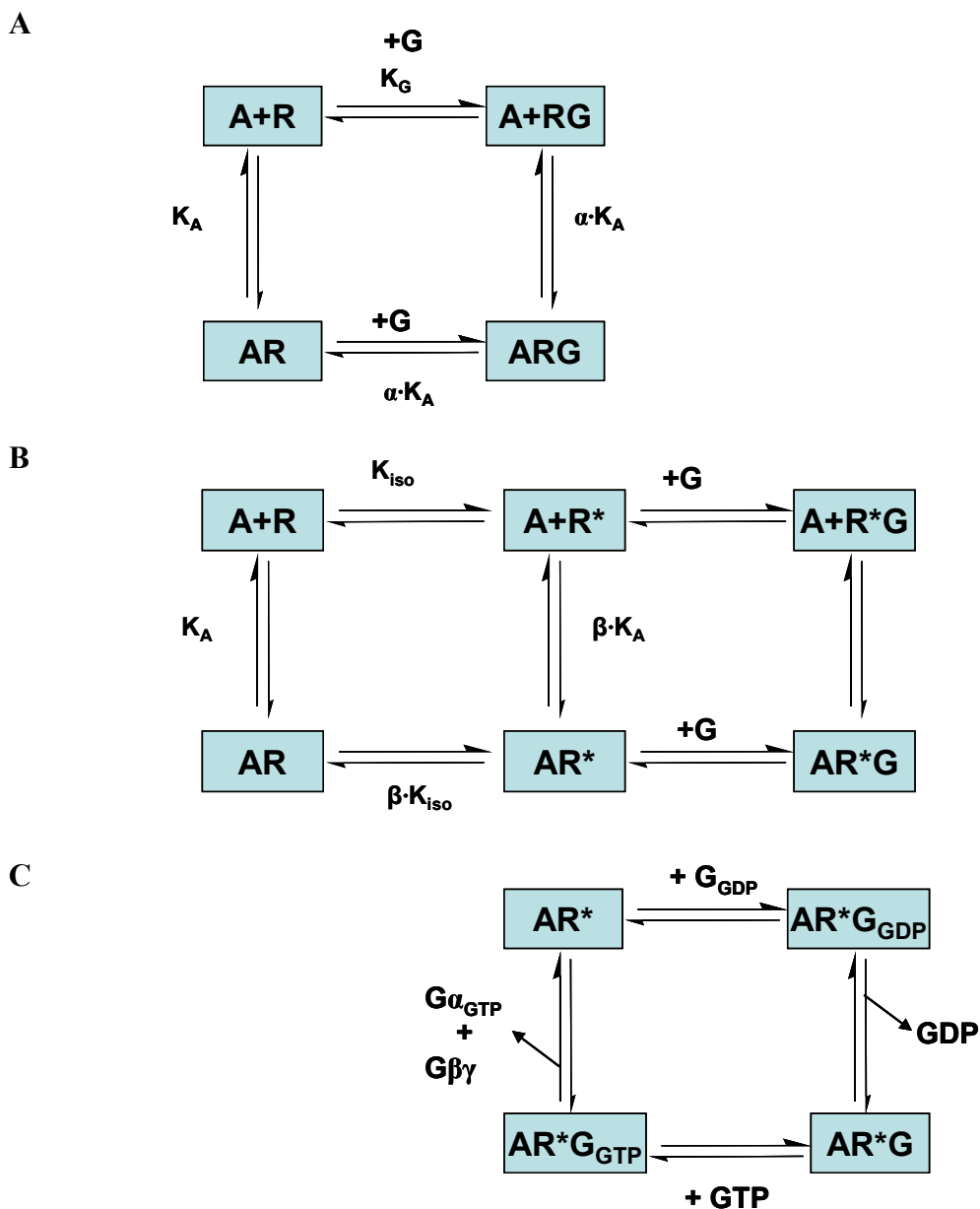


Figure 4.16 **A** The ternary complex. A represents the agonist ligand with an affinity of K_A , G represents a G protein with an affinity of K_G for the receptor, and α is a co-operativity factor reflecting the change in affinity of agonist ligand or G protein when the receptor is occupied by the other ligand (adapted from Lazareno and Birdsall).²⁰⁰ **B** Extended ternary complex. Proportions of ground state (R) and active state (R^*) are determined by the isomerisation constant (K_{iso}). β is a co-operativity factor and determines the difference of agonist affinity for the ground and active state (adapted from Lazareno and Birdsall).²⁰⁰ **C** G protein activation. Exchange of GDP/GTP on G protein activates the receptor and GTP binding induces the dissociation of $G\alpha$ from $G\beta\gamma$ (adapted from Roberts and Waelbroeck).²⁰¹

Accordingly, the G protein is activated when bound to the receptor. Agonist binding to the receptor induces G protein activation by enhancing the affinity of the receptor for the G protein. The agonist has a higher affinity for the G protein-coupled receptor (RG) than for the free receptor (R). The agonist binding contributes to the stabilisation of the ternary complex of agonist/receptor/G protein (ARG) and the extent of stabilisation should determine the efficacy of agonist action.²⁰² In the extended ternary complex model (Figure 4.16B), the receptor exists in two states, in a ground state (R) and in an activate state (R*), and the latter couples to the G protein to form the activate (R*G) high affinity state and the effective ternary complex (AR*G). An agonist (A) prefers the activate (R*) rather than the ground state (R) and shifts the receptor to the activate state.²⁰³ The agonist also stabilizes the formation of the R*G complex. Both effects of the agonist promote the formation of the ternary complex (AR*G). In the ternary complex (Figure 4.16C), the exchange of GDP for GTP on the G protein leads to the dissociation of the complex in to the $G\alpha_{GTP}$ and $G\beta\gamma$ subunits of the G protein, which regulate the activity of effector molecules.

The GTP shift represents the ratio of the affinity obtained in the presence of GTP (K_{iGTP}) or the nonhydrolysable GTP analogue Gpp(NH)p ($K_{iGpp(NH)p}$) and of the higher agonist affinity (K_H) obtained in the absence of GTP (K_{iGTP}/K_H) or Gpp(NH)p ($K_{iGpp(NH)p}/K_H$). It may provide a quantitative measurement of the agonist to promote coupling of the receptor to G protein and subsequently to determine the efficacy of the ligand within a particular assay system.^{204,205} The correlation between the GTP shift and relative efficacies in functional assays has been studied successfully for dopamine D₂ receptors,²⁰⁶ nevertheless studies carried out by other groups have not been able to demonstrate any significant correlation.^{149,207}

The study presented has verified that agonists have different binding characteristics depending on their properties as full agonists such as pramipexole or as partial agonists such as BP 897. In the absence of added guanine nucleotide, the full agonist pramipexole and compound **54** exhibit competition curves best described by a two-site binding model with higher and lower affinities (K_H and K_L) (F -test, $P < 0.001$) and by a one-site binding model in the presence of guanine nucleotides at dopamine D_{2S} receptors (F -test, $P < 0.05$). Pramipexole ($K_{iGpp(NH)p}/K_H = 1625$) and compound **54** ($K_{iGpp(NH)p}/K_H = 964$) exhibited a significant GTP shift at dopamine D_{2S} receptors. For further investigations, the efficacies of pramipexole and compound **54** need to be evaluated in a functional assay in our laboratory and to be compared to the results with the extent of the GTP shift. Binding affinities of pramipexole and compound **54** at dopamine D₃ receptors in the absence and

presence of guanine nucleotides were better described by a one-site binding model (F -test, $P < 0.05$). Pramipexole studies of other groups' best described the competition curve in the absence of GTP by a two-site binding model.¹³⁵ In this study the low ionic strength and the lack of guanine nucleotides used did not provide a biphasic curve. Competition binding of the dopaminergic agonist pramipexole and its analogue compound **54** demonstrated that Gpp(NH)p decreased affinity for dopamine D₃ receptors, increased Hill slopes of competition curves close to unity and a slight but significant GTP shift has been displayed for both compounds. GTP shifts in dopamine D₃ receptor binding have been revealed in a number of studies using different cell lines,¹⁹¹ although other groups observed a lack of guanine sensitivity.³³ Generally, the difference between the high and the low affinity state exhibited for dopamine D₃ is much smaller than obtained for dopamine D₂ receptors and consequently more delicate to detect in competition binding assays.^{22,192} In this investigation, a high affinity agonist binding and its resulting biphasic curve has only revealed for competition binding at dopamine D_{2S} receptors, but not for dopamine D₃ receptors. Accordingly, experimental considerations need to be re-evaluated. It is necessary to eliminate entire endogenous GTP of the membrane preparation to receive high-affinity agonist binding. Although membrane preparations of the different receptor subtypes have been prepared with an identical method, one possible explanation for the lack of a two-binding site model might be the existence of endogenous GTP in the membrane preparation of dopamine D₃ receptors. One might argue that then K_i control and K_i Gpp(NH)p have similar values, but the lack of sodium ions under these assay conditions could explain the difference in affinity binding in the absence and presence of Gpp(NH)p. An advanced protocol for the membrane preparation with reduced guanine nucleotides or an increase in volume to dilute any endogenous guanine nucleotides could improve the coupling of G protein to the receptor. Additionally, it is of great importance to consider that an adequate amount of G protein molecules is available for receptor-coupling. In order to calculate GTP shift data using a two-site binding model it is of immense significance to increase the number of data points. In this case, 12 - 15 concentrations in each independent experiment with an extended range using 3 different concentrations per log unit are required and determination of the relative proportion of the high and low affinity states for agonists is feasible. The more complex mathematical model requires enough data to attain statistical reliability in the fitting of a two-site model. In this experiment, only 7 concentrations applied in triplicates were used to determine binding data, an increase in data points may improve the fitting of the data and its analysis.

A possible explanation of the biphasic binding curve of agonists is still highly discussed. As explained by the extended ternary complex illustrated in Figure 4.16B, agonist binding changes the equilibrium between the ground, inactive (R) and active (R*) state of the receptor. The agonist couples to the R*G form with high agonist affinity (K_H) in the absence of GTP (Figure 4.16B). In the presence of GTP the receptor dissociates from $G\alpha_{GDP}$ which is presumed to have low agonist affinity (K_{iGTP}) (Figure 4.16C). The low affinity state (K_L) seen for agonists in the absence of GTP is hardly explainable; it may result from a depletion of G protein molecules. It has already been discussed in literature that the shape of an agonist curve in the absence of guanine nucleotides strongly depends on the stoichiometry of receptor to the G protein.²⁰⁸ Depletion of G protein could prevent the formation of the high affinity state of the receptor and agonists bind to the free receptor. It has been reported that agonist efficacy and affinity at the same receptor subtype varies between different assay systems due to coupling to different G proteins resulting in activation of diverse signaling pathways.²⁰⁹ The GTP shift is applicable when comparing different ligands under comparable conditions and therefore it may be used as ad hoc measurement of relative efficacy. The greater the GTP shift, the greater the efficacy. It is not possible to compare reference data of pramipexole due to many varying parameters under assay conditions. Different research groups have presented different K_i values, which are highly influenced by their selected assay conditions, such as radioligand and ionic strength of buffer composition.^{61,129}

An agonist activates the receptor and induces an intracellular response of the signaling system, which is referred to as efficacy. Structurally diverse agonists exhibit different degrees of agonism, i.e. full-agonism, partial agonism, inverse agonism. In order to evaluate the efficacy of an agonist, functional assays measuring receptor/G protein coupling are efficient techniques, such as the [³⁵S]GTP γ S ([³⁵S]guanosine-5'-O-(γ -thiotriphosphate)) binding assay at dopamine D₂ and D₃ receptors.^{210,211} The assay determines the increase in GDP/[³⁵S]GTP γ S exchange at G proteins stimulated via receptor activation as a result of agonist binding. The [³⁵S]GTP γ S binding assay accurately assesses the agonist efficacy and maximal functional effect, while the GTP shift assay only allows precisely to determine agonist affinity in the absence or presence of Gpp(NH)p and might provide a measure of the stabilization of the coupled form of the receptor/agonist. For a correlation between the extent of stabilization and efficacy, a comparison of the ratio of affinities of the lower and higher affinity states (K_{iGTP}/K_H) revealed in the GTP shift assay and the efficacy determined in the [³⁵S]GTP γ S binding assay is required.¹⁹⁹ Other

functional assays include second messenger methods. For dopamine D₂ and D₃ receptors the cyclic AMP accumulation assay is applied and the ability of an agonist to inhibit the stimulation of [³H]cAMP accumulation in response to forskolin is determined.^{62,212} Recently, assays based on agonist-induced stimulation of mitogen-activated protein (MAP) kinase phosphorylation,²¹³ and activation of G protein-coupled inwardly rectifying potassium channels (GIRKs) have been described for dopamine D₂ receptors,²¹³ while ERK1/2 phosphorylation has been investigated for both dopamine receptor subtypes.²¹⁴ Functional coupling of dopamine D₂ and D₃ receptors can also be assessed using a mitogenesis assay, which measures the incorporation of [³H]thymidine.²¹² It is worth mentioning, that functional assays highly depend on the expression system of receptors.⁶² For BP 897, a one-site model provided a better description of binding at dopamine D_{2S} and D₃ in the presence and absence of Gpp(NH)p. Hill coefficients were not significantly different from unity. It is noteworthy that Gpp(NH)p slightly but significantly has increased the affinity at dopamine D₃ receptor subtype for BP 897 compared to control, but did not alter affinity for dopamine D_{2S} receptors. BP 897 is a selective dopamine D₃ over D₂ receptor ligand. *In vitro* BP 897 acts as a partial dopamine D₃ receptor agonist and as a dopamine D₂ receptor antagonist.¹⁴⁰ Other investigations suggested that BP 897 might act as an antagonist rather than a partial agonist at dopamine D₃ receptors.¹⁴² Partial agonists display lower intrinsic activity than full agonist at receptors and it has been assumed that partial agonists may stabilize different activated states of receptors. They either behave as a functional antagonist in the presence of a full agonist, while in the absence of an agonist they function as an agonist. It is expected that partial agonists, like full agonists, discriminate high- and low affinity states in the absence of guanine nucleotides, but indeed a single site has been recognized for dopamine D₃ receptors. Instead, Gpp(NH)p has shifted the competition curve of BP 897 to the left and increased affinity binding. Conclusively, the uncoupled receptor state has been favoured by BP 897. In contrast, a GTP shift has not been recognized for dopamine D₂ receptor binding. This result has been expected since full antagonists have likely similar affinities for both receptor states.²¹⁵ A similar observation has been noticed for the dopamine D₂ and D₃ receptor antagonist ST 198. At dopamine D_{2S} and D₃ receptors, binding data of ST 198 have been best described by a one-site binding model. Hill coefficients did not significantly vary from unity. As already mentioned for BP 897, the presence of guanine nucleotides increased the affinity for dopamine D₃ receptors and resulted in a “reverse” GTP shift, but did not alter affinity for dopamine D_{2S} receptors. ST 198 did not discriminate high- or low affinity state at

dopamine D₂ receptors, but obviously preferred the uncoupled state of dopamine D₃ receptors. This binding behavior has been shown for inverse agonists at multiple targets,²⁰¹ among them dopamine D₂ and D₃ receptors. Inverse agonists preferentially stabilize the uncoupled state of the receptor and reduce the basal G protein activity.²¹⁶ The termination of precoupling of receptor/G protein by guanine nucleotides results in a higher affinity state for inverse agonists.^{201,217} It is noteworthy that inverse agonism is always associated with high constitutive activity, revealed as a common result of recombinant (over expressed) receptor systems,²¹⁸ but it is also found in native *in vivo* systems.²¹⁹

From this study, clear evidence has been obtained that G proteins couple to dopamine D_{2S} receptors and this course of action has been eliminated by guanosine nucleotides. For dopamine D₃ receptors, clear confirmation for G protein coupling is still missing since a biphasic binding curve for the agonist pramipexole and its derivative in the absence of Gpp(NH)p has not been revealed. One explanation of the observed results might be that assay procedure and conditions are not completely optimized and an increase in data points could improve binding outcome. Another assumption is that agonist binding to dopamine D₃ receptors might not couple to G proteins in the recombinant expression system as already recognized by other groups.^{33,191} Competition binding of the dopamine D₃ receptor partial agonist and D₂ receptor antagonist BP 897 and antagonist ST 198 resulted in unaffected binding affinities for dopamine D_{2S}. Nevertheless, a significant increase in binding affinities for dopamine D₃ receptors by addition of Gpp(NH)p and consequently a GTP shift to the left has been shown. Conclusively, the data reported show that it is likely to categorize agonist and partial agonist or antagonist by GTP shift experiments in preliminary investigations, but not to give quantitative values in terms of the effect.

4.2 Pharmacological Results and Structure-Affinity Relationships

4.2.1 Analogues of BP 897 and ST 198

Starting from our lead structure BP 897 (cf. 1.2.6), a partial agonist with high affinity binding and selectivity for dopamine D₃ receptors, series of analogues have been prepared and investigated with the aim to enlighten structure-affinity relationships for further improvement of affinity binding at dopamine D₃ receptors. Therefore, BP 897 was structurally divided into three elements: (I) a hydrophobic aryl moiety connected to an amide consisting of a naphthalen-2-carboxamide residue, (II) an alkyl spacer represented by a linear tetramethylene chain, and (III) a lipophilic basic, aryl substituted alkanamine residue, comprising a 4-(2-methoxyphenyl)piperazine moiety (Figure 4.17). This structural pattern can be applied for most dopamine D₃ receptor ligands with partial agonist and antagonist properties as the structure ST 198 (cf. 1.2.6).

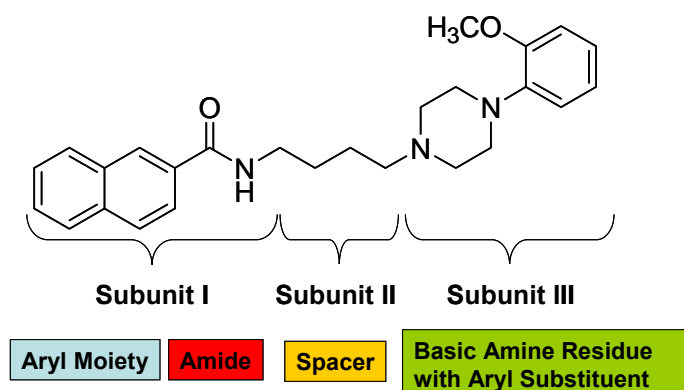


Figure 4.17 Structural pattern of BP 897.

The concept of modification consisted of the structural division of the lead structure into the three different subunits followed by a new combination of the three elements and their bioisosteric analogues. The exchange of particular substructures and as a result the rearrangement of functionalities might lead to more potent and selective dopamine D₃ receptor ligands. As a bioisosteric replacement of the naphthalen-2-carboxamide residue structural variations included cinnamide residues, (hetero)aryl substituted-, and cyclo alkyl substituted carboxamide moieties. The basic aryl alkanamine residue was either represented by the BP 897 scaffold 4-(2-methoxyphenyl)piperazine (S1) or 1,2,3,4-tetrahydroisoquinoline (S2), known as the core structure of ST 198. In the first series, the tetramethylene chain remained unchanged (Table 4.5).

Table 4.5 K_i values and Hill coefficients (in parentheses) of 4-(2-methoxyphenyl)piperazine and 1,2,3,4-tetrahydroisoquinoline derivatives.

No.	S	R	K_i [nM]		K_i (hD _{2S}) / K_i (hD ₃)
			hD _{2S}	hD ₃	
BP 897	S1		52 ± 12 (1.12 ± 0.3)	0.91 ± 0.2 (0.98 ± 0.28)	57
1	S1		44 ± 7 (1.06 ± 0.19)	0.45 ± 0.22 (0.92 ± 0.15)	98
2	S1		55 ± 17 (1.04 ± 0.18)	5.63 ± 1.81 (0.95 ± 0.33)	10
3	S1		52 ± 7 (1.09 ± 0.25)	2.04 ± 0.20 (1.02 ± 0.20)	26
4	S1		59 ± 4 (0.96 ± 0.13)	3.09 ± 0.37 (1.00 ± 0.19)	19
ST 198	S2		1272 ± 99 (0.95 ± 0.11)	8.72 ± 0.21 (0.76 ± 0.11)	146
5	S2		815 ± 56 (0.85 ± 0.08)	82 ± 14 (0.87 ± 0.23)	10
6	S2		791 ± 119 (1.08 ± 0.01)	24 ± 4 (0.86 ± 0.12)	33

Determined equilibrium dissociation constant values of BP 897 are in good agreement to literature data (K_i (D₃) = 0.92 ± 0.2 nM and K_i (D₂) = 61 ± 0.2 nM).¹⁴⁰ 4-(2-Methoxyphenyl)piperazine substituted compounds **1** - **4** have shown binding affinities in the low nanomolar to subnanomolar concentration range for dopamine D₃ receptors and nanomolar K_i values for dopamine D₂ receptors. The bioisosteric replacement of the naphthalen-2-carboxamide by heteroaromatic or alicyclic residues has not altered affinities for dopamine D₂ receptors, but has influenced affinities for dopamine D₃ receptors. The introduction of a benzo[*b*]thiophen-2-yl residue (**1**) has markedly demonstrated an improved binding with

subnanomolar affinity and enhanced selectivity for dopamine D₃ receptors compared to BP 897. Compound **1** has been already described by another research group and is known as FAUC 346 (reference data: K_i (D₃) = 0.23 ± 0.016 nM and K_i (D₂) = 52 ± 1.0 nM).¹²⁵ The benzo[*b*]thiophen-2-yl residue is also found in FAUC 365 (cf. 1.2.6), a ligand with high affinity and selectivity binding for dopamine D₃ receptors.¹²⁵ An additional heteroatom led to the basic benzo[*b*][1,4]thiazol-2-yl residue compound **2** and has not been able to improve neither affinity binding nor selectivity for dopamine D₃ receptors compared to compound **1**. Introducing alicyclic unsaturated residues (**3**, **4**) has been well tolerated, noteworthy that the double bond in 1-position (**3**) has been slightly favoured over the 3-position (**4**). The unsaturated function in vicinity to the carboxamide causes a more rigid molecule, which might affect binding affinities. Data indicate that a heteroaromatic or aromatic ring system is not of absolute necessity to achieve affine and selective ligands.

The following modifications include the introduction of the 1,2,3,4-tetrahydroisoquinoline moiety. This structural motif has been successfully applied in the cinnamoyl derivative ST 198, a dopamine D₃ receptor selective antagonist (reference data: K_i (D₃) = 12 ± 0.5 nM and K_i (D₂) = 780 ± 30 nM).⁸³ The 1,2,3,4-tetrahydroisoquinoline derivatives (**5**, **6**) have displayed moderate nanomolar affinities for dopamine D_{2S} and nanomolar affinities for dopamine D₃ receptors. The lipophilic anellated aryl residue in compound **6** has slightly increased affinity binding and selectivity for dopamine D₃ receptors compared to the thiophen-2-yl bearing compound **5** due to possible additional hydrophobic interactions with the receptor binding site. It is noteworthy that the 4-(2-methoxyphenyl)piperazine analogue **1** of compound **6** has demonstrated higher affinities for dopamine D_{2S} and D₃ receptors and also improved selectivity for dopamine D₃ receptors. This result is in good agreement with literature data.²²⁰ By replacing the 4-(2-methoxyphenyl)piperazine residue with the 1,2,3,4-tetrahydroisoquinolin-2-yl moiety the degree of rigidity of the ligand has increased. This scaffold is a structural combination of a benzyl- and a phenylethyl residue and therefore provides a rigid feature. A possible explanation of the aforementioned decline in affinity at both receptor subtypes and a decreased selectivity at dopamine D₃ receptors is an altered distance of the basic amine to the aromatic system in the 1,2,3,4-tetrahydroisoquinolin-2-yl residue compared to the phenylpiperazine moiety. Furthermore, the 4-(2-methoxyphenyl)piperazine residue is more flexible and the methoxy substitution in position 4 on the phenyl ring contributes to additional interactions with the receptor binding site. In previous studies 1,2,3,4-tetrahydroisoquinoline compounds have mostly demonstrated antagonist properties,²²¹ whereas it is assumed that the less rigid 4-(2-

methoxyphenyl)piperazine moiety of BP 897 is responsible for its partial agonist properties at dopamine D₃ receptors.

Conclusively, in the series of 4-(2-methoxyphenyl)piperazine derivatives, modifications on the naphthalen-2-carboxamide of BP 897 resulted in compounds with high affinity and selectivity for dopamine D₃ receptors (**1** - **4**). Particularly the replacement of naphthalen-2-carboxamide by benzo[*b*]thiophen-2-carboxamide provided compound **1**, also known as FAUC 346, and has demonstrated superior affinity and selectivity for dopamine D₃ compared to BP 897. Exchanging the cinnamide residue of the 1,2,3,4-tetrahydroisoquinoline derivative ST 198 with an aryl heterocycle (**5**) or annellated aryl (**6**) has resulted in ligands with nanomolar affinities and selectivity for dopamine D₃ receptors, but the modifications have not enhanced binding data when compared to ST 198.

The following development of ligands (Table 4.6) has been performed to evaluate the concept of the reversed structural rearrangement of amid functionalities. Therefore, a structurally reversed functional amide group has been linked via an alkyl spacer varying in lengths to the basic alkanamine moiety, represented by either an unsubstituted 4-phenylpiperazine (**S1**) or 1,2,3,4-tetrahydroisoquinoline (**S2**) residue. This approach has been based on the inverse amide compound ST 314 (1,5-bis(4-phenylpiperazinyl)pentan-1-one), which comprises dopamine D₃ receptor selectivity (K_i (D₃) = 6.5 ± 5.3 nM and K_i (D₂) = 467 ± 178 nM, selectivity ratio K_i (D₂)/ K_i (D₃) = 71.9) and the properties of a dopamine D₃ receptor partial agonist (intrinsic activity 0.8).²²² Here, the amine group of the amide functionality is part of the piperazine ring and is integrated into the lipophilic moiety. Moreover, the second amine of the piperazinyl system (anilino amine) has only weak basic properties. Accordingly, the amide functionality has been structurally inverted compared to the previous arrangement in the lead structure BP 897.

Due to its transformed structural characteristics, ligand-receptor interactions of inverse amides are altered. Firstly, the nitrogen of the amide has changed into a weak hydrogen bond acceptor. Subsequently, the alkyl chain has been extended to one additional carbon atom and the distance between the basic nitrogen of the alkanamino moiety (subunit III) and the amide oxygen as a hydrogen bond acceptor has been decreased. Consequently, it was of interest not only to investigate in the influence of diverse inverse amide moieties and basic alkanamino residues, but also to consider different chain lengths. It has also been investigated in the substitution pattern on the inverse amides.

Table 4.6 K_i values and Hill coefficients (in parentheses) of inverse amide compounds.

S1 **S2**

No.	S	R	n	K_i [nM]		K_i (hD _{2S}) / K_i (hD ₃)
				hD _{2S}	hD ₃	
7	S1		4	1482 ± 296 (0.84 ± 0.07)	138 ± 39 (0.85 ± 0.09)	11
8	S1		4	563 ± 135 (1.04 ± 0.08)	136 ± 20 (0.92 ± 0.02)	4
9	S1		3	1057 ± 185 (1.03 ± 0.22)	120 ± 12 (1.05 ± 0.02)	9
10	S1		4	1020 ± 99 (0.80 ± 0.11)	185 ± 66 (1.02 ± 0.20)	6
11	S1		5	841 ± 184 (1.02 ± 0.16)	25 ± 2.8 (0.98 ± 0.16)	34
12	S2		3	198 ± 69 (0.97 ± 0.14)	48 ± 14 (1.01 ± 0.06)	4
13	S2		4	2839 ± 820 (0.92 ± 0.11)	516 ± 43 (0.98 ± 0.10)	6
14	S2		3	649 ± 122 (0.93 ± 0.12)	97 ± 7 (0.89 ± 0.34)	7

In the first series the 4-phenylpiperazine residue is linked via an alkyl spacer to piperidin-1-carbonyl (**7**), 4-phenyl-1,2,3,6-tetrahydropiperidin-1-carbonyl (**8**) or 2,3-dihydro-1*H*-isoindol-1-carbonyl (**9**, **10**, **11**). The 4-phenyl-1,2,3,6-tetrahydropiperidine residue combines structural properties of the phenylpiperazine and the 1,2,3,4-tetrahydroisoquinoline moiety, while the 2,3-dihydro-1*H*-isoindole structure bears the symmetry of phenylpiperazine and the partial benzyl amine feature of 1,2,3,4-tetrahydroisoquinoline.²²²

The modification resulted in compounds with nanomolar affinities at dopamine D₃ receptors and nanomolar to micromolar affinity binding at dopamine D_{2S} receptors. Comparing compounds only varying in the inverse amide residues (**7**, **8**, and **10**) has

clearly shown an alteration in affinity binding for dopamine D_{2S} receptors but has slightly influenced affinities for dopamine D₃ receptors. Structural diminishment of the aryl-substituted alkanamine residues (**8** and **10**) to an aliphatic heterocyclic system (**7**) has been tolerated by dopamine D₃ receptors but demonstrated a decrease in affinity binding at dopamine D_{2S}. This result indicate that the presence of an aryl system substituted to the alkanamine residue is not of absolute necessity since the aliphatic heterocyclic compound still has affinities for both receptor subtypes. In the series of isoindole derivatives enlargement of the alkyl chain (**9** → **10** → **11**) has markedly affected affinity binding at dopamine D₃ receptors. Alternate binding data have been received with increasing chain lengths with the pentyl spacer bearing compound **11** demonstrating enhanced affinity binding and selectivity for dopamine D₃ receptors. It is noteworthy, that the altered arrangement into an inverse amide has changed the position and orientation of the carbonyl group. The distance between the carbonyl functionality and the basic amino group is shorter. In order to compensate the reduction of the space, the alkyl chain requests to be increased to an additional methylene group. In previous modeling studies, and also confirmed by pharmacological binding data of analogues and related structures of BP 897,¹²⁶ a tetramethylene spacer accomplish the required distance of about 6.5 Å between the basic aliphatic nitrogen and hydrogen bond acceptor for high dopamine D₃ receptor affinity binding. Consequently, the favourable alkyl length for inverse amides is a pentyl spacer, as seen in compound **11**. In the series of inverse amides this ligand has shown the highest affinity and selectivity for dopamine D₃ receptors. It is worth mentioning that ligands at the dopamine D₃ receptor adopt not only an extended but also more linear conformation, while ligands the dopamine D₂ receptor favour a more bent conformation.^{125,126} This relation has been confirmed for compounds **9**, **11** and **12** at the dopamine D₃ receptors.

Replacement of the 4-phenylpiperazine residue by a 1,2,3,4-tetrahydroisoquinoline moiety has revealed compounds with nanomolar to micromolar affinity binding for dopamine D_{2S} receptors and nanomolar affinities for dopamine D₃ receptors.. Increasing the alkyl spacer in the 2,3-dihydro-*IH*-isoindole derivatives (**12** → **13**) has demonstrated decreased binding affinities for both dopamine receptor subtypes. The remarkably reduction of affinity binding at dopamine D₂ receptors is in contrast to previous dopamine D₂ affinity data described for their structural analogues coupled to 4-phenylpiperazine (**9** → **10**). Moderate affinity binding value has been gained for the 1,2,3,4-tetrahydroisoquinoline compound (**14**) when combined with 1-phenylpiperazine. The reversed restructuring of the amide

functionality resulted in inverse amide compounds with new structural properties. The new concept provided compounds, which have been well tolerated at dopamine D₃ and at dopamine D_{2S} receptors. The inverse amide compounds presented here have evidently demonstrated the consequence of different orientations of carbonyl oxygen in the binding site and the importance of the distance between basic nitrogen and the hydrogen bonding functional group. The results obtained propose that the length of the alkyl linker connecting the basic alkanamino aryl residue to the inverse amide plays a pivotal role in affinity binding behaviour (**9** → **11**, **12** → **13**). It strongly influences the steric orientation of the ligand in the binding pocket and the interaction with the receptor binding sites. When comparing the aryl substituted basic alkanamino residues, it is important to consider that the phenylpiperazine residue is more flexible while the 1,2,3,4-tetrahydroisoquinoline moiety has increased the rigidity of the ligand. This might influence the orientation of the ligand in the binding pocket when increasing the alkyl spacer. For compound **11** the elongated alkyl spacer shifted the alkanamino residues to an optimal distance between carbonyl oxygen and basic nitrogen of the phenylpiperazine moiety and increased binding at dopamine D₃ and D_{2S} receptors and selectivity for D₃ receptors.

Conclusively, changing the structural order from an aryl carboxamide into an inverse amide has only revealed modest binding affinities and low selectivity ratios for dopamine D₃ receptor. However, the inverse amide approach provides compounds with a novel structural scaffold. Further comprehensive investigations in structural modifications and functional activities might confirm the inverse amide as a worthwhile new lead structure.

4.2.2 Benzhydrylpiperazine Derivatives

Antipsychotic drugs have become first line treatment of schizophrenia despite their interactions with several neurotransmitter receptors, including histamine H₁ receptors, serotonin 5-HT_{2A} receptors, and α_1/α_2 adrenergic receptors.¹⁰⁷ This multireceptor affinity has been considered to effect both therapeutic advantages but also adverse effects.²²³ The antagonist binding profile of antipsychotics for central histamine H₁ receptors has been well demonstrated by chlorpromazine, a phenothiazine derivative, initially developed for its antiallergic properties by Delay and Deniker in 1952.²²⁴ Additionally, histamine H₁ receptor antagonists containing tri- and tetracyclic structures display high affinity for diverse catecholamine receptors, due to the highly conserved ligand-receptor interaction of biogenic amine receptors by an aspartate (Asp) residue in transmembrane (TM) 3.^{122,225,226} Similar structural requirements of antagonists on the binding site of dopamine D₂-like receptors and histamine H₁ receptors are found in a lipophilic/aromatic moiety connected to a basic nitrogen atom²²⁵ and are often claimed as “privileged structures” for GPCRs.

In order to elucidate the structure-affinity relationships of the histamine H₁/dopamine D₂-like receptor profile, a hybrid structure development of novel benzhydrylpiperazines (diphenylmethylpiperazine residues) and analogues to identify highly affine dopamine D₃ receptor selective ligands has been investigated. An approach was undertaken by synthesizing hybrid molecules containing substructures of histamine H₁ receptor antagonists and fragments of dopamine D₃ receptor-preferring ligands. The (semi)rigid components of histamine H₁ receptor antagonists comprised basic substructures of cetirizine ([4-(4-chlorophenyl)phenylmethyl]piperazine), mianserin (4-(2,3,4,5,10,15-hexahydro-1*H*-dibenzo[*b:e*]pyrazino[2,1-*g*])azepine), ketotifen (4-[4-(10-oxo-9,10-dihydro-4*H*-benzo[4,5]cyclohepta[1,2-*b*]thiophen)-4-yliden]piperidine), loratadine (4-[(8-chloro-5,6-dihydro-11*H*-benzo[5,6]cyclohepta[1,2-*b*]pyridin)-11-yliden]piperidine), and bamipine (*N*-benzyl-*N*-piperidin-4-ylaniline). Structures of histamine H₁ receptor antagonists are shown in cf. 1.3.6. These residues were connected via a tetramethylene chain to naphthalen-2-carboxamide, cinnamide, benzo[*b*]thiophen-2-carboxamide, or phthalimide moiety, as represented in BP 897, ST 198, FAUC 365 (cf. 1.2.6) and NAN190, respectively. NAN190 (*N*-(4-[4-(2-methoxyphenyl)piperazinyl]butyl)isoindolin-1,3-dion) has demonstrated lower binding affinity and selectivity for dopamine D₃ receptors (K_i (D₃) = 38 ± 5.7 nM and K_i (D₂) = 50 ± 6 nM, selectivity ratio K_i (D₂)/ K_i (D₃) = 1) compared to BP 897, ST 198 and FAUC 365, and has shown to bind with high affinity

at the serotonin 5-HT_{1A} receptor ($K_i = 0.6$ nM).²²⁷ The phthalimide residue, comprising two amide functionalities, might represent a potential novel scaffold. A model of the hybrid design approach is illustrated in Figure 4.18.

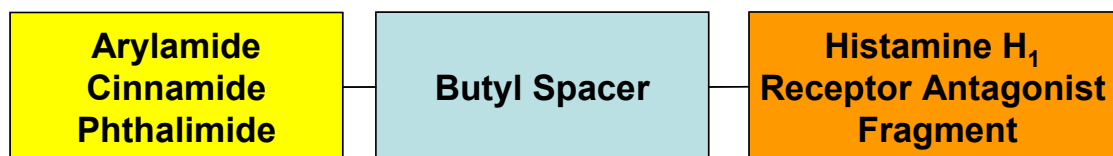


Figure 4.18 Model of the hybrid design approach.

The aim was to evaluate the influence of both, variations of diverse arylamides and related moieties, and structural modifications on the basic nitrogen atom including aryl residues, tri- and tetracyclic ring substitutions.

41 novel hybrid compounds were synthesized and binding affinities were preliminary screened using a competition binding screening with six-point measurements in duplicates only. This first rough screening was not carried out in-house but externally tested (cf. 10). Radioligand binding assays were carried out using HEK cells transfected with human D_{2S} and CHO cells transfected with human D₃ receptor cDNA and [³H]spiperone (cf. 10.1.2).¹⁹² 25 out of 41 novel hybrids that promised the most potential chemical substructures for dopamine D₃ receptor binding were selected. From each series containing different (semi)rigid histamine H₁ receptor antagonist substructures the compounds with the highest affinity and/or selectivity for dopamine D₃ receptors or related parent leads were chosen. Besides, the various aryl amide moieties such as naphthalen-2-carboxamide, and benzo[*b*]thiophen-2-carboxamide were considered and as well as phthalimide, and cinnamide residues to compare potentially bioisosteric features. Consequently, a second precise [³H]spiperone displacement binding to cloned human D_{2S}, and D₃ receptors stably transfected in CHO cells was carried out using 7 different concentrations of test compound in triplicates in at least 3 independent experiments. Determined pharmacological binding data are shown in Tables 4.8 - 4.10. For reasons of selectivity, histamine H₁ receptor affinity binding of a selected subset of compounds has been determined (Tables 4.8 - 4.10). For a comprehensive data evaluation dopamine D₂, D₃, and histamine H₁ receptor affinities of the above mentioned parent antihistaminergic H₁ receptor antagonists were assessed (Table 4.11).

As expected inconsistencies were obtained by comparing the pharmacological binding data received via rough screening using six-point measurements (see Appendix Table 4.7) and via precise competition binding assay procedures. Compound **36** has displayed K_i values of

0.3 nM at dopamine D₃ receptors and of 703 nM at hD_{2S} receptors in the rough screening assay. In the reevaluation, the binding data significantly changed for dopamine D₃ ($K_i = 140$ nM) and but did not significantly differ for dopamine D_{2S} receptors ($K_i = 573$ nM). On the contrary, similar binding affinity data at dopamine D_{2S} and D₃ receptors were received for compound **39**, although the experiments were carried out under different assay conditions. Using dissimilar binding assay conditions, including different final concentrations of radioligands, varying incubation buffers, incubation times, different host cells as an expression system for dopamine receptors, solvent for test compounds, and dissimilar reference compounds to determine non-specific binding has resulted in significantly different K_i affinity values and consequently different dopamine D₂/D₃ selectivity ratios. The tested compounds have shown calculated log*P* values in the range of 2.65 – 6.53 (cf. Appendix Table 4.7). Ligands demonstrating log*P* values in the range of 5 are not well suited for automated screening procedures due to poor solubility and might give an explanation for the observed differences of data. It is noteworthy that SAR should be predicted from data received from one and the same laboratory carrying out precise and repetitive competition binding assays. Consequently the ensuing SAR can be based only on the data presented in Tables 4.8 - 4.10, since they fulfill the above mentioned prerequisites. In the following sections, the SAR is enlightened concerning the effects of antagonist H₁ receptor fragments and it is focused on changes in dopamine D₂/D₃ receptor selective substructures.

Unsubstituted or differently substituted benzhydrylpiperazine residues based on the structural element of the antihistaminergic cetirizine have been combined with diverse aryl amides, cinnamide and phthalimide moieties (**15** - **27**). The benzhydrylpiperazine element has been substituted either with a chlorine at 4-position or methoxy group(s) at 2-position(s) of the phenyl ring(s) related to BP 897. Moreover the piperazine ring has been replaced by 1,4-diazepane. Among the series of benzhydrylpiperazine derivatives, compounds have shown nanomolar affinities for dopamine D₃ receptors and moderate nanomolar to micromolar binding affinities for dopamine D_{2S} receptors. Introduction of a piperazine ring extension to a 1,4-diazepane in the phthalimide derivative **16** and has demonstrated a 2-fold decrease in binding affinities at both dopamine D_{2S} and D₃ receptors compared to compound **15**. This reduction of binding affinity due to 1,4-diazepane substitution has also been obtained for the cinnamide containing compound **18** when extended to **22**. Compound **22** has a 3-fold decreased affinity for dopamine D₃ receptors and a 2-fold decreased affinity for D_{2S} receptors. Conclusively, ring extension has proved

to decline affinities for D_{2S} and D₃ receptors and to reduce selectivity for dopamine D₃ over D₂ receptors within these examples.

In order to evaluate the influence of variations of the aryl amide substituent, the naphthalen-2-carboxamide moiety in **17** has been replaced by cinnamide in **18**. The replacement has resulted in minor retention of affinity binding at dopamine D₃ receptors but clear reduction at D_{2S} receptors, consequently the selectivity for D₃ receptors has increased. In compounds **15** and **19** - **21** the phenyl ring of the benzhydrylpiperazine residue has been substituted with a chloro atom in 4-position. Substitution of the phthalimide moiety (**15**) by naphthalen-2-carboxamide (**19**), cinnamide (**20**) or benzo[*b*]thiophen-2-carboxamide (**21**) had only minor influence on affinity binding at dopamine D₃ receptors, but the cinnamide (**20**) and the benzo[*b*]thiophen-2-carboxamide (**21**) have shown a noticeable decrease in affinities at dopamine D_{2S} receptors compared to the naphthalen-2-carboxamide compound **19** and the phthalimide derivative **15**, resulting in a slightly increase in selectivity for dopamine D₃ receptors. The affinity and selectivity profiles of benzhydrylpiperazine derivatives **25** - **27**, which are methoxy disubstituted at 2-position of the phenyl rings, have been strongly influenced by variations of amide residues. The naphthalen-2-carboxamide residue bearing compound **25** has displayed the highest affinity for D₃ receptors, but only a 4-fold selectivity ratio for dopamine D₃ receptors, whereas the cinnamide compound **26** has been 11-fold selective for D₃ receptors versus D₂ receptors. The benzo[*b*]thiophen-2-carboxamide **27** has had only moderate affinities for D_{2S} receptors and D₃ receptors. In the ring extended series with diphenyl-1,4-diazepane the exchange from cinnamide (**22**) to benzo[*b*]thiophen-2-carboxamide (**23**) has resulted in reduced affinities for dopamine D₃ and D_{2S} receptor binding and a decrease in selectivity for dopamine D₃ over D₂ receptors.

Another aim has been the characterization of alterations in the substitution pattern on the phenyl ring(s) of the benzhydrylpiperazine residue and its consequence on the conformation of the ligand. Among the series of benzhydryl derivatives either unsubstituted or in 2-position of the phenyl rings methoxy disubstituted, compounds with cinnamide residues (**18**, **26**) have shown the highest preference for dopamine D₃ over D₂ receptors in this series. A favored binding behavior of cinnamide bearing compounds for dopamine D₃ over D₂ receptors could be obtained for compound **22** in the series with unsubstituted diphenylmethyl-1,4-diazepane derivatives. When the naphthalen-2-carboxamide compound **17** was compared to in 4-position chloro substituted (**19**) and 2-positions methoxy disubstituted (**25**) benzhydryl analogues, the affinities for D₃ receptors

Table 4.8 K_i values and Hill coefficients (in parentheses) of cetirizine-based hybrids.

No.	R	R ¹	R ²	n	K_i [nM]		$\frac{K_i}{(hD_{2S}/hD_3)}$	$\frac{K_i}{(hH_1/hH_3)}$	$\frac{K_i}{(hH_1/hD_3)}$
					hD _{2S}	hD ₃			
15		4-Cl	H	1	184 ± 66 (0.89 ± 0.01)	67 ± 18 (1.18 ± 0.26)	3	34 ± 9 (1.33 ± 0.50)	0.5
16		4-Cl	H	2	313 ± 152 (1.70 ± 0.30)	150 ± 1.7 (1.04 ± 0.70)	2	n.d. ^a	n.d. ^a
17		H	H	1	243 ± 39 (1.40 ± 0.14)	39 ± 0.8 (1.65 ± 0.42)	6	21 ± 6 (1.23 ± 0.13)	0.5
18		H	H	1	767 ± 119 (1.14 ± 0.17)	55 ± 15 (0.88 ± 0.15)	14	7 ± 0.42 (1.29 ± 0.17)	0.1
19		4-Cl	H	1	180 ± 35 (1.28 ± 0.09)	49 ± 24 (1.04 ± 0.06)	4	n.d. ^a	n.d. ^a
20		4-Cl	H	1	292 ± 39 (1.11 ± 0.30)	60 ± 16 (1.85 ± 0.75)	5	n.d. ^a	n.d. ^a
21		4-Cl	H	1	318 ± 69 (1.33 ± 0.2)	54 ± 11 (1.20 ± 0.20)	6	n.d. ^a	n.d. ^a
22		H	H	2	1261 ± 242 (1.29 ± 0.78)	144 ± 85 (1.47 ± 0.61)	9	26 ± 5 (1.30 ± 0.24)	0.2
23		H	H	2	1708 ± 852 (2.43 ± 0.21)	394 ± 70 (1.70 ± 0.61)	5	50 ± 12 (1.77 ± 0.50)	0.1
24		2-H ₃ CO	H	1	457 ± 23 (1.31 ± 0.05)	134 ± 46 (1.49 ± 0.17)	4	n.d. ^a	n.d. ^a
25		2-H ₃ CO	H ₃ CO	1	138 ± 13 (1.56 ± 0.3)	36 ± 13 (1.68 ± 0.59)	4	n.d. ^a	n.d. ^a
26		2-H ₃ CO	H ₃ CO	1	736 ± 228 (0.95 ± 0.20)	67 ± 11 (1.25 ± 0.37)	11	20 ± 5 (0.92 ± 0.15)	0.3
27		2-H ₃ CO	H ₃ CO	1	523 ± 118 (1.07 ± 0.18)	111 ± 29 (1.24 ± 0.31)	5	n.d. ^a	n.d. ^a

^an.d., not determined.

did not significantly changed, but an increase in affinity for dopamine D₂ occurred (**17** → **19** → **25**). The cinnamide derivatives **18**, **20**, and **26** showed similar results regarding the affinities for D₃ receptors. The chloro substituted compound **20** has demonstrated higher affinity binding compared to that of the unsubstituted (**18**) and methoxy disubstituted derivatives (**26**) at the dopamine D₂ receptor.

In the series of benzo[*b*]thiophen-2-carboxamide (**21**, **24**, **27**) derivatives the 4-chloro substituted compound (**21**) has displayed a 2-fold enhanced affinity for dopamine D₃ receptors compared to that of the methoxy analogues (**24**, **27**). Here introduction of the additional methoxy group (**27**) did not significantly change affinities for dopamine D₂ and D₃ receptors. In summary, modifications of the substitution pattern on the phenyl ring(s) of the benzhydryl residue have not clearly changed affinity binding for dopamine D₃ receptors when hybridized with naphthalen-2-carboxamide (**17**, **19**, **25**) or cinnamide (**18**, **20**, **26**), but binding affinities have been influenced by incorporation of benzo[*b*]thiophen-2-carboxamide (**21**, **24**, **27**). In contrary, no clear structure-activity relationship was found for dopamine D₂ receptors when substituted with different aryl amide moieties and related residues and varying substitutions on the phenyl ring with chloro or methoxy residues, reflecting putative differences in binding sites of dopamine D₃ and D₂ receptors.

In compounds **29** - **34** the tetracyclic substructure of mianserin and the tricyclic fragments of ketotifen and loratadine have been included (Table 4.9).

Incorporation of the hexahydrodibenzopyrazinoazepine (**S1**) residue, the substructure of mianserin, has displayed modest nanomolar affinity binding at dopamine D_{2S} and D₃ receptors. The bioisosteric exchange of the (aryl) amide moieties has exposed similar affinity binding values at both receptor subtypes for naphthalen-2-carboxamide (**28**) and cinnamide (**29**). For the benzo[*b*]thiophen-2-carboxamide compound (**30**) the affinity binding at dopamine D₃ receptors has been reduced 2-fold while the affinity for dopamine D_{2S} receptors has been slightly improved. The data indicate that an increase in steric bulkiness and rigidity has not revealed compounds with enhanced affinity and selectivity for dopamine D₃ receptors.

Benzothienylcycloheptadienpiperidine (**S2**), the substructure of ketotifen, has been integrated in compound **31** and **32** and the modification has resulted in moderate nanomolar binding affinities for dopamine D₃ and D_{2S} receptors. Compared to the phthalimide derivative (**31**), the naphthalen-2-carboxamide residue (**32**) has improved the

selectivity ratio for dopamine D₃ over D₂ receptors by enhancing the affinity for dopamine D₃ receptors (4-fold).

Table 4.9 *K_i* values and Hill coefficients (in parentheses) of tri- and tetracyclic compounds.

No.	S	R	<i>K_i</i> [nM]		<i>K_i</i> (hD _{2S} /hD ₃)	<i>K_i</i> [nM] hH ₁	<i>K_i</i> (hH ₁ /hD ₃)
			hD _{2S}	hD ₃			
28	S1		513 ± 217 (1.75 ± 0.05)	201 ± 153 (1.61 ± 0.27)	3	n.d. ^a	n.d. ^a
29	S1		472 ± 100 (1.47 ± 0.26)	228 ± 50 (1.06 ± 0.09)	2	7 ± 0.3 (1.40 ± 0.36)	0.03
30	S1		387 ± 97 (1.96 ± 0.03)	455 ± 158 (2.14 ± 0.36)	1	n.d. ^a	n.d.
31	S2		525 ± 66 (1.19 ± 0.10)	145 ± 52 (0.87 ± 0.11)	4	9 ± 4 (1.09 ± 0.29)	0.1
32	S2		769 ± 195 (1.01 ± 0.22)	48 ± 13 (1.29 ± 0.59)	16	26 ± 9 (1.27 ± 0.44)	0.5
33	S3		230 ± 76 (1.61 ± 0.23)	96 ± 31 (1.29 ± 0.10)	3	n.d. ^a	n.d. ^a
34	S3		261 ± 19 (1.65 ± 0.38)	177 ± 56 (1.19 ± 0.32)	2	13 ± 3 (1.52 ± 0.53)	0.1

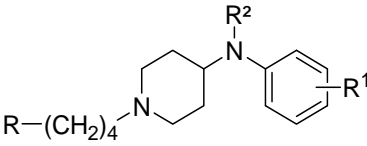
^an.d., not determined.

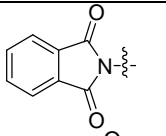
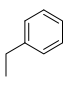
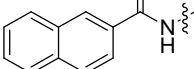
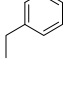
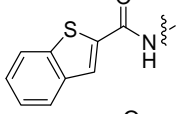
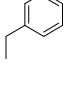
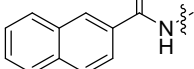
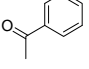
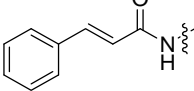
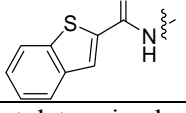
The loratadine ring system (**S3**) was included in compounds **33** and **34** and this has resulted in molecules with nanomolar affinities for dopamine D₃ receptor binding. Introducing this bulky residue has been well tolerated by dopamine D_{2S} receptors effecting improved binding affinities and clearly shown for **33** when compared to compounds **28** and **32**. As confirmed by previous findings for the series of mianserin derivatives, the naphthalen-2-carboxamide substitution has demonstrated higher affinity for dopamine D₃ receptors as the substitution with benzo[*b*]thiophen-2-carboxamide, but both aryl amide residues showed similar binding data for dopamine D₂ receptors. In summary, ketotifen

derivatives have demonstrated higher affinities and dopamine D₃ receptor-preference (**32**) than those containing mianserin (**28**) and loratadine (**33**) substructures. Comparing the different heterocyclic hybrid molecules, the loratadine hybrid approach has displayed compounds with highest affinity for dopamine D_{2S} receptors.

For a comprehensive series of potentially privileged structures of histamine H₁ receptor antagonists, derivatives of the benzyl-*N*-piperidin-4-ylaniline fragment of bamipine were synthesized (**35** - **40**) (Table 4.10).

Table 4.10 *K_i* values and Hill coefficients (in parentheses) of bamipine-based hybrids.



No.	R	R ¹	R ²	<i>K_i</i> [nM]		$\frac{K_i}{(hD_{2S} / hD_3)}$	$\frac{K_i}{hH_1}$	$\frac{K_i}{(hH_1 / hD_3)}$
				hD _{2S}	hD ₃			
35		H		340 ± 60 (1.36 ± 0.67)	225 ± 70 (1.52 ± 0.36)	2	n.d. ^a	n.d. ^a
36		H		573 ± 77 (1.55 ± 0.19)	140 ± 50 (1.93 ± 0.82)	4	n.d. ^a	n.d. ^a
37		H		423 ± 102 (1.30 ± 0.44)	60 ± 22 (1.20 ± 0.59)	7	n.d. ^a	n.d. ^a
38		2-H ₃ CO		8066 ± 242 (0.99 ± 0.18)	512 ± 66 (1.4 ± 0.47)	16	n.d. ^a	n.d. ^a
39		2-H ₃ CO	H	962 ± 7 (0.90 ± 0.14)	7.4 ± 2.6 (0.9 ± 0.01)	130	17 ± 4 (1.03 ± 0.08)	2.3
40		2-H ₃ CO	H	843 ± 40 (0.71 ± 0.05)	7.9 ± 0.6 (0.95 ± 0.19)	107	n.d. ^a	n.d. ^a

^an.d., not determined.

The bamipine substructure has been combined with phthalimide (**35**), cinnamide (**36**) or benzo[*b*]thiophen-2-carboxamide (**37**) connected via a butyl linker and the modification resulted in nanomolar affinities for dopamine D₃ and D_{2S} receptors. Among the series, the phthalimide variation has displayed the lowest affinity for dopamine D₃ and the highest affinity for D_{2S} receptors (**35**), a preference which has already been described for the cetirizine derivative **15** (Table 4.8) and the ketotifen related compound **31** (Table 4.9).

Compared to molecule **35** and **36** the benzo[*b*]thiophen-2-carboxamide (**37**) has shown improved affinity for dopamine D₃ receptor with dopamine D₃ receptor-preference. Replacement of the benzyl ring (**36**) of the bampine derivative by a benzoyl residue (**38**) and the additional introduction of a methoxy substitution in 2-position of the phenyl ring has not been tolerated and has caused a reduction of dopamine D₃ receptor binding and even a greater loss of binding at dopamine D_{2S} receptors. Assumably an additional hydrogen bond acceptor moiety has not been favored.

In the following compounds **39** and **40**, the benzyl-*N*-piperidin-4-ylaniline scaffold of bampine has been structurally diminished into a phenylaminopiperidine moiety with methoxy substitution in 2-position on the phenyl system. This modification was further varied by introducing a cinnamide residue (**39**) and a highly selective ligand has been obtained. This promising ligand has presented a pharmacological profile with low nanomolar binding data for D₃ receptors and a 130-fold selectivity for dopamine D₃ over D₂ receptors. The phenylaminopiperidine (**39**) residue is an analogue of the 4-(2-methoxyphenyl)piperazino moiety as seen in BP 897 (cf. 1.2.6). Combined with the cinnamide substructure of ST 198 (cf. 1.2.6) the modification has impressively improved affinity binding for dopamine D₃ receptors. Exchange of the cinnamide residue by the potential bioisostere benzo[*b*]thiophen-2-carboxamide (**40**) led to a slightly decrease in selectivity for dopamine D₃ over D₂. This observation has been previously described for the cetirizine derivatives (**26** → **27**).

Since many of the moieties introduced into the novel dopamine ligands are well-known histamine H₁ receptor antagonists, selected compounds were further evaluated on their histamine H₁ receptor binding properties (Table 4.8 - 4.10). Low nanomolar binding data have been obtained for the benzhydryl derivative **18** and the hexahydrodibenzopyrazinoazepine derivative **29**, both ligands are connected via a butyl linker to a cinnamide moiety. Disubstitution of methoxy groups in 2-position on the phenyl rings of the benzhydrylpiperazine residue slightly decreased binding affinity for histamine H₁ receptors (**26**) compared to its unsubstituted analogue (**18**). Extension of a piperazine ring to 1,4-diazepane (**18** → **22**) has resulted in reduced binding affinity for histamine H₁ receptors as already seen for D₂-like receptors. One may argue that the introduction of second generation histamine H₁ receptor antagonists may not be the optimal choice since these compounds have been prepared for not penetrating the brain and thereby reducing the e.g. sedating side effects. It could be shown that the physicochemical as well as the

pharmacological properties were largely changed by derivatisations performed leading to novel compounds which newly have to be investigated on the brain penetrating or multidrug resistance protein binding properties in further studies.

As intended, introducing dopamine D₂/D₃ selective (aryl) amide or imide moieties connected via a butyl linker to histamine H₁ receptor substructure analogues resulted in compounds displaying improved binding affinity profiles for dopamine D₂ and D₃ receptors compared to their parent histamine H₁ receptor antagonists, so called “antihistamines”. Hybrid compounds have demonstrated declined binding affinities at histamine H₁ receptors compared to that of the antihistamines with the exception of loratadine derivatives. In Table 4.11 it is demonstrated, that the marketed antihistaminergic drugs have shown low binding affinities for dopamine D_{2S} and D₃ receptors ($K_i \geq 1\ 000$ nM for dopamine D₂ and D₃). As expected with such a hybrid approach most of the compounds tested were more potent at histamine H₁ receptors than at dopamine D₃ or D₂ receptors. Compound **39** was the only exception and showed a 2-fold selectivity for dopamine D₃ versus histamine H₁ receptors. The binding data have demonstrated that the binding pocket of the histamine H₁ receptor tolerated additional (aryl) amide or imide residues. It may be speculated that the additional residues might positively contribute to the interaction of the molecules with the histamine H₁ receptor binding site. The positive binding data thus has reflected the close evolutionary relationship of aminergic receptors.

Table 4.11 K_i values and Hill coefficients (in parentheses) of histamine H₁ receptor antagonists.

Compound	K_i [nM]		
	hD _{2S}	hD ₃	hH ₁
Cetirizine	>150.000	>60.000	28 ± 7 (0.79 ± 0.18)
Mianserin	2563 ± 845 (0.99 ± 0.27)	1644 ± 87 (1.23 ± 0.25)	0.84 ± 0.26 (1.18 ± 0.12)
Ketotifen	4855 ± 1277 (1.09 ± 0.33)	1301 ± 762 (0.86 ± 0.37)	0.34 ± 0.07 (1.05 ± 0.13)
Loratadine	43.000 ± 2135 (0.82 ± 0.14)	>10.000	130 ± 54 (1.00 ± 0.06)
Bamipine	1925 ± 440 (1.01 ± 0.09)	1035 ± 119 (1.07 ± 0.04)	12 ± 0.87 (1.16 ± 0.51)

Conclusively, the hybrid approach combining substructures of histamine H₁ receptor antagonists and fragments of dopamine D₃ receptor-preferring ligands, related to BP 897, ST 198 and analogues, resulted in compounds showing nanomolar affinities for dopamine D₃ and nanomolar to micromolar affinities for dopamine D₂ receptors. The affinity profiles of structural modified histamine H₁ receptor antagonists have been optimized and

improved for dopamine D₂ and D₃ receptor binding. Binding affinities at histamine H₁ receptors have been decreased for mianserin- and ketotifen-related hybrids, have improved for loratadine analogues and have not mainly changed for bamipine- and cetirizine-substructure bearing compounds. Incorporation of histamine H₁ receptor antagonist substructures has been tolerated for flexible residues, such as phenylaminopiperidine and benzhydryl, while rigid and bulky tricyclic or tetracyclic ring systems were not tolerated by dopamine D₂ and D₃ receptors in this hybrid approach (Figure 4.19). Tri- and tetracyclic aromatic residue are fundamental substructures of several antipsychotics with affinities for dopamine D₂ and D₃ receptors. But in this context and applying this hybrid approach, the results might indicate a discriminating conformation of the tri- and tetracyclic aromatic residue and possibly unfavorable interaction between the basic nitrogen and the conserved Asp in TM3 in the binding pocket of dopamine D₂ and D₃ receptors. Potentially bioisosteric variations of the (aryl) amide and imide moieties had only moderate influence on D₃ receptor binding, but significantly changes on D_{2S} receptor binding were obtained as already observed in previous studies.²²⁸ In this investigation clear improvements in selectivity ratios for D₃ over D₂ receptors were gained when cinnamide substituted (Figure 4.19), with the impressively enhancement of compound **39**, exhibiting the highest affinity and selectivity for dopamine D₃ receptors. This results confirm previous investigation,¹²⁶ suggesting an improved binding of cinnamide residue due to its elongated and rigid geometry, noteworthy the linear conjugated structure. By the presented hybrid approach deeper insight into ligand binding behavior on several related aminergic receptors has been presented. This refined SAR might be useful to design more potent and selective drugs with a designed pharmacological profile on multiple targets.

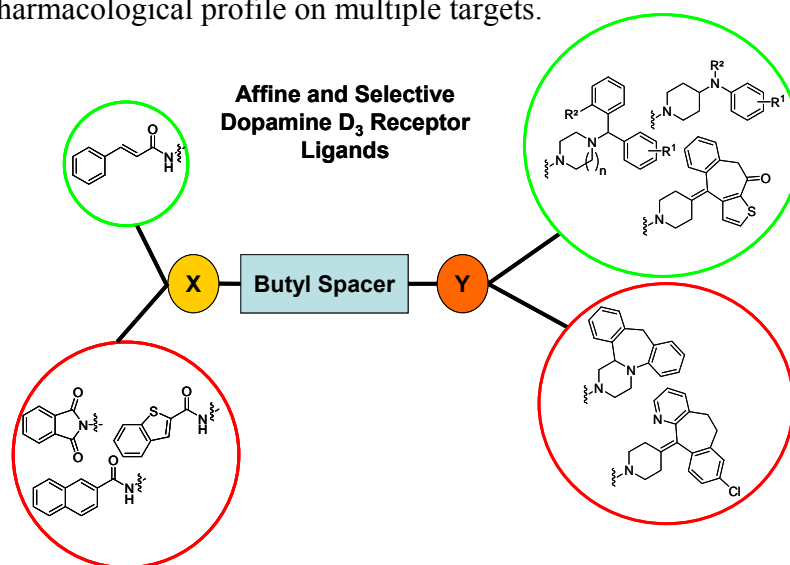
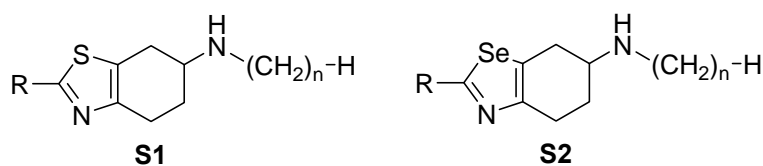


Figure 4.19 Model on performed variations. X, fragments of dopamine D₃ receptor-preferring ligands; Y, elements of histamine H₁ receptor antagonists. The green cycle indicates optimization, while the red cycle indicates negative influence.

4.2.3 Pramipexole and Etrabamine Derivatives

Considerable advances have been made in defining the pathogenesis and pathology of Parkinson's disease. The effort resulted in the development of novel drugs available for its treatment. The pharmacotherapy is still focused on the dopamine precursor levodopa (cf. 1.2) and in addition, on dopamine agonists such as pramipexole (Sifrol[®], Mirapex[®] (Boehringer Ingelheim), cf. 1.2.6). One strategy in our laboratory was the synthesis of structural variations of the full agonist pramipexole ((*S*)-(-)-2-amino-6-propylamino-4,5,6,7-tetrahydrobenzothiazole) and the structurally related dopamine agonist etrabamine (6-methylamino-4,5,6,7-tetrahydrobenzothiazole).^{133,135,229} Pramipexole has shown agonist activity at the presynaptic and postsynaptic dopamine receptors belonging to the D₂-like receptor family, with highest affinity at dopamine D₃ receptors and has been demonstrated to be efficacious in treating Parkinson's disease.⁸⁴ Etrabamine has been developed as a new long-lasting dopamine agonist for Parkinson's disease in the 1980's. It has been demonstrated to be more effective than the dopamine agonist apomorphine, has decreased the prolactin secretion and did not modify adenylyl cyclase activity.²²⁹

Starting with 6-alkylamino-4,5,6,7-tetrahydrobenzothiazole, variations were carried out by increasing the alkyl chain length on the secondary nitrogen atom in 6-position and as well, different substitution patterns in 2-position were constructed (**41** - **51**). Furthermore, modifications on the heteroaromatic moiety were derived by the replacement of the sulphur atom by a selenium atom (**52** - **54**). Results are shown in Table 4.12. Radioligand binding studies were carried out under physiological conditions with sodium ions. Competition binding curves demonstrated mostly a Hill slope not significantly different from unity and were fitted best by a one-site binding model ($P < 0.05$). In the case of calculated Hill slopes significantly different from unity, a better fit of equations indicated a one-site binding model under these assay conditions. Dissociation constants (K_i) of pramipexole are in good agreement with literature data describing the low affinity site of dopamine D_{2S} and D₃ receptors (K_i (D₂) = 1600 ± 200 nM and K_i (D₃) = 15 ± 1 nM).⁶¹ The compounds (**41** - **54**) have displayed nano- to micromolar affinity binding at dopamine D₃ receptors and micromolar affinity binding for dopamine D_{2S} receptors. Among the series of 6-alkylamino-4,5,6,7-tetrahydrobenzothiazole derivatives, an enlargement in the alkyl chain length from methyl (**41**) to ethyl (**42**) and propyl (**43**) has resulted in a clear enhanced affinity for dopamine D₃ receptor binding and moderately increased affinity at D_{2S} receptors, achieving an enhanced selectivity ratio for dopamine D₃ over D₂ receptors. The variations have not resulted in affinity binding and selectivity data superior to pramipexole.

Table 4.12 K_i values and Hill coefficients (in parentheses) of pramipexole analogues and related compounds.

No.	S	R	n	K_i [nM]		$K_i (D_{2S}) / K_i (D_3)$
				hD_{2S}	hD_3	
Pramipexole	S1	NH ₂	3	2626 ± 267 (0.66 ± 0.04)	6.59 ± 4.96 (0.72 ± 0.09)	399
41	S1	H	1	21430 ± 3846 (0.70 ± 0.05)	1112 ± 279 (0.92 ± 0.16)	19
42	S1	H	2	26490 ± 11830 (n.d.)	210 ± 24 (0.94 ± 0.02)	126
43	S1	H	3	18011 ± 5033 (0.58 ± 0.09)	93 ± 15 (0.93 ± 0.07)	194
44	S1	Cl	3	11637 ± 1481 (0.73 ± 0.11)	78 ± 2.4 (0.89 ± 0.12)	150
45	S1	Br	3	7398 ± 1482 (0.96 ± 0.08)	92 ± 10 (1.00 ± 0.19)	80
46	S1	H ₃ CO	3	18043 ± 5580 (0.86 ± 0.12)	46 ± 20 (0.71 ± 0.05)	392
47	S1	H ₅ C ₂ O	3	63960 ± 4342 (n.d.)	1205 ± 22 (0.92)	53
48	S1	H ₇ C ₃ O	3	2139 ± 945 (0.87 ± 0.11)	2302 ± 205 (1.04 ± 0.06)	0.9
59	S1	Isopropoxy	3	75925 ± 34896 (0.94 ± 0.02)	1255 ± 414 (0.82 ± 0.13)	61
50	S1	Cyclopropylethoxy	3	>1000	>1000	
51	S1	F ₃ C-H ₂ CO	3	42930 ± 14170 (0.55 ± 0.06)	1305 ± 556 (0.94 ± 0.24)	33
52	S2	H	2	8030 ± 871 (0.80 ± 0.05)	118 ± 18 (1.02 ± 0.06)	68
53	S2	Cl	2	10440 ± 2391 (0.63 ± 0.03)	272 ± 63 (0.90 ± 0.30)	38
54	S2	H ₂ N	2	1798 ± 668 (0.71 ± 0.13)	15 ± 2.6 (0.85 ± 0.17)	120

To gain further improvement, the *N*-propyl substitution has been chosen in the following compounds (**44** - **51**). Introduction of a chlorine (**44**) or bromine (**45**) atom in 2-position on the heterocyclic aryl moiety has displayed lower affinities for dopamine D₃ and D_{2S} receptors compared to pramipexole. A markedly impact on binding with higher affinity and prominent selectivity for dopamine D₃ over D_{2S} receptors has been revealed for the in 2-position methoxy substituted compound **46**, while further enlargement to ethoxy, propoxy, isopropoxy and cyclopropylethoxy residues has not been tolerated by both receptor subtypes as indicated by compounds **47** → **48** → **49** → **50**. Introduction of the 2,2,2-trifluoro-ethoxy residue in 2-position has also resulted in low binding affinities for dopamine D_{2S} and D₃ receptors and a moderate selectivity ratio (**51**). In compounds **52** - **54** the influence of exchanging the sulphur atom of the thiazole ring by a selenium atom has been investigated. The compounds possess an ethyl chain on the basic nitrogen atom in 6-position and vary in residues in 2-position. The hydrogen substituted compound **52** has demonstrated a enhanced binding profile for dopamine D₃ and D_{2S} receptors compared to the sulphur containing analogue **42**, but has not shown an improved selectivity for dopamine D₃ receptors. Incorporation of a chlorine atom in compound **53** resulted in reduced affinities for dopamine D₃ and D_{2S} receptors, while introducing an amino functionality (**54**) has clearly displayed a benefit for dopamine D_{2S} receptor and dopamine D₃ receptor binding affinities with an increased selectivity for dopamine D₃ over D₂ receptors, but has not exceeded the ratio data of pramipexole.

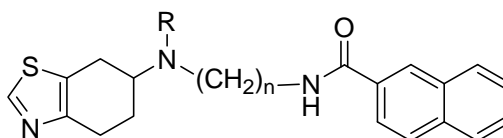
The development of pramipexole started with the rigidification of the neurotransmitter dopamine and the itemisation of the agonist apomorphine ensuing in hydroxyl substituted aminotetralin derivatives. It had always been a challenge to replace the catechol or phenol structure with a bioisosteric heteroaromatic moiety to avoid but improve metabolically instability and low oral bioavailability.¹³² Exchange of the phenol feature of aminotetralin derivatives by a more lipophilic 2-aminothiazole resulted in pramipexole.¹³³ In this investigation, clear insights into structure-affinity relationships of pramipexole derivatives have been gained. It is already known that the length of the alkyl substituent on the secondary nitrogen atom in 6-position is important for affinity binding at dopamine D₂ and D₃ receptors and best results have been demonstrated for a *N*-propyl residue, as found in pramipexole and rotigotine (cf. 1.2.6).^{133,230} The extension of the *N*-alkyl chain on the secondary basic nitrogen from methyl to ethyl and propyl (**41** → **42** → **43**) and subsequently the improved binding affinities for both dopamine receptor subtypes clearly confirm these previous results.^{132,230} The lipophilic character of the propyl chain and the

possibility of the *N*-propylamine to freely rotate might contribute to the interaction of the positive charged nitrogen under physiological conditions with the highly conserved aspartate of the dopamine D₂ and D₃ receptor. Furthermore it has been previously shown in our research group (data not shown)²³¹ and by Schneider et al.,¹³³ that a primary 6-amino function is less affine. Another outcome of this structure-affinity relationship is the importance of the amino group in 2-position of the thiazole ring. Pramipexole and compound **54** have shown an increased affinity binding for both dopamine D_{2S} and D₃ compared to the hydrogen, halogen or ether substituted compounds. The exocyclic amino group may substitute for the hydroxyl group of the catechol structure and as a hydrogen-bond donor it interacts with the serine residues in TM5 of the dopamine receptors. The methoxy substituted compound **46** has shown high affinity binding for dopamine D₃ and micromolar affinity binding for dopamine D₂ receptors, and the modification has demonstrated as remarkable selectivity for dopamine D₃ receptors comparable to pramipexole. The methoxy group, comprising electron donor properties, might interact as a hydrogen-bond acceptor with the binding site; however, further enlargement of the alkyl chain (**47** - **50**) and additional fluoro substitution (**51**) have not been tolerated at both dopamine receptor subtypes. Worth mentioning that the propoxy substituted compound **48** has shown similar micromolar binding affinities at dopamine D₃ and D₂ receptors without any receptor preference. The electron rich and withdrawing halogen atoms in compound **44**, **45**, and **53** have also decreased binding affinities compared to that of pramipexole. This can be explained by the lack of forming hydrogen bonds to the receptor binding sites. The replacement of the sulphur atom by a selenium atom increased affinities for dopamine D_{2S} and D₃ receptors (**42** → **52**). Furthermore, the selenium derivative **54** has the closest structural similarity to pramipexole and has demonstrated the highest affinity for dopamine D₃ receptors among this series of pramipexole analogues. An increase in lipophilicity due to the exchange of sulphur by selenium might cause interference with other important interaction points. Additional beneficial effects of selenium are its antioxidative and free radical scavenger properties and may possibly reduce the progression of Parkinson's disease.²³²

Positively encouraged by the results of the pramipexole analogues and related compounds (see Table 4.12), the studies have been continued and extended. It was of interest to investigate in combining two structural dopamine D₃ receptor pharmacophore elements, namely the 6-amino-4,5,6,7-tetrahydrobenzothiazole moiety and the naphthalen-2-carboxamide residue, with high affinity and selectivity for dopamine D₃ receptors in order

to further improve affinity binding and selectivity. The 6-amino-4,5,6,7-tetrahydrobenzothiazole moiety is not only the substructure of pramipexole, it also presents the structural motif of etrabamine, a dopamine agonist developed for Parkinson's disease.²²⁹ The naphthalen-2-carboxamide moiety is found in the D₃-receptor preferring compound BP 897 and has confirmed to enhance high dopamine D₃ receptor affinity binding.¹⁴⁰ It had been assumed that introducing an additional dopamine D₃ receptor pharmacophore element has a positive impact on the interaction with dopamine D₃ receptor binding sites. Therefore the naphthalen-2-carboxamide residue has been coupled to the etrabamine motif via an alkyl chain varying in length. Moreover, alterations in the substitution pattern on the basic nitrogen of the etrabamine derivative have been conducted to examine its influence on affinity binding (Table 4.13).

Table 4.13 *K_i* values and Hill coefficients (in parentheses) of naphthalen-2-carboxamide derivatives.



No.	R	n	<i>K_i</i> [nM]		<i>K_i</i> (D _{2S}) / <i>K_i</i> (D ₃)
			hD _{2S}	hD ₃	
55	C ₂ H ₅	2	2549 ± 302 (0.78 ± 0.01)	68 ± 21 (0.93 ± 0.15)	38
56	H	4	20997 ± 2552 (0.75 ± 0.16)	147 ± 30 (0.99 ± 0.23)	143
57	CH ₃	4	3824 ± 1104 (0.85 ± 0.16)	25 ± 9.6 (0.79 ± 0.13)	153
58	C ₂ H ₅	4	1567 ± 303 (0.64 ± 0.09)	2.7 ± 0.9 (1.00 ± 0.29)	580
59	C ₃ H ₇	4	873 ± 388 (0.89 ± 0.10)	1.16 ± 0.2 (1.23 ± 0.06)	753
60	Allyl	4	459 ± 83 (0.89 ± 0.18)	0.95 ± 0.2 (1.12 ± 0.05)	483
61	Propargyl	4	9078 ± 684 (0.69 ± 0.04)	7.76 ± 1.4 (1.06 ± 0.36)	1170

Compounds linked via a tetramethylene spacer (**56** – **61**) have shown low nanomolar to nanomolar affinity binding for dopamine D₃ receptors and moderate micromolar to nanomolar binding at dopamine D_{2S} receptors. Compound **56**, possessing secondary nitrogen, has displayed only moderate affinity for dopamine D₃ and resulted in a loss of

affinity binding for D_{2S} receptors compared to its tertiary analogues **57** - **61**. Compounds with an increasing saturated alkyl chain (methyl (**57**) → ethyl (**58**) → propyl (**59**)) on the basic nitrogen of the etrabamine element have demonstrated an improved binding profile with low nanomolar affinity data for the dopamine D₃ receptor and moderate micromolar to nanomolar binding affinities for dopamine D₂ receptors. Consequently, this modification has led to a superior selectivity for dopamine D₃ receptors. Shorten the tetramethylene spacer of the ethyl substituted derivative (**58**) to 2 methylene units (**55**) has significantly reduced D₃ receptor affinity and has moderately decreased D_{2S} receptor affinity. For a comprehensive investigation, the saturated propyl chain (**59**) has been replaced by an unsaturated allyl (prop-2-enyl) residue (**60**) and this variation has improved the affinity for dopamine D₃ receptors with the most promising subnanomolar K_i value in this series, although the positive impact on dopamine D_{2S} receptor binding slightly has decreased the selectivity ratio for dopamine D₃ over D₂ compared to the saturated analogue (**59**). Exchange of the allyl (**60**) by a propargyl (prop-2-ynyl) (**61**) moiety has exhibited high affinity binding for the dopamine D₃ receptor but further enhancement compared to compound **60** has not been revealed. Whereas the introduction of the propargyl residue has caused a loss of affinity binding at dopamine D_{2S} receptors and to this point the most selective compound in this current approach has been achieved.

Investigation in structure-affinity relationships has apparently demonstrated that the existence of basic tertiary nitrogen has positive impact on receptor-ligand interaction. Compound **56** has a secondary nitrogen atom and this modification has shown reduced binding affinities for both dopamine receptor subtypes. This result emphasizes the importance of the protonated nitrogen of ligands allow them to interact with Asp 110 (D₃) and Asp 114 (D₂) in TM3 and to serve as a main anchor point for receptor-ligand interaction, which is conserved among aminergic GPCRs.¹²² As already discussed for pramipexole derivatives (see Table 4.12, **43** – **51**) the enlargement of the alkyl substituent on the nitrogen atom is crucial for affinity binding and dopaminergic activity. A *N*-propyl specific binding pocket has been proposed which is responsible for hydrophobic interaction between the alkyl chain of the ligand and the binding site of the receptor.²³⁰ The pharmacological data (**57** → **58** → **59**) of this study are in good agreement with these previous studies. It is noteworthy that the unsaturated allyl residue (**60**) increased affinity binding for both receptor subtypes compared to the saturated propyl analogue (**59**) probably caused by π -electron interaction and a rigidized alkyl residue. Nevertheless, compound **60** has not enhanced selectivity for dopamine D₃ over D₂ receptors. Introducing

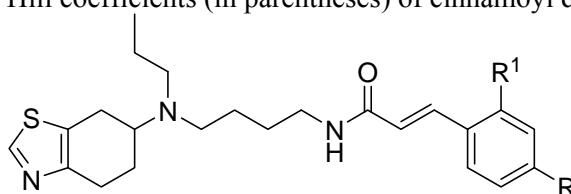
a linear and π -electron rich moiety such as a propargyl moiety (**61**) has strongly decreased dopamine D_{2S} affinity binding and moderately lowered dopamine D₃ affinity binding resulting in an superior selectivity for dopamine D₃ receptors. The propargyl residue is also found in selegilin (Movergan[®]) and rasagilin (Azilect[®]),^{233,234} two selective MAO-B-inhibitors for the treatment of Parkinson's disease. The alkynyl residue covalently binds to a flavin-cofactor and consequently causes irreversible inhibition.²¹ Moreover both compounds demonstrate neuroprotective properties and it is proposed that the propargyl moiety is involved in multiple survival signaling transduction pathways.^{26,233,235} It might be of interest to investigate in MAO-B-inhibiting activities of compound **61**. Another crucial aspect is the effect of the tetramethylene spacer as a linker. Extension of an ethyl (**55**) to a butyl spacer (**58**) has only moderate influence on dopamine D_{2S} binding affinity but has caused major improvement on dopamine D₃ receptor affinity. The extended and more linear ligand conformation has been favoured by dopamine D₃ receptors while dopamine D_{2S} receptor ligands have a bent and shorter conformation. This influence has already been described by our working group in previous studies.¹²⁶ The hydrophobic aryl moiety connected to an amide, here represented by naphthalen-2-carboxamide, has to have a certain distance to the basic nitrogen in order to allow interference with diverse interaction points in the binding site. In summary, by incorporating an additional dopamine D₃ receptor-preferring pharmacophore element compounds with enhanced affinities and high selectivity for dopamine D₃ receptors have been achieved.

Taking into account, that the tetramethylene spacer has proved to be favourable for affinity binding and selectivity for dopamine D₃ receptors and furthermore considering the positive effect on binding affinity for dopamine D₃ when the basic nitrogen is propyl substituted, a bioisosteric replacement of naphthalen-2-carboxamide by a cinnamoyl residue has consequently been constructed for further development of affinity binding and selectivity for dopamine D₃ receptors (Table 4.14). The cinnamoyl residue has been recognized in ST 198 (cf. 1.2.6) and incorporation of the structural element into molecules has demonstrated high affinity and selectivity for dopamine D₃ receptors (cf. 4.2.2).²²⁸ Furthermore, the influence of halogen substitution in *para*- and/or *ortho*-positions on the phenyl ring of the cinnamide residue has been investigated.

The halogen unsubstituted hybrid molecule **62** has demonstrated low nanomolar binding data for dopamine D₃ receptors and micromolar affinity binding at dopamine D_{2S} receptors, subsequently a high selectivity for the dopamine D₃ receptor has been revealed. Introducing chlorine substitution in *ortho*- and *para*-position (**63**) on the phenyl ring

increased affinity for dopamine D₃ and D_{2S} compared to that of the unsubstituted compound (**62**), but unfortunately this substitution pattern also reduced selectivity for dopamine D₃ receptors. Further modification on the phenyl system gave the *para*-substituted fluoro compound **64**. The fluorine incorporation has prominently improved binding and resulted in subnanomolar affinities for dopamine D₃ receptors. Whereas a diminished binding at dopamine D₂ receptors remarkable enhanced selectivity and the most affine and selective dopamine D₃ ligand not only in this series but also in the series of pramipexole and etrabamine derivatives has been recognized.

Table 4.14 K_i values and Hill coefficients (in parentheses) of cinnamoyl derivatives.



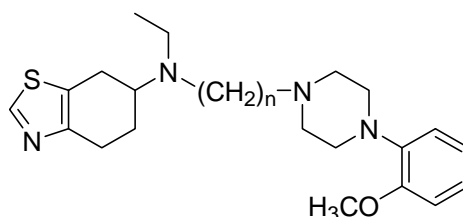
No.	R	R ¹	K_i [nM]		K_i (D _{2S}) / K_i (D ₃)
			hD _{2S}	hD ₃	
62	H	H	4015 ± 383 (0.47 ± 0.08)	8.11 ± 1.2 (1.00 ± 0.23)	495
63	Cl	Cl	445 ± 55 (0.81 ± 0.05)	2.41 ± 1.06 (1.02 ± 0.27)	185
64 (ST 625)	F	H	842 ± 35 (0.67 ± 0.02)	0.57 ± 0.04 (0.90 ± 0.22)	1477

With the exchange of the naphthalen-2-carboxamide moiety into a cinnamide residue, a bioisosteric rigid structure has been introduced. This *E*-cinnamide element, taken from ST 198, has been known as a high selective pharmacophore feature for dopamine D₃ receptors. Mono-, di-, and trisubstituted cinnamoyl derivatives have been entirely discussed in our working group,¹²⁶ but in this research the moiety has been coupled to an etrabamine residue for the first time. As expected for this structural class, the preference for dopamine D₃ receptors has been remarkably demonstrated. The fluorine monosubstitution (**64**) on the phenyl ring of the cinnamide residue has been favoured to chlorine disubstitution (**63**) and has been superior to the unsubstituted compound (**62**). The 4-fluoro substituent on the phenyl system (**64**, **ST 625**) is electron-rich and electron-withdrawing and has shown enhanced binding data with an impressive selectivity for dopamine D₃ over D₂ receptors. Additional lipophilic interaction with the receptor site might contribute to the promising results. On the other hand, a disubstitution (**63**) restricts the orientation of the cinnamide towards the basic nitrogen and the thiazole ring to a certain position and might decrease the

affinity. Compound **64** (**ST 625**) represents a promising potential radioligand for PET studies and further investigation in functional test systems and *in vivo* studies is highly required. Conclusively, the approach of combining two important dopamine D₃ receptor structural pharmacophore elements has been successful and compounds, in particular when *para*-fluoro substituted, have been achieved with high affinity and selectivity for dopamine D₃ receptors. Prospectively, to complete structure-affinity relationships differently halogen substituted cinnamoyl compounds need to be synthesised and studied.

In the first approach (Table 4.13), the aryl amide of the lead structure BP 897 has been incorporated. In the following study the basic amine aryl residue of BP 897, 4-(2-methoxyphenyl)piperazine, has been coupled to the etrabamine structure. This strategy considered different alkyl chain length as spacer while the basic nitrogen of the etrabamine residue has been substituted with an ethyl residue (Table 4.15).

Table 4.15 K_i values and Hill coefficients (in parentheses) of 4-(2-methoxyphenyl)piperazine derivatives.



No.	n	K_i [nM]		K_i (D _{2S}) / K_i (D ₃)
		hD _{2S}	hD ₃	
65	2	148 ± 23 (1.00 ± 0.06)	14 ± 1.1 (0.92 ± 0.22)	11
66	3	140 ± 22 (1.03 ± 0.1)	89 ± 1.7 (0.92 ± 0.09)	2
67	4	480 ± 51 (0.86 ± 0.18)	55 ± 16 (0.84 ± 0.13)	9

All compounds have demonstrated nanomolar binding affinities at dopamine D₃ and D_{2S} receptors with moderate preference for the dopamine D₃ receptor. Two and four methylene units as a spacer were well tolerated at dopamine D₃ receptors (**65**, **67**), while two and three methylene units have been more favored by dopamine D_{2S} receptors (**65**, **66**). By coupling a 4-(2-methoxyphenyl)piperazine residue to an etrabamine feature, a second basic tertiary amine has been introduced. Under physiological conditions at least two of the three nitrogen atoms are protonated. It is assumed that the basic aryl amine component of BP 897 is important for its partial agonism.¹²⁶ Data indicate that the additional protonated nitrogen of the ligand has been well tolerated at dopamine D_{2S} receptors, while further

improvement in binding at dopamine D₃ receptors has not been revealed. Nevertheless, due to its nanomolar affinities at both dopamine receptor subtypes, compound **66** might be an interesting and worthwhile ligand for the treatment of Parkinson's disease.

It might be of high interest to investigate in computer-based approaches and study the docking of the combined dopamine D₃ receptor pharmacophore elements bearing molecules into the binding pocket of dopamine D₃ and D₂ receptors. It is most likely that the ligands have two different orientations to allow reinforced ionic bonds of the protonated nitrogen with the highly conserved aspartate in TM3. Additionally, the results have shown that dopamine D₂ receptors favour ligands with a short and bend conformation (**65**, **66**) while dopamine D₃ receptors prefer ligands with a more linear conformation (**65**, **67**).¹²⁶ This assumption has already been confirmed by binding data of compounds **55** and **58**.

In the next step, varied heteroaryl amide moieties, including benzo[*b*]thiophen-2-carboxamide and its structural analogue benzo[*b*]thiazol-2-carboxamide, have been linked via butyl chain to the etrabamine structure (Table 4.16). The benzo[*b*]thiophen-2-carboxamide residue is taken from FAUC 365, a dopamine D₃-preferring ligand (cf. 1.2.6). In previous studies the tetramethylene spacer has been clearly preferred by dopamine D₃ receptors and consequently it has been used for further improvement of ligand binding. As already mentioned in earlier studies, the extension of the alkyl substituent on the basic nitrogen is considered to be critical to the dopaminergic activity. Therefore, evaluation of varying alkyl length has been carried out.

In the series of benzo[*b*]thiophen-2-carboxamide compounds (**68** - **71**) the growing alkyl chain on the basic nitrogen has produced molecules exhibiting steadily increasing affinity binding for dopamine D_{2S} receptors. The affinity for dopamine D₃ constantly increased from the unsubstituted (**68**) to methyl-, (**69**) and ethyl-substituted (**70**) ligand. Introduction of the ethyl substituent (**70**) on the basic nitrogen resulted in the most promising ligand within this series, demonstrating low nanomolar affinity at dopamine D₃ receptors while its affinity for dopamine D_{2S} proved to be in the micromolar range. Consequently, the modification resulted in a remarkably selectivity ratio for dopamine D₃ receptors. Further extension to propyl substitution (**71**) has slightly decreased affinity binding for dopamine D₃ receptors compared to compound **70** and accordingly lowering the selectivity ratio. Bioisosteric replacement of benzo[*b*]thiophen-2-carboxamide with a benzo[*b*]thiazol-2-carboxamide moiety has led to compound **72** and **73**. While secondary nitrogen bearing compound **72** has revealed a loss of affinity binding for dopamine D_{2S} and micromolar

affinity binding for dopamine D₃ receptors, tertiary *N*-propyl substituted compound **73** has demonstrated improved binding affinity for both dopamine receptor subtypes compared to **71** and **72**, and an increase in selectivity for dopamine D₃ receptors.

Table 4.16 K_i values and Hill coefficients (in parentheses) of heteroaryl amide derivatives.

No.	R	R ¹	K_i [nM]		K_i (D _{2S}) / K_i (D ₃)
			hD _{2S}	hD ₃	
68	H		23420 ± 1217 (1.02 ± 0.23)	292 ± 41 (0.92 ± 0.18)	80
69	CH ₃		3388 ± 388 (1.13 ± 0.20)	53 ± 5.1 (1.06 ± 0.22)	64
70	C ₂ H ₅		2496 ± 463 (0.58 ± 0.06)	2.92 ± 0.48 (0.96 ± 0.15)	855
71	C ₃ H ₇		2278 ± 105 (0.88 ± 0.12)	16 ± 6 (0.93 ± 0.17)	142
72	H		24480 ± 7580 (0.81)	1895 ± 510 (0.73 ± 0.21)	13
73	C ₃ H ₇		1667 ± 602 (0.55 ± 0.04)	4.53 ± 0.91 (1.04 ± 0.37)	368
74	C ₂ H ₅		2101 ± 327 (0.76 ± 0.13)	5.61 ± 0.3 (0.92 ± 0.24)	375
75	C ₃ H ₇		347 ± 133 (0.78 ± 0.19)	0.65 ± 0.09 (0.82 ± 0.08)	534

To further evaluate regiochemistry, the benzo[*b*]thiazole residue has been attached to the carboxamide moiety in 6-position (**74**, **75**). The *N*-ethyl substituted ligand (**74**) has displayed micromolar affinity binding for dopamine D_{2S} and nanomolar affinity and high selectivity for dopamine D₃ receptors. *N*-propyl substitution (**75**) has resulted in nanomolar

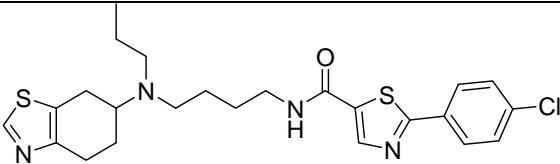
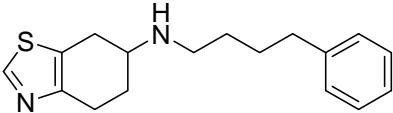
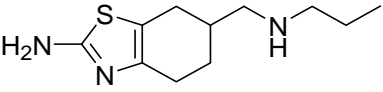
affinity for dopamine D_{2S} and subnanomolar affinity binding for dopamine D₃ receptors with improved selectivity ratio.

Heteroaromatic moieties play a major role in dopamine D₃ receptor affinity and selectivity. Introducing benzo[*b*]thiophen-2-carboxamide, benzo[*b*]thiazol-2-carboxamide, and benzo[*b*]thiazol-6-carboxamide residues led to high affine and selective dopamine D₃ receptor ligands. In this series, the FAUC 365 related compound **70** has displayed the highest selectivity for dopamine D₃ receptors. The benzo[*b*]thiophen-2-carboxamide scaffold in FAUC 365 has also proved to effect high selectivity for dopamine D₃ receptors. An additional heterocyclic nitrogen atom in molecule (**71** → **73**, **75**) has increased affinity binding for both receptor subtypes and enhanced selectivity ratio for dopamine D₃ receptors. Similar to sulphur, the nitrogen is able to form a hydrogen-bond with the binding sites of the dopamine receptor. Attaching the heteroaromatic residue in 6-position seems to be beneficial for the steric orientation of the etrabamine residue and benzo[*b*]thiazole-6-carboxamide moiety and allows stronger interaction with the dopamine receptor as indicated by compound **75**. Structural analogues of the propyl substituted etrabamine derivative **70** have been already discussed in Table 4.14 (**62** - **64**). As seen before (**56**), etrabamine derivatives with a secondary nitrogen (**68**, **72**) have shown a complete loss of affinity for dopamine D_{2S} and micromolare to moderate nanomolar affinities for dopamine D₃ receptors. Data confirm the importance of the tertiary basic nitrogen to interfere with aspartate in TM3. By varying the *N*-alkyl chain the importance of the *N*-propyl binding motif has been verified for benzo[*b*]thiazole carboxamide ligands (**72** → **73**, **74** → **75**), but it has not been demonstrated for benzo[*b*]thiophen-2-carboxamide derivatives (**68** → **71**). In summary, this process has been successfully applied by combining etrabamine derivatives with heteroaryl amide moieties.

Diverse structural elements such as a phenyl substituted thiazole carboxamide residue; a phenyl moiety or saturated propyl chain, have been coupled to either the etrabamine structure or pramipexole (Table 4.17). The etrabamine derivative **76** has been linked to a thiazole carboxamide, and this moiety has been extended by a *para*-chloro phenyl substituent. This enlargement has been well-tolerated by the dopamine D₃ receptor demonstrating nanomolar affinity binding, but introducing the lipophilic aromatic residue has caused moderate affinity binding at dopamine D_{2S}. In compound **77** the lipophilicity has been increased by combining the etrabamine motif linked via a butyl spacer to a phenyl substituent. The ligand has only displayed micromolar affinity for both dopamine receptor subtypes. The lack of hydrogen-bond donor or acceptor atoms, mostly represented by

amide functionality, and the incorporation of a lipophilic, flexible extended residue might have caused the decreased affinities. Compound **78** has close structural similarity with pramipexole. Introducing an additional methylene unit between the 2-aminotetrahydrobenzothiazole and the propylamine residue has induced a lack of affinities at dopamine D_{2S} and D₃ receptors demonstrated by binding data in the micromolar range.¹³³ This result has shown that the positions of the exocyclic amino functionality and thiazole system relative to the basic nitrogen play an important role for affinity binding.

Table 4.17 K_i values and Hill coefficients (in parentheses) of diverse structural elements.

No.	Structure	K_i [nM]		K_i (D _{2S}) / K_i (D ₃)
		hD _{2S}	hD ₃	
76		2522 ± 144 (1.08 ± 0.10)	83 ± 2 (1.16 ± 0.24)	30
77		8437 ± 195 (0.87 ± 0.21)	1447 ± 526 (1.06 ± 0.21)	6
78		>20.000	>15.000	

The combination of dopamine D₃ receptor pharmacophore features has been successfully applied; combining the etrabamine motif with aryl amide residues has resulted in compounds with high affinity and prominent selectivity for dopamine D₃ receptors. In contrast, incorporating aryl residues linked via a butyl spacer has revealed ligands which have not obviously discriminated the dopamine receptors.

Further investigations contain *in vitro* functional assays to assess intrinsic activities and also *in vivo* studies to determine the pharmacological effects. Pramipexole has demonstrated a remarkable receptor profile. It has shown a high selectivity for dopamine D₂-like receptors with highest affinity for dopamine D₃ receptors, whereas only small interaction with aminergic receptors has been noticed.^{236,237} This binding profile lowers the risk of dyskinesia and cardiovascular side-effects. Pharmacokinetic studies revealed no potential to interact with other drugs via the cytochrome P450 enzyme system.²³⁸ Pramipexole also provides neuroprotective effects and therefore may delay disease progression.⁸⁴ Consequently, prospect studies might concentrate on a homogeneity in

receptor binding profiles, pharmacokinetic properties and neuroprotective effects of the novel pramipexole and etrabamine derivatives.

It is of interest, if these large molecules still allow the receptor to change its conformation in order to fully activate the receptor. It is noteworthy to mention, that agonist binding is far more complex than antagonist binding. If agonist binding is directly measured with an agonist radioligand, then only the high affinity binding of the ligand may be observed and show higher affinity in inhibiting agonist radioligands than antagonist radioligands. Radioligand agonist competition is more relevant assessing receptor selectivity data for agonists; otherwise an overestimation of selectivity might be concluded.

In summary, introducing an additional dopamine D₃ receptor pharmacophore element into pramipexole or etrabamine resulted in numerous compounds with high affinity and remarkable selectivity for dopamine D₃ receptors. Further studies might underline the potential of the ligands as drug candidates.

4.3 Virtual Screening Leading to New Scaffolds

Due to the lack of a crystal structure of dopamine receptors an accurate three-dimensional (3D) structure of the receptor has not been available.¹²¹ Therefore ligand binding at dopamine receptors and the structural requirements for affine and subtype selective ligands is not completely resolved.¹²¹ Knowledge has principally based on investigations in structure-activity relationships of ligand binding and new lead finding is a difficult task. It is noteworthy that dopamine D₂ and D₃ receptors display a high sequence identity and the similarity of binding sites is still a challenge to obtain an improved selectivity for dopamine D₃ receptor ligands.^{24,239} Since much effort has been made in the field of chemical synthesis, investigation in computational chemistry as an alternative and worthwhile approach has been done to identify novel lead candidates with high affinity binding and dopamine D₃ receptor-preference.^{121,126,240} As one complement to HTS, ligand-based virtual screening methods have been successfully applied. Especially the support vector machine (SVM) approach, originally implemented to solve binary class/non class separation tasks,¹⁷⁷ has been introduced successfully for pharmaceutical data analysis and has shown promising applications in the prediction of GPCR ligands.^{241,242} Consequently, this method was investigated for virtual screening at dopamine D₂ and D₃ receptors in order to find new leads. Achieved and ordered compounds were pharmacologically tested (see 4.3.1). Encouraged by the results of the SVM approach, further various classification techniques were applied to succeed in novel lead identification. Clustering-based VS methods, regression-based VS and pharmacophore-based VS approaches were employed to improve the lead finding process. Identified molecules were assessed for affinity binding at dopamine D_{2S} and D₃ receptors (see 4.3.2).

4.3.1 Support Vector Machine Based Virtual Screening

Support vector machine (SVM) based virtual screening was performed to find novel lead structures with high affinity and selectivity for dopamine D₃ receptors. The detailed screening procedure is described by Byvatov et al.⁹ Generally, SVM classifiers are generated by a two step-procedure: first, sample data are described by labeled vectors and are projected to a high-dimensional space. Then the algorithm finds a class-separating linear hyperplane in this high-dimensional space, and finally, this hyperplane is projected back to the original data-space.¹⁷⁷ The aim of a classifier is to generate the hyperplane with the largest margin separating classes of a data vector. In the first step, a SVM was trained

on a reference (training) active dataset ($N = 395$) using analogues and related derivatives of BP 897 with defined K_i values of dopamine D_2 and D_3 receptor affinities. Each compound was described by a fingerprint of three-point pharmacophores (3PP). In addition to the binary SVM optimized, a regression SVM was generated to predict the logarithm of the ratio between K_i values for dopamine D_2 and D_3 receptors. By combining these models dopamine D_3 receptor-selective ligands should be identified. Virtual screening of synthetic compounds from the collection of Interbioscreen (IBS) ($N = 25,601$, release February 2004, Interbioscreen Ltd., 121019 Moscow, Russia) resulted in 169 molecules predicted to be active. Regarding poor solubility, potential chemical reactivity, and dissimilarity to dopamine leads, eleven compounds were manually selected and screened for binding affinities at dopamine D_{2S} and D_3 receptors. Data are shown in Table 4.18.

Table 4.18 Dopamine receptor affinities of compounds from the first virtual screening cycle.

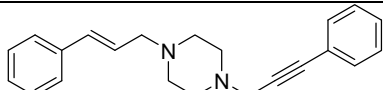
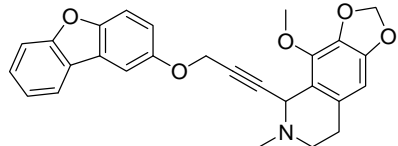
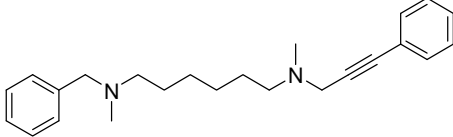
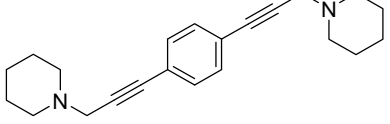
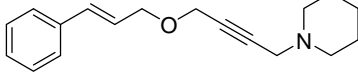
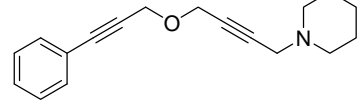
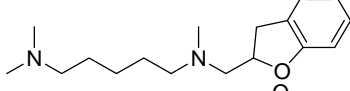
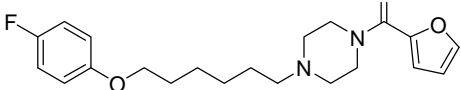
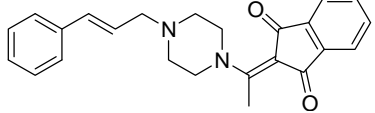
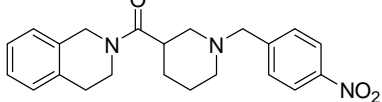
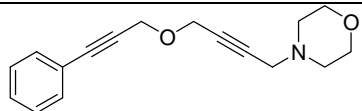
No.	Structure	K_i [μM]	
		hD_{2S}	hD_3
79		< 2	< 2
80		2 - 6	< 2
81		2 - 6	2 - 6
82		> 6	2 - 6
83		> 6	2 - 6
84		> 6	2 - 6
85		> 6	> 6
86		> 6	> 6
87		> 6	> 6
88		> 6	> 6

Table 4.18 (continued)

No.	Structure	K_i [μM]	
		hD_{2S}	hD_3
89		> 6	> 6

Although most of the compounds have shown binding affinities in the micromolar range at dopamine D_{2S} and D_3 receptors, compounds **79** and **80** have demonstrated $< 2 \mu\text{M}$ binding affinities at the dopamine D_3 receptor. Compound **80** was the most promising ligand with a $K_i(D_3) < 2 \mu\text{M}$ and $K_i(D_2) 2 - 6 \mu\text{M}$ and was used for further optimization.

For the purpose of improving dopamine D_3 receptor affinity and selectivity, an optimization of compound **80** was performed using a similarity search approach based on 3PP pharmacophores which were important for the SVM prediction. Virtual screening of the SPECS collection ($N = 229,685$, release January 2004, SPECS, 2628 XH Delft, The Netherlands) was carried out. 134 compounds were obtained and manually selected by criteria of drug-likeness, diversity and novelty. Finally, five compounds were tested for binding affinities at both dopamine receptor subtypes (Table 4.19). A short overview of the design of the experiment is shown in Figure 4.20.

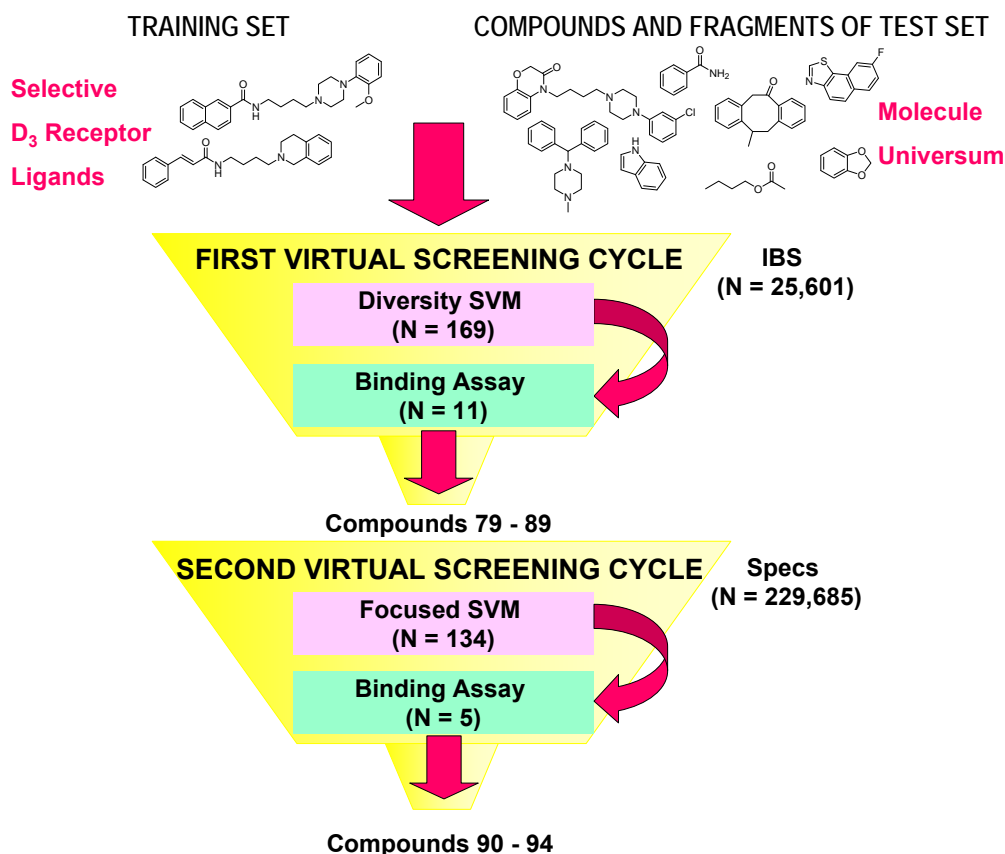
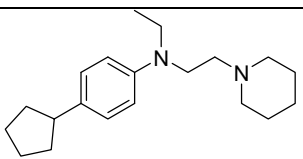
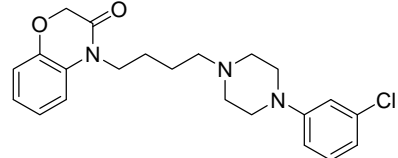
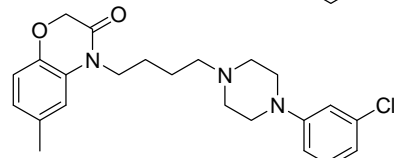
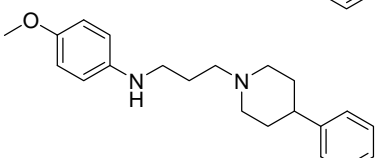
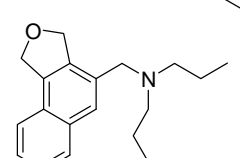
**Figure 4.20** Design of the experiment of support vector machine approach.

Table 4.19 Dopamine receptor affinities of compounds from the second virtual screening cycle (from Specs catalogue).

No.	Structure	K_i [nM]		$K_i(D_{2S}) / K_i(D_3)$
		hD_{2S}	hD_3	
90		1414 ± 516 (1.35 ± 0.43)	1408 ± 1068 (1.38 ± 0.5)	1
91		554 ± 97 (1.13 ± 0.22)	40 ± 6 (1.06 ± 0.15)	14
92		417 ± 60 (1.12 ± 0.13)	139 ± 17 (1.18 ± 0.15)	3
93		201 ± 48 (1.03 ± 0.13)	96 ± 21 (1.09 ± 0.30)	2
94		4395 ± 497 (0.87 ± 0.08)	914 ± 307 (1.10 ± 0.17)	5

In the similarity search,⁹ four out of five compounds have displayed nanomolar affinities at dopamine D₃ receptors. Compounds **91** - **93** possess the structural important features for dopamine D₂ and D₃ antagonist binding: a basic amine aryl moiety, represented by the 4-phenylpiperazine motif (**91**, **92**) as seen in BP 897 (cf. 1.2.6) or phenylpiperidine (**93**) found in the dopamine D₂-preferring haloperidol (cf. 1.2.6), a linear tetramethylene chain, and an aryl substituted hydrogen-bond acceptor. In this series the benzo[1.4]oxazin-3-one compound **91** has demonstrated high affinity binding and a clear preference for the dopamine D₃ receptor. In this molecule, the amide functionality is rigidly incorporated into the heteroaromatic moiety. This favorable orientation contributes to the binding profile. Docking of compound **91** into a homology model of dopamine D₃ has been constructed based on a 2.8 Å resolution rhodopsin crystal structure (PDB-code 1F88).⁹ Insight in protein-ligand binding interactions has been shown in Figure 4.21. In the active site the residues Asp110, Ser192, Phe345, and Phe346 are predicted to be important for ligand binding, exemplified by **91**, to the dopamine D₃ receptor. Introducing an additional methyl residue into the benzo[1.4]oxazin-3-one moiety (**92**) has clearly decreased affinity binding for dopamine D₃ receptors. In compound **94** the non-polar *N,N*-dipropyl residue was

recognized, a feature which has already described for diverse dopamine D₃ agonist such as (*R*)-(+)-7-OH-DPAT (cf. 1.2.6).

The results of the first cycle have been of limited success only and might be explained by the manual post-selection of the molecules. The goal of this investigation was a maximum of diverse and dissimilar compounds with affinity binding for dopamine D₃ receptors. This concept has resulted in reduced binding affinities for both receptor subtypes. The SVM was trained on a data set of analogues of BP 897 represented by the general structural pattern of a hydrophobic residue connected to an amide, an alkyl spacer and a basic lipophilic amine aryl moiety.^{9,243}

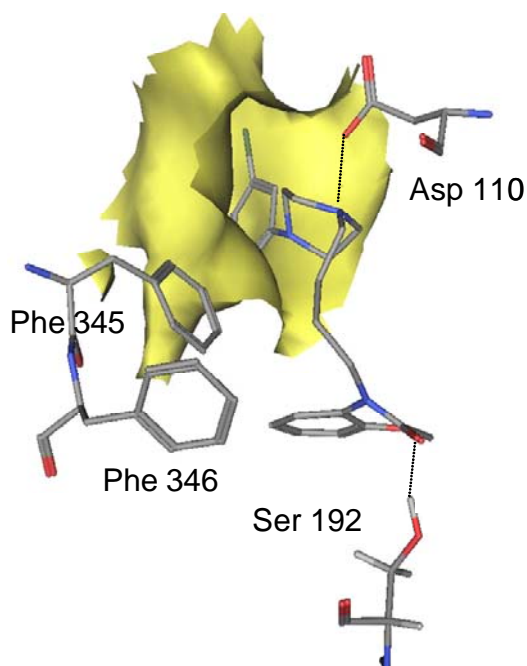


Figure 4.21 Docking of compound **91** into homology model of human dopamine D₃ receptor.⁹

In the first cycle all obtained compounds had basic tertiary nitrogen atoms, but only compounds **79** and **80** generally fulfilled requirements of this structural pattern and gave moderate binding affinities for dopamine D_{2S} and D₃ receptors. Some compounds had two basic nitrogen atoms, lacked of hydrogen-bond functionality, or demonstrated enlarged spacer with an additional ether function. This might give an explanation for the missing affinity binding. In the second cycle, a focused SVM based-similarity search was employed. All important features for interaction between ligand and dopamine receptor, such as basic nitrogen, hydrogen-bond functionality, and aromatic residue, were considered. Unfortunately, but not unexpected, compounds **91** - **93** have displayed structural similarity to the reference set, while **80**, **90**, **93** and especially **94** have contained novel structural features. These promising leads can be further optimized by chemical modifications to improve binding affinity and selectivity for dopamine D₃ receptors. The

applied iterative virtual screening cycles with SVM have been successful and lead scaffolds have been identified.

4.3.2 Lead Identification Strategies for Dopamine D₃ Receptor Ligands

To increase the success rate in the lead identification process for dopamine D₃ receptors several classification techniques were employed to generate novel lead scaffolds. Detailed procedures are described by Böcker.²⁴⁴ Clustered-based virtual screening was applied using two hierarchical clustering methods,²⁴⁵ namely NIPALSTREE and hierarchical *k*-means, and self organizing maps (SOM). 472 compounds with defined *K*_i binding affinity values at dopamine D₂ and D₃ receptors and the SPECS catalogue (released June 2003) were taken as a data set. The 472 ligands are mainly analogues of our lead structure BP 897 (cf. 1.2.6), a selective dopamine D₃ receptor partial agonist, which can be divided into three different features: (i) an aryl amide moiety, (ii) an alkyl spacer, (iii) a basic alkanamine residue with aryl substitution. All molecules were described by descriptors. Subsequently the SPECS compound collection with the included 472 compounds (N = 230,130) were virtually grouped based on similar molecular properties. SPECS molecules of clusters enriched with dopamine D₃ receptor ligands were pooled. In total 207 compounds were obtained. 17 out of 207 compounds were extracted by considering drug-like properties, the presence of positively charged nitrogen essential for receptor binding and dissimilarity to the training set. For this diverse subset of molecules binding affinities were determined at dopamine D_{2S} and D₃ receptors (Table 4.20). The design of the experiment is shown in Figure 4.22.

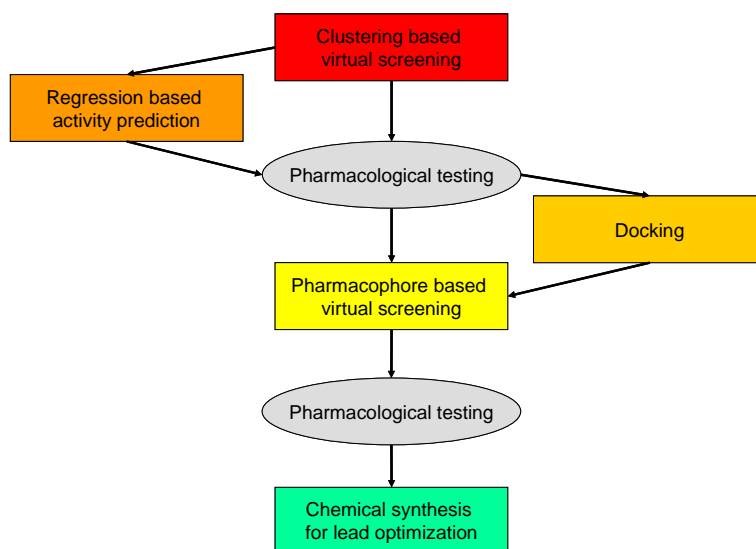


Figure 4.22 Design of the experiment of virtual screening approach.

Table 4.20 Dopamine receptor affinities of compounds from clustering-based virtual screening.

No.	Structure	K_i [nM]		K_i (D _{2S}) / K_i (D ₃)
		hD _{2S}	hD ₃	
95		901, 730 (0.88 ± 0.11)	65 ± 7.26 (0.95 ± 0.23)	12.6
96		894, 666 (0.93 ± 0.14)	289, 244 (1.11 ± 0.79)	2.9
97		7750, 4900 (0.83 ± 0.43)	1367, 621 (0.88 ± 0.34)	6.4
98		11716 ± 6172 (0.54 ± 0.06)	3212, 1935 (0.66 ± 0.34)	4.6
99		3351, 4766 (1.28 ± 0.46)	214, 297 (0.88 ± 0.25)	15.9
100		2812, 2363 (1.14 ± 0.15)	573, 572 (0.91 ± 0.05)	4.5
101		1092, 779 (1.26 ± 0.18)	983, 938 (0.63 ± 0.02)	1.0
102		>10.000 (n.d. ^a)	4526, 4280 (0.91 ± 0.28)	3.6
103		801, 743 (1.13 ± 0.26)	264 ± 163 (0.93 ± 0.20)	2.9
104		>10.000 (n.d. ^a)	2007, 2037 (0.69 ± 0.18)	8.5
105		7013, 4431 (0.97 ± 0.51)	2299, 2268 (0.80 ± 0.23)	2.5
106		23713 ± 11540 (0.76 ± 0.06)	3466, 10320 (0.72 ± 0.27)	3.4

Table 4.20 (continued)

107		>10.000 (n.d. ^a)	3016, 6542 (1.15)	12.3
108		3212, 5549 (0.61 ± 0.28)	190 ± 58 (0.99 ± 0.26)	23.1
109		>50.000 (n.d. ^a)	>5.000 (n.d. ^a)	3.7
110		216, 284 (0.90 ± 0.19)	2707, 2464 (1.24 ± 0.18)	0.1
111		495, 575 (0.78 ± 0.16)	1093, 621 (0.77 ± 0.16)	0.6

^an.d., not determined. All compounds were aligned according to the basic nitrogen.

In this series, a K_i of below 1 μ M was defined a “hit”. The pharmacological testing has revealed nine active molecules at dopamine D_3 receptors and six active compounds at dopamine D_{2S} receptors. Among these molecules, a K_i value below 300 nM at dopamine D_3 receptors has been presented by compounds **95**, **96**, **99**, **103**, **108** and at dopamine D_{2S} receptors by compound **110**. Six molecules (**98**, **102**, **104**, **106**, **107**, **109**) have demonstrated a loss of affinity binding for dopamine D_{2S} receptors ($> 10 \mu$ M) and low affinity binding for D_3 receptors (2 - 7 μ M). The most promising molecule **95** has displayed a K_i (D_3) value of 65 nM and a 13-fold preference for dopamine D_3 receptors. The ligand has the 4-(2-methoxyphenyl)piperazine motif of BP 897. Referring to the classical division of antagonists and partial agonists, the hydrophobic aryl moiety has been replaced by a non-aromatic bicycle[2.2.1]heptane residue. Aryl-thioether moieties have been noticed in compound **96** and **99** and have moderate affinities for both receptor subtypes with preference for dopamine D_3 receptors. It is noteworthy that the amide functionality is absent in compound **103** and moderate affinity for dopamine D_2 and D_3 with a slight preference for D_3 receptors has been obtained. The two ether oxygen atoms are conjugated with the phenyl ring and have a partial charge comparable to the amide

oxygen of BP 897 (partial charge calculation were performed with the software package Gaussian, data not shown).²⁴⁴ An acceptable selectivity profile (23-fold) for dopamine D₃ receptors has been obtained with the dibenzocycloheptadiene derivative **108**, a compound with similar structural features to tricyclic antipsychotic drugs such as clozapine.²²⁴ The butyrophenone derivative **110** is closely related to haloperidol (cf. 1.2.6),¹³¹ a neuroleptic drug, and as expected, it has displayed moderate affinity binding and selectivity (10-fold) for dopamine D₂ receptors. This dopamine D₂-preferring binding behavior has also been observed for compound **111**, a chromen-2-one derivative. The encouraging binding data of these structurally diverse molecules were further highlighted by the benzamide moiety as a promising linker recognized for compounds **95** - **100**. Considering the common structural requirements for dopamine D₂/D₃ receptor ligands with antagonist properties, the benzamide scaffold has been incorporated in between the aryl moiety and the basic amine aryl moiety. Benzamide residues in dopamine D₂-like compounds are already well-known. Representatives of benzamides are the atypical antipsychotics sulpride and raclopride with high affinity binding for dopamine D₂ and D₃ receptors (cf. 1.2.6).¹³² In our previous studies a replacement of an alky chain into a rigid xylene spacer resulted in moderate to good affinity binding for both dopamine subtype receptors.²⁴³ Our training set has also included these xylene spacer compounds and gave a positive impact on the screening. A clear advantage of the benzamide as a spacer is that this structure is synthetically easy accessible and synthetic modifications can be carried out with an appropriate effort. Additionally, parallel synthesis might be possible for lead optimization.

With the aim of prospectively predict the affinities for the 17 ordered compounds a regression based affinity prediction trained by support vector based regression,⁹ neural nets and partial least squares²⁴⁶ using different descriptor sets was investigated. The application to the 17 compounds was of limited success only (data not shown). This result clearly shows that in this context experimental determination of binding affinity values for new structural molecules is of absolute necessity since techniques of computational chemistry are thus far not able to predict reliable affinity values.

To enlighten the binding mode of the SPECS compounds in the binding pocket docking analysis was performed. A 3D homology model⁹ (see 4.3.1) of the dopamine D₃ receptor was employed and 17 compounds were docked using GOLD docking.²⁴⁷ The positive score values indicated a successful fitting of all compounds into the binding pocket (data not shown).²⁴⁴ The binding modes observed suggested a second alternative binding pocket for the aryl moiety. For further elucidation of this putative binding mode a pharmacophore

model for dopamine D₃ receptor antagonists was constructed requiring both aryl moieties simultaneously. A 3D pharmacophore model was used (model not shown) and containing an aromatic potential pharmacophore point (PPP) for both aryl moieties, an acceptor PPP at the position of the oxygen amide, a hydrophobic or aromatic PPP in the spacer region, an essential cationic PPP and an aromatic PPP in the amine residue. All PPPs were required as crucial except the acceptor and spacer element. The SPECS catalogue (N = 229,658) was screened and 35 molecules were identified. After manual selection considering the aspect of the diverse binding mode four molecules were ordered and tested for binding affinities at dopamine D_{2S} and D₃ receptors (Table 4.21).

Compounds **112** and **113** have shown moderate affinity and dopamine D₃ receptor-preference. Both ligands contain a benzhydrylidene substituted pyrrolidindione residue as a hydrophobic aryl moiety, and a phenylpiperazine moiety. Compound **112** demonstrates structural similarity to the phthalimide derivative NAN190 (*N*-(4-[4-(2-methoxyphenyl)piperazinyl]butyl)isoindolin-1,3-dion), which only has demonstrated slightly lower binding affinity for dopamine D₃ ($K_i = 38 \pm 6$) than for D₂ ($K_i = 50 \pm 6$) receptors.²²² Although the molecules are planar and rigidized they seem to fit into the binding site. Compound **112** contains the 4-(2-methoxyphenyl)piperazine motif of BP 897 and has shown unexpectedly good results for dopamine D₃ but also D₂ receptor binding. By replacing the methoxy functionality in 2-position with a chlorine in 3-position (**113**) on the phenyl ring the affinities for both receptors have been decreased but the selectivity ratio has not changed. The enlarged substituents in compound **114** and **115** had a negative impact on affinity binding for dopamine D₂ and D₃ receptors. The flexible dibenzylcarbamoylbenzyl substituted 1,2,3,4-tetrahydroisoquinoline (**114**) was more tolerated than the bulky and rigid benzoimidazo substituted phenylpiperazine (**115**). By comparing **112** and **114** in an alignment, the molecules split at different distances to the acceptor functionality. This might give an explanation of the dissimilar binding characteristics. In summary, several compounds were identified with novel structural elements in a short-term period and a cost-saving procedure applying different classification techniques of chemoinformatic approaches. A benzamide residue has been recognized incorporated as a spacer element. This promising scaffold is chemically easy accessible and allows performance of parallel synthesis to generate SAR of analogues.

Table 4.21 Dopamine receptor affinities of compounds from pharmacophore based virtual screening.

No	Structure	K_i [nM]		$\frac{K_i(D_{2S})}{K_i(D_3)}$
		hD _{2S}	hD ₃	
112		162 ± 26 (1.20 ± 0.12)	65 ± 9 (1.52 ± 0.23)	2.5
113		1359 ± 315 (1.78 ± 0.28)	498 ± 76 (1.25 ± 0.80)	2.7
114		1376 ± 285 (1.29 ± 0.86)	>1.000 (n.d.)	0.6
115		4392 ± 348 (0.86 ± 0.26)	2636 ± 349 (0.77 ± 0.11)	1.7

Additionally, two novel structural elements for aryl residue replacement were noticed: a non-aromatic bicycle[2.2.1]heptane and a aryl-thioether moiety. The 4-(2-methoxyphenyl)piperazine residue of BP 897, the 1,2,3,4-tetrahydroisoquinoline motif seen in ST 198 and SB 277011 (cf. 1.2.6), the butyrophenone and dibenzocycloheptadiene moieties from marketed antipsychotic drugs has been recognized by virtual screening methods. These encouraging results confirm the applicability of the employed computational techniques in early stages of the drug discovery process for new lead finding.

5 Summary

The development of novel drugs targeting GPCRs is of particular interest since modulation of subfamilies of this receptor class highly influences neurotransmission in the central nervous system. This study has focused on the development of ligands for the dopamine D₃ receptor. The receptor belongs to the dopamine D₂-like family among the biogenic amine binding GPCRs. The dopamine D₃ receptor is involved in neurological and neuropsychiatric disorders such as Parkinson's disease, schizophrenia and drug addiction. Due to its close structural similarity to the dopamine D₂ receptor subtype, it is still a challenge to identify and further optimize new leads. Therefore an *in vitro* screening assay, which also allows elucidating comprehensive structure-affinity relationships, is required.

In this investigation the implementation and evaluation of radioligand binding assays for human dopamine D_{2S} and dopamine D₃ receptors and for the related aminergic human histamine H₁ receptor stably expressed in Chinese hamster ovary (CHO) cells has been performed. Saturation binding experiments with [³H]spiperone at dopamine D_{2S} and D₃ receptors and with [³H]mepyramine at histamine H₁ receptors were carried out. The determined equilibrium dissociation constant of radioligands (K_d) and the total number of specific binding sites (B_{max}) of the receptor membrane preparations were in good agreement with reference data. Inhibition constants (K_i) of reference ligands obtained in radioligand competition binding experiments at dopamine hD_{2S}, hD₃ and histamine H₁ receptors validated the reliability and reproducibility of the assay. In order to discriminate agonists from antagonists, a GTP shift assay has been investigated for dopamine D_{2S} and D₃ receptors. In competition binding studies at dopamine D_{2S} receptors the high- and low affinity state in the absence of the GTP analogue Gpp(NH)p has been recognized for the agonists pramipexole and the seleno analogue **54**. In the presence of Gpp(NH)p a decrease in affinity, referred to as "GTP shift", has been revealed for agonists at dopamine D_{2S} and D₃ receptors. An effect of Gpp(NH)p on dopamine D_{2S} receptor binding has not been observed for the antagonists ST 198 and BP 897, while a reverse "GTP shift" has been noticed at the dopamine D₃ receptor. For the development of novel ligands with high affinity and selectivity for dopamine D₃ receptors, investigation in refined structure-affinity relationships (SAR) of analogues of the lead BP 897 has been performed. Replacement of the naphthalen-2-carboxamide of BP 897 by aryl amide residues (**1** - **4**) had a clear influence on affinity binding and selectivity for dopamine D₃ receptors. Introduction of the benzo[*b*]thiophen-2-carboxamide (**1**) has markedly improved binding with subnanomolar affinity and enhanced selectivity for dopamine D₃ receptors. Exchanging the aryl substituted basic alkanamine residue of **1** by a 1,2,3,4-

tetrahydroisoquinoline moiety (**6**) emphasized the benefit of the 4-(2-methoxyphenyl) piperazine residue of BP 897 regarding dopamine D₂ and D₃ receptor affinities. The change of particular elements of BP 897 and the rearrangement of the amide functionality resulted in inverse amide compounds with new chemical properties. Moderate affinity binding data, as obtained for the isoindol-1-carbonyl compound **11**, suggest that inverse amides provide a worthwhile new lead structure with a novel structural scaffold.

A hybrid approach combining privileged scaffolds of histamine H₁ receptor antagonists and fragments of dopamine D₃ receptor-preferring ligands, related to BP 897 and analogues has been investigated. Various benzhydrylpiperazine derivatives and related structures have shown moderate to high affinities for dopamine D₃ receptors with the impressive enhancement of the cinnamide substituted bamipine-related hybrid **39**, exhibiting the highest affinity and selectivity for dopamine D₃ receptors. Improved affinity profiles of structural modified histamine H₁ receptor antagonists for dopamine D₂ and D₃ receptors and a refined SAR has been achieved.

A SAR of derivatives of the dopamine agonist pramipexole and the related etrabamine has been studied. The propargyl substituted etrabamine derivative **61** demonstrated highest affinity and selectivity. The ligand attracts attention since neuroprotective properties have been reported for the propargyl functionality. Further development resulted in the most promising compound **64**, a cinnamide derivative with 4-fluoro substitution on the phenyl ring. Subnanomolar affinity and remarkable selectivity for dopamine D₃ receptors has aroused particular interest in this ligand due to its development potential as a radioligand for PET studies.

Radioligand binding studies in combination with virtual screening and different classification techniques of chemoinformatic methods resulted in further elucidation of SAR. New leads with novel chemical scaffolds have been found in the bicycle[2.2.1]heptane derivative **95** and the benzhydrylidene substituted pyrrolidindione **112** and can be further optimized by chemical modifications.

The outcome of the studies provides the development of various novel high affine and dopamine D₃ receptor selective ligands. Modifications of lead structures or application of chemoinformatic tools in combination with radioligand competition binding assays have resulted in new leads with different chemical scaffolds. Furthermore, a comprehensive insight into structure-affinity relationships of ligands at dopamine D₃ receptors has been revealed. This refined SAR is valuable to develop more affine and selective drug candidates with a designed pharmacological receptor profile.

6 Zusammenfassung

Das Ziel der Arbeit war die Entwicklung von neuen Liganden zur Beeinflussung der Neurotransmission im zentralen Nervensystem. Der Fokus lag auf dem Dopamin-D₃-Rezeptor, der eine wichtige Rolle bei Morbus Parkinson, Schizophrenie und Drogenmissbrauch spielt. Aufgrund seiner Strukturähnlichkeit zum Dopamin-D₂-Rezeptor ist es eine Herausforderung, neue, selektive Leitstrukturen für den Dopamin-D₃-Rezeptor zu identifizieren bzw. zu optimieren. Ein *in vitro* Testsystem ist hierfür erforderlich und ermöglicht das Aufstellen von Struktur-Wirkungsbeziehungen (SAR) und ein rationales Wirkstoffdesign.

Die Arbeit umfasste die Etablierung von Radioliganden Bindungsassays an Dopamin-D_{2S}- und -D₃-Rezeptoren, sowie am verwandten aminergen Histamin-H₁-Rezeptor, die stabil in Zelllinien von Ovarien des Chinesischen Hamsters exprimiert wurden. Sättigungsstudien wurden mit [³H]Spiperon am Dopamin-D_{2S}- und D₃-Rezeptor und mit [³H]Mepyramin am Histamin-H₁-Rezeptor durchgeführt. Die ermittelten Dissoziationskonstanten (K_d) und maximale Zahl der Bindungsstellen (B_{max}) stimmten mit den Literaturwerten überein. Die in Verdrängungsstudien bestimmten Inhibitionskonstanten (K_i) von Referenzsubstanzen am Dopamin-D_{2S}- und -D₃-Rezeptor sowie am Histamin-H₁-Rezeptor bestätigten die Zuverlässigkeit und Reproduzierbarkeit der Bindungsassays. Zur Unterscheidung der Agonisten von Antagonisten wurden „GTP-Shift“ Assays am Dopamin-D_{2S}- und -D₃-Rezeptor angewandt. Für Pramipexol und das Selenanalog **54** wurden zwei Bindungszustände mit unterschiedlichen Affinitäten (ein so genannter „high- und low affinity state“) am Dopamin-D_{2S}-Rezeptor in Abwesenheit von Gpp(NH)p beobachtet. Eine Affinitätsabnahme („GTP-Shift“) in Anwesenheit von Gpp(NH)p zeigte sich für die Agonisten am Dopamin-D_{2S}- und -D₃-Rezeptor. Dieser Einfluss des Gpp(NH)p konnte nicht für den Antagonisten ST 198 und den partiellen Agonisten BP 897 gezeigt werden. Für diese Verbindung wurde ein inverser „GTP-Shift“, also eine Affinitätsverbesserung am Dopamin-D₃-Rezeptor beobachtet.

Um neue Liganden mit hoher Affinität und Selektivität für den Dopamin-D₃-Rezeptor zu entwickeln, wurden ausführliche SAR verschiedener Derivate der Leitstruktur BP 897 und ST 198 erstellt. Der Austausch des Naphthalen-2-carboxamid-Rests von BP 897 durch verschiedene Arylamid-Strukturen (**1** – **4**) zeigte deren deutlichen Einfluss auf die Dopamin-D₃-Rezeptorbindungsaffinität und -selektivität. Die Einführung eines Benzo[*b*]thiophen-2-carboxamid-Rests führte in Verbindung **1** zu herausragender subnanomolarer Affinität am Dopamin-D₃-Rezeptor sowie zu deutlich erhöhter Selektivität im Vergleich zu BP 897. Die Variation des lipophilen basischen Amin-Restes von **1** ergab das 1,2,3,4-Tetrahydroisochinolin-Derivat **6**. Verdrängungsstudien konnten den Vorteil des 4-(2-Methoxyphenyl)piperazine-Substituenten von BP 897 bezüglich der Affinitäten am Dopamin-

D_{2S}- und -D₃-Rezeptor deutlich zeigen. Modifikationen einzelner Elemente von BP 897 und ST 198 und die veränderte Integration der Amid-Funktion in dem lipophilen Aryl-Rest führten zur Substanzklasse der inversen Amide mit neuen chemischen Eigenschaften. Moderate Bindungsaffinitäten, wie für das Isoindol-1-carbonyl-Derivat **11** gezeigt, legen nahe, dass inverse Amide eine lohnenswerte neue Leitstruktur mit andersartigem strukturellem Gerüst darstellen. In einer Hybrid-Strategie wurden Strukturelemente von Histamin-H₁-Rezeptorantagonisten mit Substrukturen von Liganden mit ausgeprägter Dopamin-D₃-Rezeptorpräferenz kombiniert. Daraus resultierten Benzhydrylpiperazin-Derivative und verwandte Substanzen mit moderater bis hoher Affinität am Dopamin-D₃-Rezeptor. Besonders hervorzuheben ist das Zimtsäureamid substituierte und zum Bamipin verwandte Hybrid **39**, welches die besten Ergebnisse in dieser Serie hinsichtlich Affinität und Selektivität am Dopamin-D₃-Rezeptor erbrachte. Verbesserte pharmakologische Profile der strukturell modifizierten Histamine-H₁-Rezeptorantagonisten am Dopamin-D_{2S}- und -D₃-Rezeptor und eine differenzierte SAR wurden erreicht.

Für Derivate des Dopaminrezeptoragonisten Pramipexol und des strukturähnlichen Etrabamin wurden SAR ausgearbeitet. Das Propargyl substituierte Etrabamin-Derivat **61** zeigte herausragende Dopamin-D₃-Rezeptoraffinität und -selektivität. Der Ligand ist von Interesse, da für den Propargyl-Rest neuroprotektive Eigenschaften berichtet wurden. Die Weiterentwicklung führte zur Verbindung **64**, einem Zimtsäureamid-Derivat mit 4-Fluor-Substitution am Phenylring. Subnanomolare Affinität und hohe Selektivität am Dopamin-D₃-Rezeptor prädestinieren **64** zur Anwendung als potentiellen PET-Radioliganden.

Radioliganden Bindungsstudien wurden auf die Ergebnisse von virtuellen Screeningstudien angewandt. Sie führten zur Identifizierung neuer Leitstrukturen und zum weiteren Verständnis der SAR. Als neue Leitstrukturen mit verschiedenartigen chemischen Gerüsten wurden unter anderem das Bicyclo[2.2.1]heptan-Derivat **95** und der Benzhydryliden substituierte Pyrrolidindion Ligand **112** gefunden. Diese können nun zur weiteren Optimierung chemisch modifiziert werden.

Die in dieser Arbeit durchgeführten Radioliganden Bindungsstudien führten zur Identifizierung, Entwicklung und Optimierung von hoch affinen und selektiven Dopamin-D₃-Rezeptor Liganden. Des Weiteren ermöglichten die Ergebnisse eine ausführliche Vertiefung der SAR. Die kombinierte Strategie von chemoinformatischen Methoden und Radioliganden Bindungsstudien hat das Finden neuer Leitstrukturen als potentielle Arzneistoffe erlaubt. Die Resultate ermöglichen in der Zukunft ein gezieltes Liganden-Design mit einem gerichteten pharmakologischen Rezeptorprofil.

7 Ausführliche Zusammenfassung

Das Ziel der Arbeit war die Entwicklung von neuen Liganden zur Beeinflussung der Neurotransmission im zentralen Nervensystem. Der Fokus lag auf dem Dopamin-D₃-Rezeptor, der zur Familie der Dopamin-D₂-ähnlichen Rezeptoren gehört. Der Dopamin-D₃-Rezeptor spielt eine wichtige Rolle bei neurologischen und psychiatrischen Erkrankungen wie Morbus Parkinson, Schizophrenie und Drogenmissbrauch bzw. -abhängigkeit. Aufgrund seiner Strukturähnlichkeit zum Dopamin-D₂-Rezeptor ist es nach wie vor eine Herausforderung neue, selektive Leitstrukturen für den Dopamin-D₃-Rezeptor zu identifizieren bzw. zu optimieren. Ein *in vitro* Testsystem ist hierfür erforderlich und ermöglicht das Aufstellen von Struktur-Wirkungsbeziehungen (SAR) und ein rationales Wirkstoffdesign.

Die Arbeit umfasste die Etablierung von Radioliganden Bindungsassays an Dopamin-D_{2S}- und -D₃-Rezeptoren, sowie an verwandten aminergen Histamin H₁-Rezeptoren, die stabil in Zelllinien von Ovarien des Chinesischen Hamsters exprimiert wurden. 115 Liganden wurden pharmakologisch an Dopamin-D_{2S}- und -D₃-Rezeptoren charakterisiert.

Die Entwicklung eines Radioliganden Bindungsassays beinhaltete Vorversuche, um optimale Testbedingungen zu finden. Hierzu gehörten unter anderem die Pufferzusammensetzung, Ionenstärke und pH-Wert Einstellung der Puffer, die Inkubationstemperatur, sowie die Herstellung der Zellmembranpräparation. In Bindungsexperimenten wurden die benötigte Proteinmenge, die Inkubationszeit und das Volumen der Waschschriffe ermittelt.

Sättigungsstudien wurden mit [³H]Spiperon am Dopamin-D_{2S}- und -D₃-Rezeptor und mit [³H]Mepyramin am Histamin-H₁-Rezeptor durchgeführt. Mit steigender Konzentration des Radioliganden war die spezifische Bindung für alle Rezeptorsubtypen gesättigt. Scatchard Analysen der spezifischen Bindungen der Radioliganden an den verschiedenen Rezeptoren waren linear. Eine einzige Bindungsstelle des jeweiligen Rezeptorsubtyps konnte bestimmt werden. Die nicht-spezifische Bindung war nicht gesättigt, stieg linear mit der Konzentration des Radioliganden an und zeigte Werte < 20% der Gesamtbindung. Die ermittelten Bindungsparameter K_d (Dissoziationskonstante) und B_{max} (maximale Zahl der Bindungsstellen) stimmten mit den Literaturwerten überein.

Die in Verdrängungsstudien bestimmten Inhibitionskonstanten (K_i) von Referenzsubstanzen am Dopamin-D_{2S}- und -D₃-Rezeptor, sowie am Histamin-H₁-Rezeptor entsprachen den Literaturwerten. Die nicht-spezifische Bindung war < 20% der Gesamtbindung und nur 10% des hinzugefügten Radioliganden wurden am jeweiligen

Rezeptorsubtyp gebunden. Diese Ergebnisse bestätigten die Zuverlässigkeit und Reproduzierbarkeit der etablierten Bindungsassays.

Für eine funktionelle Charakterisierung und zur Unterscheidung der Agonisten von Antagonisten wurden „*GTP-Shift*“ Assays am Dopamin-D_{2S}-, und -D₃-Rezeptor angewandt. Für Pramipexol und das Selenanalog **54** wurden zwei Bindungszustände mit unterschiedlichen Affinitäten (ein so genannter „high- und low affinity state“) am Dopamin-D_{2S}-Rezeptor in Abwesenheit von Gpp(NH)p, einer GTP analogen Verbindung, beobachtet. Eine Affinitätsabnahme („*GTP-Shift*“) in Anwesenheit von Gpp(NH)p zeigte sich für die Agonisten am Dopamin-D_{2S}- und -D₃-Rezeptor. Dieser Einfluss des Gpp(NH)p konnte nicht für den Antagonisten ST 198 und den partiellen Agonisten BP 897 gezeigt werden. Für diese Verbindung wurde ein inverser „*GTP-Shift*“, also eine Affinitätsverbesserung am Dopamin-D₃-Rezeptor beobachtet. Die Ergebnisse zeigen, dass eine Einteilung in Agonist, partieller Agonist and Antagonist mittels einem „*GTP-Shift*“ Assay durchführbar ist.

Um neue Liganden mit hoher Affinität und Selektivität für den Dopamin-D₃-Rezeptor zu entwickeln, wurden ausführliche Struktur-Wirkungsbeziehungen verschiedener Derivate der Leitstruktur BP 897 und ST 198 erstellt. Der Austausch des Naphthalen-2-carboxamid-Rests von BP 897 durch verschiedene Arylamid-Strukturen (**1** – **4**) zeigte deren deutlichen Einfluss auf die Dopamin-D₃-Rezeptorbindungsaffinität und -selektivität. Die Einführung eines Benzo[*b*]thiophen-2-carboxamid-Rests führte in Verbindung **1** zu herausragender subnanomolarer Affinität am Dopamin-D₃-Rezeptor sowie zu deutlich erhöhter Selektivität im Vergleich zu BP 897. Der Austausch des lipophilen basischen Aminrestes 4-(2-Methoxyphenyl)piperazine in **1** durch 1,2,3,4-Tetrahydroisochinolin, der Substruktur von ST 198, ergab Derivat **6** mit geringerer Affinität und Selektivität für den Dopamin-D₃-Rezeptor. Verdrängungsstudien konnten den Vorteil des 4-(2-Methoxyphenyl)piperazine-Substituenten von BP 897 bezüglich der Affinitäten am Dopamin-D_{2S}- und -D₃-Rezeptor, sowie die Selektivität am Dopamin-D₃-Rezeptor deutlich zeigen.

Modifikationen einzelner Elemente der Leitstruktur BP 897 und ST 198 und die veränderte Integration der Amid-Funktion in dem lipophilen Aryl-Rest führte zur Substanzklasse der inversen Amide. Diese Moleküle zeigen neuen chemischen Eigenschaften. Die Invertierung des Amids führte zu einer umgewandelten Funktionalität, neuen Orientierung des Carbonyl Sauerstoffes im Molekül, sowie zu einem veränderten Abstands des basischen Stickstoffes zum Amid im Vergleich zu den Leitstrukturen BP 897 und ST 198. Moderate Bindungsaffinitäten am Dopamin-D₂- und -D₃-Rezeptor mit mäßiger Dopamin-

D₃-Rezeptorpräferenz wurden, wie für das Isoindol-1-carbonyl Derivat **11** gezeigt, erhalten. Aufgrund dieser Ergebnisse ist die Weiterentwicklung der inversen Amide von Interesse, da sie eine lohnenswerte neue Leitstruktur mit andersartigem strukturellem Gerüst darstellen.

Aufgrund von Strukturähnlichkeiten der Antagonisten am Histamin-H₁-Rezeptor und an Dopamin-D₂-ähnlichen Rezeptoren wurde der Einfluss einer Hybridbildung dieser Liganden an Dopamin-D_{2S}- und -D₃-Rezeptoren, sowie am Histamin-H₁-Rezeptor untersucht. Substrukturen der Histamin-H₁-Rezeptorantagonisten (so genannte „Antihistaminika“) Cetirizin, Mianserin, Ketotifen, Loratadin und Bamipin wurden mit Strukturelementen der Leitstrukturen BP 897, ST 198 und analogen Verbindungen mit ausgeprägter Dopamin-D₃-Rezeptorpräferenz kombiniert. Daraus resultierten Benzhydrylpiperazin-Derivative, Moleküle mit tri- und tetrazyklischen Ringsystemen, sowie Bamipin- Analoga. Die Liganden wiesen moderate bis hohe Affinität am Dopamin-D₃-Rezeptor auf. Besonders hervorzuheben ist das Zimtsäureamid substituierte und zum Bamipin verwandte Hybrid **39**, welches die besten Ergebnisse in dieser Serie hinsichtlich Affinität und Selektivität am Dopamin-D₃-Rezeptor zeigte. Der Austausch des Zimtamid gegen einen Benzo[*b*]thiophen-2-carboxamid-Rest (**40**) erbrachte vergleichbar gute Resultate bezüglich Bindungsaffinitäten und Selektivität für den Dopamin-D₃-Rezeptor. Die Histamin-H₁-Rezeptorantagonisten ergaben am Histamin-H₁-Rezeptor eine deutliche höhere Affinität als an Dopamine-D₂- und -D₃-Rezeptoren. Die pharmakologischen Profile der neuen, strukturell modifizierten Histamine-H₁-Rezeptorantagonisten wurden für den Dopamin-D_{2S}- und D₃-Rezeptor optimiert, während die Affinitäten zum Histamin-H₁-Rezeptor, mit Ausnahme der Loratadin verwandten Substanzen, herabgesetzt wurden. Bis auf Molekül **39** zeigten alle Hybridmoleküle einer höhere Affinität zum Histamin-H₁-Rezeptor als zum Dopamin-D₂- und -D₃-Rezeptor. Die Einführung flexibler Teilstrukturen von Histamin-H₁-Rezeptorantagonisten wie Phenylaminopiperidin-Reste und Benzhydryl-Elemente wurden am Dopamin-D₃- und -D₂-Rezeptor toleriert. Sterisch anspruchsvolle und rigide Substanzen wurden in diesem Hybridansatz nur bedingt vertragen. Die Hybridstrategie ermöglichte die Entwicklung neuer Liganden mit einem gerichteten Rezeptorprofil sowie die Darstellung differenzierte Struktur-Wirkungsbeziehungen an verwandten aminergen Rezeptoren.

In Radioliganden Bindungsstudien wurde der Einfluss struktureller Variationen des Dopaminrezeptoragonisten Pramipexol und des strukturähnlichen Etrabamin untersucht. Struktur-Wirkungsbeziehungen wurden für die Dopamin-D₂- und -D₃-Rezeptoren

ausgearbeitet. Im Vergleich zu kürzeren Kettenlängen wurde eine *N*-propyl-Substitution am sekundären basischen Stickstoff (**43**) sowohl am Dopamin-D₃-Rezeptor als auch Dopamin-D₂-Rezeptor bevorzugt. Durch Einführung eines Selen-Atoms in das Strukturanalogon des Pramipexols (**54**) wurden zusätzliche antioxidative und Radikalfänger-Eigenschaften integriert. Bindungsaffinitäten im niedrigen nanomolaren Bereich und gute Selektivität für den Dopamin-D₃-Rezeptor wurden für **54** erhalten.

Die Kombination eines Dopaminrezeptoragonisten mit einem weiteren Dopamin-D₃-Rezeptor affinen Pharmakophorelement aus BP 897, ST 198 oder verwandten Substanzen führte zu Verbindungen mit hoher Affinität und Selektivität am Dopamin-D₃-Rezeptor. Das Propargyl substituierte Etrabamin-Derivat **61** zeigte herausragende Dopamin-D₃-Rezeptoraffinität und -selektivität. Der Ligand ist von großem Interesse, da für den Propargyl-Rest neuroprotektive Eigenschaften berichtet wurden. Die Weiterentwicklung führte zur Verbindung **64**, ein Zimtsäureamid-Derivate mit 4-Fluor-Substitution am Phenylring. Subnanomolare Affinität und hohe Selektivität am Dopamin-D₃-Rezeptor prädestinieren **64** zur Anwendung als potentiellen PET-Radioliganden. Das Benzo[*b*]thiophen-2-carboxamid substituierte Etrabamin-Derivat **70** zeigte eine hohe Affinität am Dopamin-D₃-Rezeptor und eine bemerkenswerte Selektivität. Die Einführung eines zusätzlichen Dopamin-D₃-affinen Pharmakophorelements in Analoga der Dopaminrezeptoragonisten Pramipexol und Etrabamin führten zu Verbindungen mit hoher Affinität und Selektivität am Dopamin-D₃-Rezeptor. Sie stellen eine neue, vielversprechende Leitstrukturserie dar. Es wird von großem Interesse sein zu untersuchen, ob die Substanzen das selektive Rezeptorbindungsprofil, die vorteilhaften pharmakokinetischen Eigenschaften und die neuroprotektiven Effekte des Pramipexols aufweisen.

Um neue Leitstrukturen mit andersartigen chemischen Grundgerüsten für den Dopamin-D₃-Rezeptor zu finden, wurden Radioliganden Bindungsassays mit virtuellen Screening Methoden kombiniert. Durch Anwendung von Verfahren, die auf der „Support Vector Machine (SVM)“ Methode beruhen, konnten in kurzer Zeit und Kosten sparend neue Leitstrukturen gefunden werden. Basierend auf einem Datensatz mit aktiven verwandten Substanzen der Leitstruktur BP 897 wurde ein SVM Model generiert und ein Substanzkatalog mit kleinen organischen Molekülen durchsucht. 11 Moleküle mit neuen Strukturelementen wurden gefunden und Bindungsaffinitäten am Dopamin-D_{2S}- und -D₃-Rezeptor ermittelt. Die Substanzen zeigten Affinitäten im molaren Bereich. Ligand **80** stellte eine viel versprechende Verbindung mit einem K_i Wert am Dopamin-D₃-Rezeptor <

2 μM und einem K_i Wert am Dopamin-D₂-Rezeptor von 2 - 6 μM dar. Er wurde für eine weitere Optimierung verwendet. Eine fokussierte SVM basierte Ähnlichkeitssuche wurde mit einem weiteren Substanzkatalog durchgeführt. 5 Moleküle wurden erhalten und im Radioliganden Bindungsassay charakterisiert. 4 der 5 Moleküle zeigten nanomolare Affinitäten am Dopamin-D₃-Rezeptor. Besonders das Benzo[1.4]oxazin-3-on-Derivat **91** mit Affinität im niedrigen nanomolaren Bereich und Dopamin-D₃-Rezeptorpräferenz ist hervorzuheben. Die Substanzen **80**, **90**, **93** und **94** besitzen neue Strukturmerkmale mit andersartigen Grundgerüsten, die zur weiteren Optimierung zur Verfügung stehen.

In weiteren Radioliganden Bindungsstudien wurden Affinitäten am Dopamin-D_{2S}- und -D₃-Rezeptor von Molekülen bestimmt, die aus verschiedenen chemoinformatischen Klassifikationstechniken resultierten. Verbindungen mit neuen chemischen Strukturelementen konnten in kurzer Zeit gefunden werden und führten zu einem tieferen Verständnis der Struktur-Wirkungsbeziehungen. Clustering basiertes virtuelles Screening eines Substanzkataloges führten zur Auswahl von 17 Substanzen. Diese wurden am Dopamin-D_{2S}- und -D₃-Rezeptor pharmakologisch getestet. Das Derivat **95** zeigte neben Bindungsaffinitäten im niedrigen nanomolaren Bereich eine deutliche Präferenz für den Dopamin-D₃-Rezeptor. Zusätzlich wies **95** mit dem Bicyclo[2.2.1]heptan Gerüst eine andersartige Struktur auf. Weitere neue Molekülelemente waren ein Aryl-Thioether-Rest (**96**, **99**) sowie Benzamide als Verbindungselement im Molekül (**95** – **100**). Dockingstudien mit einem Homologiemodell des Dopamin-D₃-Rezeptors führten zur Hypothese zweier alternativer Bindungstaschen. Ein darauf aufgebautes Pharmakophormodell identifizierte in einem virtuellen Screening den Benzhydryliden substituierten Pyrrolidindion Liganden **112** mit niedriger nanomolarer Affinität am Dopamin-D₃-Rezeptor. Er unterstützt die Hypothese der zwei Bindungstaschen. Substanz **112** ist eine neue Leitstruktur und kann nun zur weiteren Optimierung chemisch modifiziert werden.

Die in dieser Arbeit etablierten Radioliganden Bindungsassays führten zur Identifizierung, Entwicklung und Optimierung von hoch affinen und selektiven Dopamin-D₃-Rezeptor Liganden. Des Weiteren ermöglichten die Ergebnisse eine ausführliche Vertiefung von Struktur-Wirkungsbeziehungen am Dopamin-D₃- und -D₂-Rezeptor. Die kombinierte Strategie von Radioliganden Bindungsstudien und virtuellen Screening Methoden hat das Finden neuer Leitstrukturen als potentielle Arzneistoffe erlaubt. Die Resultate ermöglichen in der Zukunft ein gezieltes Liganden-Design mit einem gerichteten pharmakologischen Rezeptorprofil.

8 Abbreviations

3D	Three-dimensional
AA	Arachidonic acid
AADC	L-amino acid decarboxylase
AC	Adenylyl cyclase
ADHD	Attention deficit hyperactivity disorder
Asp	Aspartic acid
BDNF	Brain-derived neurotrophic factor
BP 897	<i>N</i> -{4-[4-(2-methoxyphenyl)piperazinyl]butyl}-2-naphtamide
cAMP	Cyclic adenosine-3',5'-monophosphate
CHO-cells	Chinese hamster ovary cells
CNS	Central nervous system
COMT	Catechol- <i>O</i> -methyltransferase
CPM	Counts per minute
CREB	Cyclic AMP response element binding protein
DA	Dopamine, 2-(3,4-dihydroxyphenyl)ethylamine
DAC	Diacylglycerol
DARPP-32	Domain-related phosphoprotein, 32 kDa
DAT	Dopamine transporter
DMSO	Dimethylsulfoxid
DOPAC	3,4-Dihydroxyphenylacetat
DOPAL	3,4-Dihydroxyphenylacetaldehyde
FRET	Fluorescence resonance energy transfer
<i>f</i> mol	Femtomol
GDP	Guanosine-5'-diphosphate
G _i	Guanine nucleotide binding protein which regulates inhibition of adenylyl cyclase
GOLD	Genetic optimization for ligand docking
GPCR	G protein-coupled receptor
G protein	Guanine nucleotide binding protein
Gpp(NH)p	5'-Guanylyl-imidodiphosphate
G _s	Guanine nucleotide binding protein which regulates the stimulation of adenylyl cyclase
GTP	Guanosine-5'-triphosphate
[³⁵ S] GTP _γ S	Guanosine-5'- <i>O</i> -(3-[³⁵ S]thiotriphosphate)

h	Hour, hours
H	Helix, helices
HVA	Homovanilic acid
HTS	High throughput screening
IC_{50}	Concentration inhibiting 50% of response
IP ₃	Inositol-1,3,5-triphosphate
IBS	Interbioscreen
IUPHAR	International Union of Pharmacology
K_d	Equilibrium dissociation constant
K_i	Dissociation constant of inhibitor, inhibition constant equilibrium
K_H	Inhibition constant of high affinity state
K_L	Inhibition constant of low affinity state
L-DOPA	L-3,4-dihydroxyphenylalanine, levodopa
LID	Levodopa-induced dyskinesia
μg	Microgram
M	Mol/L
MAO-A	Monoamine oxidase A
MAO-B	Monoamine oxidase B
MAPK	Mitogen-activated protein kinase
min	Minute, minutes
mg	Milligram
mmol	Millimol
MOE	Molecular operation environment
MPTP	1-Methyl-4-phenyl-1,2,3,6-tetrahydropyridine
MT	3-Methoxytyramine
n	Number of individual experiment
n.d.	Not determined
NIPALS	Non-linear iterative partial least squares
nM	Nanomol/L
NMDA	<i>N</i> -methyl- <i>D</i> -aspartate
NN	Neuronal networks
NPA	<i>N</i> -propylnorapomorphine
PBS	Phosphate-buffered saline
PD	Parkinson's disease

PET	Positron emission tomography
PKA	Protein kinase A
PKC	Protein kinase C
PLC	Phospholipase C
PLS	Partial least squares
PP1 or PP2A	Protein phosphatase 1 or 2A
PPP	Potential pharmacophore points
3PP	Three-point pharmacophore
QSAR	Quantitative structure-activity relationships
% R_H	% of higher affinity sites
rpm	Rotation per minute
RRA	Retrochubral area
SAR	Structure-activity relationships
SD	Standard deviation
SNe	Substantia nigra pars compacta
SOM	Self organising maps
SPECT	Single photon emission computed tomography
SVM	Support vector machine
TH	Tyrosine 3-hydroxylase
TM	Transmembrane domain
VS	Virtual screening
VTA	Ventral tegmental area

9 References

1. Ellis, C. The State of GPCR Research in 2004. *Nat Rev Drug Discovery* **3**, 577-626 (2004).
2. Palczewski, K., Kumasaka, T., Hori, T., Behnke, C.A., Motoshima, H., Fox, B.A., Le Trong, I., Teller, D.C., Okada, T., Stenkamp, R.E., Yamamoto, M. & Miyano, M. Crystal Structure of Rhodopsin: A G Protein-Coupled Receptor. *Science* **289**, 739-745 (2000).
3. Wise, A., Gearing, K. & Rees, S. Target Validation of G-protein Coupled Receptors. *Drug Discov. Today* **7**, 235-246 (2002).
4. Klabunde, T. & Hessler, G. Drug Design Strategies for Targeting G-Protein-Coupled Receptors. *ChemBioChem* **3**, 928-944 (2002).
5. Hill, S. J. G-Protein-Coupled Receptors: Past, Present and Future. *Br J Pharmacol* **147** (2006).
6. Brady, A. E. & Limbird, L. E. G Protein-coupled Receptor Interacting Proteins: Emerging Roles in Localization and Signal Transduction. *Cell Signal* **14**, 297-309 (2002).
7. Hur, E. M. & Kim, K. T. G Protein-coupled Receptor Signalling and Cross-talk: Achieving Rapidity and Specificity. *Cell Signal* **14**, 397-405 (2002).
8. Malbon, C. C. G Proteins in Development. *Nature Rev Mol. Cell Biol.* **6**, 689-701 (2005).
9. Byvatov, E., Sasse, B. C., Stark, H. & Schneider, G. From Virtual to Real Screening for D₃ Dopamine Receptor Ligands. *ChemBioChem* **6**, 997-999 (2005).
10. www.GPCR.org.
11. Horn, F., Bettler, E., Oliveira, L., Campagne, F., Cohen, F.E. & Vriend, G. GPCRDB Information System for G Protein-Coupled Receptors. *Nucleic Acids Res.* **31**, 294-297 (2003).
12. www.ebi.ac.uk.
13. Thompson, J. D., Higgins, D. G. & Gibson, T. J. CLUSTAL W: Improving the Sensitivity of Progressive Multiple Sequence Alignment through Sequence Weighting, Position-Specific Gap Penalties and Weight Matrix Choice. *Nucleic Acids Res.* **22**, 4673-4680 (1994).
14. Klabunde, T. & Evers, A. GPCR Antitarget Modeling: Pharmacophore Models for Biogenic Amine Binding GPCRs to Avoid GPCR-mediated Side Effects. *ChemBioChem* **6**, 876-889 (2005).
15. Milligan, G. G Protein-Coupled Receptor Dimerization: Function and Ligand Pharmacology. *Mol Pharmacol* **66**, 1-7 (2004).
16. O'Dowd, B. F. Ji, X., Alijaniam, M., Rajaram, R.D., Kong, M.M.C., Rashid, A., Nguyen, T. & George, S.R. Dopamine Receptor Oligomerization Visualized in Living Cells. *J Biol Chem* **280**, 37225-37235 (2005).
17. Fuxe, K. Canals, M., Torvinen, M., Marcellino, D., Terasmaa, A., Genedani, S., Leo, G., Guidolin, D., Diaz-Cabiale, Z., Rivera, A., Lundstrom, L., Langel, U., Narvaez, J., Tanganelli, S., Lluís, C., Ferre, S., Woods, A., Franco, R. & Agnati, L. F. Intramembrane Receptor-Receptor Interactions: A Novel Principle in Molecular Medicine. *J. Neural. Transm.* (2006).
18. Carlsson, A., Lindquist, M., Magnusson, T. & Waldeck, B. On the Presence of 3-Hydroxytyramine in Brain. *Science* **127**, 471 (1958).
19. Nieoullon, A. & Coquerel, A. Dopamine: A Key Regulator to Adapt Action, Emotion, Motivation and Cognition. *Curr Opin Neurol.* **16**, S3-S9 (2003).
20. Carlsson, A. A Paradigm Shift in Brain Research. *Science* **294**, 1021-1024 (2001).
21. Le Foll, B., Goldberg, S. R. & Sokoloff, P. The Dopamine D₃ Receptor and Drug Dependence: Effects on Reward or Beyond? *Neuropharmacology.* **49**, 525-541 (2005).

22. Joyce, J. N. Dopamine D₃ Receptor as a Therapeutic Target for Antipsychotic and Antiparkinsonian Drugs. *Pharmacol. Ther.* **90**, 231-259 (2001).
23. Emilien, G., Maloteaux, J. M., Geurts, M., Hoogenberg, K. & Cragg, S. Dopamine Receptors--Physiological Understanding to Therapeutic Intervention Potential. *Pharmacol. Ther.* **84**, 133-156 (1999).
24. Missale, C., Nash, S. R., Robinson, S. W., Jaber, M. & Caron, M. G. Dopamine Receptors: From Structure to Function. *Physiol. Rev.* **78**, 189-225 (1998).
25. Elsworth, J. D. & Roth, R. H. Dopamine Synthesis, Uptake, Metabolism, and Receptors: Relevance to Gene Therapy of Parkinson's Therapy. *Exp. Neurol.* **144**, 4-9 (1997).
26. Gütschow, M. & Meusel, M. Enzyme Inhibitors in Parkinson Treatment. *Pharm Unserer Zeit* **35**, 2-9 (2006).
27. Bozzi, Y. & Borrelli, E. Dopamine in Neurotoxicity and Neuroprotection: What do D₂ Receptors have to do with it? *Trends Neurosci.* **29**, 167-174 (2006).
28. Misu, Y., Goshima, Y. & Miyamae, T. Is DOPA a Neurotransmitter? *Trends Pharmacol Sci.* **23**, 262-267 (2002).
29. Shimamura, M., Shimizu, M., Yagami, T., Funabashi, T., Kimura, F., Kuroiwa, Y., Misu, Y. & Goshima, Y. L-3,4-Dihydroxyphenylalanine-induced c-Fos Expression in the CNS under Inhibition of Central Aromatic L-Amino Acid Decarboxylase. *Neuropharmacology.* **50**, 909-916 (2006).
30. Smith, Y. & Kieval, J. Z. Anatomy of the Dopamine System in the Basal Ganglia. *Trends Neurosci.* **23**, S28-S33 (2000).
31. Keibian, J. W., Petzold, G. L. & Greengard, P. Dopamine-Sensitive Adenylate Cyclase in Caudate Nucleus of Rat Brain and its Similarity to the Dopamine Receptor. *Proc Natl Acad Sci U S A* **69**, 2145-2149 (1972).
32. Keibian, J. W. & Calne, D. B. Multiple Receptors for Dopamine. *Nature* **277**, 93-96 (1979).
33. Sokoloff, P., Giros, B., Martres, M. P., Bouthenet, M. L. & Schwartz, J. C. Molecular Cloning and Characterization of a Novel Dopamine Receptor (D₃) as a Target for Neuroleptics. *Nature* **347**, 146-51 (1990).
34. Van Tol, H. H. M., Bunzow, J.R., Guan, H.C., Sunahara, R.K., Seeman, P., Niznik, H.B. & Civelli, O. Cloning of the Gene for a Human Dopamine D₄ Receptor with High Affinity for the Antipsychotic Clozapine. *Nature* **350**, 610-614 (1991).
35. Sunahara, R. K. Guan, H.C., O'Dowd, B.F., Seeman, P., Laurier, L.G., NG, G., George, S.R., Torchia, J., Van Tol, H.H.M. & Niznik, H.B. Cloning of the Gene for a Human Dopamine D₅ Receptor with Higher Affinity for Dopamine than D₁. *Nature* **350**, 614-619 (1991).
36. Neve, K. A., Seamans, J. K. & Trantham-Davidson, H. Dopamine Receptor Signaling. *J Recept Signal Transduct Res.* **24**, 165-205 (2004).
37. Huff, R. M. Signal Transduction Pathways Modulated by the D₂ Subfamily of Dopamine Receptors. *Cell Signal* **8**, 453-9 (1996).
38. Bonci, A. & Hopf, F. W. The Dopamine D₂ Receptor: New Surprises from an Old Friend. *Neuron* **47**, 335-8 (2005).
39. Stenkamp, R. E., Teller, D. C. & Palczewski, K. Rhodopsin: A Structural Primer for G-Protein Coupled Receptors. *Arch. Pharm. Chem. Life Sci.* **338**, 209-216 (2005).
40. Civelli, O., Bunzow, J. R. & Grandy, D. K. Molecular Diversity of the Dopamine Receptors. *Annu. Rev. Pharmacol. Toxicol.* **32**, 281-307 (1993).
41. Strange, P. G. Oligomers of Dopamine D₂ Receptors: Evidence from Ligand Binding. *J Mol Neurosci.* **26**, 155-160 (2005).

42. Lee, S. P., Xie, Z., Varghese, G., Nguyen, T., O'Dowd, B.F. & George, S.R. Oligomerization of Dopamine and Serotonin Receptors. *Neuropsychopharmacol* **23**, S32-S40 (2000).
43. Lee, S. P., So, C.H., Rashid, A.J., Varghese, G., Cheng, R., Lanca, A.J. O'Dowd, B.F. & George, S.R. Dopamine D₁ and D₂ Receptor Co-activation Generates a Novel Phospholipase c-mediated Calcium Signal. *J Biol Chem* **279**, 35671-35678 (2004).
44. Scarselli, M., Novi, F., Schallmach, E., Lin, R., Baragli, A., Colzi, A., Griffon, N., Corsini, G. U., Sokoloff, P., Levenson, R., Vogel, Z. & Maggio, R. D₂/D₃ Dopamine Receptor Heterodimers Exhibit Unique Functional Properties. *J Biol Chem* **276**, 30308-30314 (2001).
45. Maggio, R., Scarselli, M., Novi, F., Millan, M. J. & Corsini, G. U. Potent Activation of Dopamine D₃/D₂ Heterodimers by the Antiparkinsonian Agents, S32504, Pramipexole and Ropinirole. *J Neurochem* **87**, 631-41 (2003).
46. Torvinen, M., Marcellino, D., Canals, M., Agnati, L. F., Lluís, C., Franco, R. & Fuxe, K. Adenosine A_{2A} Receptor and Dopamine D₃ Receptor Interactions: Evidence of Functional A_{2A}/D₃ Heteromeric Complexes. *Mol Pharmacol* **67**, 400-407 (2005).
47. Rocheville, M., Lange, D.C., Kumar, U., Patel, S.C., Patel, R.C. & Patel, Y.C. Receptors for Dopamine and Somatostatin: Formation of Hetero-oligomers with Enhanced Functional Activity. *Science* **288**, 154-157 (2000).
48. Bunzow, J. R., Van Tol, H. H., Grandy, D. K., Albert, P., Salon, J., Christie, M., Machida, C. A., Neve, K. A. & Civelli, O. Cloning and Expression of a Rat D₂ Dopamine Receptor cDNA. *Nature* **336**, 783-787 (1988).
49. Giros, B., Sokoloff, P., Martres, M. P., Riou, J. F., Emorine, L. J. & Schwartz, J. C. Alternative Splicing Directs the Expression of two D₂ Dopamine Receptor Isoforms. *Nature* **342**, 923-926 (1989).
50. Guiramand, J., Montmayeur, J. P., Ceraline, J., Bhatia, M. & Borrelli, E. Alternative Splicing of the Dopamine D₂ Receptor Directs Specificity of Coupling to G-Proteins. *J Biol Chem* **270**, 7354-7358 (1995).
51. Montmayeur, J. P., Guiramand, J. & Borrelli, E. Preferential Coupling Between Dopamine D₂ Receptors and G Proteins. *Mol Endocrinol* **7**, 161-170 (1993).
52. Giros, B., Martres, M. P., Pilon, C., Sokoloff, P. & Schwartz, J. C. Shorter Variants of the D₃ Dopamine Receptor Produced Through Various Patterns of Alternative Splicing. *Biochem Biophys Res Commun* **176**, 1584-1592 (1991).
53. Sokoloff, P., Giros, B., Martres, M. P., Andrieux, M., Besancon, R., Pilon, C., Bouthenet, M. L., Souil, E. & Schwartz, J. C. Localization and Function of the D₃ Dopamine Receptor. *Arzneimittelforschung* **42**, 224-30 (1992).
54. Suzuki, M., Hurd, Y. L., Sokoloff, P., Schwartz, J. C. & Sedvall, G. D₃ Dopamine Receptor mRNA is Widely Expressed in the Human Brain. *Brain Res* **779**, 58-74 (1998).
55. Van Tol, H. H. M., Wu, C.M., Guan, H.-C., Ohara, K., Bunzow, J.R., Civelli, O., Kennedy, J., Seeman, P., Niznik, H.B. & Jovanovic, V. Multiple Dopamine D₄ Receptor Variants in the Human Population. *Nature* **358**, 149-152 (1992).
56. Zhou, Q.-Y., Grandy, D. K., Thambi, L., Kushner, J.A., Van Tol, H.H.M., Cone, R., Pribnow, D., Salon, J., Bunzow, J. R. & Civelli, O. Cloning and Expression of Human and Rat D₁ Dopamine Receptors. *Nature* **347**, 76-80 (1990).
57. Seeman, P. & Van Tol, H. H. Dopamine Receptor Pharmacology. *Curr Opin Neurol Neurosurg* **6**, 602-608 (1993).

58. Seeman, P. Dopamine Receptor Sequences. Therapeutic Levels of Neuroleptics Occupy D₂ Receptors, Clozapine Occupies D₄. *Neuropsychopharmacol* **7**, 261-284 (1992).
59. Park, S. K. Nguyen, M. D., Fischer, A., Luke, M. P., Affar el, B., Dieffenbach, P. B., Tseng, H. C., Shi, Y. & Tsai, L. H. Par-4 Links Dopamine Signaling and Depression. *Cell* **122**, 275-287 (2005).
60. Beaulieu, J. M., Sotnikova, T. D., Marion, S., Lefkowitz, R. J., Gainetdinov, R. R. & Caron, M. G. An Akt/Beta-Arrestin 2/PP2A Signaling Complex Mediates Dopaminergic Neurotransmission and Behavior. *Cell* **122**, 261-273 (2005).
61. Perachon, S., Schwartz, J. C. & Sokoloff, P. Functional Potencies of New Antiparkinsonian Drugs at Recombinant Human Dopamine D₁, D₂ and D₃ Receptors. *Eur J Pharmacol* **366**, 293-300 (1999).
62. Levant, B. The D₃ Dopamine Receptor: Neurobiology and Potential Clinical Relevance. *Pharmacol Rev* **49**, 231-52 (1997).
63. Nishi, A., Snyder, G. L. & Greengard, P. Bidirectional Regulation of DARPP-32 Phosphorylation by Dopamine. *J Neurosci* **17**, 8147-8155 (1997).
64. Kottke, T. & Stark, H. Complex Regulation of Dopamine D₂ Receptors. *Pharm Unserer Zeit* **35**, 9-11 (2006).
65. Schwartz, J. C., Diaz, J., Pilon, C. & Sokoloff, P. Possible Implications of the Dopamine D(3) Receptor in Schizophrenia and in Antipsychotic Drug Actions. *Brain Res Brain Res Rev* **31**, 277-87 (2000).
66. Pilla, M. Perachon, S., Sautel, F., Garrido, F., Mann, A., Wermuth, C. G., Schwartz, J. C., Everitt, B. J. & Sokoloff, P. Selective Inhibition of Cocaine-seeking Behaviour by a Partial Dopamine D₃ Receptor Agonist. *Nature* **400**, 371-375 (1999).
67. Levesque, D., Diaz, J., Pilon, C., Martres, M. P., Giros, B., Souil, E., Schott, D., Morgat, J. L., Schwartz, J. C. & Sokoloff, P. Identification, Characterization, and Localization of the Dopamine D₃ Receptor in Rat Brain Using 7-[³H]Hydroxy-*N,N*-di-n-propyl-2-aminotetralin. *Proc Natl Acad Sci U S A* **89**, 8155-8159 (1992).
68. Schwartz, J. C. Diaz, J., Bordet, R., Griffon, N., Perachon, S., Pilon, C., Ridray, S. & Sokoloff, P. Functional Implications of Multiple Dopamine Receptor Subtypes: the D₁/D₃ Receptor Coexistence. *Brain Res Brain Res Rev* **26**, 236-242 (1998).
69. Diaz, J. Pilon, C., Le Foll, B., Gros, C., Triller, A., Schwartz, J. C. & Sokoloff, P. Dopamine D₃ Receptors Expressed by All Mesencephalic Dopamine Neurons. *J Neurosci* **20**, 8677-8684 (2000).
70. Gurevich, E. V. & Joyce, J. N. Distribution of Dopamine D₃ Receptor Expressing Neurons in the Human Forebrain: Comparison with D₂ Receptor Expressing Neurons. *Neuropsychopharmacol* **20**, 60-80 (1999).
71. Kim, K. M., Gainetdinov, R. R., Laporte, S. A., Caron, M. G. & Barak, L. S. G protein-coupled Receptor Kinase Regulates Dopamine D₃ Receptor Signaling by Modulating the Stability of a Receptor-Filamin-Beta-Arrestin Complex. A Case of Autoreceptor Regulation. *J Biol Chem* **280**, 12774-12780 (2005).
72. Sautel, F., Griffon, N., Levesque, D., Pilon, C., Schwartz, J. C. & Sokoloff, P. A Functional Test Identifies Dopamine Agonists Selective for D₃ versus D₂ Receptors. *Neuroreport* **6**, 329-332 (1995).
73. Xu, M., Koeltzow, T. E., Cooper, D. C., Tonegawa, S. & White, F. J. Dopamine D₃ Receptor Mutant and Wild-type Mice Exhibit Identical Responses to Putative D₃ Receptor-selective Agonists and Antagonists. *Synapse* **31**, 210-215 (1999).
74. Parkinson, J. *An Essay on the Shaking Palsy* (London, 1817), book.
75. Müller, T. Hefter, H., Hueber, R., Jost, W.H., Leenders, K.L., Odin, P. & Schwarz, J. Is Levodopa Toxic? *J Neurol* **251**, 44-46 (2004).

76. Arai, H., Furuya, T., Mizuno, Y. & Mochizuki, H. Inflammation and Infection in Parkinson's Disease. *Histol Histopathol* **21**, 673-8 (2006).
77. Jenner, P. Dopamine Agonists, Receptor Selectivity and Dyskinesia Induction in Parkinson's Disease. *Curr Opin Neurol* **16**, S3-S7 (2003).
78. Bezard, E., Brotchie, J. M. & Gross, C. E. Pathophysiology of Levodopa-Induced Dyskinesia: Potential for New Therapies. *Nat Rev Neurosci* **2**, 577-588 (2001).
79. Jenner, P. Pharmacology of Dopamine Agonists in the Treatment of Parkinson's Disease. *Neurology* **58**, S1-S8 (2002).
80. Junghanns, S., Glockler, T. & Reichmann, H. Switching and Combining of Dopamine Agonists. *J Neurol* **251**, S6, VI/19-23 (2004).
81. Junghanns, S., Fuhrmann, J. T., Simonis, G., Oelwein, C., Koch, R., Strasser, R. H., Reichmann, H. & Storch, A. Valvular Heart Disease in Parkinson's Disease Patients Treated with Dopamine Agonists: A Reader-Blinded Monocenter Echocardiography Study. *Mov Disord* (2006).
82. Jenner, P. A Novel Dopamine Agonist for the Transdermal Treatment of Parkinson's Disease. *Neurology* **65**, S3-5 (2005).
83. Bezard, E., Ferry, S., Mach, U., Stark, H., Leriche, L., Boraud, T., Gross, C. & Sokoloff, P. Attenuation of Levodopa-Induced Dyskinesia by Normalizing Dopamine D₃ Receptor Function. *Nat Med* **9**, 762-767 (2003).
84. Moller, J. C. & Oertel, W. H. Pramipexole in the Treatment of Parkinson's Disease: New Developments. *Expert Rev Neurother* **5**, 581-586 (2005).
85. Iravani, M. M., Haddon, C. O., Cooper, J. M., Jenner, P. & Schapira, A. H. Pramipexole Protects Against MPTP Toxicity in Non-Human Primates. *J Neurochem* **96**, 1315-1321 (2006).
86. Pan, T., Xie, W., Jankovic, J. & Le, W. Biological Effects of Pramipexole on Dopaminergic Neuron-associated Genes: Relevance to Neuroprotection. *Neurosci Lett* **377**, 106-109 (2005).
87. Gupta, S., Vincent, J. L. & Frank, B. Pramipexole: Augmentation in the Treatment of Depressive Symptoms. *CNS Spectr* **11**, 172-175 (2006).
88. Ekbom, K. A. Restless Legs Syndrome. *Acta Med Scand* **158**, 4-122 (1945).
89. Thorpy, M. J. New Paradigms in the Treatment of Restless Legs Syndrome. *Neurology* **64**, S28-33 (2005).
90. Vignatelli, L., Billiard, M., Clarenbach, P., Garcia-Borreguero, D., Kaynak, D., Liesiene, V., Trenkwalder, C. & Montagna, P. EFNS Guidelines on Management of Restless Legs Syndrome and Periodic Limb Movement Disorder in Sleep. *Eur J Neurol* **13**, 1049-1065 (2006).
91. Kushida, C. A. Pramipexole for the Treatment of Restless Legs Syndrome. *Expert Opin Pharmacother* **4**, 441-451 (2006).
92. Bogan, R. K., Fry, J. M., Schmidt, M. H., Carson, S. W. & Ritchie, S. Y. Ropinirole in the Treatment of Patients with Restless Legs Syndrome: A US-Based Randomized, Double-Blind, Placebo-Controlled Clinical Trial. *Mayo Clin Proc* **81**, 17-27 (2006).
93. Zareba, G. Rotigotine: A Novel Dopamine Agonist for the Transdermal Treatment of Parkinson's Disease. *Drugs Today* **42**, 21-28 (2006).
94. Clemens, S., Rye, D. & Hochman, S. Restless Legs Syndrome: Revisiting the Dopamine Hypothesis From the Spinal Cord Perspective. *Neurology* **67**, 125-130 (2006).
95. Rowley, M., Bristow, L. J. & Hutson, P. H. Current and Novel Approaches to the Drug Treatment of Schizophrenia. *J. Med. Chem.* **44**, 477-501 (2001).
96. Wong, A. H. & Van Tol, H. H. Schizophrenia: From Phenomenology to Neurobiology. *Neurosci Biobehav Rev* **27**, 269-306 (2003).

97. Willner, P. The Dopamine Hypothesis of Schizophrenia: Current Status, Future Prospects. *Int Clin Psychopharmacol* **12**, 297-308 (1997).
98. Carlsson, A. The Neurochemical Circuitry of Schizophrenia. *Pharmacopsychiatry* **39**, S10-4 (2006).
99. Snyder, S. H. The Dopamine Hypothesis of Schizophrenia: Focus on the Dopamine Receptor. *Am J Psychiatry* **133**, 197-202 (1976).
100. Abi-Dargham, A. & Laruelle, M. Mechanism of Action Of Second Generation Antipsychotic Drugs in Schizophrenia: Insights from Brain Imaging Studies. *Eur Psychiatry* **20**, 15-27 (2005).
101. Laruelle, M., Frankle, W. G., Narendran, R., Kegeles, L. S. & Abi-Dargham, A. Mechanism of Action of Antipsychotic Drugs: From Dopamine D₂ Receptor Antagonism to Glutamate NMDA Facilitation. *Clin Ther.* **27**, S16-24 (2005).
102. Lindsley, C. W., Shipe, W. D., Wolkenberg, S. E., Theberge, C. R., Williams, D. L. Jr., Sur, C. & Kinney, G. G. Progress Towards Validating the NMDA Receptor Hypofunction Hypothesis of Schizophrenia. *Curr Top Med Chem* **6**, 771-785 (2006).
103. Millan, M. J. N-methyl-D-aspartate Receptors as a Target for Improved Antipsychotic Agents: Novel Insights and Clinical Perspectives. *Psychopharmacol (Berl)* **179**, 30-53 (2005).
104. Sokoloff, P., Diaz, J., Le Foll, B., Guillin, O., Leriche, L., Bezard, E. & Gross, C. The Dopamine D₃ Receptor: A Therapeutic Target for the Treatment of Neuropsychiatric Disorders. *CNS Neurol Disord Drug Targets* **5**, 25-43 (2006).
105. Leriche, L., Diaz, J. & Sokoloff, P. Dopamine and Glutamate Dysfunctions in Schizophrenia: Role of the Dopamine D₃ Receptor. *Neurotox. Res.* **6**, 63-71 (2004).
106. Laszy, J., Laszlovszky, I. & Gyertyan, I. Dopamine D₃ Receptor Antagonists Improve the Learning Performance in Memory-Impaired Rats. *Psychopharmacol (Berl)* **179**, 567-575 (2005).
107. Kroeze, W. K., Hufeisen, S. J., Popadak, B. A., Renock, S. M., Steinberg, S., Ernsberger, P., Jayathilake, K., Meltzer, H. Y. & Roth, B. L. H₁-Histamine Receptor Affinity Predicts Short-Term Weight Gain for Typical and Atypical Antipsychotic Drugs. *Neuropsychopharmacol* **28**, 519-526 (2003).
108. Wonodi, I., Hong, L. E. & Thaker, G. K. Psychopathological and Cognitive Correlates of Tardive Dyskinesia in Patients Treated with Neuroleptics. *Adv Neurol.* **96**, 336-349 (2005).
109. Jann, M. W. Implications for Atypical Antipsychotics in the Treatment of Schizophrenia: Neurocognition Effects and a Neuroprotective Hypothesis. *Pharmacotherapy* **24**, 1759-1783 (2004).
110. Tarazi, F. I., Zhang, K. & Baldessarini, R. J. Dopamine D₄ receptors: Beyond Schizophrenia. *J Recept Signal Transduct Res* **24**, 131-47 (2004).
111. Corrigan, M. H., Gallen, C. C., Bonura, M. L. & Merchant, K. M. Effectiveness of the Selective D₄ Antagonist Sonepiprazole in Schizophrenia: A Placebo-Controlled Trial. *Biol Psychiatry* **55**, 445-451 (2004).
112. Millan, M. J. Multi-Target Strategies for the Improved Treatment of Depressive States: Conceptual Foundations and Neuronal Substrates, Drug Discovery and Therapeutic Application. *Pharmacol Ther* **110**, 135-370 (2006).
113. Cassano, P., Lattanzi, L., Fava, M., Navari, S., Battistini, G., Abelli, M. & Cassano, G. B. Ropinirole in Treatment-Resistant Depression: A 16-Week Pilot Study. *Can J Psychiatry* **50**, 357-360 (2005).
114. Bertaina-Anglade, V., La Rochelle, C. D. & Scheller, D. K. Antidepressant Properties of Rotigotine in Experimental Models of Depression. *Eur J Pharmacol* **548**, 106-114 (2006).

115. Lemke, M. R., Brecht, H. M., Koester, J., Kraus, P. H. & Reichmann, H. Anhedonia, Depression, and Motor Functioning in Parkinson's Disease During Treatment with Pramipexole. *J Neuropsychiatry Clin Neurosci* **17**, 214-220 (2005).
116. Zarate, C. A. Jr., Payne, J. L., Singh, J., Quiroz, J. A., Luckenbaugh, D. A., Denicoff, K. D., Charney, D. S. & Manji, H. K. Pramipexole for Bipolar II Depression: A Placebo-Controlled Proof of Concept Study. *Biol Psychiatry* **56**, 54-60 (2004).
117. Carroll, F. I., Howell, L. L. & Kuhar, M. J. Pharmacotherapies for Treatment of Cocaine Abuse: Preclinical Aspects. *J. Med. Chem.* **42**, 2721-2736 (1999).
118. Koob, G. F. Dopamine, Addiction and Reward. *Semin Neurosci* **4**, 139-148 (1992).
119. Bannon, M. J. The Dopamine Transporter: Role in Neurotoxicity and Human Disease. *Toxicol Appl Pharmacol* **204**, 355-360 (2005).
120. Segal, D. M., Moraes, C. T. & Mash, D. C. Up-Regulation of D₃ Dopamine Receptor mRNA in the Nucleus Accumbens of Human Cocaine Fatalities. *Mol. Brain Res* **45**, 335-339 (1997).
121. Varady, J. Wu, X., Fang, X., Min, J., Hu, Z., Levant, B. & Wang, S. Molecular Modeling of the Three-Dimensional Structure of Dopamine 3 (D₃) Subtype Receptor: Discovery of Novel and Potent D₃ Ligands through a Hybrid Pharmacophore- and Structure-Based Database Searching Approach. *J. Med. Chem.* **46**, 4377-4392 (2003).
122. Strange, P. G. The Energetics of Ligand Binding at Catecholamine Receptors. *Trends Pharmacol Sci* **17**, 238-244 (1996).
123. Ishiguro, M. Ligand-Binding Modes in Cationic Biogenic Amine Receptors. *ChemBioChem* **5**, 1210-1219 (2004).
124. Sartania, N. Role of the Conserved Serine Residue in the Interaction of Agonists with D₃ Dopamine Receptors. *J Neurochem* **72**, 2621-2624 (1999).
125. Bettinetti, L., Schlotter, K., Hubner, H. & Gmeiner, P. Interactive SAR Studies: Rational Discovery of Super-Potent and Highly Selective Dopamine D₃ Receptor Antagonists and Partial Agonists. *J. Med. Chem.* **45**, 4594-4597 (2002).
126. Hackling, A. Ghosh, R., Perachon, S., Mann, A., Holtje, H. D., Wermuth, C. G., Schwartz, J. C., Sippl, W., Sokoloff, P. & Stark, H. *N*-(ω -(4-(2-Methoxyphenyl)piperazin-1-yl)alkyl)carboxamides as Dopamine D₂ and D₃ receptor Ligands. *J. Med. Chem.* **46**, 3883-3899 (2003).
127. Newman, A. H., Grundt, P. & Nader, M. A. Dopamine D₃ Receptor Partial Agonists and Antagonists as Potential Drug Abuse Therapeutic Agents. *J. Med. Chem.* **48**, 3663-3679 (2005).
128. Akunne, H. C., Towers, P., Ellis, G. J., Dijkstra, D., Wikstrom, H., Heffner, T. G., Wise, L. D. & Pugsley, T. A. Characterization of Binding of [³H]PD 128907, a Selective Dopamine D₃ Receptor Agonist Ligand, to CHO-K1 Cells. *Life Sci* **57**, 1401-1410 (1995).
129. Coldwell, M. C., Boyfield, I., Brown, T., Hagan, J. J. & Middlemiss, D. N. Comparison of the Functional Potencies of Ropinirole and Other Dopamine Receptor Agonists at Human D₂(long), D₃ and D_{4.4} Receptors Expressed in Chinese Hamster Ovary Cells. *Br J Pharmacol* **127**, 1696-1702 (1999).
130. Millan, M. J., Cussac, D., Milligan, G., Carr, C., Audinot, V., Gobert, A., Lejeune, F., Rivet, J.M., Brocco, M., Duqueyroux, D., Nicolas, J.P., Boutin, J.A., Newman-Tancredi, A. Antiparkinsonian Agent Piribedil displays Antagonist Properties at Native, Rat, and Cloned, Human Alpha(2)-adrenoceptors: Cellular and Functional Characterization. *J Pharmacol Exp Ther* **297**, 876-887 (2001).
131. Janssen, P. A. The Pharmacology of Haloperidol. *Int J Neuropsychiatry* **3**, S10-18 (1967).

132. Luedtke, R. R. & Mach, R. H. Progress in Developing D₃ Dopamine Receptor Ligands as Potential Therapeutic Agents for Neurological and Neuropsychiatric Disorders. *Curr. Pharm. Des.* **9**, 643-671 (2003).
133. Schneider, C. S. & Mierau, J. Dopamine Autoreceptor Agonists: Resolution and Pharmacological Activity of 2,6-diaminotetrahydro-benzothiazole and an Aminothiazole Analogue of Apomorphine. *J. Med. Chem.* **30**, 494-498 (1987).
134. Dutta, A. K. et al. Synthesis and biological characterization of novel hybrid 7-{(2-(4-phenyl-piperazin-1-yl)-ethyl)-propyl-amino}-5,6,7,8-tetrahydro-naphthalen-2-ol and their heterocyclic bioisosteric analogues for dopamine D₂ and D₃ receptors. *Bioorg Med Chem.* **12**, 4361-4374 (2004).
135. Mierau, J., Schneider, F. J., Ensinger, H. A., Chio, C. L., Lajiness, M. E. & Huff, R. M. Pramipexole Binding and Activation of Cloned and Expressed Dopamine D₂, D₃ and D₄ Receptors. *Eur J Pharmacol* **290**, 29-36 (1995).
136. Horn, A. S., Tepper, P., Van der Weide, J., Watanabe, M., Grigoriadis, D. & Seeman, P. Synthesis and Radioreceptor Binding Activity of N-0437, a New Extremely Potent and Selective D₂ Receptor Agonist. *Pharm Weekbl., Sci. Ed.* **7**, 208-211 (1985).
137. Lenz, C., Haubmann, C., Hübner, H., Boeckler, F. & Gmeiner, P. Fancy Bioisosteres: Synthesis and Dopaminergic Properties of the Endiayne FAUC 88 as a Novel Non-aromatic D₃ Agonist. *Bioorg Med Chem* **13**, 185-192 (2005).
138. Audinot, V., Newman-Tancredi, A., Gobert, A., Rivet, J. M., Brocco, M., Lejeune, F., Gluck, L., Desposte, I., Bervoets, K., Dekeyne, A. & Millan, M. J. A Comparative in Vitro and in Vivo Pharmacological Characterization of the Novel Dopamine D₃ Receptor Antagonists (+)-S 14297, Nafadotride, GR 103,691 and U 99194. *J Pharmacol Exp Ther* **287**, 187-197 (1998).
139. Austin, N. E. Avenell, K. Y., Boyfield, I., Branch, C. L., Hadley, M. S., Jeffrey, P., Johnson, C. N., Macdonald, G. J., Nash, D. J., Riley, G. J., Smith, A. B., Stemp, G., Thewlis, K. M., Vong, A. K. & Wood, M. D. Design and Synthesis of Novel 2,3-dihydro-1H-isoindoles with High Affinity and Selectivity for the Dopamine D₃ Receptor. *Bioorg Med Chem Lett* **11**, 685-688 (2001).
140. Preti, A. BP-897 Bioprojet. *Curr Opin Investig Drugs* **1**, 110-115 (2000).
141. Wood, M. D., Boyfield, I., Nash, D. J., Jewitt, F. R., Avenell, K. Y. & Riley, G. J. Evidence for Antagonist Activity of the Dopamine D₃ Receptor Partial Agonist, BP 897, at Human Dopamine D₃ Receptor. *Eur J Pharmacol* **407**, 47-51 (2000).
142. Wicke, K. & Garcia-Ladona, J. The Dopamine D₃ Receptor Partial Agonist, BP 897, is an Antagonist at Human Dopamine D₃ Receptors and at Rat Somatodendritic Dopamine D₃ Receptors. *Eur J Pharmacol* **424**, 85-90 (2001).
143. Cervo, L., Carnovali, F., Stark, J. A. & Mennini, T. Cocaine-Seeking Behavior in Response to Drug-Associated Stimuli in Rats: Involvement of D₃ and D₂ Dopamine Receptors. *Neuropsychopharmacol* **28**, 1150-1159 (2003).
144. Garcia-Ladona, F. J. & Cox, B. F. BP 897, a Selective Dopamine D₃ Receptor Ligand with Therapeutic Potential for the Treatment of Cocaine-Addiction. *CNS Drug Rev* **9**, 141-158 (2003).
145. Leopoldo, M., Berardi, F., Colabufo, N. A., De Giorgio, P., Lacivita, E., Perrone, R., Tortorella, V. Structure-Affinity Relationship Study on N-(4-(4-Arylpiperazin-1-yl)butyl)arylcaboxamides as Potent and Selective Dopamine D₃ Receptor Ligands. *J. Med. Chem.* **45**, 5727-5735 (2002).
146. Dubuffet, T., Newman-Tancredi, A., Cussac, D., Audinot, V., Loutz, A., Millan, M. J. & Lavielle, G. Novel Nenzopyrano[3,4-c]pyrrole Derivatives as Potent and Selective Dopamine D₃ Receptor Antagonist. *Bioorg Med Chem Lett* **9**, 2059-2064 (1999).

147. Geneste, H., Backfisch, G., Braje, W., Delzer, J., Haupt, A., Hutchins, C. W., King, L. L., Lubisch, W., Steiner, G., Teschendorf, H. J., Unger, L. & Wernet, W. Synthesis and SAR of Highly Potent and Selective Dopamine D₃-Receptor Antagonists: Quinolin(di)one and Benzazepin(di)one Derivatives. *Bioorg Med Chem Lett* (2005).
148. Geneste, H., Amberg, W., Backfisch, G., Beyerbach, A., Braje, W.M., Delzer, J., Haupt, A., Hutchins, C. W., King, L. L., Sauer, D.R., Unger, L. & Wernet, W. Synthesis and SAR of Highly Potent and Selective Dopamine D₃-Receptor Antagonists: Variations on the 1*H*-Pyrimidin-2-one Theme. *Bioorg Med Chem Lett* **16**, 1934-1937 (2006).
149. Hill, S. J., Ganellin, C.R., Timmerman, H., Schwartz, J. C., Shankley, N.P., Young, J.M., Schunack, W., Levi, R. & Haas, H.L. International Union of Pharmacology. XIII. Classification of Histamine Receptors. *Pharmacol Rev* **49**, 253-278 (1997).
150. Blandina, P., Efooudebe, M., Cenni, G., Mannaioni, P. & Passani, M. B. Acetylcholine, Histamine, and Cognition: Two Sides of the Same Coin. *Learn. Mem.* **11**, 1-8 (2004).
151. Ito, C. The Role of the Central Histaminergic System on Schizophrenia. *Drug New Perspect* **17**, 383-387 (2004).
152. Hough, L. B. Genomix Meets Histamine Receptors: New Subtypes, New Receptors. *Mol Pharmacol* **59**, 415-419 (2001).
153. Gantz, I., Schaffer, M., DeVelle, J., Logsdon, C., Campbell, V., Uhler, M. & Yamada, T. Molecular Cloning of a Gene Encoding the Histamine H₂ Receptor. *Proc Natl Acad Sci USA* **88**, 429-433 (1991).
154. Yamashita, M., Fukui, H., Sugama, K., Horio, Y., Ito, S., Mizuguchi, H. & Wada, H. Expression Cloning of a cDNA Encoding the Bovine Histamine H₁ Receptor. *Proc Natl Acad Sci USA* **88**, 11515-11519 (1991).
155. Arrang, J. M., Garbarg, M. & Schwartz, J. C. Auto-Inhibition of Brain Histamine Release Mediated by a Novel Class (H₃) of Histamine Receptors. *Nature* **302**, 832-837 (1983).
156. Lovenberg, T. W., Roland, B.L., Wilson, S.J., Jiang, X., Pyati, J., Huvar, A., Jackson, M.R. & Erlander, M.G. Cloning and Functional Expression of the Human Histamine H₃ Receptor. *Mol Pharmacol* **55**, 1101-1107 (1999).
157. Jablonowski, J. A., Carruthers, N. I. & Thurmond, R. L. The Histamine H₄ Receptor and Potential Therapeutic uses for H₄ Ligands. *Mini-Rev. Med.Chem.* **4**, 993-1000 (2004).
158. Parsons, M. E. & Ganellin, C. R. Histamine and its Receptors. *Br J Pharmacol* **147**, S127-S135 (2006).
159. Fujimoto, K., Horio, Y., Sugama, K., Ito, S., Liu, Y.Q. & Fukui, H. Genomic Cloning of the Rat Histamine H₁ Receptor. *Biochem Biophys Res Commun* **190**, 294-301 (1993).
160. Horio, Y., Mori, Y., Higuchi, I., Fujimoto, K., Ito, S. & Fukui, H. Molecular Cloning of the Guinea-Pig Histamine H₁ Receptor Gene. *J Biochem* **114**, 408-414 (1993).
161. Inoue, I., Taniuchi, I., Kitamura, D., Jenkins, N.A., Gilbert, D.J., Copeland, N.G. & Watanabe, T. Characteristics of the Mouse Genomic Histamine H₁-Receptor Gene. *Genomics* **36**, 178-181 (1996).
162. De Backer, M. D., Gommeren, W., Moereels, H., Nobels, G., Van Gompel, P., Leysen, J. E. & Luyten, W. H. Genomic Cloning, Heterologous Expression and Pharmacological Characterization of a Human Histamine H₁ Receptor. *Biochem. Biophys. Res. Commun.* **197**, 1601-1608 (1993).

163. Leurs, R., Smit, M. J. & Timmerman, H. Molecular Pharmacological Aspects of Histamine Receptors. *Pharmacol. Ther.* **66**, 413-463 (1995).
164. Bakker, R. A., Schoonus, S. B., Smit, M. J., Timmerman, H. & Leurs, R. Histamine H₁-Receptor Activation of Nuclear Factor-Kappa B: Roles for G $\beta\gamma$ - and G $\alpha(q/11)$ -subunits in Constitutive and Agonist-Mediated Signaling. *Mol Pharmacol* **60**, 1133-1142 (2001).
165. Ito, C. The Role of Brain Histamine in Acute and Chronic Stresses. *Biomed Pharmacother* **54**, 263-267 (2000).
166. Kazmierczak, H., Pawlak-Osinska, K. & Kazmierczak, W. Betahistidine in Vertebrobasilar Insufficiency. *Int Tinnitus J* **10**, 191-193 (2004).
167. James, A. & Thorp, M. Meniere's Disease. *Clin Evid*, 742-750 (2004).
168. Ohta, K., Hayashi, H., Mizuguchi, H., Kagamiyama, H., Fujimoto, K., Fukui, H. Site-directed Mutagenesis of the Histamine H₁ Receptor: Roles of Aspartic Acid (107), Asparagine(198) and threonine(194). *Biochem. Biophys Res Commun* **203**, 1096-1101 (1994).
169. Leurs, R., Smit, M. J., Meeder, R., Ter Laak, A. M. & Timmerman, H. Lysine 200 Located in the Fifth Transmembrane Domain of the Histamine H₁ Receptor Interacts with Histamine but not with all H₁ Agonists. *Biochem. Biophys Res Commun* **214**, 110-117 (1995).
170. Van der Burg, W. J., Bonta, I. L., Delobelle, J., Ramon, C. & Vargaftig, B. A Novel Type of Substituted Piperazine with High Antiserotonin Potency. *J. Med. Chem.* **13**, 35-38 (1970).
171. Venkatesh, S. & Lipper, R. A. Role of the Development Scientist in Compound Lead Selection and Optimization. *J Pharm Sci* **89**, 145-154 (2000).
172. Bleicher, K. H., Bohm, H. J., Muller, K. & Alanine, A. I. Hit and Lead Generation: Beyond High-Throughput Screening. *Nat Rev Drug Discov* **2**, 369-378 (2003).
173. Bajorath, J. Integration of Virtual and High-Throughput Screening. *Nat Rev Drug Discov* **1**, 882-894 (2002).
174. Jain, A. K., Murty, M. N. & Flynn, P. J. Data Clustering: A Review. *ACM Computing Surveys* **31**, 265-323 (1999).
175. Chen, X., Rusinko, A. I. & Young, S. S. Recursive Partitioning Analysis of a Large Structure-Activity Data Set Using Three-Dimensional Descriptors. *J. Chem. Inf. Comput. Sci.* **38**, 1054-1062 (1998).
176. Renner, S. & Schneider, G. Fuzzy Pharmacophore Models From Molecular Alignments for Correlation-Vector-Based Virtual Screening. *J. Med. Chem.* **47**, 4653-4664 (2004).
177. Cortes, C. & Vapnik, V. Support-Vector Networks. *Machine Learning* **20**, 273-297 (1995).
178. Manallack, D. T. & Livingstone, D. J. Neural Networks in Drug Discovery: have they Lived up to their Promise? *Eur J Med Chem.* **34**, 195-208 (1999).
179. Hayes, G., Biden, T. J., Selbie, L. A. & Shine, J. Structural Subtypes of the Dopamine D₂ Receptor are Functionally Distinct: Expression of the Cloned D_{2A} and D_{2B} Subtypes in a Heterologous Cell Line. *Mol Endocrinol* **6**, 920-926 (1992).
180. Bradford, M. M. A Rapid and Sensitive Method for the Quantitation of Microgram Quantities of Protein Utilizing the Principle of Protein-Dye Binding. *Anal Biochem* **72**, 248-254 (1976).
181. Smit, M. J., Timmerman, H., Hijzelendoorn, J. C., Fukui, H. & Leurs, R. Regulation of the Human Histamine H₁ Receptor Stably Expressed in Chinese Hamster Ovary Cells. *Br J Pharmacol* **117**, 1071-1080 (1996).

182. Cheng, Y. & Prusoff, W. H. Relationship Between the Inhibition Constant (K₁) and the Concentration of Inhibitor which causes 50 per cent Inhibition (I₅₀) of an Enzymatic Reaction. *Biochem Pharmacol* **22**, 3099-3108 (1973).
183. Graeser, D. & Neubig, R. R. in *Signal Transduction A Practical Approach* (ed. Milligan, G.) 1-29 (Oxford University Press, Oxford, 1992).
184. Chang, C.-C. & Lin, C.-J. LIBSVM: a Library for Support Vector Machines. (2001).
185. Hulme, E. C. & Birdsall, N. J. M. in *Receptor-Ligand Interactions A Practical Approach* (ed. Hulme, E. C.) (Oxford University Press, Oxford, 1992).
186. Keen, M. (ed.) *Receptor Binding Techniques*. (Humana Press, Totowa, 1999).
187. Gardner, B. R., Hall, D. A. & Strange, P. G. Agonist Action at D₂(short) Dopamine Receptors Determined in Ligand Binding and Functional Assays. *J Neurochem* **69**, 2589-2598 (1997).
188. Seeman, P. & Van Tol, H. H. Deriving the Therapeutic Concentrations for Clozapine and Haloperidol: the Apparent Dissociation Constant of a Neuroleptic at the Dopamine D₂ or D₄ Receptor Varies with the Affinity of the Competing Radioligand. *Eur J Pharmacol* **291**, 59-66 (1995).
189. Vanhauwe, J. F., Fraeyman, N., Francken, B. J., Luyten, W. H. & Leysen, J. E. Comparison of the Ligand Binding and Signaling Properties of Human Dopamine D(2) and D(3) Receptors in Chinese Hamster Ovary Cells. *J Pharmacol Exp Ther* **290**, 908-916 (1999).
190. Vile, J. M., D'Souza, U. M. & Strange, P. G. [³H]nemonapride and [³H]spiperone Label Equivalent Numbers of D₂ and D₃ Dopamine Receptors in a Range of Tissues and Under Different Conditions. *J Neurochem* **64**, 940-943 (1995).
191. Castro, S. W. & Strange, P. G. Coupling of D₂ and D₃ Dopamine Receptors to G-Proteins. *FEBS Lett* **315**, 223-226 (1993).
192. Sokoloff, P., Andrieux, M., Besancon, R., Pilon, C., Martres, M. P., Giros, B. & Schwartz, J. C. Pharmacology of Human Dopamine D₃ Receptor Expressed in a Mammalian Cell Line: Comparison with D₂ Receptor. *Eur J Pharmacol* **225**, 331-337 (1992).
193. Strange, P. G. Mechanisms of Inverse Agonism at G-protein-coupled receptors. *Trends Pharmacol Sci* **23**, 89-95 (2002).
194. Hall, D. A. & Strange, P. G. Evidence that Antipsychotic Drugs are Inverse Agonists at D₂ Dopamine Receptors. *Br J Pharmacol* **121**, 731-736 (1997).
195. Anthes, J. C., Gilchrest, H., Richard, C., Eckel, S., Hesk, D., West Jr., R.E., Williams, S.M., Greenfeder, S., Billah, M., Kreutner, W. & Egan, R.W. Biochemical Characterization of Desloratadine, a Potent Antagonist of the Human Histamine H₁ Receptor. *Eur J Pharmacol* **449**, 229-237 (2002).
196. Keabadian, J. W., Tarazi, F. I., Kula, N. S. & Baldessarini, R. J. Compounds Selective For Dopamine Receptor Subtypes. *Drug Discov Today* **2**, 333-340 (1997).
197. Traiffort, E., Leurs, R., Arrang, J. M., Tardivel-Lacombe, J., Diaz, J., Schwartz, J. C. & Ruat, M. Guinea Pig Histamine H₁ Receptor. I. Gene cloning, Characterization, and Tissue Expression Revealed by in Situ Hybridization. *J Neurochem* **62**, 507-518 (1994).
198. DeLean, A., Stadel, J. M. & Lefkowitz, R. J. A Ternary Complex Model Explains the Agonist Specific Binding Properties of the Adenylyl Cyclase-Coupled β-Adrenergic Receptor. *J. Biol. Chem.* **255**, 7108-7117 (1980).
199. Payne, S. L., Johansson, A. M. & Strange, P. G. Mechanisms of Ligand Binding and Efficacy at the Human D₂(short) Dopamine Receptor. *J Neurochem* **82**, 1106-1117 (2002).

200. Lazareno, S. & Birdsall, N. J. M. in *G Protein-Coupled Receptors* (eds. Haga, T. & Berstein, G.) 8-10 (CRC Press, 1999).
201. Roberts, D. J. & Waelbroeck, M. G Protein Activation by G Protein Coupled Receptors: Ternary Complex Formation or Catalyzed Reaction? *Biochem Pharmacol* **68**, 799-806 (2004).
202. Kent, R. S., De Lean, A. & Lefkowitz, R. J. A Quantitative Analysis of Betaadrenergic Receptor Interactions : Resolution of High and Low Affinity States of the Receptor by Computer Modeling of Ligand Binding Data. *Mol Pharmacol* **17**, 14-23 (1980).
203. Weiss, J. M., Morgan, P. H., Lutz, M. W. & Kenakin, T. P. The Cubic Ternary Complex Receptor Occupancy Model. *J Theor Biol* **181**, 381-397 (1996).
204. Lahti, R. A., Figur, L. M., Piercey, M. F., Ruppel, P. L. & Evans, D. L. Intrinsic Activity Determinations at the Dopamine D₂ Guanine Nucleotide Binding Protein Coupled Receptor. Utilisation of Receptor State Binding Affinities. *Mol Pharmacol* **42**, 432-438 (1992).
205. Harley, E. A., Middlemiss, D. M. & Ragan, C. I. Relationship Between Inhibition of Cyclic AMP Production in Chinese Hamster Ovary Cells Expressing the Rat D₂(444) Receptor and Antagonist/Agonist Binding Ratios. *Br J Pharmacol* **115**, 1307-1313 (1995).
206. Kenakin, T. The Classification of Seven Transmembrane Receptors in Recombinant Expression Systems. *Pharmacol Rev* **48**, 413-463 (1996).
207. Gardner, B. & Strange, P. G. Agonist action at D₂(long) Dopamine Receptors: Ligand Binding and Functional Assays. *Br J Pharmacol* **124**, 978-984 (1998).
208. Christopoulos, A. & El-Fakahany, E. E. Qualitative and Quantitative Assessment of Relative Agonist Efficacy. *Biochem Pharmacol* **58**, 735-748 (1999).
209. Cordeaux, Y., Nickolls, S. A., Flood, L. A., Graber, S. G. & Strange, P. G. Agonist Regulation of D(2) Dopamine Receptor/G Protein Interaction. Evidence for Agonist Selection of G Protein Subtype. *J Biol Chem* **276**, 28667-28675 (2001).
210. Weiland, T. & Jakobs, K. H. Measurement of Receptor-stimulated Guanosine 5'-O-(gamma-thio)triphosphate Binding by G proteins. *Methods Enzymol* **237**, 3-13 (1994).
211. Newman-Tancredi, A., Cussac, D., Audinot, V., Pasteau, V., Gavaudan, S. & Millan, M. J. G Protein Activation by Human Dopamine D₃ Receptors in High-Expressing Chinese Hamster Ovary Cells: A Guanosine-5'-O-(3-[³⁵S]thio)-triphosphate Binding and Antibody Study. *Mol Pharmacol* **55**, 564-574 (1999).
212. Pilon, C., Levesque, D., Dimitriadou, V., Griffon, N., Martres, M. P., Schwartz, J. C. & Sokoloff, P. Functional coupling of the Human Dopamine D₃ Receptor in a Transfected NG 108-15 Neuroblastoma-Glioma Hybrid Cell Line. *Eur J Pharmacol* **268**, 129-139 (1994).
213. Gay, E. A., Urban, J. D., Nichols, D. E., Oxford, G. S. & Mailman, R. B. Functional Selectivity of D₂ Receptor Ligands in a Chinese Hamster Ovary hD_{2L} Cell Line: Evidence for Induction of Ligand-Specific Receptor States. *Mol Pharmacol* **66**, 97-105 (2004).
214. Wong, S. K. A 384-well Cell-based Phospho-ERK Assay for Dopamine D₂ and D₃ receptors. *Anal Biochem* **333**, 265-272 (2004).
215. Kenakin, T. Principles: Receptor Theory in Pharmacology. *Trends Pharmacol Sci* **25**, 186-192 (2004).
216. Vanhauwe, J. F., Josson, K., Luyten, W. H., Driessen, A. J. & Leysen, J. E. G-Protein Sensitivity of Ligand Binding to Human Dopamine D(2) and D(3) Receptors Expressed in Escherichia Coli: Clues for a Constrained D(3) Receptor Structure. *J Pharmacol Exp Ther* **295**, 274-283 (2000).

217. Newman-Tancredi, A., Verrièle, L., Chaput, C. & Millan, M. J. Labelling of Recombinant Human and Native Rat Serotonin 5-HT_{1A} Receptors by a Novel, Selective Radioligand, [³H]S15535: Definition of its Binding Profile using Agonists, Antagonists and Inverse Agonists. *Naunyn Schmiedebergs Arch Pharmacol* **357**, 205-217 (1998).
218. Costa, T. & Herz, A. Antagonists with Negative Intrinsic Activity at Delta Opioid Receptors Coupled to GTP-binding Proteins. *Proc Natl Acad Sci U S A* **86**, 7321-5 (1989).
219. Schwartz, J. C., Morisset, S., Rouleau, A., Ligneau, X., Gbahou, F., Tardivel-Lacombe, J., Stark, H., Schunack, W., Ganellin, C.R. & Arrang, J.M. Therapeutic Implications of Constitutive Activity of Receptors: the Example of the Histamine H₃ Receptor. *J Neural Transm* **64**, S1-S16 (2003).
220. Murray, P. J. A Novel Series of Arylpiperazines with High Affinity and Selectivity for the Dopamine D₃ Receptor. *Bioorg Med Chem Letters* **5**, 219-222 (1995).
221. Stemp, G., Ashmeade, T., Branch, C. L., Hadley, M. S., Hunter, A. J., Johnson, C. N., Nash, D. J., Thewlis, K. M., Vong, A. K., Austin, N. E., Jeffrey, P., Avenell, K. Y., Boyfield, I., Hagan, J. J., Middlemiss, D. N., Reavill, C., Riley, G. J., Routledge, C. & Wood, M. Design and Synthesis of Trans-*N*-[4-[2-(6-cyano-1,2,3,4-tetrahydroisoquinolin-2-yl)ethyl]cyclohexyl]-4-quinolinecarboxamide (SB-277011): A Potent and Selective Dopamine D(3) Receptor Antagonist with High Oral Bioavailability and CNS Penetration in the Rat. *J. Med. Chem.* **43**, 1878-1885 (2000).
222. Mach, U. R. Synthese und Struktur-Wirkungsbeziehungen neuer rezeptorselektiver Dopamin-D₂ and D₃-Liganden, Ph. D. Thesis, im *Fachbereich Chemische und Pharmazeutische Wissenschaften, Johann Wolfgang Goethe-Universität, Frankfurt am Main*, (2003).
223. Richelson, E. & El-Fakahany, E. Changes in the Sensitivity of Receptors for Neurotransmitters and the Actions of Some Psychotherapeutic Drugs. *Mayo Clin Proc* **57**, 576-582 (1982).
224. Shen, W. W. A History of Antipsychotic Drug Development. *Compr Psychiatry* **40**, 407-414 (1999).
225. Nonaka, H., Otaki, S., Ohshima, E., Kono, M., Kase, H., Ohta, K., Fukui, H. & Ichimura, M. Unique Binding Pocket for KW-4679 in the Histamine H₁ Receptor. *Eur J Pharmacol* **345**, 111-117 (1998).
226. Cusack, B., Nelson, A. & Richelson, E. Binding of Antidepressants to Human Brain Receptors: Focus on Newer Generation Compounds. *Psychopharmacology* **114**, 559-565 (1994).
227. Hjorth, S. & Sharp, T. Mixed Agonist/Antagonist Properties of NAN-190 at 5-HT_{1A} Receptors: Behavioural and In Vivo Brain Microdialysis Studies. *Life Sci* **46**, 955-963 (1990).
228. Mach, U. R., Hackling, A. E., Perachon, S., Ferry, S., Wermuth, C. G., Schwartz, J. C., Sokoloff, P. & Stark, H. Development of Novel 1,2,3,4-tetrahydroisoquinoline Derivatives and Closely Related Compounds as Potent and Selective Dopamine D₃ Receptor Ligands. *ChemBioChem* **5**, 508-518 (2004).
229. Ponzio, F., Algeri, S., Garattini, S., Cioce, V., Rusconi, L., Sacchetti, G., Manuel, C., Notelle, C., Duvert, L., Legeai, J. Behavioural and Biochemical Studies on 6-Methylamino-4,5,6,7-tetrahydrobenzothiazole (14.839JL), a New Potent Dopaminergic Agonist. *Pharmacol Res Commun* **19**, 555-565 (1987).
230. Hacksell, U., Svensson, U., Nilsson, J.L.G., Hjorth, S., Carlsson, A., Wikström, H., Lindberg, P. & Sanchez, D. *N*-Alkylated 2-Aminotertalins: Central Dopamine-Receptor Stimulating Activity. *J. Med. Chem.* **22**, 1469-1475 (1979).

231. Stark, H. Dopamin-D₃-Rezeptorliganden als pharmakologische Werkzeuge und potentielle Arzneistoffe, Habilitationsschrift, im *Fachbereich Pharmazie, Freie Universität Berlin, Berlin*, (1998).
232. Stadtman, T. C. Selenium Biochemistry--Selected Topics. *Adv Inorg Biochem* **10**, 157-175 (1994).
233. Ebadi, M. Brown-Borg, H., Ren, J., Sharma, S., Shavali, S., El ReFaey, & H. Carlson, E. C. Therapeutic Efficacy of Selegiline in Neurodegenerative Disorders and Neurological Diseases. *Curr Drug Targets* **7**, 1513-1529 (2006).
234. Bonuccelli, U. & Del Dotto, P. New Pharmacologic Horizons in the Treatment of Parkinson's Disease. *Neurology* **67**, S30-S8 (2006).
235. Weinreb, O., Amit, T., Bar-Am, O., Sagi, Y., Mandel, S. & Youdim, M. B. Involvement of Multiple Survival Signal Transduction Pathways in the Neuroprotective, Neurorescue and APP Processing Activity of Rasagiline and its Propargyl moiety. *J Neural Transm Suppl*, 457-465 (2006).
236. Piercey, M. F. Pharmacology of Pramipexole, a Dopamine D₃-Preferring Agonist useful in Treating Parkinson's Disease. *Clin Neuropharmacol* **21**, 141-151 (1998).
237. Millan, M. J., Maiorini, L., Cussac, D., Audinot, V., Boutin, J. A. & Newman-Tancredi, A. Differential Actions of Antiparkinson Agents at Multiple Classes of Monoaminergic Receptor. I. A Multivariate Analysis of the Binding Profiles of 14 Drugs at 21 Native and Cloned Human Receptor Subtypes. *J Pharmacol Exp Ther* **303**, 791-804 (2002).
238. Kvernmo, T., Hartter, S. & Burger, E. A Review of the Receptor-Binding and Pharmacokinetic Properties of Dopamine Agonists. *Clin Ther* **28**, 1065-1078 (2006).
239. Joyce, J. N. & Millan, M. J. Dopamine D₃ Receptor Antagonists as Therapeutic Agents. *Drug Discov Today* **10**, 917-925 (2005).
240. Boeckler, F., Ohnmacht, U., Lehmann, T., Utz, W., Hubner, H. & Gmeiner, P. CoMFA and CoMSIA Investigations Revealing Novel Insights into the Binding Modes of Dopamine D₃ Receptor Agonists. *J. Med. Chem.* **48**, 2493-2508 (2005).
241. Burbidge, R., Trotter, M., Buxton, B. & Holden, S. Drug Design by Machine Learning: Support Vector Machines for Pharmaceutical Data Analysis. *Comput. Chem.* **26**, 5-14 (2001).
242. Byvatov, E. & Schneider, G. Support Vector Machine Applications in Bioinformatics. *Appl Bioinformatics* **2**, 67-77 (2003).
243. Hackling, A. E. & Stark, H. Dopamine D₃ Receptor Ligands with Antagonist Properties. *ChemBioChem* **3**, 946-961 (2002).
244. Böcker-Felbek, A. D. Identification of Structure Activity Relationships in Primary Screening Data of High-Throughput Screening Assays, Ph. D. Thesis, im *Fachbereich Biochemie, Chemie und Pharmazie, Johann Wolfgang Goethe-Universität, Frankfurt am Main*, (submitted 2006).
245. Böcker, A., Schneider, G. & Teckentrup, A. NIPALSTREE: A New Hierarchical Clustering Approach for Large Compound Libraries and its Application to Virtual Screening. *J. Chem. Inf. Model.* **46**, 2220-2229 (2006).
246. Smola, A. J. & Schölkopf, B. A Tutorial on Support Vector Regression. *NeuroCOLT Technical Report Series* (1998).
247. Verdonk, M. L., Cole, J. C., Hartshorn, M. J., Murray, C. W. & Taylor, R. D. Improved Protein-Ligand Docking Using GOLD. *Proteins* **52**, 609-23 (2003).
248. Wermuth, C. G., Mann, A., Garrido, F., Lecomte, J., Schwartz, J.-C. & Sokoloff, P. Preparation of *N*-Piperazinylbutyl- and *N*-Piperidinylbutyl 2-Naphthamide Derivatives and as D₃ Receptor Agonists. *Chem. Abstr.* **127**, Eur. Pat. 0779284, (1997).

10 Pharmacological Experimental Procedures

10.1 Radioligand Binding Assays

10.1.1 Dopamine D_{2S} and D₃ Receptor Binding Assays

CHO-D_{2S} cells, expressing the recombinant human D₂(short) dopamine receptor gene,¹⁷⁹ were grown in Dulbecco's modified Eagle's medium/nutrient mixture F12 1:1 mixture supplemented with 2 mM glutamine, 10% fetal bovine serum, and 10 $\mu\text{l}\cdot\text{ml}^{-1}$ penicillin/streptomycin in an atmosphere of 5% CO₂ at 37 °C (Gibco™, Karlsruhe, Germany). Human D₃ receptors stably expressed in CHO cells as previously described by Sokoloff *et al.*¹⁹² were used. The cell line was cultured in Dulbecco's modified Eagle's medium supplemented with 2 mM glutamine, and 10% dialyzed fetal bovine serum, and were grown in an atmosphere of 5% CO₂ at 37 °C (Gibco™). Human D_{2S}- and D₃ receptors expressing cell lines were grown to confluence. The medium was removed, and the cells were washed with 10 ml PBS buffer (140 mM NaCl, 3 mM KCl, 1.5 mM KH₂PO₄, 8 mM Na₂HPO₄, pH 7.4) at 4 °C. After removing the wash buffer, the cells were scraped from the flasks into 15 ml of ice-cold media, and centrifuged at 3,000 rpm for 10 min at 4 °C. After centrifugation the medium was removed and the supernatant resuspended in ice-cold Tris-HCl buffer containing 5 mM MgCl₂, pH 7.4 and disrupted with a Polytron and centrifuged at 20,000 rpm, for 30 min at 4 °C. The pellet was resuspended by sonication in ice-cold Tris-HCl buffer (containing 5 mM MgCl₂, pH 7.4), membrane aliquots were stored at -70 °C. Determination of membrane protein was carried out by the method of Bradford.¹⁸⁰ Cell membranes containing human D_{2S} and D₃ receptors from CHO cells were thawed, rehomogenized with sonication at 4 °C in Tris-HCl, pH 7.4 containing 120 mM NaCl, 5 mM KCl, 2 mM CaCl₂ and 1 mM MgCl₂ (incubation buffer), and incubated with 0.2 nM [³H]spiperone (106 Ci·mmol⁻¹, Amersham Biosciences, Freiburg, Germany), and drug diluted in incubation buffer. Nonspecific binding was determined in the presence of 10 μM BP 897 (prepared by same of the authors).²⁴⁸ Incubations were run at 25 °C for 120 min, and terminated by rapid filtration through PerkinElmer GF/B glass fibre filters (PerkinElmer Life Sciences, Rodgau, Germany) coated in 0.3% polyethylenimine (Sigma-Aldrich, Taufkirchen, Germany) using an Inotech cell harvester (Inotech AG, Dottikon, Switzerland). Unbound radioligand was removed with four washes of 1 ml of ice-cold 50 mM Tris-HCl buffer, pH 7.4, containing 120 mM NaCl. The filters were soaked in 9 ml Beta plate scint scintillator and counted using a PerkinElmer MicroBeta[®]Trilux scintillation counter (PerkinElmer Life Sciences). Competition binding data were analyzed by the software GraphPad Prism™ (2000, version

3.02, San Diego, CA, USA), using non-linear least squares fit. For detailed screening the compounds have been tested at seven concentrations in triplicate carrying out three to five separate binding experiments for human dopamine D_{2S} and for human dopamine D₃ receptors and expressed as mean \pm standard error of the mean (SEM). K_i values were calculated from the IC_{50} values according to Cheng-Prusoff equation.¹⁸²

10.1.2 Preliminary Dopamine D_{2S} and D₃ Receptor Binding Screening

Cell culture was carried out using standard procedures. Human dopamine D_{2S} and D₃ receptors were expressed in stably transfected Human Embryonic Kidney (HEK) and Chinese hamster ovary (CHO) cells, respectively. The CHO-D₃ cells were cultured at 37°C in Dulbecco's Modified Eagle Medium (DMEM, Cambrex Bio Sciences, Rockland Inc) supplemented with 10% dialysed fetal calf serum (Invitrogen, Co, Carlsbad, CA), 100 Units/ml penicillin-streptomycin (Cambrex, Bio Sciences, Rockland Inc), HEPES 20 mM, pH = 7.4 and 2 mM glutamine (Cambrex, Bio Sciences, Rockland Inc) in an atmosphere of 5% CO₂.¹⁹² The HEK-D_{2S} cell line was obtained following transfection by pCDNA3.1-D2S expressing vector. HEK-D_{2S} were cultured at 37°C in Dulbecco's Modified Eagle Medium (DMEM-NUT.F-12, Cambrex, Bio Sciences, Rockland Inc) supplemented with 10% fetal calf serum (Cambrex, Bio Sciences, Rockland Inc), 100 Units/ml penicillin-streptomycin (Cambrex, Bio Sciences, Rockland Inc), HEPES 20 mM, pH=7.4, 400µg/ml geneticin (Cambrex, Bio Sciences, Rockland Inc) and 2 mM glutamine (Cambrex, Bio Sciences, Rockland Inc) in an atmosphere of 5% CO₂. Incubations containing 2 nM [³H]spiperone (specific activity 15 Ci/mmol, Perkin Elmer Life Sciences, Boston, MA) were run in duplicate in 0.1% polyethylenimine (PEI) (Sigma-Aldrich, Inc, St.Louis, MI) coated multiscreen GF/B 96 wells microplates (Millipore, Billerica, MA). Incubations were started by adding per well 250 µl membrane suspension diluted to 10 µg protein/ml. 2 µl of tested compounds diluted in dimethyl sulfoxide (Sigma-Aldrich, Inc, St.Louis, MI) were added in increasing final concentrations, at 0.1, 1, 10, 100, 1 000 or 10 000 nM. Non specific binding was measured in the presence of 5 µM haloperidol (Sigma-Aldrich, Inc, St.Louis, MI). Incubations were run 1 hour at room temperature and stopped by vacuum filtration. Filters were washed 4 times by 250 µl of ice-cold binding buffer. Then 50 µl of Optiphase Supermix scintillation cocktail (Perkin Elmer, Boston, MA) was added and the filters were counted by liquid scintillation on the 14.50 microbeta Trilux counter (Wallac-PerkinElmer, Boston, MA). IC_{50} values representing the concentrations to 50% of maximal inhibition were calculated by nonlinear regression using the Origin 6.0 software (microcal

software, Inc, Northampton, MA). K_i values were derived from the formula $K_i = IC_{50}/(1+L/K_d)$ where L is the concentration of [3 H]spiperone and K_d its dissociation constant.¹⁸²

10.1.3 Histamine H_1 Receptor Binding Assay

CHO- H_1 cells, stably expressing the recombinant human H_1 histamine receptor gene in CHO-K1 cells,¹⁸¹ were grown in Dulbecco's modified Eagle's medium supplemented with 2 mM glutamine, 10% fetal bovine serum, and 100 IU/mL penicillin G, 100 μ g/mL streptomycin, and 0.1 mM nonessential amino acids in an atmosphere of 5% CO_2 at 37 °C (GibcoTM, Karlsruhe, Germany). At confluence, the cells were washed with 10 mL ice-cold PBS buffer (140 mM NaCl, 3 mM KCl, 1.5 mM KH_2PO_4 , 8 mM $NaHPO_4$, pH 7.4), scraped into ice-cold HEPES binding buffer (20 mM HEPES, 10 mM $MgCl_2$, 100 mM NaCl, pH 7.4), and homogenized with sonication. Membranes were pelleted at 20,000 rpm for 30 minutes at 4 °C, rehomogenized in HEPES buffer using a hand potter, and stored in liquid nitrogen. Protein concentrations were determined according to the method of Bradford.¹⁸⁰

Cell membranes were thawed, rehomogenized with sonication at 4 °C into ice-cold HEPES binding buffer, and incubated with [3 H]mepyramine (1.0 nM; 28 Ci·mmol⁻¹, Amersham Biosciences, Freiburg, Germany), and drug was diluted in HEPES buffer. Nonspecific binding was determined in the presence of 10 μ M Chlorphenaminhydrogenmaleat (Sigma-Aldrich, Taufkirchen, Germany). Incubations were run at 25 °C for 120 min, and terminated by rapid filtration through PerkinElmer GF/B glass fibre filters (PerkinElmer Life Sciences, Rodgau, Germany) coated in 0.3% polyethylenimine (Sigma-Aldrich, Taufkirchen, Germany) using an Inotech cell harvester (Inotech AG, Dottikon, Switzerland). Unbound radioligand was removed with four washes of 1 ml of ice-cold HEPES buffer. The filters were soaked in 9 ml Beta plate scint scintillator and counted using a PerkinElmer MicroBeta[®] Trilux scintillation counter (PerkinElmer Life Sciences). Competition binding data were analyzed by the software GraphPad PrismTM (2000, version 3.02, San Diego, CA, USA), using non-linear least squares fit. For detailed screening the compounds have been tested at seven concentrations in triplicate carrying out three to five separate binding experiments for human histamine H_1 receptors and expressed as mean \pm standard error of the mean (SEM). K_i values were calculated from the IC_{50} values according to Cheng-Prusoff equation.¹⁸²

10.1.4 GTP Shift Assay

GTP shift competition binding experiments for dopamine D_{2S} and D₃ receptors are carried out under similar assay conditions as competition binding experiments with few modifications. Frozen cell membrane preparations with human dopamine D_{2S} or D₃ receptors were thawed, rehomogenized in control buffer (Tris 50 mM, KCl 5 mM, CaCl₂ 1 mM, MgCl₂ 2 mM, HCl ad pH 7.4) using ultrasonic waves (duty cycle constant, 10 sec) at 4 °C. Final membrane protein concentrations of dopamine D_{2S} receptors was 10 µg/200 µL and for D₃ receptors 2 µg/200 µL. Test compound and [³H]spiperone were diluted in control buffer (final concentration 0.2 nM). Either 50 µL of test compound dilution or 50 µL of control buffer to determine total binding or 50 µL of 10 µM BP897 in control buffer to measure non-specific binding were applied. In the next step, 50 µL GTP-binding buffer (NaCl 120 mM (4-fold concentrated), Tris 50 mM, KCl 5 mM, CaCl₂ 1 mM, MgCl₂ 2 mM, HCl ad pH 7.4), 50 µL control buffer or 50 µL 100 µM Gpp(NH)p in GTP-binding buffer were added to the microtiter plate, respectively. Finally, 50 µL 0.2 nM [³H]spiperone (final concentration) and 50 µL cell membrane suspension were applied. Samples were incubated at 25 °C for 2 h and terminated by rapid filtration through GF/B glass fibre filters, presoaked for 30 min and at 4 °C in 0.3% polyethylenimine solution, using a cell harvester. Unbound radioligand was removed with four washes of 300 µL ice-cold wash buffer. Filters were dried at 55 °C for 50 – 60 min in the oven and afterwards soaked in 9 mL scintillant. Bound radioactivity was counted (5 min/well) in a β-counter at 45% counter efficiency. Competition binding data were analyzed by the software GraphPad Prism™ (2000, version 3.02, San Diego, CA, USA), using non-linear least squares fit. Assays were carried out in triplicates and at least 3 independent experiments using 96-well plates.

11 Appendix

Table 4.1 $-\log K_d$ values derived from [^3H]spiperone saturation experiments.

Receptor	Non-specific binding	$-\log K_d^a$
hD_{2S}	10 μM BP897	9.97 \pm 0.05
hD₃	10 μM BP897	9.66 \pm 0.06
hD₃	10 μM haloperidol	9.66 \pm 0.05

^aValues ($-\log K_d$) are mean \pm SD of at least three independent experiments performed in triplicates.

Table 4.2 $-\log K_d$ values derived from [^3H]mepyramine saturation experiments.

Receptor	Non-specific binding	$-\log K_d^a$
hH₁	10 μM chlorpheniramine	8.89 \pm 0.02

^aValues ($-\log K_d$) are mean \pm SD of at least three independent experiments performed in triplicates.

Table 4.3 $-\log K_i$ values and Hill coefficients (in parentheses) of determined dopamine reference compounds.

Compound	$-\log K_i$ (hD _{2S}) ^a	$-\log K_i$ (hD ₃) ^a
BP 897	7.29 \pm 0.09 (1.12 \pm 0.30)	9.05 \pm 0.11 (0.98 \pm 0.28)
Haloperidol	8.65 \pm 0.05 (0.95 \pm 0.05)	8.33 \pm 0.02 (1.04 \pm 0.15)
(S)-(-)-Nafadotride	8.19 \pm 0.01 (1.03 \pm 0.05)	n.d. ^b
(S)-(-)-Raclopride	8.35 \pm 0.01 (1.07 \pm 0.12)	8.63 \pm 0.17 (0.85 \pm 0.14)
Spiperone	9.57 \pm 0.02 (0.99 \pm 0.15)	9.17 \pm 0.04 (1.02 \pm 0.22)
ST 198	5.90 \pm 0.03 (0.95 \pm 0.11)	8.06 \pm 0.01 (0.76 \pm 0.11)
U 99194A	5.42 \pm 0.08 (0.84 \pm 0.16)	6.52 \pm 0.14 (0.82 \pm 0.06)

^aValues ($-\log K_i$) are mean \pm SD of at least three independent experiments performed in triplicates.

^bn.d., not determined.

Table 4.4 $-\log K_i$ values and Hill coefficients (in parentheses) of determined histamine reference compounds.

Compound	$-\log K_i$ (hH ₁) ^a
Bamipine	7.92 ± 0.03 (1.16 ± 0.51)
Cetirizine	7.56 ± 0.10 (0.79 ± 0.18)
Chlorpheniramine	7.77 ± 0.07 (1.00 ± 0.19)
Diphenhydramine	7.46 ± 0.02 (0.86 ± 0.07)
Fexofenadine	7.48 ± 0.03 (0.86 ± 0.12)
Ketotifen	9.48 ± 0.08 (1.05 ± 0.13)
Loratadine	6.91 ± 0.16 (1.00 ± 0.06)
Mepyramine	8.76 ± 0.03 (0.79 ± 0.02)
Mianserin	9.10 ± 0.14 (1.18 ± 0.12)

^aValues ($-\log K_i$) are mean ± SD of at least three independent experiments performed in triplicates.

Figure 4.8, 4.9 Pramipexole binding at dopamine D_{2S} and D₃ receptors (Hill coefficients in parentheses).

hD _{2S}					
$-\log K_H^a$	% R _H ^a	$-\log K_L^a$	n ^b	$-\log K_i$ Gpp(NH)p ^a	n ^b
8.52 ± 0.13	23 ± 7	6.49 ± 0.21	3	5.31 ± 0.08 (0.80 ± 0.12)	4
hD ₃					
$-\log K_{i \text{ control}}^a$		n ^b	$-\log K_i$ Gpp(NH)p ^a		n ^b
8.90 ± 0.02 (0.72 ± 0.21)		3	7.93 ± 0.12 (0.94 ± 0.20)		4

^aValues are mean ± SD of independent experiments.

^bNumber of experiments performed in triplicates.

Figure 4.10, 4.11 Compound **54** binding at dopamine D_{2S} and D₃ receptors (Hill coefficients in parentheses).

hD_{2S}					
$-\log K_H^a$	% R_H^a	$-\log K_L^a$	n^b	$-\log K_i$ Gpp(NH)p ^a	n^b
8.63 ± 0.22	33 ± 5	6.74 ± 0.08	3	5.61 ± 0.05 (0.69 ± 0.09)	4
hD₃					
$-\log K_{i \text{ control}}^a$	n^b	$-\log K_i$ Gpp(NH)p ^a	n^b		
8.51 ± 0.10 (0.78 ± 0.17)	3	7.73 ± 0.08 (0.89 ± 0.22)	3		

^aValues are mean ± SD of independent experiments.^bNumber of experiments performed in triplicates.**Figure 4.12, 4.13** BP 897 binding at dopamine D_{2S} and D₃ receptors (Hill coefficients in parentheses).

hD_{2S}			
$-\log K_{i \text{ control}}^a$	n^b	$-\log K_i$ Gpp(NH)p ^a	n^b
7.10 ± 0.003 (1.18 ± 0.27)	3	7.28 ± 0.02 (1.30 ± 0.20)	3
hD₃			
$-\log K_{i \text{ control}}^a$	n^b	$-\log K_i$ Gpp(NH)p ^a	n^b
8.76 ± 0.04 (0.80 ± 0.21)	3	9.12 ± 0.07 (1.10 ± 0.03)	3

^aValues are mean ± SD of independent experiments.^bNumber of experiments performed in triplicates.**Figure 4.14, 4.15** ST 198 binding at dopamine D_{2S} and D₃ receptors (Hill coefficients in parentheses).

hD_{2S}			
$-\log K_{i \text{ control}}^a$	n^b	$-\log K_i$ Gpp(NH)p ^a	n^b
5.74 ± 0.03 (0.84 ± 0.10)	4	5.97 ± 0.06 (0.86 ± 0.18)	4
hD₃			
$-\log K_{i \text{ control}}^a$	n^b	$-\log K_i$ Gpp(NH)p ^a	n^b
7.26 ± 0.05 (0.86 ± 0.06)	3	8.12 ± 0.07 (0.93 ± 0.16)	4

^aValues are mean ± SD of independent experiments.^bNumber of experiments performed in triplicates.

Table 4.5 $-\log K_i$ values and Hill coefficients (in parentheses) of 4-(2-methoxyphenyl)piperazine and 1,2,3,4-tetrahydroisoquinoline derivatives.

No.	$-\log K_i^a$	
	hD_{2S}	hD_3
BP 897	7.29 \pm 0.09 (1.12 \pm 0.30)	9.05 \pm 0.11 (0.98 \pm 0.28)
1	7.36 \pm 0.08 (1.06 \pm 0.19)	9.39 \pm 0.21 (0.92 \pm 0.15)
2	7.27 \pm 0.12 (1.04 \pm 0.18)	8.27 \pm 0.15 (0.95 \pm 0.33)
3	7.29 \pm 0.05 (1.09 \pm 0.25)	8.69 \pm 0.04 (1.02 \pm 0.20)
4	7.23 \pm 0.03 (0.96 \pm 0.13)	8.51 \pm 0.05 (1.00 \pm 0.19)
ST 198	5.90 \pm 0.03 (0.95 \pm 0.11)	8.06 \pm 0.01 (0.76 \pm 0.11)
5	6.09 \pm 0.03 (0.85 \pm 0.08)	7.09 \pm 0.08 (0.87 \pm 0.23)
6	6.11 \pm 0.06 (1.08 \pm 0.01)	7.62 \pm 0.08 (0.86 \pm 0.12)

^aValues ($-\log K_i$) are mean \pm SD of at least three independent determinations performed in triplicates.

Table 4.6 $-\log K_i$ values and Hill coefficients (in parentheses) of inverse amide compounds.

No.	$-\log K_i^a$	
	hD_{2S}	hD_3
7	5.84 \pm 0.09 (0.84 \pm 0.07)	6.87 \pm 0.13 (0.85 \pm 0.09)
8	6.26 \pm 0.11 (1.04 \pm 0.08)	6.87 \pm 0.06 (0.92 \pm 0.02)
9	5.98 \pm 0.08 (1.03 \pm 0.22)	6.92 \pm 0.04 (1.05 \pm 0.02)
10	5.99 \pm 0.04 (0.80 \pm 0.11)	6.75 \pm 0.17 (1.02 \pm 0.20)
11	6.08 \pm 0.09 (1.02 \pm 0.16)	7.61 \pm 0.05 (0.98 \pm 0.16)
12	6.72 \pm 0.15 (0.97 \pm 0.14)	7.34 \pm 0.14 (1.01 \pm 0.06)
13	5.56 \pm 0.13 (0.92 \pm 0.11)	6.29 \pm 0.04 (0.98 \pm 0.10)
14	6.19 \pm 0.09 (0.93 \pm 0.12)	7.00 \pm 0.03 (0.89 \pm 0.34)

^aValues ($-\log K_i$) are mean \pm SD of at least three independent determinations performed in triplicates.

Table 4.7 Clog*P* value, and preliminary pharmacological screening results for human dopamine D₂ and D₃ receptor binding affinities.

Compound	Clog <i>P</i>	<i>K_i</i> [nM] ^a	
		hD _{2s}	hD ₃
15	5.31	559	28.0
16	5.41	226	42.9
17	5.93	457	11.1
18	5.28	652	6.2
19	6.49	587	2.5
20	5.84	963	2.5
21	6.53	1000	17.7
22	5.38	161	40.9
23	6.08	633	36.9
24	5.84	626	3.60
25	5.68	313	15.2
26	5.02	972	15.2
27	5.72	619	22.8
28	6.33	1324	>1000
29	5.68	429	50.2
30	6.37	4925	>1000
31	4.22	1149	99.1
32	5.41	>1000	10.9
33	5.57	n.d.	n.d.
34	6.46	849	2.7
35	5.30	128	>1000
36	6.49	703	0.3
37	6.53	1570	31.1
38	5.38	4620	>1000
39	3.18	>1000	10.8

^aValues (-log*K_i*) received by six-points measurements performed in duplicates in one experiment (external tested). Clog*P* values were provided by Dr. U. Mach.

Table 4.8 -log*K_i* values and Hill coefficients (in parentheses) of cyclizine-based hybrids.

No.	-log <i>K_i</i> ^a		
	hD _{2s}	hD ₃	hH ₁
15	6.75 ± 0.14 (0.89 ± 0.01)	7.19 ± 0.13 (1.18 ± 0.26)	7.48 ± 0.12 (1.33 ± 0.50)
16	6.54 ± 0.21 (1.70 ± 0.30)	6.83 ± 0.01 (1.04 ± 0.70)	n.d. ^b
17	6.62 ± 0.07 (1.40 ± 0.14)	7.41 ± 0.01 (1.65 ± 0.42)	7.69 ± 0.13 (1.23 ± 0.13)
18	6.12 ± 0.07 (1.14 ± 0.17)	7.27 ± 0.11 (0.88 ± 0.15)	8.16 ± 0.03 (1.29 ± 0.17)
19	6.75 ± 0.09 (1.28 ± 0.09)	7.35 ± 0.23 (1.04 ± 0.06)	n.d. ^b
20	6.54 ± 0.06 (1.11 ± 0.30)	7.24 ± 0.11 (1.85 ± 0.75)	n.d. ^b
21	6.50 ± 0.09 (1.33 ± 0.2)	7.27 ± 0.09 (1.20 ± 0.20)	n.d. ^b
22	5.90 ± 0.08 (1.29 ± 0.78)	6.89 ± 0.20 (1.47 ± 0.61)	7.60 ± 0.08 (1.30 ± 0.24)

Table 4.8 (continued)

No.	$-\log K_i^a$		
	hD_{2S}	hD_3	hH_1
23	5.80 \pm 0.17 (2.43 \pm 0.21)	6.41 \pm 0.08 (1.70 \pm 0.61)	7.32 \pm 0.11 (1.77 \pm 0.50)
24	6.34 \pm 0.02 (1.31 \pm 0.05)	6.88 \pm 0.24 (1.49 \pm 0.17)	n.d. ^b
25	6.86 \pm 0.04 (1.56 \pm 0.3)	7.46 \pm 0.15 (1.68 \pm 0.59)	n.d. ^b
26	6.15 \pm 0.13 (0.95 \pm 0.20)	7.18 \pm 0.08 (1.25 \pm 0.37)	7.71 \pm 0.12 (0.92 \pm 0.15)
27	6.29 \pm 0.11 (1.07 \pm 0.18)	6.97 \pm 0.12 (1.24 \pm 0.31)	n.d. ^b

^aValues ($-\log K_i$) are mean \pm SD of at least three independent experiments performed in triplicates.

^bn.d., not determined.

Table 4.9 $-\log K_i$ values and Hill coefficients (in parentheses) of tri- and tetracyclic compounds.

No.	$-\log K_i^a$		
	hD_{2S}	hD_3	hH_1
28	6.32 \pm 0.18 (1.75 \pm 0.05)	6.77 \pm 0.30 (1.61 \pm 0.27)	n.d. ^b
29	6.33 \pm 0.09 (1.47 \pm 0.26)	6.65 \pm 0.09 (1.06 \pm 0.09)	8.19 \pm 0.02 (1.40 \pm 0.36)
30	6.42 \pm 0.10 (1.96 \pm 0.03)	6.36 \pm 0.16 (2.14 \pm 0.36)	n.d. ^b
31	6.28 \pm 0.05 (1.19 \pm 0.10)	6.86 \pm 0.18 (0.87 \pm 0.11)	8.08 \pm 0.21 (1.09 \pm 0.29)
32	6.12 \pm 0.11 (1.01 \pm 0.22)	7.33 \pm 0.12 (1.29 \pm 0.59)	7.60 \pm 0.15 (1.27 \pm 0.44)
33	6.66 \pm 0.17 (1.61 \pm 0.23)	7.00 \pm 0.15 (1.29 \pm 0.10)	n.d. ^b
34	6.62 \pm 0.02 (1.65 \pm 0.38)	6.77 \pm 0.15 (1.19 \pm 0.32)	7.90 \pm 0.09 (1.52 \pm 0.53)

^aValues ($-\log K_i$) are mean \pm SD of at least three independent experiments performed in triplicates.

^bn.d., not determined.

Table 4.10 $-\log K_i$ values and Hill coefficients (in parentheses) of bamipine-based hybrids.

No.	$-\log K_i^a$		
	hD_{2S}	hD_3	hH_1
35	6.47 ± 0.08 (1.36 ± 0.67)	6.66 ± 0.13 (1.52 ± 0.36)	n.d. ^b
36	6.25 ± 0.06 (1.55 ± 0.19)	6.88 ± 0.18 (1.93 ± 0.82)	n.d. ^b
37	6.38 ± 0.11 (1.30 ± 0.44)	7.24 ± 0.15 (1.20 ± 0.59)	n.d. ^b
38	5.09 ± 0.01 (0.99 ± 0.18)	6.29 ± 0.06 (1.40 ± 0.47)	n.d. ^b
39	6.02 ± 0.01 (0.90 ± 0.14)	8.15 ± 0.14 (0.92 ± 0.01)	7.78 ± 0.12 (1.03 ± 0.08)
40	6.07 ± 0.02 (0.71 ± 0.05)	8.10 ± 0.03 (0.95 ± 0.19)	n.d. ^b

^aValues ($-\log K_i$) are mean ± SD of at least three independent experiments performed in triplicates.

^bn.d., not determined.

Table 4.11 $-\log K_i$ values and Hill coefficients (in parentheses) of histamine H_1 receptor antagonists.

No.	$-\log K_i^a$		
	hD_{2S}	hD_3	hH_1
Cetirizine	<4	<4.5	7.56 ± 0.10 (0.79 ± 0.18)
Mianserin	5.61 ± 0.13 (0.99 ± 0.27)	5.78 ± 0.02 (1.23 ± 0.25)	9.10 ± 0.14 (1.18 ± 0.12)
Ketotifen	5.33 ± 0.12 (1.09 ± 0.33)	5.93 ± 0.27 (0.86 ± 0.37)	9.48 ± 0.08 (1.05 ± 0.13)
Loratadine	4.37 ± 0.02 (0.82 ± 0.14)	<5	6.91 ± 0.16 (1.00 ± 0.06)
Bamipine	5.72 ± 0.10 (1.01 ± 0.09)	5.99 ± 0.05 (1.07 ± 0.04)	7.92 ± 0.03 (1.16 ± 0.51)

^aValues ($-\log K_i$) are mean ± SD of at least three independent experiments performed in triplicates.

Table 4.12 $-\log K_i$ values and Hill coefficients (in parentheses) of pramipexole analogues and related compounds.

No.	$-\log K_i^a$	
	hD_{2s}	hD_3
Pramipexole	5.58 ± 0.04 (0.66 ± 0.04)	8.26 ± 0.31 (0.72 ± 0.09)
41	4.67 ± 0.07 (0.70 ± 0.05)	5.97 ± 0.11 (0.92 ± 0.16)
42	4.61 ± 0.20 (n.d. ^b)	6.68 ± 0.05 (0.94 ± 0.02)
43	4.76 ± 0.11 (0.58 ± 0.09)	7.04 ± 0.07 (0.93 ± 0.07)
44	4.94 ± 0.05 (0.73 ± 0.11)	7.11 ± 0.01 (0.89 ± 0.12)
45	5.14 ± 0.09 (0.96 ± 0.08)	7.04 ± 0.05 (1.00 ± 0.19)
46	4.76 ± 0.13 (0.86 ± 0.12)	7.37 ± 0.22 (0.71 ± 0.05)
47	4.20 ± 0.03 (n.d. ^b)	5.92 ± 0.01 (0.92)
48	5.69 ± 0.20 (0.87 ± 0.11)	5.64 ± 0.04 (1.04 ± 0.06)
49	4.14 ± 0.21 (0.94 ± 0.02)	5.92 ± 0.13 (0.82 ± 0.13)
50	<6	<6
51	4.38 ± 0.15 (0.55 ± 0.06)	5.92 ± 0.20 (0.94 ± 0.24)
52	5.10 ± 0.05 (0.80 ± 0.05)	6.93 ± 0.07 (1.02 ± 0.06)
53	4.99 ± 0.10 (0.63 ± 0.03)	6.57 ± 0.10 (0.90 ± 0.30)
54	5.77 ± 0.18 (0.71 ± 0.13)	7.83 ± 0.07 (0.85 ± 0.17)

^aValues ($-\log K_i$) are mean ± SD of at least three independent experiments performed in triplicates.

^bn.d., not determined.

Table 4.13 $-\log K_i$ values and Hill coefficients (in parentheses) of naphthalen-2-carboxamide derivatives.

No.	$-\log K_i^a$	
	hD_{2s}	hD_3
55	5.60 ± 0.05 (0.78 \pm 0.01)	7.19 ± 0.16 (0.93 \pm 0.15)
56	4.68 ± 0.05 (0.75 \pm 0.16)	6.84 ± 0.09 (0.99 \pm 0.23)
57	5.43 ± 0.12 (0.85 \pm 0.16)	7.62 ± 0.19 (0.79 \pm 0.13)
58	5.81 ± 0.09 (0.64 \pm 0.09)	8.60 ± 0.15 (1.00 \pm 0.29)
59	6.09 ± 0.19 (0.89 \pm 0.10)	8.94 ± 0.07 (1.23 \pm 0.06)
60	6.34 ± 0.08 (0.89 \pm 0.18)	9.03 ± 0.09 (1.12 \pm 0.05)
61	5.04 ± 0.03 (0.69 \pm 0.04)	8.11 ± 0.08 (1.06 \pm 0.36)

^aValues ($-\log K_i$) are mean \pm SD of at least three independent determinations performed in triplicates.

Table 4.14 $-\log K_i$ values and Hill coefficients (in parentheses) of cinnamoyl derivatives.

No.	$-\log K_i^a$	
	hD_{2s}	hD_3
62	5.40 ± 0.04 (0.47 \pm 0.08)	8.09 ± 0.07 (1.00 \pm 0.23)
63	6.35 ± 0.05 (0.81 \pm 0.05)	8.65 ± 0.23 (1.02 \pm 0.27)
64	6.08 ± 0.02 (0.67 \pm 0.02)	9.25 ± 0.03 (0.90 \pm 0.22)

^aValues ($-\log K_i$) are mean \pm SD of at least three independent experiments performed in triplicates.

Table 4.15 $-\log K_i$ values and Hill coefficients (in parentheses) of 4-(2-methoxyphenyl)piperazine derivatives.

No.	$-\log K_i^a$	
	hD_{2s}	hD_3
65	6.83 ± 0.07 (1.00 \pm 0.06)	7.87 ± 0.04 (0.92 \pm 0.22)
66	6.86 ± 0.07 (1.03 \pm 0.1)	7.05 ± 0.01 (0.92 \pm 0.09)
67	6.32 ± 0.05 (0.86 \pm 0.18)	7.27 ± 0.14 (0.84 \pm 0.13)

^aValues ($-\log K_i$) are mean \pm SD of at least three independent determinations performed in triplicates.

Table 4.16 $-\log K_i$ values and Hill coefficients (in parentheses) of heteroaryl amide derivatives.

No.	$-\log K_i^a$	
	hD_{2s}	hD_3
68	4.63 ± 0.02 (1.02 \pm 0.23)	6.54 ± 0.06 (0.92 \pm 0.18)
69	5.47 ± 0.05 (1.13 \pm 0.20)	7.28 ± 0.04 (1.06 \pm 0.22)
70	5.61 ± 0.08 (0.58 \pm 0.06)	8.54 ± 0.07 (0.96 \pm 0.15)
71	5.64 ± 0.02 (0.88 \pm 0.12)	7.82 ± 0.16 (0.93 \pm 0.17)
72	4.62 ± 0.14 (0.81)	5.73 ± 0.13 (0.73 \pm 0.21)
73	5.79 ± 0.16 (0.55 \pm 0.04)	8.35 ± 0.09 (1.04 \pm 0.37)
74	5.68 ± 0.07 (0.76 \pm 0.13)	8.25 ± 0.02 (0.92 \pm 0.24)
75	6.48 ± 0.16 (0.78 \pm 0.19)	9.19 ± 0.06 (0.82 \pm 0.08)

^aValues ($-\log K_i$) are mean \pm SD of at least three independent experiments performed in triplicates.

Table 4.17 $-\log K_i$ values and Hill coefficients (in parentheses) of diverse structural elements.

No	$-\log K_i^a$	
	hD_{2s}	hD_3
76	5.60 ± 0.02 (1.08 \pm 0.10)	7.08 ± 0.01 (1.16 \pm 0.24)
77	5.07 ± 0.01 (0.87 \pm 0.21)	5.88 ± 0.19 (1.06 \pm 0.21)
78	<5	<5

^aValues ($-\log K_i$) are mean \pm SD of at least three independent experiments performed in triplicates.

Table 4.18 Dopamine receptor affinities of compounds from the first virtual screening cycle.

No.	$-\log K_i^a$	
	hD_{2S}	hD_3
79	> 5.7	> 5.7
80	5.2 – 5.7	> 5.7
81	5.2 – 5.7	5.2 – 5.7
82	< 5.2	5.2 – 5.7
83	< 5.2	5.2 – 5.7
84	< 5.2	5.2 – 5.7
85	< 5.2	< 5.2
86	< 5.2	< 5.2
87	< 5.2	< 5.2
88	< 5.2	< 5.2
89	< 5.2	< 5.2

^aValues ($-\log K_i$) are mean \pm SD of two independent experiments performed in triplicates.

Table 4.19 Dopamine receptor affinities of compounds from the second virtual screening cycle.

No.	$-\log K_i^a$	
	hD_{2S}	hD_3
90	5.88 ± 0.17 (1.35 ± 0.43)	6.04 ± 0.43 (1.38 ± 0.5)
91	6.26 ± 0.08 (1.13 ± 0.22)	7.41 ± 0.07 (1.06 ± 0.15)
92	6.36 ± 0.06 (1.12 ± 0.13)	6.86 ± 0.06 (1.18 ± 0.15)
93	6.71 ± 0.11 (1.03 ± 0.13)	7.03 ± 0.09 (1.09 ± 0.30)
94	5.36 ± 0.05 (0.87 ± 0.08)	6.07 ± 0.18 (1.10 ± 0.17)

^aValues ($-\log K_i$) are mean \pm SD.

^bNumber of experiments performed in triplicates.

Table 4.20 Dopamine receptor affinities of compounds from clustering-based virtual screening.

No.	$-\log K_i^a$			
	hD_{2s}	n^b	hD_3	n^b
95	6.05, 6.14 (0.88 ± 0.11)	2	7.19 ± 0.05 (0.95 ± 0.23)	3
96	6.05, 6.18 (0.93 ± 0.14)	2	6.54, 6.61 (1.11 ± 0.79)	2
97	5.11, 5.31 (0.83 ± 0.43)	2	5.86, 6.21 (0.88 ± 0.34)	2
98	4.97 ± 0.22 (0.54 ± 0.06)	3	5.49, 5.71 (0.66 ± 0.34)	2
99	5.47, 5.32 (1.28 ± 0.46)	2	6.67, 6.53 (0.88 ± 0.25)	2
100	5.55, 5.63 (1.14 ± 0.15)	2	6.24, 6.24 (0.91 ± 0.05)	2
101	5.96, 6.11 (1.26 ± 0.18)	2	6.01, 6.03 (0.63 ± 0.02)	2
102	<5.00 (n.d.) ^c	2	5.34, 5.37 (0.91 ± 0.28)	2
103	6.10, 6.13 (1.13 ± 0.26)	2	6.65 ± 0.31 (0.93 ± 0.20)	4
104	<5.00 (n.d.) ^c	2	5.70, 5.69 (0.69 ± 0.18)	2
105	5.15, 5.36 (0.97 ± 0.51)	2	5.64, 5.64 (0.80 ± 0.23)	2
106	4.67 ± 0.27 (0.76 ± 0.06)	3	5.46, 4.99 (0.72 ± 0.27)	2
107	<5.00 (n.d.) ^c	2	5.52, 5.18 (1.15, n.d.)	2
108	5.49, 5.26 (0.61 ± 0.28)	2	6.74 ± 0.13 (0.99 ± 0.26)	3
109	<5.00 (n.d.) ^c	2	5.18, 5.36 (n.d.) ^c	2
110	6.67, 6.55 (0.90 ± 0.19)	2	5.57, 5.61 (1.24 ± 0.18)	2
111	6.31, 6.24 (0.78 ± 0.16)	2	5.96, 6.21 (0.77 ± 0.16)	2

^aValues ($-\log K_i$) are mean ± SD.

^bNumber of experiments performed in triplicates.

^cn.d., not determined.

Table 4.21 Dopamine receptor affinities of compounds from pharmacophore based virtual screening.

No	$-\log K_i^a$		$-\log K_i^a$	
	hD_{2S}	n^b	hD_3	n^b
112	6.80 \pm 0.07 (1.20 \pm 0.12)	4	7.19 \pm 0.06 (1.52 \pm 0.23)	3
113	5.87 \pm 0.10 (1.78 \pm 0.28)	3	6.31 \pm 0.07 (1.25 \pm 0.80)	4
114	5.87 \pm 0.09 (1.29 \pm 0.86)	3	5.50, 5.39 (n.d.) ^c	2
115	5.36 \pm 0.03 (0.86 \pm 0.26)	3	5.54, 5.62 (0.77 \pm 0.11)	2

^aValues ($-\log K_i$) are mean \pm SD.^bNumber of experiments performed in triplicates.^cn.d., not determined.

12 Curriculum Vitae

PERSONAL DATA

DATE OF BIRTH 02/10/1973
PLACE OF BIRTH Bad Nauheim, Germany

PROFESSIONAL EXPERIENCE

J. W. Goethe-University, Frankfurt, Germany 02/2002 - 04/2006
PERFORMANCE OF PH.D. THESIS IN PHARMACEUTICAL SCIENCES
“Development of Novel Ligands Influencing Neurotransmission in the Central Nervous System”. Supervisor: Professor Dr. H. Stark, Institute of Pharmaceutical Chemistry.

TEACHING ASSISTANT, LECTURER 02/2002 - 04/2006
Teaching Lectures and Practical Training Courses for Students of Pharmaceutical Sciences in “Qualitative and Quantitative Analysis of Drugs According to European Pharmacopeia”.

Brunnen Apotheke, Dieburg, Germany 01/2001 - 12/2001
PHARMACIST

Kur-Apotheke, Bad Nauheim, Germany 06/2000 - 12/2000
PHARMACIST

EDUCATION

CERTIFIED PHARMACIST 08/2000

THIRD PHARMACEUTICAL EXAMINATION 07/2000

SECOND PHARMACEUTICAL EXAMINATION 04/1999

J. W. Goethe-University, Frankfurt, Germany

FIRST PHARMACEUTICAL EXAMINATION 09/1996

J. W. Goethe-University, Frankfurt, Germany

STUDIES OF OECOTROPHOLOGICAL SCIENCES 10/1993 - 03/1994
Justus-Liebig-University, Giessen, Germany

ABITUR 1993
St. Lioba Gymnasium, Bad Nauheim, Germany

TRAINING

Unité De Neurobiologie Et Pharmacologie Moléculaire, (INSERM), 04/2002
Centre Paul Broca, Paris, France

Practical Training in Radioligand Competition Binding Assays, Pharmacological Functional Assays and Cell Culture. Supervisor: Dr. P. Sokoloff.

Department of Pharmacy, King’s College, London, England 11/1999 - 05/2000
Research Studies in Pharmacognosy: “Investigation of Constituents of Helonias with Reference to Possible Estrogenic Activity”. Supervisor: Prof. Dr. P. Houghton.

Georgen Apotheke, Darmstadt, Germany 05/1999 - 11/1999
Trainee Program for Pharmacists.

13 Publications

PUBLICATIONS

Byvatov, E., Sasse, B.C., Stark, H., and Schneider, G. From Virtual to Real Screening for D₃ Dopamine Receptor Ligands. *ChemBioChem*, **2005**, *6*, 997-999.

Petroianu, G., Arafat, K., Sasse, B.C., and Stark, H. Multiple Enzyme Inhibitions by Histamine H₃ Receptor Antagonists as Potential Procognitive Agents, *Pharmazie*, **2006**, *61*, 179-182.

Noeske, T., Sasse, B.C., Stark, H., Parsons, C.G., Weil, T., and Schneider, G. Predicting Compound Selectivity by Self-Organizing Maps: Cross-Activities of Metabotropic Glutamate Receptor Antagonists. *ChemMedChem*, **2006**, *1*, 1066-1068.

Sasse, B.C., Mach, U.R., Leppanen, J., Calmels, T. and Stark, H. Benzhydrylpiperazine Derivatives as High Affine and Selective Dopamine D₃ Receptor Ligands, submitted.

Böcker, A.[§], Sasse, B.C.[§], Nietert, M., Stark, H., and Schneider, G. GPCR Targeted Library Design: Novel Dopamine D₃ Receptor Ligands. ([§]Both authors contributed equally to the work), *ChemMedChem*, **2007**, accepted.

POSTER

Sasse, B., Perachon, S., Schwartz, J.-C., Sokoloff, P., and Stark, H. Congeners of Pramipexole as Dopamine D₃ Receptor Ligands. *XVIIth International Symposium on Medicinal Chemistry*, Barcelona, Spain, September 1-5, **2002**.
Drugs Future **2002**, *27* (Suppl. A), 437, P461.

Sasse, B.C., Byvatov, E., Richter, C. Schneider, G., and Stark, H. Support Vector Machine for Novel Lead Findings with Dopamine D₃ Receptor Ligands. *Deutsche Pharmazeutische Gesellschaft - Annual Meeting*, Mainz, Germany, October 5-8, **2005**.
Abstract Book, 123, C94.

Sasse, B.C., Böcker, A., Schneider, G., and Stark, H. Classification Techniques in Chemoinformatics: Lead Identification Strategies for Dopamine D₃ Receptor Ligands. *Frontiers in Medicinal Chemistry*, Medicinal Chemistry Divisions of GDCh and DPhG, Frankfurt am Main, Germany, March 12-15, **2006**.
Abstract Book, 120.

Saur, O., Sasse, B.C., Mach, U. R., Leppanen, J., Calmels, T., and Stark, H. Bamipine-Based Amides as Dopamine D₂ and D₃ Receptor Ligands. *Frontiers in Medicinal Chemistry*, Medicinal Chemistry Divisions of GDCh and DPhG, Frankfurt am Main, Germany, March 12-15, **2006**.
Abstract Book, 120.

Kubas, H., Sasse, B.C., Mach, U.R., Leppanen, J., Calmels, T., and Stark, H. Cyclizine-Based Dopamine D₃ Receptor Ligands. *Frontiers in Medicinal Chemistry*, Medicinal Chemistry Divisions of GDCh and DPhG, Frankfurt am Main, Germany, March 12-15, **2006**.
Abstract Book, 121.

Schübler, M., Sasse, B.C., Mach, U.R., Leppaenen, J., Calmels, T., and Stark, H. Tri- and Tetracyclic Compounds as D₃ Dopamine Receptor Ligands. *Frontiers in Medicinal Chemistry*, Medicinal Chemistry Divisions of GDCh and DPhG, Frankfurt am Main, Germany, March 12-15, **2006**.

Abstract Book, 122.

Kottke, T., Sasse, B.C., Mach, U R., Leppaenen, J., Calmels, T., and Stark, H. Binding Studies of Dopamine D₂/D₃ Receptor Ligands Having Structural Histamine H₁ Receptor Antagonist-Related Scaffolds. *Frontiers in Medicinal Chemistry*, Medicinal Chemistry Divisions of GDCh and DPhG, Frankfurt am Main, Germany, March 12-15, **2006**.

Abstract Book, 123.

Kubas, H., Sasse, B.C., Mach, U.R., Leppaenen, J., Calmels, T., and Stark, H. Dopamine D₂-like Receptor Ligands by Fragment-based Approach. *XIXth International Symposium on Medicinal Chemistry*, Istanbul, Turkey, August 29-September 2, **2006**.

Drugs Future **2006**, 31 (Suppl. A), 137-138, P193.

Saur, O., Sasse, B.C., Mach, U. R., Leppaenen, J., Calmels, T., and Stark, H. Bامipine- and Mianserin-Based Amines as Dopamine D₂ and D₃ Receptor Ligands. *XIXth International Symposium on Medicinal Chemistry*, Istanbul, Turkey, August 29-September 2, **2006**.

Drugs Future **2006**, 31 (Suppl. A), 137-138, P193.

Kottke, T., Sasse, B.C., Mach, U R., Leppaenen, J., and Stark, H. Binding Properties of Dopamine D₃ Receptor Ligands Using Privileged Structures. *Joint Meeting 2006*, German Pharmaceutical Society with Czech Pharmaceutical Society and Hungarian Society for Pharmaceutical Sciences, Marburg, Germany, October 4-7, **2006**.

Noeske, T., Derksen, S., Sasse, B.C., Stark, H., Parsons, C.G., Weil, T., and Schneider, G. Selectivity Profiles for Ligands of Family C GPCRs. *2nd German Conference on Chemoinformatics*, 20. CIC-Workshop, Goslar, Germany, November 12-14, **2006**.